The expression of potential molecular candidates for chloride ion channels in primary human granulocytes and granulocytic cell lines

By

Kirsty-Anne Kirk, RN (Dip) HE, BA (Hons), MSc, PGCME, FHEA

A thesis submitted in complete fulfilment of the requirements of the University of East Anglia for the degree of Doctor of Philosophy

Norwich Medical School
Faculty of Medicine and Health Sciences
University of East Anglia

Submitted July 2014

DECLARATION

I declare that the work submitted in this thesis was undertaken and completed by myself unless otherwise acknowledged, and has not been accepted in any previous application for a degree with any other institution.

Kirsty Kirk

July 2014

ABSTRACT

INTRODUCTION AND HYPOTHESIS: The project aims to identify potential candidates for chloride (Cl^-) ion channels in granulocytes, and granulocytic cell lines. It is hypothesised that Cl^- ion channels, in particular hBest1, are implicated in the role of granulocytes in response to inflammation.

METHODOLOGY: Two main methodologies were used; laboratory techniques and systematic review. Laboratory techniques included RT-PCR, flow cytometry and western blot analysis to characterise the expression of hANO1, hBest1 and hCLCA1 as potential chloride ion channels in granulocytes and granulocytic cell lines. Systematic review was performed to identify whether chloride ion channels are up-regulated in COPD and asthma.

RESULTS: RT-PCR demonstrated hCLCA1 expression in granulocytes and eosinophils but not HL60. hBest1 and hBest3 was expressed in all 3 cell types. In granulocytes, flow cytometry demonstrated greater hCLCA1 protein expression intracellularly, compared to hBest1 protein, and greater hBest1 plasma membrane expression compared to hCLCA1 ($P<0.05$). There was a negative correlation between hBest1, and hCLCA1 but also a weak negative correlation between hBest1 and hANO1 ($P<0.05$). Granulocytes stimulated with IL-13 over 24 hours, had a greater protein expression both intracellularly and at the plasma membrane. There was increased migration of HL60s when transfected with hBest1, in response to fMLP ($P<0.05$). Systematic review did not support the project due to limitations.

CONCLUSIONS: There is a complex relationship between hBest1, hCLCA1 and hANO1 which may contribute to the function of granulocytes. HBest1 protein expression peaked 24 hours after continuous stimulation with IL-13. This correlates with peak symptom expression in diseases such as COPD and asthma. It is suggested that hBest1 has a role in migration and activation of granulocytes, through regulation of cell shape and volume. It is concluded that hBest1 is a novel therapeutic target in the control of symptoms in chronic inflammatory lung diseases.

CONTENTS

LIST OF FIGURES

LIST OF TABLES

ABBREVIATIONS

9AC	Anthracene-9-carboxylic acid
AHR	Airway hyper-responsiveness
ANO	Anoctamin
ATP	Adenosine triphosphate
BCA	Bicinchoninic acid assay
Best	Bestrophin
BSA	Bovine serum albumin
Ca^{2+}	Calcium
CaCC	Calcium activated chloride channels
cAMP	Cyclic adenosine monophosphate
cDNA	Complementary deoxyribonucleic acid
CF	Cystic fibrosis
CFPAC	Cystic fibrosis pancreatic duct adenocarcinoma cell
CFTR	Cystic fibrosis transmembrane conductance regulator
Char-LCP	Charcot-Leyden crystal protein
CHO	Chinese hamster ovary
Cl^-	Chloride
CLIC	Chloride intracellular channel
COPD	Chronic obstructive pulmonary disease
Cys-LT	Cysteinyl-leukotrienes
DAPI	4',6-diamidino-2-phenylindole
dbcAMP	N^6,2'-0-dibutyryladenosine 3':5'-cyclic monophosphate sodium
dEoL-1	Differentiated EoL-1
dH_2O	Deionised water
DIDS	4,4'-diisothiocyanatostilbene-2,2'-disulphonic acid

DMEM	Dulbecco's Modified Eagle Medium
DNA	Deoxyribonucleic acid
EDTA	Ethylenediaminetetraacetic acid
ELISA	Enzyme-linked immunosorbent assay
EoL-1	Eosinophilic leukaemia cell line
EtBr	Ethidium bromide
FACS	Fluorescence-activated cell sorting
FBS	Foetal bovine serum
FCS	Foetal calf serum
FITC	Fluorescein isothiocyanate
fMLP	Formyl-methionyl-leucyl-phenylalanine
FSC	Forward scatter
GFP	Green fluorescent protein
H^+	Hydrogen
HCl	Hydrogen chloride
HEK-	Prefix for HEK293. Human embryonic kidney
HL60	Human promyelocytic leukemia cells
HPACC	Health Protection Agency Culture Collections
IAA94	*R*(+)-[(6,7-dichloro-2-cyclopentyl-2,3-dihydro-2-methyl-1-oxo-1H-inden-5yl)-oxy] acetic acid 94
IL-	Pre-fix (ie IL-13, IL-5). Interleukin
K^+	Potassium
KRB	Krebs ringer buffer
LB	Lysogeny broth
MBP	Major basic protein
MCS	Multiple cloning site
MQAE	*N*-[ethoxycarbonylmethyl]-6-methoxy-quinolinium bromide
mRNA	Messenger ribonucleic acid

NaCl	Sodium chloride
NAEC	Nasal airway epithelial cells
NADPH	Nicotinamide adenine dinucleotide phosphate
NCBI	National Center for Biotechnology Information
NPPB	5-nitro-2-(3-phenylpropylamino) benzoic acid
PBS	Phosphate buffered saline
PE	Phycoerythrin
PFA	Paraformaldehyde
PI	Propidium iodide
PMN	Polymorphonuclear cells
RAO	Recurrent airway obstruction
RCF	Relative centrifugal force
RNA	Ribonucleic acid
RPMI	Roswell Park Memorial Institute. RPMI 1640 media
RT-PCR	Reverse transcriptase polymerase chain reaction
SAEC	Small airway epithelial cells
SCF	Stem cell factor
SDS	Sodium dodecyl sulphate
SSC	Side scatter
STAT6	Signal transducer and activator of transcription 6
TBE	Tris-borate-EDTA
TBST	Tris-buffered saline with tween (0.5%)
TGF	Transforming growth factor
TMD	Transmembrane domains
TMEM-	Prefix indicating a member of the anoctamin family. Example TMEM16A for anoctamin1
TNF	Tumour necrosis factor
UTP	Uridine5'-triphosphate
VWA	Von Willebrand factor domain A

ACKNOWLEDGEMENTS

Completing this thesis has been a long and steep journey but without the help, guidance, love and support from a number of people, I would never have reached the summit.

Firstly, the sound judgement, and gentle perseverance of my supervisors, John and Darren. Accepting my quirks and flaws, the rough and smooth, and kept me on the right track with their belief in me.

UEA staff and students for accepting me into the fold and supporting with collegial advice. My managers at UCS for both financial and emotional support. In particular, Bob, not only my line manager but colleague, and friend. He has always kept the faith.

My family. Where to start? Mum, for backing me in everything I do, for getting up at 05.30 to look after the kids in the rain, sleet and snow, for celebrating my successes and picking me up when I'm down. My Mum, my best friend. Dad, your level head, wise words, or practical nature and your so very dry sense of humor! And Nana, dear Nana, as always, for you.

My dear husband, Chris. You walked into my life, and we turned yours upside down. Your love, belief and sheer stubbornness has been my backbone.

And my babies, you are my reason for being, my reason to get up and strive on, you are my life. And you keep me grounded, when life gets hard, you always remind me what's important, and what's real.

Finally, my dear friends. My girls, Marita and Eleanor. My life has been a roller coaster and you've ridden it all the way with me!

There are too many, and words are never enough, but thank you all.

CHAPTER 1: INTRODUCTION

1.1 Inflammatory airway diseases and the role of potential chloride ion channel candidates in granulocyte function within inflammatory airways.

Asthma and chronic obstructive pulmonary disease (COPD) have one of the highest morbidity and mortality rates in western society (Barnes, 2008; Sturton *et al.*, 2008; Knight *et al.*, 2012).

Asthma and COPD are both considered inflammatory airway diseases and have similar clinical manifestations, overlapping pathophysiology, and similar treatment strategies. Currently, asthma and COPD are treated predominantly with inhaled corticosteroids and inhaled bronchodilators (Polosa & Blackburn, 2009; Knight *et al.*, 2012). Exaccerbations of COPD can also be treated with non-invasive positive pressure ventilation. In addition, both diseases are associated with increased incidences of hospitalisation, decreasing quality of life associated with symptoms, high morbidity and physical disability (Knight *et al.*, 2012). There are, however, different aetiologies for asthma and COPD (Gonem *et al.*, 2012). It is widely acknowledged that tobacco smoking is the main risk factor in COPD whereas asthma can be considered either an atopic disease with acute exaccerbations triggered by allergens, viral infections or air pollution, such as tobacco smoke (Polosa & Blackburn, 2009; Gonem *et al.*, 2012; Knight *et al.*, 2012), or non-atopic. Non-atopic asthma is also considered intrinsic where there are no external triggers to symptom exacerbation, and often as a result of hypersensitivity. General clinical manifestations for asthma are respiratory wheezing, variable airway obstruction, dyspnoea and cough, whereas COPD has differences (Polosa & Blackburn, 2009). In COPD, mucous clearance is limited, there is greater association with respiratory failure and cardiac failure (*cor*

pulmonale) and less variation in obstruction to airflow (Polosa & Blackburn, 2009). In addition, asthma symptoms are responsive to glucocorticoid therapies whereas the response in COPD is limited. Gonem *et al* (2012) have highlighted five domains that can be used to phenotype asthma and COPD according to clinical manifestation (Table 1.1 summarises domains).

Domain	Descriptor	Clinical manifestation
A	Airway hyper-responsiveness (AHR)	Narrowing of the airways related to sensitivity and reactivity of smooth muscle. Airflow obstruction and dyspnoea. Considered a symptom that is variable
B	Bronchitis	Airway inflammation. Asthma is considered eosinophilic and COPD neutrophilic
C	Cough reflex hypersensitivity	Dry cough associated with asthma. COPD often presents with a productive cough that has poor clearance. Variable symptom.
D	Damage to airways and lung parenchyma	Thickening of the bronchial wall, airway remodelling with fibrosis, hypertrophy of smooth muscle in airways, emphysema and bronchiectasis, airway collapse and angiogenesis
E	Extra-pulmonary factors	These are factors that may impact upon presentation of disease and examples include obesity and rhinosinusitis

Table 1.1: Five domains to phenotype asthma and COPD: Five domains have been highlighted by Gonem *et al.* (2012) to assist in phenotyping respiratory disease, particularly asthma and COPD. Domains are labelled A-E and the associated clinical manifestations are supported by Polosa and Blackburn (2009) and Knight *et al.* (2012)

Within the five domains there are variations according to identified disease. Airway hyper-responsiveness (refer to domain A in table 1.1 for definition) is common to COPD and asthma however, in asthma, this is typically reversed by the use of bronchodilators with resultant variable airflow obstruction (Gonem *et al.*, 2012; Knight *et al.*, 2012). COPD is considered to have a fixed obstruction to airflow and prolonged AHR which is associated with airway remodelling and fibrosis of the lung tissue. The cough that presents in asthma is often non-productive in response to inhaled glucocorticoid therapies, however in COPD, there is increased mucous production, with difficulty in clearance (Polosa & Blackburn, 2009; Gonem *et al.*, 2012). Another marked difference between the pathophysiological abnormalities of COPD and asthma is the damage to airways. In asthma, there is hypertrophy of smooth muscle, however COPD has greater destruction of alveoli (Gonem *et al.*, 2012). Figure 1.1 outlines the differences observed in the pathophysiologies of COPD and asthma, with related aetiology.

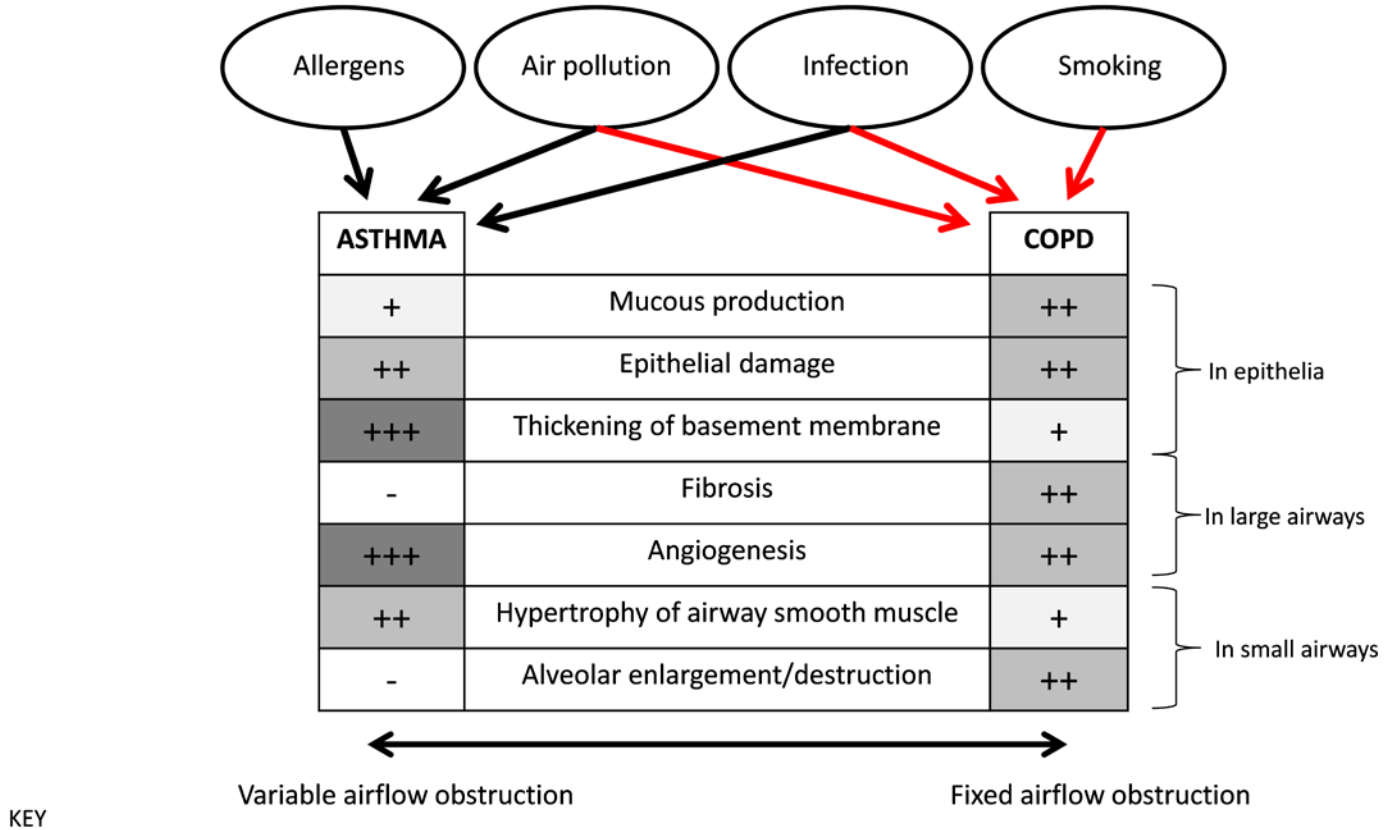

KEY

-	Not usual
+	Mild (comparatively)
++	Moderate (comparatively)
+++	Severe (comparatively)

Figure 1.1: Different pathophysiological abnormalities observed in COPD and Asthma: The figure is adapted from Gonem *et al* (2012). This shows the differing aetiologies associated with COPD and asthma and comparable pathological abnormalities. Each abnormality is presented with indication as to the extent it affects both asthma (left column) and COPD (right column). – denoted that it is not expected, += mild, ++=moderate and +++=severe. Of note, asthma is associated with a dry cough where as COPD has a productive cough with limited clearance. Of clinical importance, asthma is considered to have variable airflow obstruction as it is often reversible with bronchodilators.

The presence of leukocytes in inflammatory and allergic airway diseases, such as asthma, cystic fibrosis (CF) and COPD, has been well documented (Martínez-Antón *et al.*, 2006; Holgate & Polosa, 2008; Vercelli, 2008). The function of granulocytes within this process remains contentious (Walsh *et al.*, 2007; Matsumoto *et al.*, 2008). Granulocytes (also termed polymorphonuclear cells (PMN)) are so named because of the presence of granules in the cytoplasm and the varying nuclear shapes. The term "granulocytes" will be used in the general discussion as this is the predominant term used within the cited studies and literature. Within the discussion of experimental methods and results in this thesis, the term PMN will be predominantly used for granuocytes as cell type was determined by nuclear shape. Often, the term PMN refers to neutrophils as these are the most abundant cell type in granulocytes, with neutrophils constituting 60-70% of all leukocytes (Bauman, 2006). Comparably, 2-4% of leukocytes are eosinophils and less than 1% are basophils (Gibbs, 2005; Bauman, 2006). For the purpose of this thesis, PMN will refer to a mixed population of granulocytes, which includes neutrophils, eosinophils and basophils in their relative abundance.

Asthma and COPD were, historically, considered to be the same disease process with differing clinical manifestations (Barnes, 2008; Gonem *et al.*, 2012). Sturton *et al* (2008) however, has suggested that they are different diseases, marked clearly by distinctive inflammatory mediators. Furthermore, Barnes (2008) proposed that different sub-types of PMNs were involved within these processes, and that the resulting clinical symptoms, were characteristic to each lung pathology. Gonem *et al.* (2012) identified the symptoms of asthma and stated that these are mediated by eosinphils, mast cells and $CD4^+$ cells. It has been suggested

that eosinophils are specifically implicated in airway hyper-responsiveness and fibrosis as a source of fibrogenic factors (Barnes, 2008; Raap & Wardlaw, 2008). This is associated with the atopic nature of the disease and variable symptom expression. COPD however is mediated by macrophages and neutrophils which are associated with the relative fixed airflow obstruction and that symptoms tend to be persistent with minimal variation (Gonem *et al.*, 2012). Specifically, neutrophils have a functional role in the over-production of sputum (Barnes, 2008). However, people with severe (refractory) asthma, that is insensitive to corticosteroid therapy, have been found to have a higher percentage of sputum neutrophils, compared to eosinophils (Choi *et al.*, 2012). This has been linked to a role in persistent airway obstruction. There are overlapping symptoms of asthma and COPD. There are some differences in disease manifestation enabling diagnosis, however often patients do not fit the expected pattern. These individuals should be phenotyped according to the domains highlighted in Table 1.1 and treatment should be focussed upon the manifestations rather than a pre-defined strategy based upon diagnosis (Gonem *et al.*, 2012).

Current treatment strategies appear to focus upon smooth muscle and reduction of inflammation and the management of mucus hypersecretion. As summarised in figure 1.1, mucus hypersecretion is predominantly characteristic of COPD, whereas asthma is associated with a dry cough. Clearance of mucus is limited in COPD which may cause bacterial infection, and exaccaerbation of clinical symptoms (Gonem *et al.*, 2012). Therefore, treatment of symptoms in COPD include airway hydration to assist in mucociliary clearance (Graeber *et al.*, 2013). Chloride (Cl^-) channels, however, may prove a novel target for pharmacological intervention to assist in the hydration of airway epithelia, and clearance of

mucus, through fluid flux associated with chloride movement. For the purpose of this project, the term chronic inflammatory lung disease will be used in relation to results, to encompass the overlapping symptoms of diseases that chloride ion channels and granulocyte function may impact upon.

Chloride channels may also be implicated in the function of granulocytes as they mediate the clinical symptoms of chronic inflammatory lung diseases. Chloride ion channels allow the passage of chloride ions via passive diffusion. This is through pores in either the plasma membrane or membrane of intracellular organelles (Altenberg, 2005). Chloride ion channels perform a variety of functions in a number of cellular processes including; regulation of cell volume, pH control of lysosomes and stabilisation of membrane potential (Eggermont, 2004; Cheng *et al.*, 2008; Linley *et al.*, 2009). When the gene encoding a chloride channel mutates, channelopathies and dysfunction occur. This can result in diseases such as osteoporosis, renal calculi, cystic fibrosis, epilepsy and myotonia (Planells-Cases & Jentsch, 2009). The presenting disease is dependent upon the position, type and functional properties of the chloride channel that is affected by the gene mutation. The function of these channels may have a further role in other physiological processes, particularly within inflammation and allergic responses. For example, Cheng *et al* (2008) have suggested that chloride ion channels have a role in migration and activation of immune cells in inflammatory and allergic lung responses. In this instance, chloride ion channels would be implicated in airway inflammation and granulocyte recruitment as highlighted previously in Figure 1.1 and Table 1.1.

Chloride (Cl^-) flux governs the movement of fluid, secondary to Cl^- channel stimulation. Cl^- channels are passive in that Cl^- efflux or influx is dependent upon the difference between intracellular and extracellular concentrations (Jentsch *et al.*, 2005). This has been highlighted by Suzuki *et al* (2006) who implicate this in both cell volume regulation, and transport of water and salts across membranes. In this case, Cl^- movement is coupled with Na^+ and therefore fluid by creation of an osmotic gradient (Jentsch *et al.*, 2002; Suzuki *et al.*, 2006). There appears a clear role for this process in inflamed airway epithelia (Duta *et al.*, 2006). The transport of fluid into inflammatory airways governs the clearance of mucus by directly affecting the composition. This is well documented in the pathology of CF which clearly underlines the role of Cl^- channels in fluid transport.

This project aims to further discussion, by examining the expression of and function of Cl^- channels in granulocyte function, with specific reference to inflammatory airway diseases. In order to achieve this aim, it is first necessary to present an argument elucidating the role of granulocytes in airway diseases. Following this, there will be discussion as to the role that Cl^- channels have, clarifying how the sub-types may impact on their function within PMNs. Finally, the molecular candidates for Cl^- channels will be identified and the evidence surrounding their structure and function presented. This will be linked to overall granulocyte function in inflammatory airway diseases.

1.1.1 The role of granulocytes in inflammatory airway diseases

1.1.1.1 Neutrophils

Neutrophils have been identified as the main pro-inflammatory mediator in COPD (KanKaanranta *et al.*, 2010; Gonem *et al.*, 2012) and cystic fibrosis (CF) (Illek *et al.*, 2008; Jacquot *et al.*, 2008). The presence of neutrophils is evident in CF lung even in the absence of bacterial infections indicating a role for them within the disease process (Freedman *et al.*, 2002; Ulrich *et al.*, 2010). Barnes (2008) states that while COPD can be considered neutrophilic, other inflammatory pathologies such as asthma, are considered eosinophilic (Figure 1.2 shows morphological differences in nucleus of neutrophils and eosinophils using DAPI staining and microscopy). This is due to differences within the chemotactic factors that are released during the inflammatory phases of these diseases. This is supported by Martínez-Antón *et al* (2006), and Tintinger *et al* (2005) who also highlights the role of neutrophils in CF and acute respiratory distress syndrome. Importantly, neutrophils have been indicated in the inflammatory processes of non-eosinophilic asthma (Tintinger *et al.*, 2005). The role of neutrophils within asthma is indicated by Barnes (2008) who states that while the neutrophil count remains within normal limits in mild asthma, there is a marked increase during severe asthmatic exacerbations.

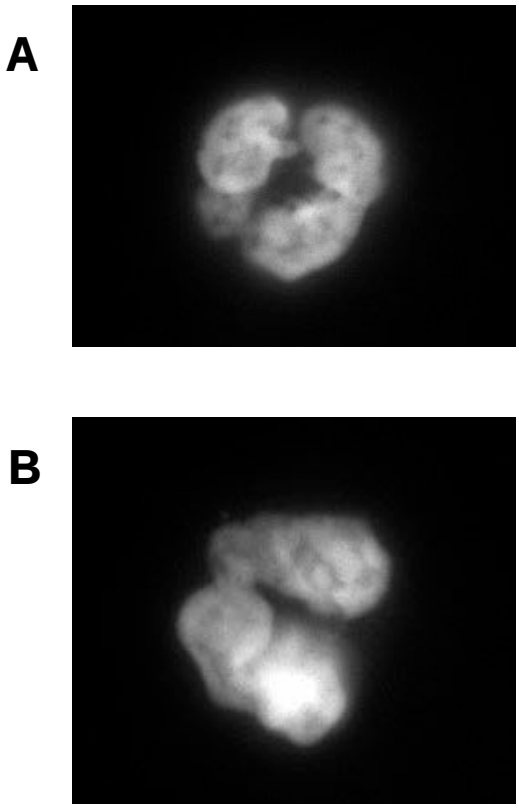

Figure 1.2: Nucleus of neutrophils and eosinophils under microscopy: Figure showing images of a neutrophil and eosinophil stained with DAPI for nucleus visualisation, at 60x magnification. **A)** DAPI stained neutrophil with clear multi-lobed nucleus and **B)** distinct bi-lobed nucleus of an eosinophil.

A role of neutrophils within inflammation is to phagocytose microbes and pathogens (Lollike *et al.*, 2002). Within inflammatory airway diseases chemotaxins attract neutrophils into tissues as a result of inflammation (Tintinger *et al.*, 2005). An integral part of the inflammatory process is respiratory burst of neutrophils (Menegazzi *et al.*, 1999). Respiratory

burst, also referred to as oxidative burst, is a process by which immune cells, such as neutrophils, rapidly release chemicals known as reactive oxygen species. These chemicals are essential for the degradation of bacteria and debris that are internalised by neutrophils during phagocytosis (Page & Pitchford, 2013).

It has been shown that neutrophils are stimulated by Tumour Necrosis Factor-α (TNF-α) only when they are fixed by fibronectin and immobilized, as in inflammatory lung disease (Menegazzi *et al.*, 1999). In the Menegazzi *et al* (1999) study it was demonstrated that β_2 integrin was required to cross-link neutrophils with fibronectin in inflamed tissues. By using inhibitors of chloride efflux, they showed that β_2 integrin cross-linking triggers Cl^- ion efflux which is responsible for respiratory burst. However, the Cl^- transport inhibitors that were used were the family of 2-aminomethyl-4-(1,1-dimethylethyl)-6-iodophenol hydrochloride (MK-447) which have been suggested in an earlier study by Parnham *et al* (1979) to effect the mononuclear cell count (Harada *et al.*, 1983). There may, therefore, be an impact upon neutrophils within the study. In the process of respiratory burst, superoxide anions are produced by activation of nicotinamide adenine dinucleotide phosphate-oxidase (NADPH oxidase) released from lysosomes (Tintinger & Anderson, 2004; Femling *et al.*, 2006). This relationship was supported by another study where lysosomal fusion and stimulation was not affected by the alternative Cl^- channel blocker DIDS (4,4'-diisothiocyanostilbene-2,2'-disulphonic acid) (Korchak *et al.*, 1980). In this study lysosomes did not release their contents however stimulation of lysosome-lysosome fusion remained evident. This supports the hypothesis that chloride flux is involved in the process of respiratory burst in neutrophils.

In COPD inhaled irritants, such as tobacco smoke, may initiate the release of chemotaxins (Barnes, 2008). CXC-chemokinase ligand 1 (CXCL1) and CXC-chemokinase ligand 8 (CXCL8) have been identified as the main candidates for chemotaxis, which are induced by the closely related interleukin-17 (IL-17) and IL-17F (Laan *et al.*, 2001). While neutrophil infiltration during inflammation has a therapeutic effect, prolonged periods of inflammation can lead to tissue damage. This is due to neutrophil mediated phagocytotic enzymes affecting surrounding tissue (Tintinger *et al.*, 2005). Alveolar damage, which presents as emphysema in COPD, is a direct result of neutrophil activation (Taraseviciene-Stewart *et al.*, 2006). In particular, the release of neutrophil elastase from the cytosol contributes to this pathology. This may also explain the presence of neutrophils in severe asthmatic exacerbations, as suggested by Holgate and Polosa (2008). They identified IL-17A as being over expressed in asthmatic airways, due to T-cell mediation which would initiate chemotaxin release. While poorly understood, neutrophil attraction and activation in asthma occurs when the onset is secondary to viral infections, or tobacco smoke inhalation and has been supported by mouse model studies using a neutrophil elastase antibody (Lee *et al.*, 2007).

A common symptom of inflammatory airway diseases is the overproduction of mucus within the airways (Martínez-Antón *et al.*, 2006). It has been suggested that mucus production occurs due to hyper secretion by, or hyperplasia of, goblet cells (Rogers, 2003; Martínez-Antón *et al.*, 2006; Barnes, 2008). In turn, neutrophils have been indicated in the up-regulation of MUC5AC genes in COPD and asthma, resulting in both hyper secretion and hyperplasia of goblet cells (Rogers, 2003; Caramori *et al.*, 2004; Barnes, 2008). Martínez-Antón *et al* (2006) argue that the increase in mucus production and the relationship to

inflammatory processes still remains unclear. In this study, they suggest hyper secretion is due primarily, to eosinophils. In contrast to Barnes (2008) and Rogers (2003), however, Martínez-Antón *et al* (2006) suggest that instead of MUC5A, it is MUC1, MUC4 and MUC8 that are indicated in hyper secretion. It should be noted that in this study, the sample size of bilateral nasal polyps was 38, of which 22 were from asthmatic airways. No samples were taken using COPD samples to compare the potential differences in primary inflammatory cells. In addition, the relationship between nasal epithelia and epithelia from the lower respiratory tract, as affected in COPD, remains an area for clarification when considering the up-regulation of mucus producing genes.

It has been suggested that goblet cell hyperplasia, and therefore mucus production, is due to up-regulation of calcium activated chloride ion channels, such as CLCA (Rogers, 2003). This will be discussed in section 1.1.3.3, however it has been shown that CLCA may not be a chloride ion channel itself, but rather a regulator of endogenous chloride ion channels (Gruber & Pauli, 1999b; Gibson *et al.*, 2005; Hamann *et al.*, 2009). Tintinger *et al* (2005) states that prior to recruitment of neutrophils and activation of pro-inflammatory processes, there is a marked increase in cytosolic calcium. This potential relationship will be discussed in further detail in section 1.1.3.3.

1.1.1.2 Eosinophils

In contrast to neutrophils, eosinophils are strongly implicated within the pathophysiology of asthma (Cheng *et al.*, 2008; Raap & Wardlaw, 2008; Kim *et al.*, 2010; Spencer & Weller, 2010). In addition, there has been a direct link between the termination of inflammatory processes in asthma

and apoptosis in human eosinophils (KanKaanranta *et al.*, 2010). Barnes (2008) reports that the infiltration of eosinophils is evident in the bronchial biopsies of asthmatics. Indeed, Kyoh *et al* (2008) suggest a direct correlation between the number of activated eosinophils in airways, and the severity of symptoms displayed in asthma. Eosinophils have been specifically implicated in late responses of asthma, with eosinophil count at its peak after 24 hours following exposure to an allergen (O'Byrne *et al.*, 2004; Holgate & Polosa, 2008). O'Byrne, *et al* (2004) also acknowledge that eosinophils cannot be held solely accountable for all symptoms during exacerbation of asthma. They claim that approximately half of patients exhibit high levels of eosinophils within their blood stream. This may be due to other factors, such as inhaled toxins (such as atmospheric pollutants), or viruses, which trigger an onset of symptoms in the asthmatic patient. Matsumoto, Tamari *et al* (2008) also poses the question as to whether eosinophilia can be considered a cause of symptom exacerbation, or whether it is purely a marker of disease. Despite whether a marker or cause, the presence of eosinophils in sputum, tissues or blood may be dependent on the mode of stimulation, and attraction of eosinophils to the site of inflammation.

Simon and Simon (2007) claim that eosinophilic disorders are either extrinsic or intrinsic in nature. Extrinsic eosinophilia is attributable to allergen stimulation, mediated by immunoglobulin-E (IgE) whereas intrinsic is non IgE mediated. Asthma may involve eosinophilia as a result of exposure to allergens (Holgate & Polosa, 2008), therefore being IgE mediated. Hegab, *et al* (2004) suggests that some individuals, however, have a genetic susceptibility due to markers on chromosome 5q31-q33. These markers contain genes which code for IL-4 and IL-13. In the event of allergen exposure, eosinophils are released from bone marrow in

response to T-cell mediated cytokine release (Kim *et al.*, 2010; Walsh & August, 2010). Rosenberg, Phipps *et al* (2007) states that T-cells produce T-helper 2 (T_H2) cells which in turn secrete the cytokines IL-4, IL-5 and IL-13 (Willis-Karp, 2004; Simon & Simon, 2007; Spencer & Weller, 2010). The evidence appears to suggest that these cytokines form a positive feedback cycle where IL-4 and IL-13 indirectly further increase eosinophilia. In contrast to previous suggestions (Holgate & Polosa, 2008) that eosinophils are activated in late phase asthmatic response, it has been argued that eosinophils act in early responses to T_H2 inducing agents, such as in asthma. This in turn activates T_H2 immune responses (Spencer & Weller, 2010). This suggests a dynamic interaction between eosinophils and T cells which contribute to the initiation and effects of innate immunity.

It has been suggested that as part of the positive feedback mechanism, mature eosinophils produce IL-4 (Raap & Wardlaw, 2008) and IL-13 which induce polarisation of T_H2 cells (Spencer & Weller, 2010; Walsh & August, 2010). The unique nature of eosinophils as a leukocyte means that these cytokines are pre-formed and stored in granules within cells ready for secretion in response to specific stimuli. Rosenberg *et al* (2007) identifies the role of IL-4 in eosinophilia. The secretion of IL-4 further increases T_H2 cell development, and cause airway epithelia to release cytokines (such as IL-4, IL-5 and IL-13) which attract eosinophils to the site of inflammation (O'Byrne *et al.*, 2004). IL-13 has been suggested to regulate the synthesis of IgE (Willis-Karp, 2004). Kariyawasam and Robinson (2007) also state that IL-13 induces differentiation of fibroblasts into myofibroblasts, and is therefore implicated in the production of collagen. Eosinophilia may be as a result of these two pro-inflammatory cytokines working together (Willis-Karp, 2004). It has been shown,

however, that the response to IL-13 in asthma phenotypes varies according to the distinct cell type upon which it is acting (Lee *et al.*, 2001). Human epithelial cells, bronchial smooth muscle and human fibroblasts were stimulated with IL-13. RNA was extracted and protein expression analysed using Western blot analysis (Lee *et al.*, 2001). This showed that gene expression varied among cells which results in differing asthma phenotypes. This highlighted that IL-13 activated a common transcription factor (STAT6) however the resultant gene expression varied. That IL-13 stimulates differing gene expression is a result of the receptor sub-unit that may be present or activated in a given cell type. Lee *et al.* (2001) stated that IL-13 will bind to one of 3 receptors; common IL-4 receptor and one of 2 subunits of the IL-13 receptor (alpha1 and alpha2). The resultant gene expression is dependent upon the pathway and receptor that IL-13 binds to. Therefore, the symptoms of asthma may not be due to eosinophilia alone but a response to direct IL-13 stimulation of airway cells, and the receptor that IL-13 binds to (common IL-4 receptor, or IL-13 receptor subunit alpha1 or alpha2). It has been demonstrated in murine models that STAT6 can be suppressed by using an IL-13 receptor antagonist (Lee *et al.*, 2001), and as a result, the symptoms of asthma were prevented. This was supported in a later study whereby STAT6 was suppressed and so IL-13 mediated asthma phenotypes were controlled (Nakano *et al.*, 2006). This study however appears to link IL-13 and chloride channels as STAT6 was suppressed using niflumic acid, a specific calcium activated chloride channel blocker. They also showed that IL-13 directly up-regulated mCLCA3 (human homologue hCLCA1).

In contrast, there appears clear evidence suggesting that IL-5 is essential in the process of eosinophilia in airway inflammation (Kim *et al.*,

2010; Spencer & Weller, 2010). This cytokine is required for the terminal differentiation of eosinophils into their mature form (O'Byrne *et al.*, 2004; Kariyawasam & Robinson, 2007; Spencer & Weller, 2010). IL-5 is subsequently implicated in the recruitment and activation of these eosinophils at the site of inflammation (Berlin *et al.*, 2004; Matsumoto *et al.*, 2008). Simon and Simon (2007) also stated that IL-5 has an important role in the survival of eosinophils. This was supported by Rosenberg, Phipps *et al* (2007) who claim that in the absence of IL-5, eosinophils undergo spontaneous apoptosis *in vitro*. This has been supported by a recent study whereby apoptosis was enhanced by histone deacetylase in the absence of IL-5, considered to prolong the survival of polymorphonuclear cells (KanKaanranta *et al.*, 2010). They suggested that this was only evident in terminally differentiated PMNs. In addition to these functions, IL-5 has been suggested to contribute to the positive feedback mechanisms by stimulating eosinophil production of IL-13 (Willis-Karp, 2004).

Further contribution to the inflammatory process is the attraction of activated T_H2 cells which release of IL-4, IL-5 and IL-13. T_H2 cells are attracted to the site of airway inflammation as a result of chemokine ligand 17 (CCL17) and chemokine ligand 22 (CCL22) interacting with CC-chemokine receptor 4 (CCR4) (Liu, 2006). Differentiated eosinophils are also attracted to the site of inflammation by chemokines (such as CC-chemokine 5 and CC-chemokine 11) released from airway epithelial cells (Holgate & Polosa, 2008; Vercelli, 2008). In addition, airway epithelial cells are responsible for recruiting mucosal mast cells to the epithelial surface through release of stem cell factor (Barnes, 2008). Activated mast cells contribute to inflammation by release of histamine from granules but in addition also release cytokines IL-4, IL-5 and IL-13 (Galli

et al., 2005; Barnes, 2008). Berlin, Lincoln *et al* (2004) suggests that mast cell stem cell factor (SCF) also has an important role in eosinophil recruitment acting via IL-5 directly in the epithelial cells of airways. They suggest that when SCF is inhibited, there is a reduction in the cytokine IL-5. As a result of IL-4, IL-5 and IL-13, eosinophils are then differentiated and recruited to the area of inflammation as outlined previously, resulting in eosinophil influx (Holgate & Polosa, 2008). Xanthou *et al* (2003) also suggest that airway epithelial cells release chemokine ligand-11 (CCL11), further recruiting eosinophils by acting upon CCR3. At the site of inflammation, activated eosinophils release pro-inflammatory and cytotoxic proteins, such as eosinophil peroxidise and major basic protein which contribute to the severity of disease symptoms (Raap & Wardlaw, 2008; Kim *et al.*, 2010). (Figure 1.3 is a diagrammatic summary of chemokine and cytokine interactions)

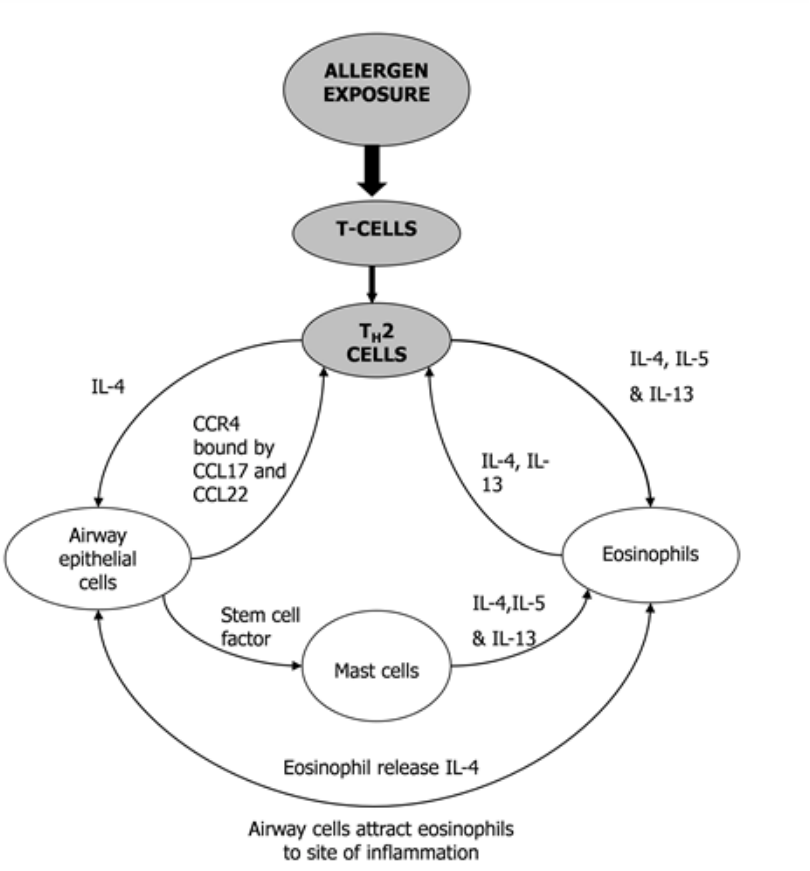

Figure 1.3: Summary of cytokine and chemokine reactions in eosinophils: Diagram (personal) to summarise the complex and positive feedback cytokine and chemokine reactions. Information extracted from previous discussion. Allergen exposure results in T-helper 2 cell responses namely IL-4, IL-5 and IL-13 release. Airway epithelia recruit mucosal mast cells to epithelial surface, through mast stem cell factor, and release cytokines to attract eosinophils to the site of inflammation. Additional response is chemokine receptor 4 (CCR4) binding chemokine ligand 17 and 22 (CCL17 and CCL22 respectively) which forms the positive feedback and further activation of the TH2 cells. IL-5 is thought to be involved in the terminal differentiation of eosinophils, survival of mature cells and the stimulation of eosinophils to produce IL-13. Together with IL-13, eosinophil release of IL-4 from granules polarises TH2 cells so forming a positive feedback response

Another protein in both eosinophil and basophil granules is the Charcot-Leyden crystal protein (Char-LCP) which has been directly associated with asthmatic inflammation (Leonidas *et al.*, 1995). It has been shown that there are distinct differences between major basic protein (MBP) and Char-LCP. Therefore, when eosinophils degranulate, Char-LCP may have distinct functional properties in inflammation (Gleich *et al.*, 1976). This is supported in a study whereby the human myeloid leukaemia cell line (AML14) was stimulated with the pro-inflammatory cytokine IL-13 and IL-5 (Paul *et al.*, 1994). In this instance mRNA encoding Char-LCP was produced and the expressed protein examined using Western Blot analysis. This demonstrated up-regulation of Char-LCP in response to these cytokines. Char-LCP was considered to have lysophospholipase (LPL) activity which may account for a role in inflammation (Leonidas *et al.*, 1995). More recently however, it has been shown that Char-LCP is not an LPL itself but may interact with this enzyme group in eosinophils (Ackerman *et al.*, 2002). Char-LCPs are now considered to be a member of the galectin family (Leonidas *et al.*, 1995; Dyer & Rosenberg, 1996). One role of galectins includes inhibition of inflammation and allergic responses. Therefore, there are clear implications for inhibition of allergic responses and chronic inflammation for Char-LCP in eosinophils and basophils.

While the recruitment and activation of eosinophils appears well documented, the role of these remains a contentious issue (Berlin *et al.*, 2004; Kariyawasam & Robinson, 2007; Barnes, 2008). Walsh *et al* (2007) has suggested that the lack of clarity regarding the role of eosinophils is due to inadequate cell models. Indeed, many authors quote studies that

have been performed using mice however Rosenberg *et al* (2007) highlight the inadequacies in these results by outlining the fundamental differences between human eosinophils and those found in mice. While both cells stain in a similar fashion, it has been noted that the granules are very different in nature. For example, human eosinophils express large numbers of IgE receptors whereas mouse eosinophils don't, the mouse eosinophil also has limited degranulation (Rosenberg *et al.*, 2007). It has been suggested that release of toxins from secondary granules have a direct impact upon the function of eosinophils (Jacobsen *et al.*, 2007). Therefore, this may have a large impact on the functional role of eosinophils in the mouse and human models. This difference is also of particular relevance when considering the role that IgE plays in the recruitment of eosinophils in inflammatory responses.

Despite the concerns involved in applying findings from mouse studies to human eosinophils, the mouse model remains the most prevalent. It has been heavily suggested that a role of eosinophils is to stimulate airway hyper-responsiveness (AHR) (O'Byrne *et al.*, 2004; Willis-Karp, 2004; Kariyawasam & Robinson, 2007; Venge, 2010). Berlin, Lincoln *et al* (2004) however, claims that AHR may not be directly associated with the presence of eosinophils, but due to activation of such by direct release of mast cell stem cell factor within the lung. As a result of activation, eosinophils are stimulated to release cytokines causing AHR, as demonstrated in the laboratory of Berlin *et al* (2004). In these experiments, anti-stem cell factor was administered to mice. Airway hyper-responsiveness was measured along with enzyme-linked immunosorbent (ELISA) assays for chemokines and cytokines. These were animal studies and as such, should be applied to human eosinophils with caution. More recently, Kyoh *et al* (2008) implicates cysteinyl-

leukotrienes (cys-LTs), derived from eosinophil membrane, in the process of bronchoconstriction (Jame *et al.*, 2007). This may contribute to the symptomatic AHR demonstrated in the asthmatic lung. In contrast, mouse studies have demonstrated that T cell expression of IL-5 is a key candidate in the stimulation of AHR by initiating spontaneous degranulation of eosinophils (Kariyawasam & Robinson, 2007; Walsh & August, 2010). Controversially, it has been demonstrated in human studies that IL-5, while increasing the number of eosinophils, does not impact on AHR. In these studies, humanised anti-IL-5 monoclonal antibodies were given to human, mildly allergic subjects (Leckie *et al.*, 2000). As a result, there was a decrease in eosinophil numbers in blood and sputum, but with no reduction in AHR. Simon and Simon (2007) claims that this may be as a result of continued activation of T-cells further releasing IL-5 but that continued AHR may be due to minimal reduction of eosinophils in sputum. This is supported by Rosenberg et al (2007) who show that anti IL-5 antibodies result in a significant decrease in peripheral eosinophils, while there remains a presence of these cells in lung tissue (Kariyawasam & Robinson, 2007). These controversies within eosinophils and their role in AHR however further confirm the difficulties in transferring mouse studies to the human lung.

It has been suggested (Barnes, 2008) that while AHR is unaffected by anti-IL-5 antibody mediated reduction in eosinophils, there is an impact on fibrosis within sub-epithelial cells in airways. As a result, eosinophils have been implicated in the incidence of fibrosis in asthmatic airways. Prolonged activation of eosinophils, and therefore inflammation, results in increased fibrosis due to degranulation and release of cytotoxins which damage epithelial cells. Kariyawasam and Robinson (2007) identify the key toxins as major basic protein (Cheng *et al.*, 2008), eosinophilic

cationic protein, eosinophil derived neurotoxin and eosinophil derived peroxidase (Holgate & Polosa, 2008), which in turn produces reactive oxygen molecules. In addition to the direct fibrinolytic damage caused by these chemicals, further damage may also be stimulated due to triggering local tissue activity (Kariyawasam & Robinson, 2007). These processes contribute to the maintenance and progression of tissue injury and repair (Holgate & Polosa, 2008). As stated previously, IL-5 is essential in the activation, and therefore degranulation of eosinophils and tissue re-modelling (fibrosis), however Willis-Karp (2004) suggest that IL-13 is responsible for fibrosis. While in asthmatic airways, this has been demonstrated in murine studies, it is also implicated in fibrosis of other inflammatory lung diseases, including COPD. The exact mechanism for this remains unclear. One possible process is that IL-13 up-regulates arginase I, an enzyme which results ultimately in the synthesis of collagen through hydrolysis of L-arginine (Willis-Karp, 2004). Whilst not relating IL-13 to fibrosis, a recent study (Siddiqui *et al.*, 2009) used flow cytometry to demonstrate that in human asthmatic subjects, IL-13 was up-regulated in comparison to healthy humans. The up-regulation of IL-13 was predominantly in peripheral T cells with some suggestion of an increased expression in eosinophils, however this was non-significant. This supports the hypothesis that there is involvement of the peripheral blood inflammatory cells in asthma and that the responses seen may not be localised entirely in airway epithelium. Kariyawasam and Robinson (2007) support the role of IL-13 in fibrosis, and suggest that eosinophils are a source of the chemotactic factor for fibroblasts, transforming growth factor-β_1 (TGF- β_1).

In addition to the role eosinophils play in AHR, airway remodelling (Raap & Wardlaw, 2008; Allakhverdi *et al.*, 2009), and fibrosis, there is evidence

to suggest that they have an important role in increased mucus production in asthma (Walsh & August, 2010). Eosinophil influx in inflammatory asthmatic airways up-regulates the genes MUC1, MUC4 and MUC5B which causes mucus hyper secretion (Martínez-Antón *et al.*, 2006). In this study using bilateral nasal polyp cells, it was shown that a reduction in eosinophils directly decreases the expression of MUC8 in patients receiving steroid treatments. This may indicate a treatment pathway for mucus hyper secretion in inflammation and therefore, asthma. It should be noted however that the experiment contained no samples from patients with COPD and further experiments may be necessary to clarify the relationship between eosinophils and mucus secretion in other inflammatory airway disorders. While Kariyawasam and Robinson (2007) and Jame et al (2007) acknowledge the potential role for eosinophils in increased mucus secretion, they link this to the presence of cys-LTs derived from cell membranes (Kyoh *et al.*, 2008). The process for this remains relatively undefined.

1.1.1.3 Basophils

Historically, the role of basophils was not considered important in inflammatory airway diseases (Nouri-Aria & Durham, 2004; Gibbs, 2005). In contrast however, Marone *et al* (2005) claims that they have a pivotal role in antigen stimulated allergic asthmatic responses (Heinemann *et al.*, 2005). Basophils have been found in the sputum and biopsies of asthmatic individuals, particularly after an acute episode of bronchoconstriction (Nouri-Aria & Durham, 2004). The decreased basophil count, comparable with other essential inflammatory cells may indicate either selective recruitment (Heinemann *et al.*, 2005), or is a result of lower differential numbers. In which case, this may inform

findings relating to potency of their actions once stimulated. While there appears little evidence supporting the role of basophils in other inflammatory airway disorders, there are emerging research papers implicating their role in non IgE mediated response. This includes those stimulated by parasites and viruses (Gibbs, 2005). This may have some impact on inflammation in the airways during COPD and CF, perhaps in the presence of viral inflammation.

The mechanism of recruitment and activation of basophils in allergic airways remains unclear (Nouri-Aria & Durham, 2004; Heinemann *et al.*, 2005). As basophils constitute less than 1% of leukocytes, Gibbs (2005) suggests that this may be a contributory factor in the limited evidence supporting their recruitment. With such small numbers, purification of such cells becomes problematic. In addition, Nouri-Aria and Durham (2004) suggested that securing an appropriate antibody for fluorescent labelling had previously been unsuccessful until recently, resulting in either unstable antibodies, or those that are not specific enough to accurately evaluate the data. It appears that there are currently two main antibodies for use (BB-1 and 2D7) in labelling basophils that have contributed to the current evidence supporting their role (Gibbs, 2005). Using these antibodies, they have been identified in late phase responses (Holgate & Polosa, 2008).

Basophil count increases by 7 hours following antigen stimulation (O'Byrne *et al.*, 2004). The relatively late onset may be because they are not present in healthy tissue (Marone *et al.*, 2005). When stimulated, basophils differentiate in bone marrow and emerge into vasculature as mature cells, for migration to sites of tissue inflammation (Gibbs, 2005). Nouri-Aria and Durham (2004) have shown that during allergic asthmatic

exacerbation, the numbers of basophils in peripheral blood increases slightly, possibly two-fold. In contrast, the numbers in the inflamed tissue can be increased markedly, as much as one hundred-fold. These were demonstrated in nasal brushings and so may not be truly representative of those found in bronchial cells. The late responses of basophils may also be due to an agonistic relationship with eosinophils. Both PMN subtypes differentiate from a shared common stem cell precursor; CD34 stem cell in bone marrow (Nouri-Aria & Durham, 2004; Allakhverdi *et al.*, 2009). The basophil count appears to peak before the eosinophil count and is reduced by approximately 24 hours following antigen stimulation (O'Byrne *et al.*, 2004). At this point, as stated in section 1.1.1.2, eosinophilia begins to become evident. This relationship may indicate the role of basophils in eosinophilia and there is evidence demonstrating that basophils release the cytokines IL-4 (Khodoun *et al*, 2004) and IL-13 (Willis-Karp, 2004).

Heinemann *et al* (2005) have shown that stem cell factor (SCF) plays an essential role in the recruitment and survival of basophils. Initially, SCF induces CD11b up-regulation of basophils. In fact, their studies have suggested that SCF is responsible for the selective recruitment of basophils. In their experiment, basophils were demonstrated to be selectively recruited, preferentially to either eosinophils or neutrophils. This was in response to chemotaxis only in the presence of SCF. When SCF was applied alone, there was no basophil migration evident. A secondary finding within this experiment was that survival of basophils was enhanced by the increase in IL-3 anti-apoptotic effects in the presence of SCF. These results appear interesting and offer some insight into the potential mechanisms of basophil migration.

It has been suggested that basophils are recruited to tissues primarily due to the T_H2 cytokine, IL-13, for which basophils have membrane receptors (Nouri-Aria & Durham, 2004; Willis-Karp, 2004). Marone et al (2005) have highlighted that basophils themselves produce IL-13, peaking at approximately 8 hours following antigen stimulation (Nouri-Aria & Durham, 2004). IL-13 is a pro-inflammatory cytokine in itself which may indicate that basophils are responsible both for the onset, and maintenance of allergic inflammation in asthmatic airways (Plath *et al.*, 2001; Gibbs, 2005).

While there appears a clear need for IL-13 in the recruitment of basophils to inflammatory tissues, IL-3 is also essential for the maturation of basophils within bone marrow before release into the circulation (Gibbs, 2005; Holgate & Polosa, 2008; Allakhverdi *et al.*, 2009). Additionally, IL-3 is required for movement of these mobilised basophils from vasculature and across airway endothelium (Gibbs, 2005). It has been acknowledged however that the role of IL-3 is not singularly important in these processes and that other chemokines, such as eotaxin, are required for this, as are mast cells (Gibbs, 2005). Marone *et al* (2005) propose that basophils and mast cells serve a complementary relationship to one another. In their paper, they highlight that, at the site of tissue inflammation, mast cells are responsible for the production of IL-3 and IL-5. This, in turn, increases the secretion of histamine and production of IL-4 by basophils (Khodoun *et al.*, 2004). Basophils are believed to express CD40 ligand which causes IL-4, and IL-13 release, but in addition, proliferation of B-cells, and therefore, increased IgE synthesis (Gibbs, 2005). As a result of IL-4 production, there is a reciprocal increase in the production of cytokines by mast cells. Nouri-Aria and Durham (2004) suggest that the release of IL-4 peaks at 6 hours following exposure to

antigens and in their study have demonstrated that the presence of IL-4 increases in bronchial biopsies, and is directly correlated to the number of basophils. Part of this positive feedback mechanism is the resultant increase in IgE synthesis, mediated by IL-4 (Jacobsen *et al.*, 2007; Vercelli, 2008; Allakhverdi *et al.*, 2009). This may also be responsible for the continued activation of mast cells, resident within inflamed tissues (Nouri-Aria & Durham, 2004). The presence of IL-4 may encourage T_H2 responses (Gibbs, 2005). This includes the release of cytokines IL-4 and IL-13, and pro-inflammatory mediators which may enable continuation of late phase allergic inflammation, and further increased migration of basophils. It has more recently been shown that basophils are antigen-presenting cells which directly impact upon Th2 responses in allergy and inflammation (Sokol *et al.*, 2009; Ito *et al.*, 2011).

Histamine release from basophils is widely considered an integral role in the inflammatory process in allergic inflammatory airways (Nouri-Aria & Durham, 2004). Histamine also has a critical role in the bronchoconstriction that is characteristic in asthma (Barnes, 2008). This is acknowledged by Marone et al (2005) who also indicate that histamine plays a large part in the long term clinical symptoms of allergic asthma. Histamine release occurs following antigen stimulation. In turn, this causes cross linking and activation of the IgE surface receptor, $F_{C\varepsilon}RI$ in basophils (Nouri-Aria & Durham, 2004; Gibbs, 2005; Marone *et al.*, 2005; Vercelli, 2008). The result of histamine release is to regulate the function of immune cells (Marone *et al.*, 2005). Through this process, basophils may induce chemotaxis of mast cells, and increase lysosomal enzyme release. Histamine may also serve to regulate basophil recruitment by binding to receptors, whereby the release of other cytokines from

basophils appear to form a positive feedback mechanism (Marone *et al.*, 2005).

It has been suggested that in addition to histamine release, cross linking of $F_{C\varepsilon}RI$ receptors can also induce LTC_4, a member of the cysteinyl leukotriene (cysLT) family (Nouri-Aria & Durham, 2004; Gauvreau *et al.*, 2005). This may be relevant in the clinical symptoms of allergic asthma as the increase in cysLTs in turn causes bronchoconstriction (Gauvreau *et al.*, 2005). In addition, there is an increase in mucus secretion, and on a cellular level, there is enhancement of eosinophil survival and basophil accumulation. This appears in accordance with the findings of Nouri-Aria and Durham (2004) who reported a correlation between the number of peripheral basophils, and airway responsiveness. While Heinemann et al (2005) support the notion of basophil involvement in increased AHR, they relate it to the increased presence of SCF. AHR may be a result of basophil degranulation, as basophils share common granules with eosinophils. These include major basic protein and eosinophil peroxidise (Jacobsen *et al.*, 2007) which has been reported in section 1.1.1.2 as involved in local tissue activity. The conflicting reports may be due to lack of suitable cell line models to fully examine the receptors and activities of activated basophils. While receptors for cysLTs have been determined on progenitor cells (for basophils and eosinophils) they have yet to be evaluated on mature basophils (Gauvreau *et al.*, 2005). In one study, a weak receptor for cysLT1 was identified (Gauvreau *et al.*, 2005). It should be noted however, as acknowledged by the authors, their sample came from humans whose allergic status was unknown and so results in allergic asthmatic patients should be applied with caution.

Airway remodelling is associated with structural changes in asthma and linked to declining lung function (Kariyawasam & Robinson, 2007). There is also a link between airway remodelling and poor regulation of $F_{C\varepsilon}RI$ cells (Marone *et al.*, 2005). This is not clearly quantified however, clear evidence in the role of basophils in angiogenesis of asthmatic airways has been presented. Basophils have been shown to release angiogenic factors from the granules (Marone *et al.*, 2005). This may directly contribute to airway remodelling.

There appears little clarity, and much controversy as to both the mechanism for recruitment and activation, and the role of basophils in allergic asthmatic airways. This may be due to small numbers of cells within total leucocyte population, poor cell models, or inadequate antibodies. It has also been shown that basophils are antigen presenting cells which may directly impact upon responses to allergens. Advances continue and so this remains an area clearly in need of further investigation.

1.1.2 Chloride ion channels

Chloride (Cl^-) channels have been extensively studied for several years. While many of them conduct several different anions, chloride remains the most prevalent, and so they are named chloride ion channels (Jentsch *et al.*, 2002). Non-specific Cl^- channels may also form due to the clustering of several peptides in the plasma membrane (Suzuki *et al.*, 2006). One of the problems in studying Cl^- ion channels is the lack of specific agents that can block these channels, as many commercial Cl^- channel blockers also affect other ion channels (Leblanc *et al.*, 2005; Greenwood & Leblanc, 2007). These issues have historically made experimentation, and clear identification of the roles of Cl^- channels, problematic (Coelho *et al.*, 2004).

With advances in the field, several Cl^- channels have now been identified and cloned. However, the method of classification of Cl^- ion channels varies. Cl^- channels may be classified according to their functions or the method of regulation of the conductance (Jentsch *et al.*, 2002; Suzuki *et al.*, 2006). Cl^- channels may also be classified according to their position within the cell, either on the membrane or within the intracellular organelles. This is discussed by Jentsch *et al* (2002) who highlight that none of these methods of classification are without issue. This is due to the lack of clear boundaries between the classes, for example, there is often more than one method of regulation for a single channel. In their review they suggest that a more appropriate definition of Cl^- ion channel would be based upon molecular candidates, or identified gene families. Cl^- channels can be classified according to their size of single conductance, and there have been three classes suggested (Suzuki *et al.*, 2006).

Those with an *in vivo* conductance of less than 10 picosiemens (pS) are considered "small" and include the ClC family, cystic fibrosis transmembrane conductance regulator (CFTR) and Bestrophin. CLCA1 and GABAA genes are "middle" sized channels having a conductance of 10-100 pS whereas the *tweety* homolog 3 (TTYH3) gene has a "large" conductance of over 100 pS. While this appears a relatively simple method of classification, it defines little about either the structure or function of such Cl^- channels. It has been stated (Suzuki *et al.*, 2006) that the conductance size of channels can merge across the sub-classes depending on their state of opening. Using classes of conductance, it is difficult to identify the structure of these families as the transmembrane domains (TMDs) are variable and do not appear to relate to the conductance. For example, TTYH3 has been identified as possessing between five and six TMDs, bestrophin has four, and CFTR and ClCs have between ten and twelve (Jentsch *et al.*, 2002; Suzuki *et al.*, 2006) (Figure 1.4 presents some predicted models of transmembrane spanning regions). While these molecular candidates will be considered in more depth later, they are presented at this point to highlight the difficulties with Cl^- channel classification based upon conductance. In addition, there appears no clear relationship between regulation of Cl^- channels and their conductance. As such, regulation has been used as an independent method of classification (Leblanc *et al.*, 2005; Suzuki *et al.*, 2006; Greenwood & Leblanc, 2007).

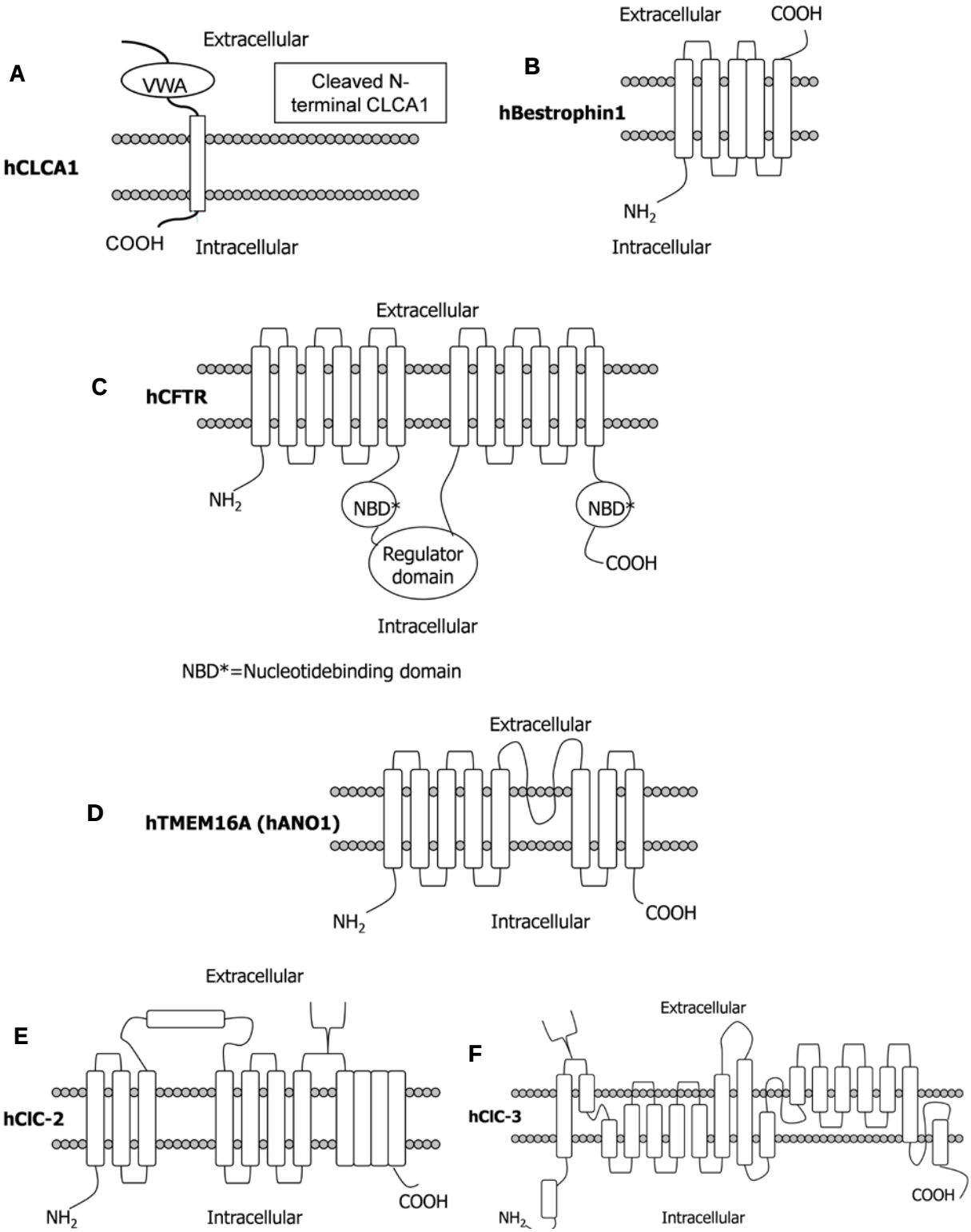

Figure 1.4: Potential chloride ion channel structure (full title on following page)

Figure 1.4: Potential chloride ion channel structure: Diagrams A-D are adapted from (Winpenny *et al.*, 2009). Diagram E adapted from (Ahmen *et al.*, 2000) and F adapted from (Robinson *et al.*, 2004) A. Topological model of hCLCA showing 1 transmembrane domain (discussion in 1.1.3.3 regarding numbers of transmembrane domains) with von Willebrand factor domain A (VWA) located near to the remaining C-terminal and demonstrating the cleavage of N-terminal. B. Human bestrophin 1 with 5 transmembrane domains. C. Represents human CFTR as having 12 transmembrane domains which are separated along the phospholipid bilayer by a regulator domain and two nucleotide binding domains as ATP binding sites. D. Shows the 8 transmembrane spanning regions of human TMEM16A, also referred to as ANO1. E. and F. portray the different topology models for ClC-2 and ClC-3. Whilst in the same family, the number of membrane spanning domains differs and segmented portions of the channel

Five categories of Cl^- channel have been identified (Greenwood & Leblanc, 2007) based on their mechanism of activation; 1. cAMP/PKA activated, 2. membrane voltage gated, 3. ligand gated, 4. cell volume activated (also known as swell activated) and 5. calcium activated (CaCC), (Jentsch *et al.*, 2002; Suzuki *et al.*, 2006), (Figure 1.5). Leblanc *et al* (2005) suggest, however that CaCC channels are ligand gated in their nature. Therefore, the distinction appears to be that ligand gated channels are regulated by extracellular ligands and are widely documented to be primarily associated with $GABA_A$ receptors (inhibitory neurotransmitters) (Jentsch *et al.*, 2002; Greenwood & Leblanc, 2007). In contrast, CaCC channels are controlled by intracellular ion ligands (Suzuki *et al.*, 2006). For the purpose of this thesis, ligand gated

channels will not be discussed due to their relationship to neurotransmitters and not granulocytes or inflammatory airway diseases.

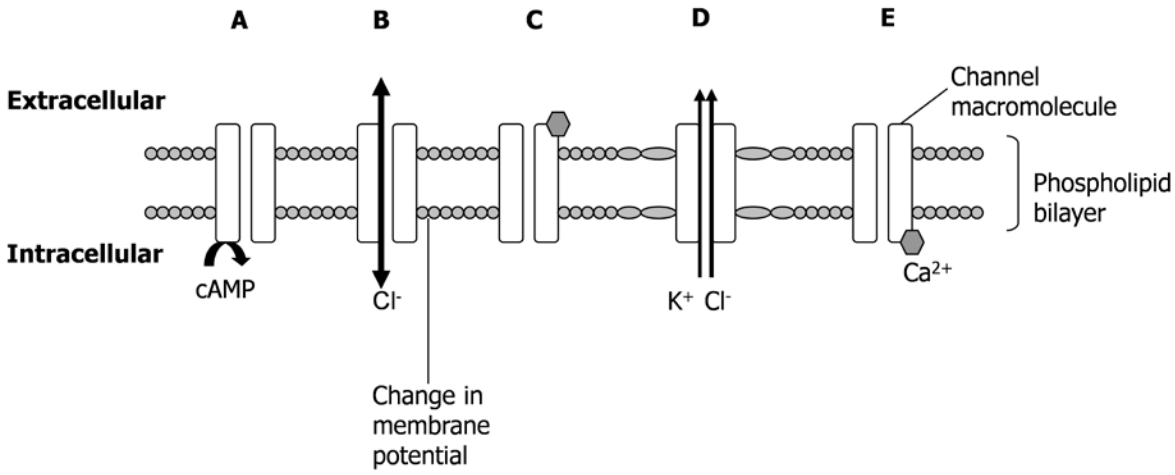

Figure 1.5: Five proposed chloride ion channel categories:
Diagrammatic representation of five propsed chloride ion channel categories (Jentsch *et al.*, 2002; Suzuki *et al.*, 2006). A. cAMP dependent chloride ion channel such as CFTR which is a cAMP-activated ATP-gated anion channel. B. Represents a voltage gated chloride ion channel whereby the change in membrane potential causes the channel to open and allow chloride passage through the membrane via a selectivity filter. The response is either inhibitory or excitatory depending on the electrochemical potential for chloride in a given cell. C. Ligand gated ion channel which refers to an extracellular ligand required to activate the channel. D. Diagrammatic representation of a volume regulated chloride ion channel. The channel opens in response to tension within the membrane allowing chloride and potassium to exit the cell, which in turn allows passage of intracellular fluid and therefore reduce cellular volume. E. A Ca^{2+} activated chloride ion channel which acts in a similar way to C with the exception that the ion ligand is intracellular such as an increase in intracellular Ca^{2+}

For overall cell volume regulation the movement Cl^- governs the movement of fluid, secondary to volume gated Cl^- channel stimulation. Cl^- channels are passive in that Cl^- efflux or influx is dependent upon the difference between intracellular and extracellular concentrations (Jentsch *et al.*, 2005). This has been highlighted by Suzuki *et al* (2006) who implicates this in both cell volume regulation, and transport of water and salts across membranes. In this case, Cl^- movement is coupled with Na^+ and therefore fluid by creation of an osmotic gradient (Jentsch *et al.*, 2002; Suzuki *et al.*, 2006). There appears a clear role for this process in inflamed airway epithelia (Duta *et al.*, 2006). The transport of fluid into inflammatory airways governs the clearance of mucus by directly affecting the composition. This is well documented in the pathology of CF which clearly underlines the role of Cl^- channels in fluid transport.

This highlights the difficulty in both classification of Cl^- channels, and the definition of their function within granulocytes. It has become clear however, that in order to establish this, there needs to be further clarity as to the molecular candidates for these channels, particularly within granulocytes. For the purpose of this project this will include ClCs, CFTR, CLCA and Bestrophin. Tables 1.2-1.9 present some key references used in the discussion of molecular candidates.

Protein Identity	Tissue expression of gene	Key role	References
hCLCA1	Airway epithelia	Mucus production via cell signalling Ion channel regulator	(Zhou *et al.*, 2001; Hoshino *et al.*, 2002; Gibson *et al.*, 2005; Hauber *et al.*, 2007; Hegab *et al.*, 2007; Hauber *et al.*, 2008; Hamann *et al.*, 2009)
	Intestinal epithelia	Mucus production	(Gruber *et al.*, 1998)
	Uterus, stomach, testis, kidney, foetal spleen	Ion channel regulator	(Agnel *et al.*, 1999)
	Brain	Cell signalling	(Zhang *et al.*, 2007)
hCLCA2	Optic nerve	Cell signalling	(Piirsoo *et al.*, 2009)
	Kidney	Cell signalling/ion channel regulator	(Elble *et al.*, 2006)
	Lung, trachea and mammary gland	Cell signalling/ion channel regulator	(Agnel *et al.*, 1999; Gruber *et al.*, 1999)
	Cornea, skin, vagina, larynx	Cell signalling/ion channel regulator	(Itoh *et al.*, 2000; Connon *et al.*, 2004; Connon *et al.*, 2005)
hCLCA3	Spleen, trachea, breast, thymus and lung	Cell signalling	(Gruber & Pauli, 1999b)
hCLCA4	Colon, bladder, brain, uterus, trachea, prostate, stomach and mammary gland	Cell signalling	(Agnel *et al.*, 1999)
	Nasal epithelium	Cell signalling	(Mall *et al.*, 2003)
	Optic nerve	Cell signalling	(Piirsoo *et al.*, 2009)

Table 1.2: Key references human CLCA1-4 (hCLCA1-4): Table summarising some of the key references used to formulate the discussion for human CLCA1-4 (hCLCA1-4), with tissue expression and postulated function identified within the literature

Protein Identity	Tissue expression of gene	Key role	References
mCLCA1	Smooth muscle of portal vein	Ion channel regulation	(Britton *et al.*, 2002)
	Intestine, spleen, bone marrow, trachea, aorta, brain	Secretion	(Leverkoehne *et al.*, 2002; Leverkoehne *et al.*, 2006; Roussa *et al.*, 2010)
	Dorsal root ganglia, intestine, cecum, brain	Secretion	(Al-Jumaily *et al.*, 2007)
	Breast		(Gruber & Pauli, 1999c)
mCLCA2	Intestine	Secretion	(Leverkoehne *et al.*, 2006; Al-Jumaily *et al.*, 2007; Roussa *et al.*, 2010)
	Breast		(Gruber & Pauli, 1999c; Leverkoehne *et al.*, 2002)
	Intestine, trachea, colon, thymus, bladder, epididymus, skin	Secretion	(Leverkoehne *et al.*, 2002)
	Dorsal root ganglia, cecum	Secretion	(Al-Jumaily *et al.*, 2007)
mCLCA3	Airway epithelial mucus cells	Secretion/ion channel regulation	(Zhou *et al.*, 2001; Leverkoehne & Gruber, 2002;

			Brouillard *et al.*, 2005; Gibson *et al.*, 2005)
	Stomach, uterus, colon	Secretion	(Komiya *et al.*, 1999)
	Intestine	Secretion	(Komiya *et al.*, 1999; Leverkoehne *et al.*, 2006)
mCLCA4	Smooth muscle ; bladder, intestine, stomach, uterus, aorta and lung	Cell signalling	(Elble *et al.*, 2002; Leverkoehne *et al.*, 2006)
	Epithelial cells	Cellular processing and regulation	(Huan *et al.*, 2008)
mCLCA5	Squamous epithelium (keratinocytes)	Maturation	(Braun *et al.*, 2010)
	Eye, intestine and spleen	Cancer cell adhesion	(Evans *et al.*, 2004)
	Dorsal root ganglion		(Al-Jumaily *et al.*, 2007)
mCLCA6	Intestines	Secretion	(Bothe *et al.*, 2008)
	Stomach	Secretion	(Evans *et al.*, 2004)

Table 1.3: Key references mouse CLCA1-6 (mCLCA1-6): Table to summarise some of the key references used to formulate the discussion for mouse CLCA1-6 (mCLCA1-6), with tissue expression and postulated function identified within the literature

Protein Identity	Tissue expression of gene	Key role	References
bCLCA1	Trachea	Secretion	(Cunningham *et al.*, 1995)
bCLCA2	Lung endothelium		(Cunningham *et al.*, 1995; Elble *et al.*, 2006)
eCLCA1	Small airways	Cell signalling	(Anton *et al.*, 2005; Ryhner *et al.*, 2008; Gerber *et al.*, 2009)
eCLCA2	Olfactory neurons	Cell signalling	(KanehisaLaboratories, 2009)
pCLCA1	Colon and retinal epithelia	Secretion/channel regulator	(Gaspar *et al.*, 2000; Loewen *et al.*, 2002a; Loewen *et al.*, 2002b; Loewen *et al.*, 2003; Loewen *et al.*, 2004; Plog *et al.*, 2009)
rCLCA1	Salivary cells, ileum, lung	Secretion	(Yamazaki *et al.*, 2005; Ishibashi *et al.*, 2006)
rCLCA2	Cerebellum, cerebrum, kidney, stomach, spinal cord, lung small intestine	Cell signalling?	(Yoon *et al.*, 2006)
rCLCA4	Uterus, lung and heart	Cell signalling	(Song *et al.*, 2009)

Table 1.4: Key references mixed species CLCA: Table to summarise some of the key references used to formulate the discussion for bovine (b), equine (e), porcine (p) and rat (r) CLCAs, with tissue expression and postulated function identified within the literature

Protein Identity	**Tissue expression of gene**	**Key role**	**References**
hBest 1	Retinal pigment epithelium	Volume regulation	(Marmorstein *et al.*, 2002; Tsunenari *et al.*, 2003; Fischmeister & Hartzell, 2005; Hagen *et al.*, 2005; Yu *et al.*, 2006; Milenkovic *et al.*, 2007; Mullins *et al.*, 2007; Yu *et al.*, 2007; Burgess *et al.*, 2008; Eksandh *et al.*, 2008; Milenkovic *et al.*, 2008; Qu & Hartzell, 2008; Xiao *et al.*, 2008; Boon *et al.*, 2009; Davidson *et al.*, 2009; Milenkovic *et al.*, 2009; Qu *et al.*, 2009; Xiao *et al.*, 2009)
	Retinal pigment epithelium	Ion channel regulation	(Yu *et al.*, 2008)
	Colon epithelium	Cell proliferation	(Spitzner *et al.*, 2008)
	Pancreatic duct	Secretion	(Marsey & Winpenny,

	epithelial cells		2009)
	Airway/intestinal epithelium	Secretion	(Duta *et al.*, 2004; Kunzelmann *et al.*, 2007; Kunzelmann *et al.*, 2009)
hBest2	Kidney, bronchial epithelium	Secretion, membrane conductance	(Tsunenari *et al.*, 2003; Qu & Hartzell, 2008; Milenkovic *et al.*, 2009)
	Non-pigmented ciliary epithelium	Secretion/fluid regulation	(Zhang *et al.*, 2010)
hBest3	Skeletal muscle	Cell Signalling ?	(Stöhr *et al.*, 2002)
	Testis and retina		(Tsunenari *et al.*, 2003)
hBest4	Airway epithelium	Membrane conductance	(Milenkovic *et al.*, 2009)
	Testis and brain		(Tsunenari *et al.*, 2003)
	Kidney and ovary membrane (cell lines)		(Tsunenari *et al.*, 2006)

Table 1.5: Key references human bestrophin 1-4 (hBest1-4): Table to summarise some of the key references used to formulate the discussion for human bestrophin 1-4 (hBest1-4), with tissue expression and postulated function identified within the literature

Protein Identity	**Tissue expression of gene**	**Key role**	**References**
mBest1	Retinal pigment epithelium	Volume regulation	(Bakall *et al.*, 2003; Marmorstein *et al.*, 2006; Neussert *et al.*, 2010)
	Trachea	Secretion	(Barro-Soria *et al.*, 2008; Barro-Soria *et al.*, 2009)
	Renal collecting duct	Ion channel regulation, cell proliferation	(Aldehni *et al.*, 2009; Barro-Soria *et al.*, 2009; O'Driscoll *et al.*, 2009)
	Dorsal root ganglia, brain	Ion channel regulation	(Boudes *et al.*, 2009; Park *et al.*, 2009)
mBest2	Trachea	Secretion	(Barro-Soria *et al.*, 2008)
	Nasal, eye, colon epithelia, trachea, brain, lung and kidney	Secretion	(Bakall *et al.*, 2008; Zhang *et al.*, 2009)
	Olfactory sensory neurons	?	(Pifferi *et al.*, 2006; Pifferi *et*

			al., 2009b)
	Colon	Secretion	(Yu *et al.*, 2010)
	Salivary glands	Secretion	(Srivastava *et al.*, 2008)
mBest3	Heart	Ion conductance	(O'Driscoll *et al.*, 2008; Srivastava *et al.*, 2008)
	Parotid gland	?	(Srivastava *et al.*, 2008)
	Vascular smooth muscle	Conductance	(Qu *et al.*, 2010)

Table 1.6: Key references mouse bestrophin 1-3 (mBest1-3): Table to summarise some of the key references used to formulate the discussion for mouse bestrophin 1-3 (mBest1-3), with tissue expression and postulated function identified within the literature

Protein Identity	Tissue expression of gene	Key role	References
Drosophila Best1	? derived from cell line *drosophila S2*	Ion transport	(Chien *et al.*, 2006; Chien & Hartzell, 2007)
Drosophila Best2		Ion transport	(Chien *et al.*, 2006)
Drosophila Best3		Ion transport	(Chien *et al.*, 2006)
Drosophila Best4		Ion transport	(Chien *et al.*, 2006)
Canine Best1	Retinal pigment epithelium	Volume regulation	(Guziewicz *et al.*, 2007)
Rat Best1	Retinal pigment epithelium	Volume regulation	(Rosenthal *et al.*, 2005)
Rat Best2	Olfactory epithelial	Cell differentiation and proliferation	(Klimmeck *et al.*, 2009)
Rat Best3	Vascular smooth muscle	Ion transport	(Matchkov *et al.*, 2008)
Xenopus Best1	Embryo	Embryogenesis	(Qu *et al.*, 2003; Onuma *et al.*, 2009)
Xenopus Best2	Embryo	Embryogenesis	(Qu *et al.*, 2003; Onuma *et al.*, 2009)
Porcine Best1	Eye	Ion regulation	(Stanton *et al.*, 2006)

Table 1.7: Key references multi-species Bestrophins: Table to summarise some of the key references used to formulate the discussion for drosophila, canine, rat, xenopus and porcine bestrophins, with tissue expression and postulated function identified within the literature

Protein Identity	Tissue expression of gene	Key role	References
ClC-0	Ubiquitous	Chloride ion regulation, regulation of membrane potential	(Pusch *et al.*, 1995; Middleton *et al.*, 1996; Ludewig *et al.*, 1997; Bykova *et al.*, 2006; Engh *et al.*, 2007)
ClC-1	Skeletal muscle	Voltage stabilization	(Steinmeyer *et al.*, 1991; Steinmeyer *et al.*, 1994; Fahlke *et al.*, 1996; Fahlke *et al.*, 1997a; Fahlke *et al.*, 1997b; Fahlke *et al.*, 1998; Rychkov *et al.*, 1998)
ClC-2	Ubiquitous	Volume regulation	(Jentsch *et al.*, 1995)
	T cells, B cells, neutrophils and myeloid cells	Activation, cell volume and shape regulation	(Jiang *et al.*, 2002)
ClC-3	Brain, kidney, skeletal muscle, retina, lung	Ion regulator	(Duan *et al.*, 1997)
	Neutrophils	Activation	(Moreland *et al.*, 2006; Moreland *et al.*, 2007; Davis-Volk *et al.*, 2008)
	T cells, B cells, neutrophils and myeloid cells	Activation, cell volume and shape regulation	(Jiang *et al.*, 2002)
ClC-4	Brain, heart,	Ion	(Picollo & Pusch, 2005)

	skeletal muscle	regulation/antiporter	
	B cells, neutrophils	Activation, cell volume and shape regulation	(Jiang *et al.*, 2002)
ClC-5	Kidney, myeloid cells	Chloride ion regulation, cell cycle progression	(Jiang *et al.*, 2004; Picollo & Pusch, 2005)
	T cells, B cells,	Activation, cell volume and shape regulation	(Jiang *et al.*, 2002)
ClC-6	Ubiquitous	Volume regulation, stabilization of membrane potential	(Eggermont *et al.*, 1997; Neagoe *et al.*, 2010)
ClC-7	Kidney, testis, skeletal muscle, brain, bone	Ion regulation/antiporter	(Kornak *et al.*, 2001; Wartosch *et al.*, 2009)
ClC-Ka	Kidney	Fluid regulation in urine, chloride ion regulation	(Markovic & Dutzler, 2007; Picollo *et al.*, 2007; Zifarelli *et al.*, 2010)
ClC-Kb	Ubiquitous	Volume regulation	(Jeck *et al.*, 2000; Picollo *et al.*, 2007)

Table 1.8: Key references human ClC family: Table to summarise some of the key references used to formulate the discussion for human ClC-0-7, ClC-Ka and ClC-Kb, with tissue expression and postulated function identified within the literature

Protein Identity	Tissue expression of gene	Key role	References
mANO1	Oesophagus, bladder, breast	Epithelial secretion	(Rock *et al.*, 2007)
	Epithelial cells; eye, inner ear, blood vessel walls, olfactory nerves, lung	Secretion, action potential generation, smooth muscle contraction, chloride conductance, apoptosis, cell proliferation	(Schroeder *et al.*, 2008; Yang *et al.*, 2008; Almaça *et al.*, 2009; Gritli-Linde *et al.*, 2009; Schreiber *et al.*, 2010)
	Trachea smooth muscle and epithelia	Embryonic development of trachea	(Rock *et al.*, 2008; Huang *et al.*, 2009)
mANO2	Epithelial cells	Chloride conductance	(Schroeder *et al.*, 2008; Pifferi *et al.*, 2009a)
	Neuronal and muscle tissue	Chloride conductance	(Schreiber *et al.*, 2010)
mANO3	Neuronal and muscle tissue, eye, cartilage and bone	?	(Gritli-Linde *et al.*, 2009; Schreiber *et al.*, 2010)
mANO4	Neuronal and muscle tissue	?	(Schreiber *et al.*, 2010)
mANO5	Neuronal and muscle tissue	?	(Schreiber *et al.*, 2010)
mANO6	Epithelial tissue	Chloride conductance and secretion	(Schreiber *et al.*, 2010)

	Neuronal, eye, olfactory neurons, mouth, cartilage, bone, skin, teeth	Chloride conductance and secretion	(Gritli-Linde *et al.*, 2009)
mANO7	Epithelial tissues	Chloride conductance	(Schreiber *et al.*, 2010)
mANO8	Epithelial tissues	?	(Schreiber *et al.*, 2010)
	Neuronal tissues, eye, ear, olfactory and nasal epithelia, mouth, cartilage, bone, skin, teeth	?	(Gritli-Linde *et al.*, 2009)
mANO9	Epithelial tissues	?	(Schreiber *et al.*, 2010)
	Neuronal tissues, eye, ear, olfactory and nasal epithelia, mouth, cartilage, bone, skin, teeth	?	(Gritli-Linde *et al.*, 2009)
mANO10	Epithelial tissue	?	(Schreiber *et al.*, 2010)

Table 1.9: Key references mouse anoctamin 1-10 (mANO 1-10) (also known as TMEM16) family: Table to summarise some of the key references used to formulate the discussion for mouse ANO1-10, with tissue expression and postulated function identified within the literature

1.1.3 Potential molecular candidates for chloride ion channels in granulocytes

1.1.3.1 ClC

This small conductance gene family currently consists of ten members; ClC-0, ClC-1-7, ClC-Ka and ClC-Kb (Jentsch *et al.*, 2002; Suzuki *et al.*, 2006; Cheng *et al.*, 2008; Jentsch, 2008). The structure of these proteins has been reported to be similar across the members, having between 10-12 TMDs, a transmembrane transport domain and a soluble regulatory domain (Dutzler, 2006). Despite the structural similarities, these proteins have a variety of functions which appear dependent upon three main variables. These being the primary function, either as a Cl^- channel or a Cl^-/H^+ antiporter (Dutzler, 2006; Matulef & Maduke, 2007), their cellular position (either intravesicular or within the cell membrane) or the tissue location (Jentsch, 2008). There also appears to be some differences across the family members with regard to their regulation. ClCs can be either voltage or volume gated (Jentsch *et al.*, 2002; Suzuki *et al.*, 2006) and fast gated acting on an individual pore, or slow gated also known as common gating (Jentsch *et al.*, 2002; Bykova *et al.*, 2006). All of these factors impact upon the perceived function of each member.

The ClC family have classically been considered as voltage gated Cl^- channels (Jentsch *et al.*, 2002; Moreland *et al.*, 2006; Suzuki *et al.*, 2006) however, ClC-2 and ClC-3 have been identified as volume gated Cl^- channels (Duta *et al.*, 2006; Suzuki *et al.*, 2006). Jentsch *et al* (2002) have suggested that members ClC-0, ClC-1, ClC-2, ClC-Ka and –Kb are membrane bound whereas all other members are located within

intracellular organelles, namely lysosomal vesicles (Jentsch *et al.*, 2005; Mummery *et al.*, 2005; Cheng *et al.*, 2008). It has been suggested that those within intracellular vesicles have a clear role in regulating pH within lysosomes, and are in fact not classical Cl^- channels but Cl^-/H^+ antiporters (Jentsch *et al.*, 2005; Picollo & Pusch, 2005). This is supported by Iyer *et al* (2002), however their focus was on bacteria. This must be considered cautiously in relation to human tissues due to the differences in molecular structure between vertebrates and bacteria (Chen, 2005).

1.1.3.2 CFTR

The cystic fibrosis transmembrane conductance regulator (CFTR) has been implicated in the pathology of cystic fibrosis (CF) (Boucher, 2007; Bangel *et al.*, 2008; Moran & Zegarra-Moran, 2008). CFTR is considered a cAMP activated channel as activation of the channel can only occur when protein kinase A is stimulated. This causes an increase in intracellular cAMP (Jentsch *et al.*, 2002; Boucher, 2007). While they are considered a member of the ATP-Binding Cassette (ABC) family, they have also been discovered to be a Cl^- channel in their own right (Schwiebert *et al.*, 1999; Sheppard & Welsh, 1999; Suzuki *et al.*, 2006; Moran & Zegarra-Moran, 2008). The location of these channels has been identified as primarily the apical lung epithelia (Yoshimura *et al.*, 1991), pancreatic ducts (Bubien, 2001; Sanz *et al.*, 2010), colon (Ntimbane *et al.*, 2009), and cardiac muscle (Horowitz *et al.*, 1993). There has also been evidence to suggest CFTR in lymphocytes (Krauss *et al.*, 1992; Lepple-Wienhues *et al.*, 2001) and more specifically, neutrophils (Painter *et al.*, 2006; Painter *et al.*, 2010).

Dysfunction of the CFTR channel in inflammatory airways causes a decrease in Cl^- secretion into the airway lumen. As a result, there is decreased fluid movement resulting in classical clinical symptoms of CF. Primarily the increased viscosity of mucus within airways and increased infection (Jentsch *et al.*, 2002; Mummery *et al.*, 2005; Suzuki *et al.*, 2006; Boucher, 2007; Döring & Gulbins, 2009). It has also been suggested that CFTR dysfunction can regulate other ion channels such as outwardly rectifying Cl^- channels (Jentsch *et al.*, 2002) and epithelial Na^+ channels (ENaC).

It has been hypothesised that CFTR inhibits Na^+ absorption through ENaC which in CF is compromised by depletion of the CFTR gene. In this instance, there is hyper-absoprtion of Na^+ through ENaC and reduction in Cl^- secretion via CFTR which alters the balance of fluid movement across the apical membrane of airway cells. Hyper-abosorption of Na^+ further increases airway dehydration (Jentsch *et al.*, 2005; Suzuki *et al.*, 2006; Boucher, 2007). Boucher (2007) supports this citing a study using CF mice whereby increased Na^+ absorption due to absence of CFTR increased pro-inflammatory cytokine release from airway epithelia (Terheggen-Lagro *et al.*, 2005). This in turn may lead to increased migration of neutrophils and the neutrophilia observed in CF lungs. Freedman *et al* (2002) however has shown in CFTR knockout mice that neutrophil levels were not different from wild type mice suggesting that CFTR mediated cytokine release may not impact upon migration. Murine models of CFTR should be considered with caution when applying to human cells as there is markedly less CFTR in healthy murine tissue and some differences in phenotypes (Bangel *et al.*, 2008). The suggestions here however are tentatively supported by clinical trials in humans.

Human studies examining bronchoalveolar lavage have demonstrated increased IL-8 in CF airways compared to non-CF airways (Khan *et al.*, 1995; Bonfield *et al.*, 1999). It has been suggested that this is a direct result of CFTR dysfunction and directly correlates with neutrophil migration (Chmiel *et al.*, 2002). The migration of neutrophils is increased due to cytokine secretion from airway epithelial cells, as a result of imbalanced ion transport.

1.1.3.3 CLCA

The CLCA gene family was first discovered in 1995 (Cunningham *et al.*, 1995) and since then, has been the focus of many articles trying to elucidate the structure and function of the family members (Britton *et al.*, 2002; Leblanc *et al.*, 2005; Patel *et al.*, 2009; Winpenny *et al.*, 2009). There are several isoforms of CLCA including; 4 human (hCLCA1-4), 6 murine (mCLCA1-6), 5 rat (Piirsoo *et al.*, 2009), 2 porcine (pCLCA1-2) and 2 bovine (bCLCA1-2) (Elble *et al.*, 1997; Loewen & Forsyth, 2005). In addition, Anton et al (2005) reported the first equine CLCA (eCLCA1) which has a similar homolog to hCLCA1 and mCLCA3. And more recently, the Kanehisa Laboratories (2009) have examined eCLCA2.

The human CLCA homologues have a distinct and differential pattern of tissue expression (Loewen & Forsyth, 2005; Patel *et al.*, 2009). This may be related to the genomic organization. hCLCA1-4 genes have cDNA sequence identities from 52% to 92% and are found in chromosome 1 (1p31-22) and run consecutively (Gruber & Pauli, 1999a; Pauli *et al.*, 2000; Loewen & Forsyth, 2005). These are ordered with hCLCA2 being the most 5', hCLCA1, hCLCA4 and hCLCA3 as most 3' in the gene cluster loci (Patel *et al.*, 2009; Piirsoo *et al.*, 2009). One mechanism of temporal

gene expression control is thought to be by such gene clustering. It has been argued however that the clustering of the CLCA genes has no regulatory significance (Gruber & Pauli, 1999a).

The protein level of CLCA expression remains unclear however each isoform has a different structure and function (Loewen & Forsyth, 2005). With the exception of hCLCA3, the human CLCA homologues have a precursor translation protein product of approximately 125 kDa. This is product is then thought to cleave, via a proteolytic cleavage site, to subunits of approximately 90 kDa of N-terminal product and 35kDa of C-terminal product (Gruber & Pauli, 1999b; Pauli *et al.*, 2000; Patel *et al.*, 2009). In contrast, hCLCA3 has a premature stop codon and a shorter protein product (approximately 37kDa) (Gruber & Pauli, 1999b). A common feature of all the human CLCA homologues is that they have a protein-protein interaction domain known as the von Willebrand factor type A (VWA). This is found directly adjacent to the N-terminal however the structure of this differes in each isoform (Abdel-Ghany *et al.*, 2001; Patel *et al.*, 2009). hCLCA2 VWA contains a β4-integrin binding site whereas the other isoforms bind proteins using a highly conserved set of five residues (metal ion-dependent adhesion site) (Loewen & Forsyth, 2005; Patel *et al.*, 2009).

In addition to differences in tissue gene expression, protein size, and VWA domains, there are differences in the structure of the four human homologues and how they cleave. Both N-terminal and C-terminal products of hCLCA1, along with full length protein, have been found secreted into media when expressed in human cell lines (Gibson *et al.*, 2005; Mundhenk *et al.*, 2006). In contrast, hCLCA2 C-terminal protein products remain membrane bound, secreting the N-terminal product

(Elble *et al.*, 2006; Pawlowski *et al.*, 2006). hCLCA3 has been considered to be completely secreted whilst hCLCA4, similar to hCLCA2, maintains a membrane bound C-terminus (Patel *et al.*, 2009; Plog *et al.*, 2012).

The prediction of transmembrane domain (TMD) number for each human CLCA isoform differs. hCLCA1 has several potential models. One suggests that there are four TMDs however and alternative suggestion is that there is only one (Pauli *et al.*, 2000; Loewen & Forsyth, 2005). hCLCA1 was also considered to possess 5 TMDs (Suzuki *et al.*, 2006). This was in contrast previous studies suggesting that hydropathy analysis of hCLCA1 discovered 4 TMDs (Gruber *et al.*, 1998). Hamann *et al* (2009) have alternatively stated that there are no transmembrane domains evident at all for CLCA proteins (Gibson *et al.*, 2005). hCLCA2 however, is considered to have five TMDs. In contrast, the hCLCA3 contains two internal stop codons which create open reading frames coding for two sequences. One stop codon in hCLCA3 terminates the polypeptide sequence before any potential TMDs, therefore producing a secreted hCLCA3 product. The second open reading frame codes a second polypeptide which lacks a signal peptide (Gruber & Pauli, 1999b; Loewen & Forsyth, 2005; Patel *et al.*, 2009). To date, there is limited evidence on the structure of hCLCA4. Experimental data using porcine and murine orthologs (pCLCA4a and mCLCA6 respectively) suggest that hCLCA4 also secretes the N-terminal and that the C-terminal product is bound to the cell membrane by at least one TMD (Plog *et al.*, 2012).

Whilst there are similarities in the structure of each CLCA isoform, the differences between them may impact upon potential functions. As their name suggests, these proteins were originally considered to be Ca^{2+} activated Cl^- channels (Gruber & Pauli, 1999b; Britton *et al.*, 2002).

Greenwood and Leblanc (2007) however state that the evidence for this is weak as there is disparity between properties of Ca^{2+} activated Cl^- channels and CLCAs.

As discussed, some CLCA isoforms have been considered secretory proteins which exit a cell and re-binds externally (hCLCA1 and hCLCA3), whereas others cleave the N-terminal portion and maintain a cell membrane bound product with TMDs (Gruber & Pauli, 1999b; Jentsch *et al.*, 2002). In one study, Gibson *et al* (2005) used bioinformatics analysis which differs from previous studies using hydrophobicity analysis. They found that the N-terminal cleavage products of hCLCA1 were found in the broncho-alveolar lavage fluid of patients with asthma where hCLCA1 is strongly up-regulated in airway epithelia and goblet cells (Rogers, 2003; Tyner *et al.*, 2006). This further supports the hypothesis that it is a secreted protein. However, all isoforms have been shown to possess protein-protein binding sites (VWA) (Loewen & Forsyth, 2005; Patel *et al.*, 2009). These would bind to alternative chloride ion channels. CLCA proteins have therefore been considered regulators of functional aspects of some ion channels, and the expression of endogenous Cl^- channels within cell membranes (Loewen *et al.*, 2002a; Gibson *et al.*, 2005; Leblanc *et al.*, 2005; Suzuki *et al.*, 2006; Greenwood & Leblanc, 2007).

CLCAs have been implicated in cell-cell adhesion in carcinoma and as a tumor suppressor (Pauli *et al.*, 2000; Piirsoo *et al.*, 2009). That CLCAs have a role in Cl^- channel conductance also appears well established in that an increase in CLCA expression leads to an increase in Cl^- conductance and efflux (Britton *et al.*, 2002; Loewen *et al.*, 2002a; Gibson *et al.*, 2005; Loewen & Forsyth, 2005; Hamann *et al.*, 2009). It should be

noted however that the evidence appears to come from a variety of CLCA members and so application across the group should be considered with caution.

The role of CLCA in chloride conductance remains unclear and appears reliant upon whether it is secreted or cleaved leaving a membrane bound portion (Loewen & Forsyth, 2005; Pawlowski *et al.*, 2006; Piirsoo *et al.*, 2009). It has been shown that on addition of a Ca^{2+} ionophore (ionomycin) CLCA proteins were activated. This produced an outwardly rectifying current, as examined under patch clamping, which was inhibited by a chloride conductance inhibitor (DIDS) (Cunningham *et al.*, 1995; Gruber *et al.*, 1998). This was supported with a later murine study of mCLCA5 (homologue of hCLCA2) and mCLCA6 (homologue hCLCA4) which showed that ionomycin stimulated a current in HEK293 transfected cells, that had a reversal potential that was correlated to the equilibrium potential for chloride. This was not found in cells that weren't transfected with mCLCA5 or mCLCA6, or mock transfected (Evans *et al.*, 2004). Whilst this contributes evidence that they are involved in Ca^{2+} activated chloride conductance, the method remains unclear. Secreted proteins hCLCA1 and hCLCA3 may modulate this by activation of an alternative Ca^{2+} activated chloride channel. For CLCAs with membrane bound portions, the protein-protein binding site may bind to alternative channels. It has been suggested that this is due to the metal ion-dependent adhesion site in the VWA binding calcium in CLCA proteins, which in turn alter the conductivity of other chloride ion channels (Loewen & Forsyth, 2005). It has been argued however that hCLCA3 may not have any biological function (Loewen & Forsyth, 2005).

There remains difficulty in clearly defining the structure of CLCAs, and mapping channel activity to sequences for CLCAs. Therefore, functional role of CLCAs remains contentious (Pawlowski *et al.*, 2006). There is mounting evidence to suggest a role for the CLCA family of proteins in Ca^{2+} chloride conductance but not as a channel directly transporting chloride in itself. CLCA proteins may indirectly be involved in chloride conductance, therefore, by interacting with alternative calcium activated chloride channels in a potential signalling capacity (Loewen & Forsyth, 2005; Pawlowski *et al.*, 2006; Patel *et al.*, 2009).

The CLCA1 gene has been considered to be asthma specific in airway epithelial cells (Lloyd & Saglani, 2010). This was demonstrated in both murine and human models whereby mCLCA3 and hCLCA1 respectively were up-regulated in response to Th2 cytokines simulating asthma (Zhou *et al.*, 2001). More recently, IL-13 has been shown to up-regulate mCLCA3 which supports this (Nakano *et al.*, 2006). It appears that the role of hCLCA1 in asthma and inflammatory airway diseases is mucus production (Izuhara *et al.*, 2009). Overexpression of hCLCA1 leads to hyperplasia of airway goblet cells and mucus hyper secretion (Rogers, 2003) via increased Cl^- efflux, and therefore fluid movement following osmotic gradients (Gruber & Pauli, 1999b; Gibson *et al.*, 2005). This was supported by a study using rats whereby niflumic acid directly affected mucous production by blocking CLCA1 (Hegab *et al.*, 2007).

Anton *et al* (2005) also suggest that blocking hCLCA1 can decrease airway inflammation in these pathophysiologies and use equine CLCA clones as a model. It appears unclear however, as to whether there are local effects on epithelial cells, a decrease in migration of granulocytes, or whether there are actions of granulocytes themselves. Equine studies are

also not considered a strong model for use in human asthma or COPD due to the environmental effects of stabling, such as dust irritation. There appears no published evidence supporting the expression of CLCA proteins in granulocytes. However, Anton et al (2005) suggest that mCLCA3 (which is of a similar isoform to hCLCA1) acidifies mucin granule content of goblet cells (Gibson *et al.*, 2005). If a similar relationship were apparent in granulocytes, there may be both intracellular and extracellular responses. Theses responses include release of inflammatory cytokines and granule content, resulting in respiratory burst and airway inflammation (Gibson *et al.*, 2005).

hCLCA1 may also be implicated in cell maturation, which could be applicable to granulocytes. The findings of Loewen and Forsyth (2005) support this claiming that mCLCA3 increases Cl^- conductance to balance H^+-ATPase processes. This restores electrical neutrality following granule acidification in cell maturation processes. Again it should be noted that this is speculative as no published evidence supports expression of CLCA in granulocytes. There are clear indications that further studies are needed, particularly structural and functional studies to elucidate the role of CLCAs in granulocyte function.

1.1.3.4 Bestrophin

Bestrophin is a protein that was discovered in 2002 (Sun *et al.*, 2002). There are four homologues in humans; hBest1-4. It has also been described in animals, including mice, Gram negative bacteria and some fungi (Hagen *et al.*, 2005). Bestrophin proteins are considered Ca^{2+} activated Cl^- channels regardless of their locality (Suzuki *et al.*, 2006; Greenwood & Leblanc, 2007; Kunzelmann *et al.*, 2007; Barro-Soria *et al.*,

2010). That they are Cl^- channels is supported by Leblanc *et al* (2005) who suggest that they are sensitive to the specific Cl^- channel blocker DIDS (4,4'-diisothiocyanatostilbene-2,2'-disulphonic acid) (Barro-Soria *et al.*, 2010). Unlike CLCA proteins, there also appears consensus that they are membrane bound, having 4-6TMDs (Leblanc *et al.*, 2005; Greenwood & Leblanc, 2007).

These proteins appear to be self-regulating. Qu et al (2006) found in their study that bestrophins have a C-terminus that regulates their activity (Hagen *et al.*, 2005; Qiang *et al.*, 2007). While this seems to support an independent role for bestrophin, Kunzelmann et al (2007) have suggested that a Cl^- selective filter has been found only on the second TMD. They postulated that bestrophins may therefore work in a complementary relationship with another protein. It has been suggested that CLCA and bestrophin may be complementary partners in Ca^{2+} activated Cl^- channels and resultant Cl^- movement (Loewen & Forsyth, 2005). In a recent study (Barro-Soria *et al.*, 2010), it was demonstrated however, that human bestrophin1 did not appear on the membrane of epithelial cells, but presented evidence that it localises to the endoplasmic reticulum (Kunzelmann *et al.*, 2009). In these cells, bestrophin1 assists intracellular calcium signalling and was linked to activation of TMEM16A (anoctamin1), an alternate Ca^{2+} activated Cl^- channel.

Bestrophins have been linked to the pathology of Best's disease, macular dystrophy of the retina. This is due to dysfunction of the bestrophin Cl^- channel and fluid shifts following osmotic gradients (Duta *et al.*, 2004; Qu *et al.*, 2004; Chien *et al.*, 2006). It has also been shown that hBest1 is permeable to HCO_3^- which directly causes fluid shift in disease processes (Qu & Hartzell, 2008). While this is linked to the retina, the movement of

fluid may have functional implications for granulocytes. Fluid movement particularly impacts cell volume regulation implicated in migration to areas of inflammation, and suggests that bestrophins are dual activated by both Ca^{2+} and cell volume (Chien & Hartzell, 2007). The evidence presented for bestrophin1 in retinal pigment epithelium cells has been questioned as electro-physical properties of such are not altered by mutations of bestrophin 1 and in knock-out mice, ocular pathology is not evident (Kunzelmann *et al.*, 2009). If the hypothesis of bestrophin1 implication in retinal fluid movement can be proven, it may also be suggested to play an important role in the production of mucus in inflammatory airways (Duta *et al.*, 2004; Barro-Soria *et al.*, 2010). Unfortunately however, there appears no published evidence supporting the presence of bestrophin in granulocytes.

There appears a need, therefore, for further examination into the expression of bestrophin, potentially coupled with other proteins such as CLCA, in granulocytes, and discussion as to their function in humans.

1.1.3.5 TMEM16A and tweety (hTTYH3) as potential candidates

While the above outline the major candidates for Cl^- channels in granulocytes, it must be acknowledged that there are some putative Cl^- channels which may be considered in the future. Due to the apparent lack of evidence either for Cl^- channels in granulocytes, or hTTYH3 and TMEM16A, it remains difficult to relate these to either eosinophils, neutrophils or basophils. They may however be potential candidates for Cl^- channels in need of further investigation.

Tweety was originally discovered as the flightless gene in flies (Suzuki *et al.*, 2006) but has however been identified as having human homologs (Suzuki, 2006). One of these is the human tweety, hTTYH3, which is a large conductance Ca^{2+} -activated Cl^- channel, and also a cell volume regulated channel. Suzuki (2006) suggests that by investigating this particular protein, we may gain more information about other channels, particularly those involved in the maintenance of body fluid volumes. In addition, it seems an appropriate candidate to explore for granulocyte roles, such as cell shape and size regulation during inflammatory migration.

Another potential target for investigation is TMEM16A, also referred to as Anoctamin1 (ANO1). TMEM16A was identified by three groups (Caputo *et al.*, 2008; Schroeder *et al.*, 2008; Yang *et al.*, 2008). This has been identified as one of 10 homologues in a family of proteins (Kunzelmann *et al.*, 2009; Schreiber *et al.*, 2010). Schroeder *et al* (2008) highlight this family of proteins, stating that they are found within the cell membrane of *Xenopus* oocytes, however that function is currently unknown. They hypothesise from their studies that they are Ca^{2+} activated Cl^- channels responsible for stabilising membrane potentials. They may also be present on the membranes of intracellular organelles (Rock *et al.*, 2008), which if present in granulocytes, may impact upon the inflammatory response and respiratory burst, particularly in chronic airway diseases. It has been argued recently that whilst ANO1 itself acts as a Cl^- channel, the structure and properties of the homologous group will vary according to tissue and cell site. Indeed, the structure for ANO1-8 has been predicted and suggests that these homologues may function as chloride ion channels. ANO9 and 10 structure and function remains unpredicted (Kunzelmann *et al.*, 2009). There is clear evidence

(Schreiber *et al.*, 2010) for ANO1 in airway epithelial cells in mice, and mice lacking in ANO1 display a general defect in epithelial electrolyte transport. Electrolyte transport has a direct impact upon the movement of fluid across epithelial cells. This influences the consistency of mucus in airway cells particularly, and mice lacking ANO1 will mimic the pathology of cystic fibrosis in that mucus becomes thick and clearance is reduced (Rock *et al.*, 2008; Kunzelmann *et al.*, 2009; Schreiber *et al.*, 2010). It has been shown in laboratory experiments that ANO1 null mice have a decrease in mucocilliary clearance (Kunzelmann *et al.*, 2009).

Anoctamins 1, 6-10 have been found predominantly in epithelial cells however ANO2-ANO5 have been found in neuronal and muscle tissues (Schreiber *et al.*, 2010). This may further impact upon the symptoms of chronic inflammatory lung disease, due to failure of smooth muscle contraction (Kunzelmann *et al.*, 2009).

This supports the role of ANO1 in chloride conductance and particularly the implications for mucus clearance in inflammatory lung diseases. As yet, the presence of this protein has not been described in human granulocytes.

1.1.3.6 CLIC

The first chloride intracellular channel (CLIC) was characterised in bovine kidney cortex (Redhead *et al.*, 1992; Landry *et al.*, 1993) and named p64. The human homologue, NCC27, was later cloned in a myelomonocytic cell line and localised to the cell nucleus (Valenzuela *et al.*, 1997). This was named CLIC1. Conversely, it was later shown using immunofluorescent microscopy that CLIC1 is present throughout the

cytoplasm of cells (Berryman & Bretscher, 2000), and is also an integral membrane protein (Tonini *et al.*, 2000). Therefore, CLIC1 can be one of two structures; soluble globular protein or integral membrane protein (Littler *et al.*, 2010). CLIC1, with the other members of the CLIC family, have been described as a "metamorphic proteins" (Murzin, 2008; Littler *et al.*, 2010). This is due to their ability to form more than one stable structure. CLIC1 can be either a soluble monomer or an oxidised dimeric state. The transition between monomer and channel involves membrane docking and insertion of the N-terminal through the phospholipids bilayer (Littler *et al.*, 2010). This reversible reaction makes function difficult to establish. Early electrophysiological studies have shown that several membrane insertions of the CLIC1 protein through the phospholipid membrane acts as a chloride ion channel (Valenzuela *et al.*, 1997; Tonini *et al.*, 2000). In support it has been shown that when CLIC1 is added to a buffer, it will insert into synthetic phospholipid bilayers (Tulk *et al.*, 2002). The function for CLIC1 is predominantly chloride transport (Berryman & Bretscher, 2000).

CLIC2 was first identified as a protein of 243 amino acids (Heiss & Poustka, 1997). It has been shown in similar electrophysiological studies that this also integrates phospholipid membranes and is therefore considered a chloride ion channel structure which creates a loop in the C-terminal allowing possible recognition of neighbouring proteins (Cromer *et al.*, 2007). The postulated function of CLIC2 is linked directly to this structural feature. It has been suggested that CLIC2 may have a role in the suppression of Ca^{2+} release intracellularly (Board *et al.*, 2004; Littler *et al.*, 2010).

As CLIC1, the later identified CLIC3 has also been primarily localised in the nucleus of cells (Qian *et al.*, 1999). Qian et al (1999) suggest that the CLIC family of proteins are not themselves chloride channels as they lack the ability to span the membrane. However, they may modulate chloride channel activity. It was shown that the COOH-terminal tail of CLIC3 reacts with mitogen-activated protein (MAP) kinases and so may be involved in cell growth regulation (Qian *et al.*, 1999).

It has been shown that CLIC4 acts as an ion channel (Chuang *et al.*, 1999). It has been considered that the transmembrane domain at the N-terminus may assist in the insertion of CLIC4 into the phospholipid membrane (Singh & Ashley, 2007). The selectivity of this channel, however, is poor and there has been suggestion that is may not be an exclusive anion channel but may also transport cations such as potassium (Singh & Ashley, 2007; Singh *et al.*, 2007; Littler *et al.*, 2010). Like CLIC1, CLIC4 appeared to be diffuse throughout the cytoplasm of human placenta (Berryman & Bretscher, 2000). However, in human kidney cells, CLIC4 has been found predominantly in the apical membrane and endoplasmic reticulum (Edwards, 1999; Littler *et al.*, 2010). The variance in locality may have implications for the functions of CLIC4. It has been implicated in the biogenesis of some neuropeptides, secondary to changes in Cl^- permeability either directly as a channel, or as a channel regulator (Chuang *et al.*, 1999). They may also have an important role in the formation of collateral arterial circulation through angiogenesis (Littler *et al.*, 2010).

CLIC5 was identified in 2000 using placental microvilli (Berryman & Bretscher, 2000). It has been shown that CLIC5, like CLIC1 and CLIC4 will integrate phospholipid membranes and act as a non-selective ion

channel (Singh & Ashley, 2007; Singh *et al.*, 2007). There is strong evidence to suggest that CLIC5 may have an important function within muscle cells. Berryman and Bretscher (2000) demonstrated through expressional analysis that CLIC5 was expressed at higher levels in skeletal muscle and heart tissue. They used biochemical fractionation and immuno-labelling to show that sub-cellular distribution of CLIC5 was at the apical membrane of polarised epithelial cells. Within muscle cells, CLIC5 may have an important functional role as it interacts directly with the actin cytoskeleton and so may be acting as a scaffolding protein (Littler *et al.*, 2010).

The human homologue CLIC6 was first cloned in 2003 (Friedli *et al.*, 2003). This followed from the rabbit orthologue, Parchorin, which was expressed in the cytosol primarily but also identified in the apical membrane of gastric glands (Nishizawa *et al.*, 2000). In contrast to the other members of the CLIC family, human CLIC6 possesses a long N-terminal end, and is the largest member with 704 amino acid residues (Friedli *et al.*, 2003). As yet, whether CLIC6 functions as a chloride channel is yet to be confirmed (Friedli *et al.*, 2003; Griffon *et al.*, 2003). It was shown that it localises to the plasma membrane however Griffon et al did not demonstrate any changes to chloride conductance in HEK293 transfected cells (Griffon *et al.*, 2003).

1.1.4 Evidence for Cl^- channel candidates in granulocytes

1.1.4.1 Volume gated Cl^- channels

Volume gated Cl^- channels are activated when there is an increase in the tension of cellular plasma membrane (Suzuki *et al.*, 2006). This process allows the regulation of both Cl^- and K^+, and therefore the transport of fluid across the cell membrane. The dysfunction of these channels have been implicated in mice with degraded retina, and the presence of large conductance volume regulated Cl^- channel has been well documented in renal cells (Suzuki *et al.*, 2006). It has been suggested in a recent review (Salmon & Ahluwalia, 2009) that neutrophils may contain a swell activated chloride ion channel. This channel may be stimulated in activated neutrophils in order to counteract the phagocyte, NADPH oxidase, generated depolarisation. This may provide a link between neutrophils, inflammatory responses in airways and chloride ion channels in humans. However, the evidence to support the role of swell activated chloride ion channels in either granulocytes or in inflammatory airway diseases remains limited. The reason may be a lack of clarity surrounding the molecular candidates for such channels, or that they have currently not been clearly identified in many cell types, making research into structure and function problematic (Jentsch *et al.*, 2002; Suzuki *et al.*, 2006). Despite this, it has been suggested that volume gated anion channels, through control over cell volume, have a role to play in cellular differentiation and apoptosis (Zholos *et al.*, 2005). While this may have a direct impact upon granulocytes, this is not clarified.

Ducharme *et al* (2007) supports the role of volume gated channels in the control of cell volume and continues to suggest that ClC-2, ClC-3 and Bestrophin 1-4 have been identified as protein candidates. These were identified, however, in the neurological immune cells, microglia. In this instance, volume gated channels were implicated in cellular migration, as a response to chemotactic stimuli. This was, however, in murine samples. The question remains, therefore, can this be applied to either humans, or granulocytes?

The molecular candidates implicated in granulocytes, particularly eosinophils are shown in the earlier findings of Schwingshackl *et al* (2000). In this study, CFTR, ClC-2, ClC-3, ClC-4, ClC-5 and ClC-6 were identified using reverse transcriptase polymerase chain reaction (RT-PCR). It was demonstrated that the only proteins studied that were expressed in eosinophils were ClC-3. An advantage of this study was that they used asthmatic patients and so would account for any up-regulation of genes during inflammatory processes in the airways. Their conclusions, however, support the role of Cl^- channels in eosinophils, with respect to regulation of cellular volume. This is implicated in the process of cellular migration, as eosinophils need to decrease their volume for extravasation and infiltration into inflamed tissues (Schwingshackl *et al.*, 2000; Agrawal *et al.*, 2008).

It has been suggested that Cl^- ion channels involved in volume regulation have an essential role in phagocytotic functions and cellular migration (Cheng *et al.*, 2008). This is because they govern cell shape changes (Moreland *et al.*, 2006). These Cl^- channels must, in which case, be membrane bound to facilitate transmembrane transport of water and salts (Moreland *et al.*, 2006; Jentsch, 2008).

Controversially, it has been shown that ClC-3 was directly linked to phagocytosis and respiratory burst activity (Moreland *et al.*, 2006). The release of superoxides and perpetuation of inflammatory tissue damage is a further result of this process. Moreland *et al* (2006) have shown that ClC-3 is located in secretory vesicles. In this study, they showed that ClC-3 knockout mice demonstrated a decrease in NADPH oxidase function. Therefore, a decrease in neutrophil respiratory burst. It may be suggested that in addition to a role in pH regulation of such vesicles, stimulation of these may trigger membrane bound channels that are involved in fluid transport, and therefore cell shape changing. They also demonstrated that by decreasing anion activity, migration of neutrophils decreased. It should be noted that experiments were on mice and therefore application to humans should be considered cautiously. To further strengthen their argument, however, supporting the role of ClC-3 in neutrophil action, they found that the mice used in their experiment died of sepsis when ClC-3 was inhibited, in contrast to the control mice who did not. They suggested that this was due to the blocked anion channel decreasing NADPH oxidase activity. It has been shown, however, that tamoxifen, a swell activated chloride channel inhibitor, decreased respiratory burst but that in neutrophils, it did not inhibit swell activated chloride conductance (Ahluwalia, 2008). This suggests that there may be alternative modulation of chloride channels. For example, extracellular pH may have an important role in regulation of ClC-3 rather than swell activation.

Other members of the ClC gene family are not clearly linked to granulocytes however this appears to be due to a lack of performed experiments, rather than suggesting there is no function in these cells.

The observed role of this family is to regulate electrical excitability, maintain transepithelial water and salt transport and maintenance of intracellular organelle pH (Dutzler *et al.*, 2002; Bykova *et al.*, 2006; Cheng *et al.*, 2008). Differing ClC members have been found in specific target organs. For example, those involved in the renal disease processes Bartter syndrome and Dent's disease are suggested to be ClC-Ka and ClC-5 respectively and can be found in kidney cells (Dutzler *et al.*, 2002; Suzuki *et al.*, 2006; Jentsch, 2008). A role for ClC-K in the defence against inflammatory airway diseases has also been suggested (Mummery *et al.*, 2005). Using the human model for sub-mucosal gland cells, Calu-3, Mummery *et al* (2005) demonstrated that ClC-K compensated for dysfunction of the CFTR Cl^- channel by increasing Cl^- conductance. This may indicate that as yet, functions for members of the ClC family are not entirely known and suggests the need for further experimentation, with particular reference to granulocytes and their function.

1.1.4.2 Voltage gated Cl^- channels

Greenwood and Leblanc (2007), Jentsch *et al* (2002) and Suzuki *et al* (2006) have suggested that voltage gated Cl- channels are encoded by the ClC gene family, specifically ClC-1. This is of specific relevance in skeletal muscle as these membrane bound Cl^- channels are responsible for the regulation of cellular electrical excitability (Jentsch *et al.*, 2002). In this process, resting membrane potential is stabilised by an influx of Cl^- to counteract the influx of Na^+ or Ca^{2+}.

Secondly, Cl^- ion channels can lead to an excitatory response in alternative cells, such as smooth muscle where the electrochemical potential for chloride is higher than the resting potential. In this instance

the opening of Cl^- drives chloride outward and the membrane to an excitatory depolarisation voltage of -20mV (Suzuki *et al.*, 2006). In this instance, open Cl^- channels cause an increase of intracellular Ca^{2+}, as a response to a second messenger system which may drive depolarisation. The result is an increase in vascular tone (Jentsch *et al.*, 2002). This raises the question as to how these channels may impact upon granulocyte function; are they excitatory or a stabilizing agent? If voltage gated Cl^- channels are excitatory in granulocytes, this may result in some of the inflammatory processes outlined above.

Simchowitz *et al* (1993) have suggested that, in neutrophils, Cl^- channels are opened in response to chemotaxis, and as a result the membrane depolarizes which may support the hypothesis of excitation in granulocytes. In contrast, Krause and Welsh (1990) argue that while membrane depolarization is an excitable response in many cells (i.e. skeletal), in neutrophils, this is an inhibitory effect. They suggest that a negative feedback mechanism occurs where there is a reduction in production of oxygen radicals, and a decrease in the release of granules. While this examines whether membrane depolarization is excitatory or inhibitory, it does not clarify the role of voltage regulated channels in this process. In one early study, three ion channels were identified in neutrophils; voltage gated K^+ channels, and Ca^{2+} activated K^+ and Cl^- channels (Krause & Welsh, 1990). This study, however, used blood samples from healthy donors only and so may not account for up-regulation of proteins during inflammation, such as in asthma, COPD or CF. In contrast, Schwingshackl *et al* (2000), suggested that in response to Cl^- channel stimulation, eosinophils are activated. As a result of eosinophil activation, there is a release of superoxides, respiratory burst, and a release of toxins (Femling *et al.*, 2006). In their experiment, they

demonstrated that Cl^- flux was blocked by the application of anti-asthmatic drugs. Schwingshackl *et al* (2000) also implicate ClC-3 as the Cl^- channel responsible for respiratory burst in eosinophils. Their samples were taken from asthmatic subjects which allows clearer application to Cl^- channels in granulocyte function, focused upon airway inflammatory diseases. In a similar study using human T lymphocytes, application of 4,4'-diisothiocyanatostilbene-2,2'-disulphonic acid (DIDS) and 5-nitro-2-(3-phenylpropylamino) benzoic acid (NPPB) inhibited cell signalling and activation (Phipps *et al.*, 1996). This was also demonstrated in an earlier study using B lymphocytes (McCann *et al.*, 1990). This study used the mouse model to block chloride ion channels and measure single channel conductance. This supports the role of chloride ion channels in the activation of lymphocytes and so may support a similar role in granulocytes.

In contrast however, Agrawal et al (2008) showed that activation of Cl^- channels decreased eosinophil activation in their research using human asthmatic subjects. This suggests that depolarisation has an inhibitory effect. In this study, an anti-asthmatic drug currently used in Japan (suplatast tonsilate) was applied and the effects upon chemotaxis, migration and respiratory burst recorded. This was done with and without the presence of Cl^- channel blockers, including; DIDS, anthracene-9-carboxylic acid (9AC), gadolinium chloride, *R*(+)-[(6,7-dichloro-2-cyclopentyl-2,3-dihydro-2-methyl-1-oxo-1H-inden-5yl)-oxy] acetic acid 94 (IAA94), and NPPB. This was in order to establish the relationship between eosinophil action and Cl^- channels. These contrasting studies add further confusion, however studies of eosinophil Cl^- channel function remain problematic as molecular candidates remain

largely unknown (Agrawal *et al.*, 2008). To elucidate these, may provide a target for treatment in asthma.

In contrast, it has been shown that volume sensitive chloride channels in the plasma membrane are responsible for whole cell conductance of chloride (Ross *et al.*, 1994; Lepple-Wienhues *et al.*, 1998). Alternatively lymphocytes may have a cAMP dependent Cl^- ion channel. It has been shown using peripheral blood samples from CF patients that this chloride channel may be similar to that found in the epithelial airway cells and dysfunction may lead to some of the symptoms in this disease (Chen *et al.*, 1989; Bubien *et al.*, 1990). In a replicate study this was not supported (Hagiwara *et al.*, 1989) however this may be due to density of the chloride channel or phase of cell cycle. This may account for the difficulties in obtaining data from granulocytes. Wang et al (2006) further examined lymphocytes and chloride channels. In this study they found that, by blocking chloride channels with DIDS in conjunction with the inhibitor of calcium entry SK&F 96365, there was a significant reduction in ClC-3 mRNA. This was in comparison with either blocking agents being applied alone. This suggests that the lymphocyte chloride channels may be calcium activated. Further elucidation of structure and function of chloride ion channels is required to postulate a role in granulocytes.

1.1.4.3 Calcium-activated Cl^- channels

Despite having identified gene families for CaCC channels, Suzuki *et al* (2006) claims that the structure and function of these channels remains unclear. Therefore, the role of these channels is difficult to assess in relation to granulocytes. There appears to be a role for these such as in cellular migration, or maturation, particularly in neutrophils, (Krause &

Welsh, 1990). Tintinger *et al* (2005) also suggest that prior to onset of inflammatory processes in neutrophils (superoxide production, degranulation, adhesion and synthesis of IL-8), there is an increase in cytosolic Ca^{2+}. The relationship between this and Cl^- channel stimulation is not discussed however it supports the hypothesis that Cl^- channels may have a role within neutrophil function.

1.1.4.4 cAMP-activated channels

CFTR has been identified in lymphocytes and neutrophils (Painter *et al.*, 2006; Painter *et al.*, 2010). In neutrophils, is has been shown that in CF defective cells, the transport of chloride is decreased, and therefore the bactericidal properties of neutrophils is reduced (Painter *et al.*, 2006). This was shown using immunofluorescence staining, reverse transcriptase polymerase chain reaction and immunoblotting. Painter *et al* (2010) claims that chloride is essential in phagosomal function, activation of neutrophils and infection defence (Jacquot *et al.*, 2008). Activation of neutrophils in CF lung is known to cause inflammatory responses. This is due to production of proteases and reactive oxygen species resulting in a reduction of mucociliary bacterial clearance (Jacquot *et al.*, 2008).

Figure 1.6 presents a diagrammatical summary of postulated chloride channel functions.

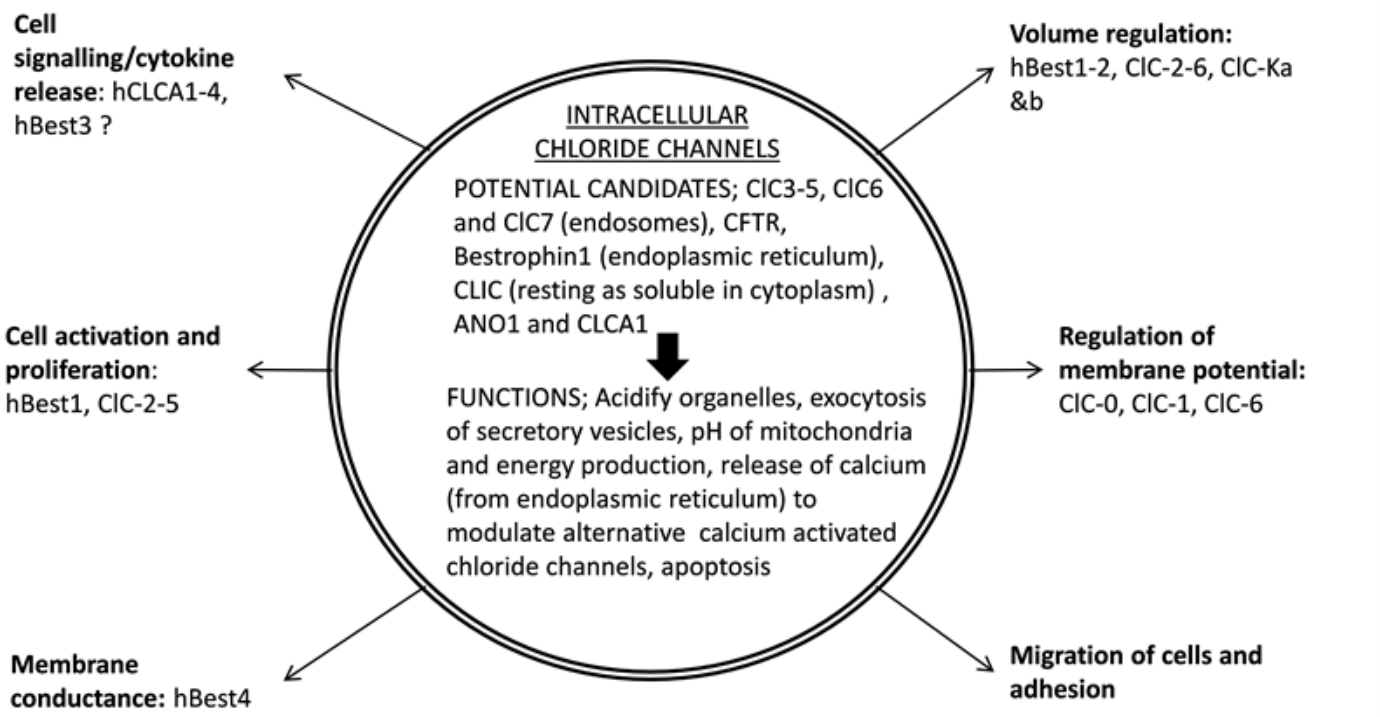

Figure 1.6: Diagrammatical summary of postulated chloride channel functions. The functions of chloride channels within cells may be dependent upon cell type and localisation within the cell. This figure presents a summary of overall postulated functions of chloride ion channels, adapted from Cheng *et al* (2008)

1.1.5 Summarising remarks; Cl^- channels and granulocyte function

The evidence presented appears to implicate granulocytes in inflammatory processes, which can be applied to airway pathologies such as asthma and COPD. However, the recruitment and roles of each granulocyte subtype is not often presented with absolute clarity or application to human airway diseases. By examining the role of chloride channels within granulocyte function the function of granulocytes may become more evident.

The role of Cl^- channels has been discussed, in order to firstly; elucidate the role of granulocytes in chronic inflammatory lung diseases, and secondly; to identify potential molecular candidates for such channels.

What remains consistent is the need for further research in all of these areas, particularly linking to human granulocytes. If the molecular proteins for Cl^- channels on granulocytes could be clearly identified, an in-depth analysis of their structure and function within specific cells could ensue. This in turn would add evidence supporting the role of Cl^- channels within granulocytes, and ultimately, clarify how these cells may first be stimulated, attracted, and act in response to inflammatory airway diseases.

In summary, there is a clearly identified need to discover which Cl^- channel protein and gene families are present in granulocytes.

1.2 Hypothesis and rationale

The evidence is clear that granulocytes have a role to play in chronic inflammatory lung diseases, such as COPD and asthma. The lung pathology of these diseases differs with differing clinical manifestations. This may be due to differing cells involved in the inflammatory process, such as agranulocytes, or granulocytes. That white blood cells migrate to inflammatory tissues is clearly documented however there appears to be little evidence to identify which chloride ion channels are up-regulated, if at all, in granulocytes. If up-regulation of a specific chloride ion channel is evident, then there needs to be further clarity as to the potential role of this in granulocytes in chronic inflammatory lung diseases.

The aim of this project is to elucidate potential candidates for chloride ion channels in granulocytes. A second aim is to provisionally explore the potential role of human bestrophin 1 in granulocyte function.

Human bestrophin 1 has been selected as a focus for experimental work as one of the potential candidates for chloride ion channels. The discussion presented within the introduction has identified that chloride ion channels are implicated in the function of granulocytes particularly through cell volume regulation, activation and proliferation of cells, cell signalling through cytokine release and regulation of alternative ion channels (see figure 1.6) (Agrawal *et al.*, 2008; Cheng *et al.*, 2008). It has also been shown that prior to the recruitment and activation of pro-inflammatory processes in specifically neutrophils, there is a significant increase in cytosolic calcium (Tintinger *et al.*, 2005). This suggests that chloride ion channels in granulocytes may be calcium activated, of which human bestrophin 1 is a prime candidate (Kunzelmann *et al.*, 2007;

Barro-Soria *et al.*, 2010). Anoctamin 1 is also considered a calcium activated chloride ion channel (Schroeder *et al.*, 2008) however it has been shown that hBest1 may modulate its activity (Barro-Soria *et al.*, 2010). This further suggests that hBest1 requires focus. As stated, there are a number of chloride ion channels which may prove candidates for chloride ion channels in granulocytes. hBest1, however, also appears to be commonly implicated with the key functions associated with chloride ion channels in granulocytes (Cheng *et al.*, 2008) (figure 1.6).

Experimental aims will be drawn together and applied to inflammatory lung diseases following a systematic review of the evidence for up-regulation of chloride ion channels in inflammatory lung diseases.

It is hypothesized that chloride ion channels, specifically focussed upon human Bestrophin 1, are up-regulated in granulocytes during inflammatory lung disease processes. It is suggested that up-regulation impacts upon the functional role of granulocytes and are a novel therapeutic target in the management of symptoms in these disease processes. hBest1 may modulate activity and regulation of alternative channels such as hANO1. Additionally, hBest1 may have a role in granulocyte volume regulation through fluid shifts. It is hypothesised that changes in cell volume and shape will directly impact upon cellular migration and activation. hBest1 up-regulation may have therapeutic inflammatory effects such as allowing phagocytosis through cell shape modulation. Alternatively however, up-regulation of hBest1 in granulocytes over a prolonged period of time may cause tissue damage. In this instance, hBest1 may be implicated in respiratory burst, airway fibrosis and airway hyper-responsiveness. The evidence suggests a

positive correlation between granulocyte accumulation in COPD and asthma, and exacerbation of symptoms.

It is hypothesised therefore, that hBest1 is implicated in the role of granulocytes in chronic inflammatory lung dieases. It is hypothesised that hBest1 is a novel therapeutic target for pharmacological interventions in chronic inflammatory lung diseases, for the control and management of symptoms. It is acknowledged, however, that there are a number of targets which require investigation, and that hBest1 is among them.

CHAPTER 2: MATERIALS AND METHODS

2.1 Cell and tissue culture

2.1.1 Commercial cell lines

2.1.1.1 EoL-1 cell line

The commercial human eosinophilic leukaemia cell line (EoL-1) was supplied by the Health Protection Agency Culture Collections (HPACC), United Kingdom. The country of origin being Japan. Cells are non-adherent and were suspended in RPMI 1640 with 4mM L-glutamine (Invitrogen, UK) supplemented with 10% foetal bovine serum (BioSera, East Sussex, UK), 100 IU/ml penicillin and 100 mg/ml streptomycin, and cultured in a T75 flask. Cultures were incubated at 37^{o}C in humidified 5% CO_2. Concentration of cells was maintained between 5 x 10^5 cells/ml and 1 x 10^6 cells/ml according to HPACC recommendations, and at approximately 60-80% confluence. Concentration was established by using trypan blue solution (Sigma-Aldrich, UK) (section 2.1.1.5). EoL-1 cells were re-suspended according to concentration and confluence by centrifuging at 150 relative centrifugal force (RCF) for 8 minutes at 4 ^{o}C to pellet cells and re-suspending in media as outlined above.

2.1.1.2 dEoL-1

EoL-1 cells in media (as in 2.1.1.1) were split into T25 flasks and re-suspended to 5 x 10^5 cells/ml. N^6, 2'-0-dibutyryladenosine 3':5'-cyclic monophosphate sodium (dbcAMP, Sigma, UK), was diluted with deionised water (dH_2O) to 100mg/ml, alliquoted and stored at -20 ^{o}C according to manufacturer instructions. 250 µl (25mg) of dibutyryl cAMP was added to each flask. Cells were cultured for 9 days with re-stimulation with

dbcAMP and readjustment of cell numbers to 5 x 10^5 cells/ml every 3 days. After day 9, cells were examined under microscopy to establish differentiation and therefore dEoL-1 cells.

2.1.1.3 HL60 cells

HL60 cells were obtained from Dr Dietmar Steverding (Norwich Medical School, UEA). HL60 cells are a commercial human promyelocytic leukaemia cell used as a model for human polymorphonuclear cells (PMNs). HL60 cells are also non-adherent and suspended in media. They were cultured using the same method as the EoL1 cells. Cells were seeded into a T75 flask in RPMI 1640 with 4mM L-glutamine (Invitrogen, UK) supplemented with 20% foetal bovine serum (FBS) (BioSera, East Sussex, UK), 100 IU/ml penicillin and 100 µg/ml streptomycin. FBS was increased to 20% to improve culture growth. Cultures were incubated at 37^{o}C in humidified 5% CO_2. The concentration of cells was maintained between 5 x 10^5 cells/ml and 1 x 10^6 cells/ml according to HPACC recommendations for culture, and at approximately 60-80% confluence.

2.1.1.4 Epithelial cells

A variety of commercially available cells have been used including A549 (derived from human alveolar basal epithelial tumours), SAEC (primary non-cancerous small airway epithelial cells), NAEC (nasal epithelial cell line), Calu-3 (human sub-mucosal cell line), CHO (Chinese hamster ovary), Vero-SG (kidney from the African green monkey), HEK293 (human embryonic kidney) and CFPAC (cystic fibrosis pancreatic duct

adenocarcinoma cell). These have been used in order to act as a control for PMN data and also for transfection of purified bestrophin cDNA.

Each of the epithelial cell lines were cultured in either T25 or T75 flasks with the appropriate media (Table 2.1). Media for each cell line was supplemented with 10% foetal calf serum, 100 IU/ml penicillin and 100 µg/ml streptomycin. All media changed 3 times per week (supplied by Invitrogen, UK). Cells were incubated at $37^{O}C$ in 5% CO_2 and grown to $1x10^5$ cells/cm^2.

Cell line	**Media**
A549	Dulbeccos Modified Eagles Media (DMEM) with 4mM L-glutamine (Invitrogen, UK)
SAEC	Bronchial Epithelial Basal Media (Lonza Walkersville, Switzerland)
NAEC	Bronchial Epithelial Basal Media (Lonza Walkersville, Switzerland)
Calu-3	DMEM with 4mM L-glutamine (Invitrogen, UK)
CHO	Minimum Essential Medium Eagle with 4mM L-glutamine (Invitrogen, UK)
Vero-SG	DMEM glutamax (Invitrogen, UK)
HEK293	DMEM with 4mM L-glutamine (Invitrogen, UK)
CFPAC	DMEM with 4mM L-glutamine (Invitrogen, UK)

Table 2.1: Culture media used for each epithelial cell line:
Epithelial cell lines used and the recommended culture media for growth. Information for growth media from cell providers and HPACC recommendations

2.1.1.5 Trypan and kimura staining

To establish cell viability, and to calculate cellular concentration, cells were stained with trypan blue (Sigma Aldrich, UK). Cells were stained at a dilution factor of 2. This was 10µl trypan with 10µl cell solution. Stained cells were applied to the plate of a haemocytometer and visualised under 40x magnification.

Stained cells were visualised and any blebbing of the cell, or excess blue staining was noted and these cells were not considered viable. Viable cells were visualised as bright, clear cells which were consistently uniform in shape. The viable cells were counted in four large squares of the haemocytometer field and an average number of cells per large haemocytometer square calculated (N). To convert the observed cell count into a calculation of cells/ml the following calculation was used

$$\text{Cells/ml} = N \times 10^4 \times \text{dilution factor}$$

This concentration was used to resuspend cells as appropriate for experimentation or tissue culture.

Kimura staining was used to differentiate PMNs. This was used at a concentration of 1:10 where 10µl cell suspension was added to 90µl kimura stain. Eosinophils cytoplasm stained green, whereas monocytes and neutrophils did not.

2.1.2 Primary cells

2.1.2.1 Peripheral blood and PMN purification

Peripheral blood was harvested by trained phlebotomists from healthy human donors following informed consent. Ethics approval for the study had been obtained from the Faculty of Health Ethics Committee (Appendix 1 for letter of approval). Polymorphonuclear cells were purified using dextran sedimentation and percol density gradient separation, with lysis steps to remove remaining red blood cells. Protocol outlined in figure 2.1

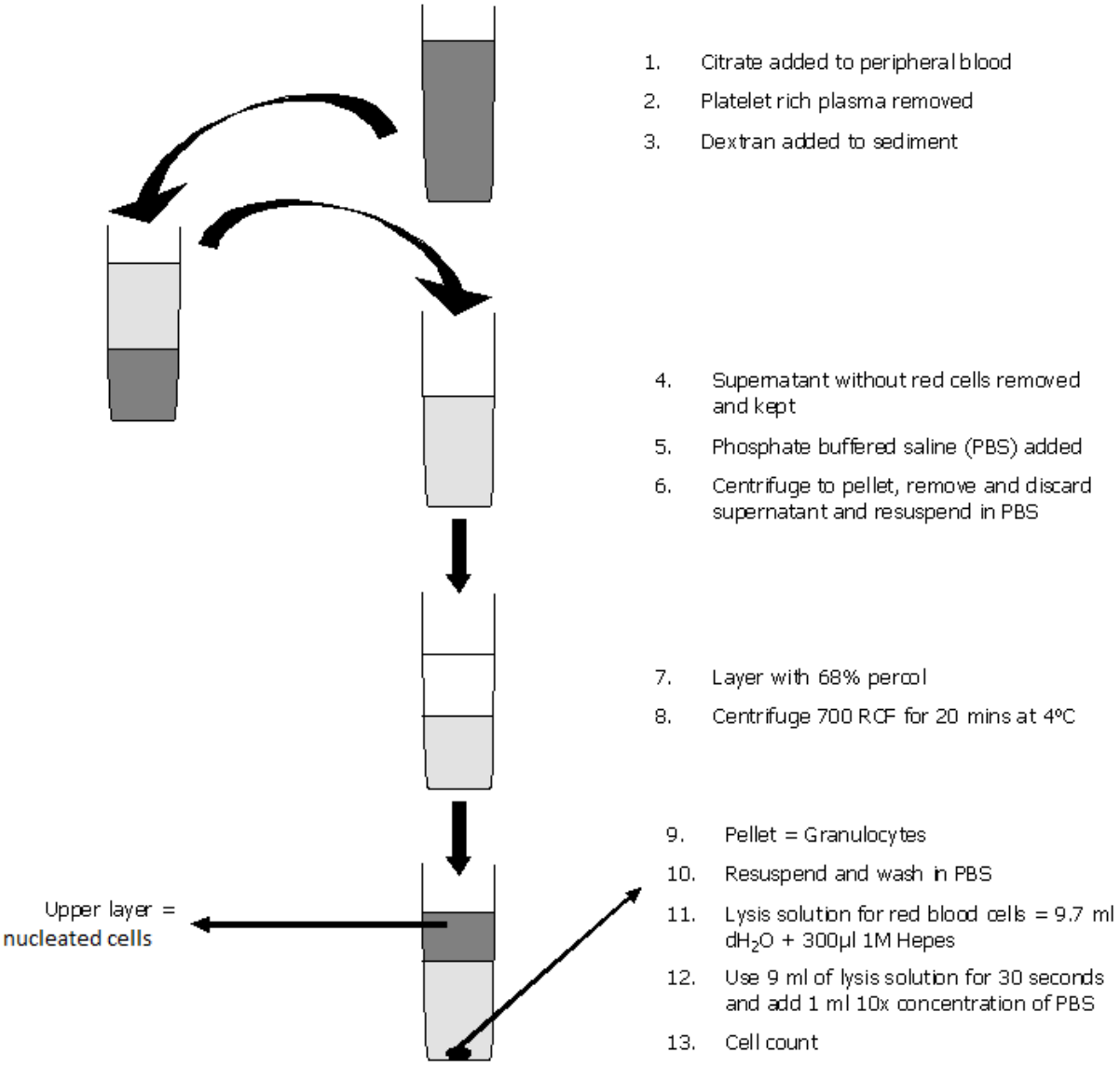

Figure 2.1: Protocol for preparation of peripheral blood: Protocol for purification of PMNs from whole blood using dextran sedimentation techniques. Dextran is added to whole blood to sediment red blood cells and supernatant removed for further processing. Sample centrifuged and pellet resuspended in phosphate buffered saline (PBS). Percol added and further centrifuge to pellet PMNs. PBS and Hepes supplied by Invitrogen, UK

40ml of harvested peripheral blood was added to 4ml of sodium citrate tribasic as an anticoagulant. This was centrifuged, without brake, at 350 RCF, 21 ^{o}C, for 20 minutes. Serum was aspirated from the top of the sample and discarded. Remaining cells were re-suspended to 40ml in PBS with gentle agitation of cell pellet. 10ml of 6% dextran was added to the 40ml sample, mixed and allowed to sediment for removal of red blood cells. The sample was incubated for 30 minutes at room temperature. Following this, the supernatant (upper layer) was removed and kept, red blood cells isolated with dextran sedimentation discarded. Supernatant contained nucleated cells and some contaminating red blood cells. These cells were centrifuged to form a pellet (350 RCF for 6 min at 21 ^{o}C) and washed with PBS. Supernatant was removed to leave 5-10ml and the pellet which was then re-suspended in the remaining supernatant. 10ml of 69% percoll was added to falcon tubes and equal volumes of the suspension layered on top of this. The sample was centrifuged at 700 RCF for 20 minutes at 21 ^{o}C to force the PMNs through the percoll to the bottom of the tube, leaving an upper monocyte layer which was removed and discarded. The percoll supernatant was then removed and the PMN pellet washed with PBS as per previously described wash step. In order to lyse contaminating red blood cells, a hypotonic shock solution (9.7ml deionised water with 300µl of 1M Hepes buffer solution) was prepared and 9ml added to the cell pellet and incubated at room temperature for 30 seconds. 1ml of 10 times concentrated PBS was added to make the solution isotonic and avoid lysis of PMNs.

In order to purify the PMN population, negative selection of eosinophils from neutrophils was used. This technique was used throughout all blood preparation as the isolated neutrophils had minimal eosinophil

contamination. Contamination of eosinophils was considered by RT-PCR (section 2.3). The signal for mixed PMNs was much brighter than those for purified eosinophils for any commonly detected band (ie hBest1 and hBest3). It was deduced therefore that the weaker signal for any eosinophils would not create a false positive where there may not have been mRNA in PMNs. In this instance, mixed PMNs were considered over 90% neutrophils and any contamination minimal. This was not considered significant to impact upon the results for mixed PMNs. Human CD16 purified antibody (Invitrogen, UK) was applied to the cells and the sample added to a membrane column using a magnetic field to filter neutrophils which were labelled with beaded CD16. CD16 is more prevalent in neutrophils however there is some present in eosinophils. To ensure maximal purification, cells were distinguished morphologically under light microscopy at 60x magnification (see figure 1.1 for DAPI stained images) using DAPI, and 40x magnification using kimura staining. No monocyte contamination was observed on differential counts. The sample was cell counted using trypan staining and haemocytometer techniques as described above.

2.1.3 Microscopy for cellular morphology

Cells were trypan stained using the method outlined in 2.1.1.5 and visualized under a light microscope at 40 x magnification to establish cell viability. Morphological changes, such as blebbing, indicated that cells were not viable. Cell suspensions were cytospun onto Superfrost microscope slides by readjusting cell concentration to 1 x 10^6 cells/ml and adding 50-100µl of cell suspension to each chamber in the Shandon Double Cytofunnel (Thermo Electron Corp, Cheshire, UK). Each chamber was clamped to the glass slide and cytospun at 500 RCF for 5 minutes. Cells were either fixed prior to, or following, cytospinning using 4% paraformaldehyde (PFA) for 15 minutes, protected from light, at 4 ^oC. To establish nuclear morphology, DAPI dihydrochloride nucleic acid stain was used. DAPI (Invitrogen, UK) 10mg vial of dry powder was reconstituted with 2ml dH_2O to yield a 5mg/ml stock solution. This was alloquoted to 50µl and stored at -20 ^oC until required. For use, stock DAPI solution was diluted to 1:2000 with PBS and 10-20µl applied to the surface of the slide over the area of cells. Slides were incubated for 15 minutes at room temperature, protected from light. Following incubation, DAPI was removed and the surface of the slide rinsed with non-sterile PBS three times. The cell area was then covered with Fluoromount-G (SouthernBiotech, Birmingham, UK) for fluorescence and 22mm^2 cover slips were applied. Slides were left to set at 4 ^oC, protected from light, for 30 minutes and the cover slips were fixed. Prepared slides stored at 4 ^oC until required.

Cells that were immunolabelled were cytospun directly onto glass slides and fixed and mounted as per above.

Immunolabelled and DAPI stained slides were examined using fluorescent microscopy on AxioCam©. The microscope was prepared as per manufacturer instructions. Microscope slides were oil submerged and visualized under 60x magnification using appropriate filters for staining; Blue for DAPI stained, GFP for immunolabelled with either Alexafluor 488 or FITC (see table 2.3). For PMNs or EoL-1 and dEoL-1 cells, images captured using multidimensional acquisition and "z-stacking" appropriate to measured cell sizes.

2.1.4 Cytokine stimulation

Granulocytes (PMNs) and purified eosinophils were washed and resuspended in fresh media at a concentration of $1x10^6$ cells/ml. 1 ml aliquots were placed in 24 well plates. Cytokines (IL-4, IL-5 and IL-13) were added to the appropriate wells at a final concentration of 10ng/ml for each cytokine. Plates were incubated at 37^0C, 5% CO_2 humidified air for either 24 or 48 hours according to the defined time course. Following incubation, cells were washed in PBS and resuspended in lysis buffer for RT-PCR analysis or in staining buffers for flow cytometry (Sections 2.2.1 and 2.3.1). All cytokine stimulations were performed under sterile conditions.

2.2 RNA expression and DNA sub-cloning

2.2.1 Reverse transcriptase polymerase chain reactions

2.2.1.1 Preparation of mRNA

mRNA was prepared using two methods; TRIzol® preparation and cell lysate preparation for smaller cell yields.

2.2.1.1.1 TRIzol® preparation of mRNA

Cells were centrifuged at 200 RCF, room temperature, for 2.5 minutes and washed using PBS (as described previously). 800µl TRIzol® (Invitrogen, UK) was added to the cell pellet and vortex used to re-suspend. 200µl chloroform was added and repeat vortex to mix. This was incubated for 3 minutes at room temperature. To separate RNA from the organic phase, the samples were centrifuged at 13000 RCF, 4°C for 15 minutes and the upper clear RNA removed and transferred into a sterile eppendorf. The equivalent volume of isopropanol was added and repeat vortex to mix. The sample was then incubated for 10 minutes at room temperature. A repeat 15 minute centrifuge at 4°C, 13000 RCF to pellet RNA was performed and supernatant removed and discarded. 1ml 70% ethanol (made with nuclease free water) was added to the RNA pellet and gently mixed. The sample was centrifuged as described above and the ethanol supernatant removed and discarded allowing the RNA pellet to air dry. Finally, RNA was re-suspended in nuclease free water and stored at -20°C until required for use.

2.2.1.1.2 Cell lysate preparation

For smaller cell numbers, such as purified eosinophils, cell lysis buffer supplied by Signosis (Signosis Inc, California) was used according to the manufacturer's protocol. All preparations were performed on ice. Cell numbers from $1x10^4$ to $1x10^5$ were centrifuged at 200RCF at 4°C for 2.5 minutes and washed with ice cold PBS. Cells were snap frozen at -80°C after being re-suspended in 100µl ice-cold cell lysis buffer. Samples were incubated on ice for 20 minutes and then centrifuged at 4°C, 10000 RCF for 2 minutes. Supernatant was heated for 15 minutes at 75°C and stored at -20°C until required for use.

2.2.1.1.3 Analysis of concentration and purity of RNA

Samples were all analysed for purity and concentration using NanoDrop™ 2000 (Thermo Scientific). 1µl of sample was analysed by applying it directly to the pedestal of the NanoDrop™. Measurement was taken of the sample to acquire concentration in ng/µl and final concentration of sample used at 1µg per reaction.

2.2.1.2 RT-PCR reaction

Reverse transcription polymerase chain reactions were all performed using a one-step kit (One-step RT-PCR kit, Qiagen, UK). Master mix was prepared in accordance with manufacturer's handbook as per the following Table 2.2. For all RT-PCR reactions, β actin was used as a positive control. Negative controls were performed for each sample which were preparations of the master mix (Table 2.2) without addition of template RNA.

REAGENT	**CONCENTRATION**	**VOLUME PER REACTION (µl)**
Buffer (5x)	1x	5
dNTP mix	400µM of each dNTP	1
"Q" solution (5x)	1x	5
Enzyme mix	-	1
RNAse inhibitor*	5 units/reaction	2
Primer A	0.6µM	1.5
Primer B	0.6µM	1.5
RNAse free water	-	Variable
Template RNA	1µg/reaction	Variable
TOTAL VOLUME		**25µl**

Table 2.2: Master mix for one-step RT-PCR: Table showing concentration and volumes of components of the Qiagen one-step RT-PCR kit used for reactions. * RNAse inhibitor optional but used due to nature of cells (ie PMNs). RNAse inhibitor supplied by Qiagen, UK.

Primers were designed using Invitrogen OligoPerfect™ primer designer tool (Invitrogen, UK). The nucleotide sequence for each, and expected size of band in base pairs is presented in Table 2.3. Each primer pair was analysed using the primer design tool, Primer-BLAST (available via www.ncbi.nlm.nih.gov/tools/primer-blast see figure 2.2 for an example analysis using hCLCA1 KW (mid) primers). This utilises the Primer3 interface to check existing primers and to ensure that each pair of primers spanned an intron, or that at least one of the primers was located at an exon-exon junction as recommended. The purpose of this in primer design is to ensure that only cDNA is amplified during the PCR process and not genomic DNA (Ye *et al.*, 2012). All primer pairs listed in Table 2.3 spanned an intron with the exception of hBest1 (5 mid). Primer pair hBest1 (5 mid) also did not have either the sense, or antisense primer that was located at an exon-exon junction. This primer was not used for any RT-PCR. Of the other primer pairs (Table 2.3), several also had one primer located at an exon-exon junction; hCLCA1 KW (mid), hCLCA2 (b), hANO4, hANO5 and hANO6. Several primers were tested to amplify hCLCA1, hCLCA2, hCLCA3 and hBest1. These were kindly donated by Laura Marsey (Winpenny Lab, UEA, 2004); using primers identified by previous papers (Gruber *et al.*, 1998) or designed using OligoPerfect™ primer designer tool. Primers used for RT-PCR have all been analysed using Primer-BLAST (Figure 2.2 for example), and been successfully sequenced (see section 2.2.1.3.2). For all hCLCA1 reactions, primer pair hCLCA1 KW (mid) was used, for hCLCA2, primer pair hCLCA2 (b), and for hBest1, primer pair hBest1 (mid) was used.

PRIMER	ACCESSION NUMBER	BAND SIZE (bp)	SENSE	ANTISENSE
hCLCA1 JW	NM_001285.3	572	5’-gatacagtgtaaaagtgcggg-3’	5’-gtgcaatgttggatatttctg-3’
hCLCA1 KW (mid)*		322	5’-tgtccaaaatgacaggaggt-3’	5’-gatttggaggtaggccattt-3’
hCLCA1 (Gruber *et al.*, 1998)		510	5’-gaaatggagctgtctctcag-3’	5’-ctgctccattatccagtagttc-3’
hCLCA1 (3)		454	5’-gaaggggccctgagtaattc-3’	5’-cgtcaaatactccccatcgt-3’
hCLCA1 (8)		502	5’-aagcacatgggaagtgatcc-3’	5’-gatggcaccacttgtttga-3’
hCLCA2	NM_006536.5	529	5’-ctagtctttggattccaggaac-3’	5’-ctttcgctcctcctcatttc-3’
hCLCA2 (a)		370	5’-acctgccacatggaaagct-3’	5’-ctttttccaggaacggggg-3’
hCLCA2 (b)*		518	5’-gaaaggatttgaggtggttgaa-3’	5’-gctgttcctggaatccaaagac-3’
hCLCA2 (c)		424	5’-ttgacctggaagctgtaaaagt-3’	5’-acccattgctgttaaaactcct-3’
hCLCA3	NM_004921	517	5’-ctcctaatggtaatcattctc-3’	5’-gttacaatatgtatgaaccatttg-3’
hCLCA3 (a)*		508	5’-gaaaaaacacagctaggcta -3’	5’-attggcttcatggatggctt-3’

hCLCA4 (3)	NM_012128.3	481	5’-cttccatctgctctggaattaaata-3’	5’-gaaattttccattattgttccactg-3’
hBest1 (3)	NM_004183.3	407	5’-ggacatgtactggaataagccc-3’	5’-gtctgtggggcactgtagta-3’
hBest1 (5)		488	5’-gtattgcgacagctacatccag-3’	5’-atccagtcgtaggcatacaggt-3’
hBest1 (mid)*		460	5’-acctgtatgcctacgactggat-3’	5’-ctggaactccatctcctctttg-3’
hBest1 (5 mid)		312	5’-ctgtatcagaggccaggcta-3’	5’-ggttggtgattgttccaaag-3’
hBest2	NM_017682.2	420	5’-agtttgaaaacctgaactcatccta-3’	5’-agaaagttggtctcaaagtcatcat-3’
hBest3	NM_032735.2	515	5’-acaagtgacagctccatgttcttac-3’	5’-ttttagaaaggtatcaccagggtct-3’
hBest4	NM_153274.2	609	5’-tttgagacaaatcagctcatagacc-3’	5’-atccctgtcttgaactttctcttct-3’
hANO1	NM_018043.5	275	5’-tgatcttcaaggctttcctg-3’	5’-gctgcttcagcttcaggtag-3’
hANO2	NM_020373.2	208	5’-ctccggagtacatggaaatg-3’	5’-cttgccaattccagagagaa-3’
hANO3	NM_031418.2	153	5’-tgatagacctctgcctccag-3’	5’-ttttcccactgaggtatgga-3’
hANO4	NM_178826.3	202	5’-tgaatgccagcttgtctgta-3’	5’-aaaacacgaggtgctcaaag-3’
hANO5	NM_213599.2 (Transcript variant 1)	337	5’-tgggtcaccttatttttgga-3’	5’-ttgacctgctttaaggatgc-3’

hANO6	NM_001025356.2 (Transcript variant 1)	200	5’-gttttggaaccctggtcttt-3’	5’-gaatgcgttcttcttcctga-3’
hANO7	NM_001001891.3 (Transcript variant NGEP-L)	220	5’-ttcaccctcaaggtgttcat-3’	5’-acctcctgcatgttgttgat-3’
hANO8	NM_020959.2	261	5’-gtgcctcgtctgtgtcttct-3’	5’-gaggctcaggtacgagttga-3’
hANO9	NM_001012302.2	174	5’-gacgggcctcttagtctttc-3’	5’-attgtcaaagaggtgggtga-3’
hANO10	NM_018075.3	221	5’-gacagtgaagccctgaagaa-3’	5’-cgaggcaaagatcacgtact-3’
Beta Actin	NM_001101.3	456	5’-gcatcctcaccctgaagtac-3’	5’-cacgcactgtaattcctctt-3’
ClC3	NM_173872.2	259	5’-accagctacaatggctttcct-3’	5’-tccaccacgatctccattggg-3’

Table 2.3: Primers used for reverse transcription polymerase chain reactions: Table presents nucleotide sequence for primers used in RT-PCR including accession numbers (National Centre for Biotechnology Information, US, National Library of Medicine) and expected size of band in base pairs. Primers all designed using OligoPerfect^{TM} primer designer supplied by Invitrogen, UK. Primers hCLCA1 KW (mid), hCLCA2 (b), hCLCA3 (a) and hBest1 (mid) marked with * to indicate that these primers were used for experimental RT-PCR and have undergone Primer-BLAST analysis and successful sequencing (see section 2.2.1.3.2) to ensure cDNA amplification and specificity of primers.

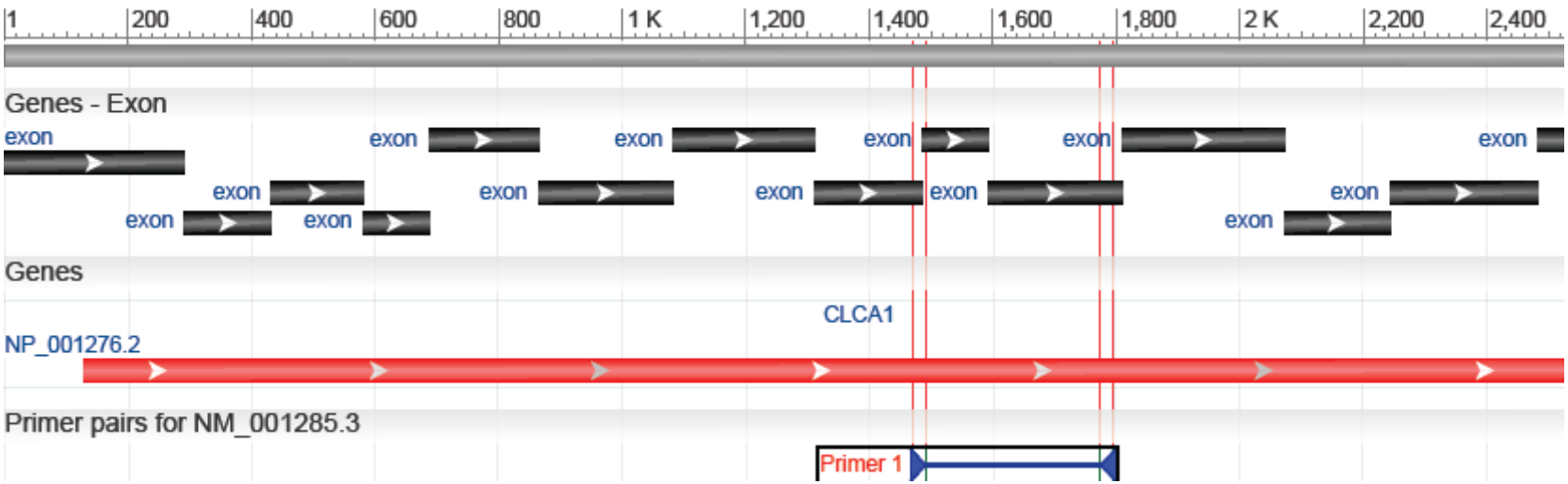

Figure 2.2: Analysis of primer pair hCLCA1 KW (mid) using Primer-BLAST: Example analysis of primers using Primer-BLAST (available via www.ncbi.nlm.nih.gov/tools/primer-blast). hCLCA1 KW (mid) primers (shown in blue) aligned against the sequence for hCLCA1 (accession number NM_001285.3) showing exon positions. Primer pairs either spanned an intron or had at least one primer per pair located at an exon-exon junction. Primers all analysed to ensure that cDNA only was amplified and not genomic DNA.

All solutions, primers and template RNA was defrosted on ice and master mix prepared as per Table 2.2. All RNA samples were analysed using NanoDrop™ (section 2.2.1.1.3) to establish concentration and purity of samples before adding to the master mix. Eppendorfs were placed into the PTC-100 Programmable Thermal Controller (MJ Research Inc.) for thermal cycling in accordance with the handbook for Qiagen One-Step RT-PCR kit, depicted in Table 2.4.

THERMAL STEP	TIME	TEMPERATURE
1. Reverse transcription	30 minutes	50 °C
2. Initial PCR activation step	15 minutes	95 °C
3-step cycling (steps 3-5 repeated total of 40 times)		
3. Denaturing	1 minute	94 °C
4. Annealing	1 minute	52 °C
5. Extension	1.5 minutes	72 °C
6. Final extension	10 minutes	72 °C
7. Maintenance and storage	Variable	4 °C

Table 2.4: Thermal cycling for RT-PCR: All thermal cycling steps for RT-PCR as per Qiagen One-Step RT-PCR handbook (Qiagen, UK)

On completion of thermal cycling, samples were prepared by adding loading buffer (Bioline, UK) at 1:5 concentration. Samples were then analysed by electrophoresis on an agarose gel, using a quantifiable molecular marker (Hyperladder ^{TM} I, Bioline, UK).

2.2.1.3 Analysis

2.2.1.3.1 Electrophoresis

Electrophoresis was performed using agarose gel and tris-borate-EDTA (TBE) buffer for a running media to separate DNA. A 1.5% agarose gel was prepared using the following protocol;

1. 50 ml TBE + 0.75 g agarose into conical flask and heat used to dissolve agarose
2. Solution cooled
3. 2µl ethidium bromide (EtBr) (Sigma, UK) added and solution poured into gel case with appropriate size comb for number of samples inserted
4. Gel allowed to set for 15 minutes

The 1.5% agarose gel was placed into an electrophoresis bath containing TBE as a running buffer. The first and last lanes contained Hyperladder^{TM} I and 10-15µl (variable dependent on size of comb used for well-size) of prepared samples were loaded into remaining wells. Controls were loaded as per section 2.2.1.2. Electrophoresis was set to run at 100V for 40-60 minutes.

On completion, the gel was removed from the TBE buffer and placed into an ultraviolet light box to visualise RT-PCR bands. The size of banding was established by comparison to the ladders loaded and considered likely to represent the anticipated DNA if comparable to expected band size (see table 2.3).

To confirm visual results, bands of DNA were excised from the agarose gel using a scalpel, and sent for sequence confirmation at the Genome Enterprise Centre (section 2.2.1.3.2).

2.2.1.3.2 Sequence confirmation

Once excised, the slice of agarose gel was prepared to purify the DNA using the QIAquick® gel extraction kit (Qiagen, UK). Figure 2.3 demonstrates the overall protocol used for this as outlined in the QIAquick® handbook. Once prepared, samples along with primers, were sent to the Genome Enterprise Centre for nucleotide sequence confirmation. These were then aligned with the nucleotide sequences available on NCBI for each gene of interest, using BioEdit software (Section 3.4, Figure 3.8 for an example of sequence alignment images produced).

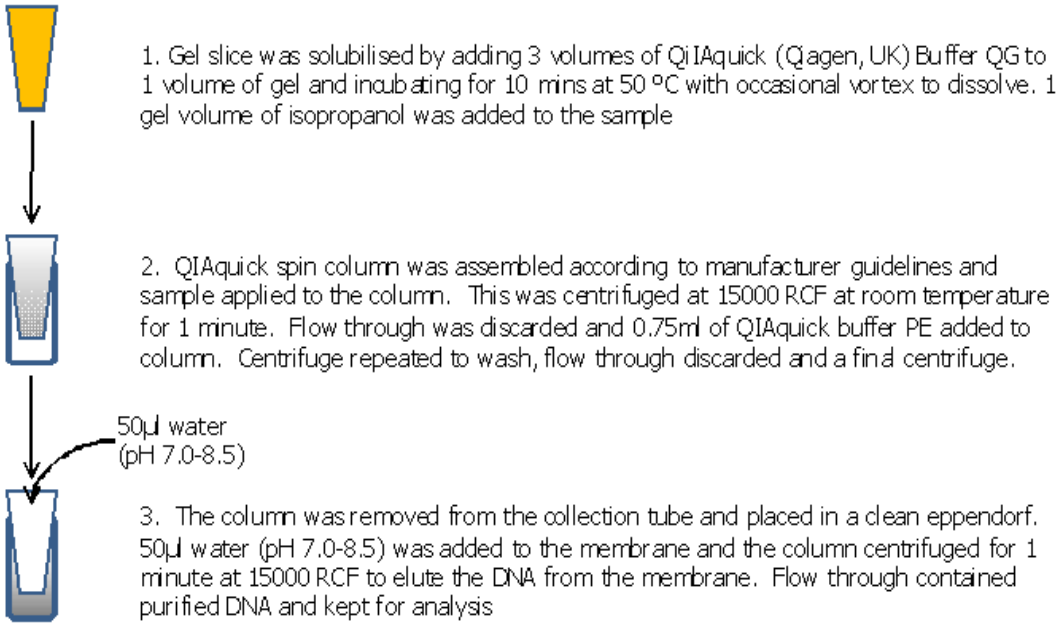

Figure 2.3: Process for DNA extraction from agarose gel slice: QIAquick gel extraction kit was used to purify DNA from an agarose gel slice. Agarose gel slice with band of interest was solubilised and applied to a spin column . DNA was eluted from the membrane. Samples were sent to the Genome Enterprise Centre for sequence confirmation

2.2.1.3.3 Semi-quantification of results

Bands visualised on RT-PCR were analysed using densitometry techniques to semi-quantify results. Statistical analysis was performed as outlined in section 2.6. Ethidium bromide gels were placed under an ultraviolet lamp to visualise bands. Images were captured onto floppy disk and then converted to bitmap images. Images were opened in ImageJ software (developed by the National Institute for Health, available via http://rsb.info.nih.gov/ij/). Using ImageJ, bands were selected and the optical density of each was recorded (as a product of the area of band in

pixels, and mean grey area as an average of the grey of all pixels in a band). Samples were normalised against the optical density for β actin;

Optical density of sample selected band / optical density of β actin

The results were statistically analysed (section 2.6) to establish potential correlations between genes expressed.

It is important to note that this process is semi-quantification and not exact quantification.

2.2.2 Sub-cloning

2.2.2.1 Transformations of plasmids into bacteria

Commercially prepared sub-clone competent cells, DH5 α *E. Coli*, were used for transformations. All competent cells and plasmids were defrosted on ice and 100ng of each plasmid containing DNA of interest was added to 50µl of cells and further incubated on ice for 30 minutes with gentle mixing.

Following incubation, cells were exposed to heat shock for 40 seconds at 42^0C and further incubated on ice for 2 minutes. Each sample was added to 500µl of LB broth and incubated for 1 hour at 37^0C. Samples were diluted to 1:10 and 100µl spread onto agar plates and incubated at 37^0C overnight until single colonies could be visualised. An individual colony was harvested and added to 250ml LB broth and incubated overnight at 37^0C. To make LB broth; 10g Tryptone, 5g yeast extract, 5g NaCl and 1g D-glucose were mixed and made up to 1000ml with dH_2O. To make agar plates, 5g agar was added to 250ml LB broth and autoclaved to dissolve. Specific antibiotics were added according to which the vector was resistant to, at a final concentration of 100µg/ml. Table 2.5 presents all vectors used and the antibiotic resistance for each.

Gene of interest	Vector	Plasmid name	Antibiotic resistance
hBest1	pRK5	pRK5-hBest1-IRES-eGFP	Ampicillin
hBest2	pRK5	pRK5-hBest2	Ampicillin
mBest2	pRK5	pRK5-mBest2	Ampicillin
hBest3	pBS	pBS-hBest3	Ampicillin
hBest4	pRK5	pRK5-hBest4-c-termRIMtag	Ampicillin

Table 2.5: Vectors used for transformations: Table presenting all vectors and plasmids used for transformation into DH5 α *E. Coli* competent cells with antibiotic resistance for selection

2.2.2.2 Purification of cDNA

Glycerol stocks of transformed bacteria were prepared by adding 800µl of LB broth containing cells, to 200µl glycerol and stored at -80^{0}C for future use. Transformed cells were then processed using a Qiagen (UK) Midi-Prep kit for purification of cDNA following manufacturer recommendations;

1. LB broth solution decanted into cornings tubes and centrifuged at 8000RCF for 15 minutes at 4^{0}C to pellet bacteria
2. 4ml of buffer P1 was added and the tube vortexed to mix
3. 4ml of buffer P2 was added and the tube vortexed to mix turning the solution blue. This was incubated at room temperature for 5 minutes

4. 4ml of chilled buffer P3 was added turning the solution white and incubated on ice for 15 minutes
5. The sample was centrifuged for 30 minutes at 20000RCF, 4^0C and supernatant pipette off and applied to equilibrated (using buffer QBT) Qiagen Filter 100 columns
6. The filter was washed with 10ml buffer QC and a repeat wash with a further 10ml allowing the run through to drain to waste
7. Filter units were placed into clean corning tubes to elute DNA by applying 5ml buffer QF
8. 3.5ml isopropanol was added to flow through to precipitate the DNA and immediately centrifuged at 15000RCF for 30 minutes at 4^0C
9. The supernatant was discarded and the DNA pellet was washed with 2ml of room temperature 70% ethanol (made with nuclease free water). The sample was re-centrifuged at 15000RCF for 10 minutes
10. The supernatant was discarded and the pellet allowed to air dry for 10 minutes
11. Cell pellet was re-suspended in 10mM Tris-Cl, pH 8.5 and stored in -80^0C

2.2.2.3 Restriction digestion

Each sub-cloned plasmid was validated by using restriction digest techniques to extract the DNA of interest, and analysis using electrophoresis on an agarose gel as outlined previously (Section 2.2.1.3) for 1.5 hours at 100V. The band identified at the correct size for bestrophin 1-4 was excised and sent for sequence analysis as outlined in

Section 2.2.1.3.2. All bands were confirmed by 100% sequence analysis. Vector maps were obtained from BD PharMingen technical data and used to establish the enzymes required to digest out the multiple cloning site (MCS) for each of the vectors used for bestrophin 1-4 transformations and sub-cloning of cDNA. 20ng of DNA was used in an eppendorf, and 1µl of the appropriate enzyme buffer (supplied with enzyme) was added. 6.5µl of H_2O was added and finally 0.5µl of each enzyme (Table 2.6). All enzymes and buffers supplied by Roche, UK. Samples were incubated for 1 hour at 37 °C in a water-bath and analysed on an agarose gel. Each sample was analysed against a control for the entire plasmid (no enzyme therefore uncut), linearized plasmid (one enzyme only added) and with cDNA cut out (both enzymes used).

Sample	Vector	Enzyme A (start of MCS)	Enzyme B (end of MCS)
pRK5-hBest1-IRES-eGFP	pRKS	Cla1	KpnI (100µg/ml BSA added as per manufacturer instruction)
pRK5-hBest2	pRKS	Cla1	KpnI (100µg/ml BSA added as per manufacturer instruction)
pBS-hBest3	pBS	Kpn1	SaCl
pRK5-hBest4-c-termRIMtag	pRKS	Cla1	KpnI (100µg/ml BSA added as per manufacturer instruction)

Table 2.6: Enzymes used for restriction digest of plasmids: Table presenting the plasmid names and identified vectors. Vector maps were used to establish the multiple cloning site that each DNA of interest was inserted into during transformations. Enzymes used to cut plasmid at MCS to either linearise or completely cut out the cDNA of interest.

2.2.2.4 Transfection of cDNA

Purified cDNA was transfected into cell lines using JetPRIME™ transfection reagent (Polyplus Transfection, France). Protocol according to the manufacturers recommendations. CHO cells were used to transfect hBest1 and analyse with Western blot and RT-PCR to establish antibody specificity. CHO were used as they were previously screened using RT-PCR techniques and no evidence of bestrophin 1-4 mRNA was found. HL60 cells were transfected with hBest1 for functional analysis.

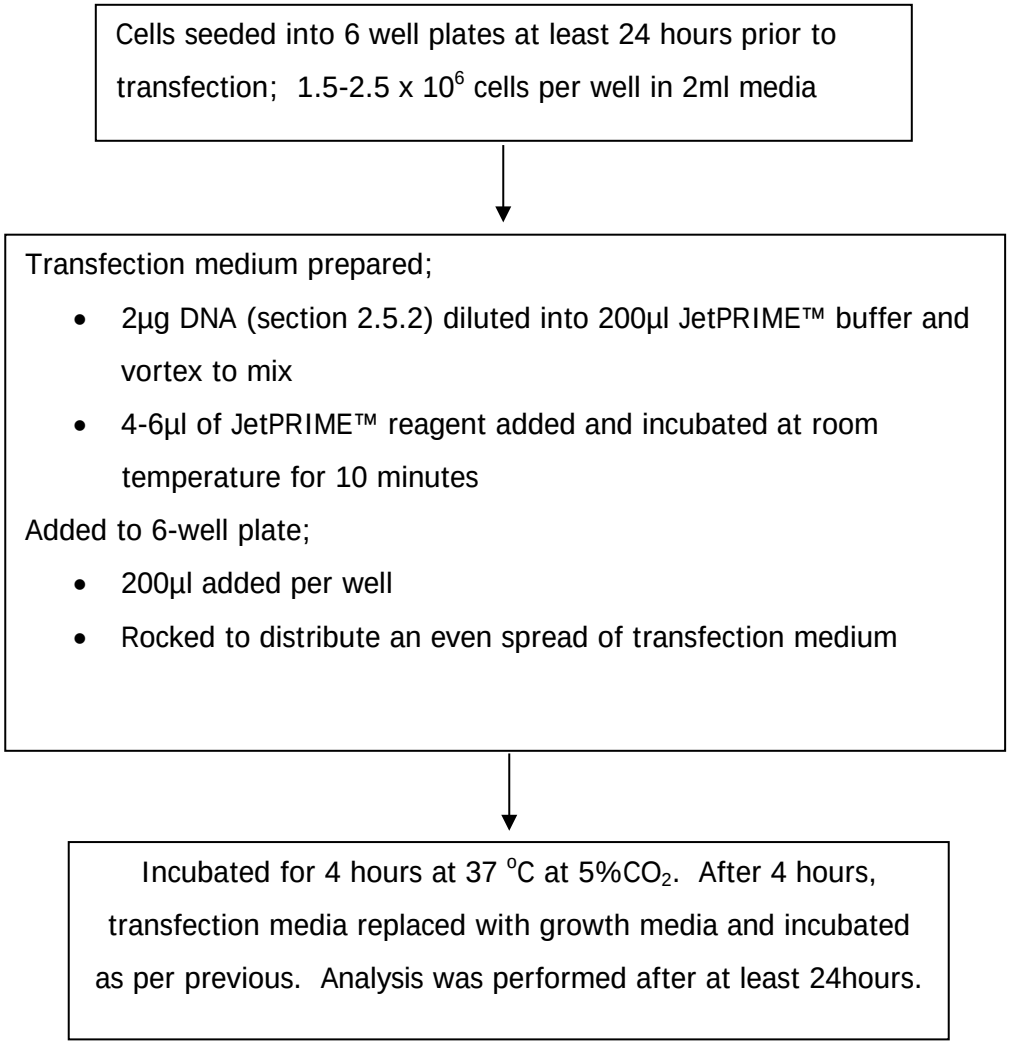

2.3 Protein expression

2.3.1 Flow cytometry

2.3.1.1 Method for immunolabelling with primary and secondary antibodies

All cells were cultured as outlined in section 2.1. For immunolabelling, cells were re-suspended to 1 x 10^6 cells/ml. Table 2.7 outlines the stock solutions for immunocytochemistry preparation.

Requirement for immunolabelling	Contents of solution
Surface staining buffer	PBS + 1% bovine serum albumin (BSA)
Surface wash buffer	PBS
Intracellular staining buffer	PBS + 1% BSA + 0.5% Triton*
Intracellular wash buffer	PBS + 0.5% Triton

Table 2.7: Stock solutions for immunolabelling: Solutions prepared for surface staining and intracellular staining of cells for flow cytometry. Phosphate buffered saline (PBS) was used with additives of bovine serum albumin (BSA) and triton as appropriate. BSA was used as a block for non-specific binding sites. *Triton (Sigma, UK) used for intracellular staining to permeabilise cell membranes

Cells were readjusted for cellular concentration and removed from the stock culture. The removed sample was centrifuged at 200 RCF for 5 minutes at room temperature. Supernatant was removed and discarded and the pellet re-suspended in 4% PFA for 10 minutes at 4 ^{o}C to fix. Fixation prior to immunolabelling was required as PBS has been found to

cleave hCLCA1 from cell surfaces and therefore potentially cause a false negative result (Gibson *et al.*, 2005). The suspension was re-centrifuged at 200 RCF and the supernatant removed and discarded whilst the cell pellet was re-suspended in the appropriate wash buffer according to whether cells were surface stained or intracellularly stained (Table 2.7). This was repeated three times to wash the cells. Cells were centrifuged at 200 RCF and the pellet re-suspended in 100µl of staining buffer appropriate to either surface or intracellular protocol, and incubated for 15 minutes at 4 ^{o}C to prevent non-specific binding by allowing BSA blocking. A comparative experiment for blocking non-specific binding sites was performed. Samples were incubated for 5 mins, 10 mins, 20 mins and 40 mins in goat serum prior to primary antibody staining. There was no discernible difference in results, or isotype control results, therefore all subsequent staining was performed with BSA blocking. Primary antibodies were added to a final concentration of 10µg/ml in 100µl of cell suspension (Table 2.8 lists primary and secondary antibodies used in flow cytometry) and incubated at 4 ^{o}C for 30 minutes, protected from light to prevent photo-bleaching. Cells were centrifuged at 200 RCF to pellet, and were washed in the appropriate wash buffer three times as outlined above (Table 2.7).

PRIMARY ANTIBODY	CONCENTRATION OF PRIMARY ANTIBODY	DETAILS (number and supplier) PRIMARY	SECONDARY ANTIBODY (all added at a concentration of 1:200)	SUPPLIER OF SECONDARY ANTIBODY
Mouse IgG1 (purified) for isotype control	10µg/ml in 100µl	MG100; Invitrogen, UK	Goat anti-mouse with FITC (green) or phycoerythrin (PE)(red) conjugate Goat anti-mouse Alexa Fluor ® 488	Beckham Coulter Invitrogen
Rabbit IgG1 (purified)	1µg in 100µl	AbD Serotec, UK	Donkey anti-rabbit Alexa Fluor ® 488	Invitrogen
Mouse anti-human CD44 monoclonal	10µg/ml in 100µl	MCA2726T; AbD Serotec, UK, clone 156-3C11	Goat anti-mouse with FITC conjugate Goat anti-mouse Alexa Fluor ® 488	Beckham Coulter Invitrogen
Mouse anti-siglec 8 monoclonal for surface stain of eosinophil markers	1µg in 100µl	Clone 3H1; Sigma-Aldrich	Goat anti-mouse with FITC or PE conjugate Goat anti-mouse Alexa Fluor ® 488	Beckham Coulter Invitrogen

Annexin V fluorescein conjugate (FITC)	2µl in 100µl of Ca^{2+} buffered PBS	Invitrogen	NA	NA
Propidium iodide nucleic acid stain	5µl in 200µl	Sigma-Aldrich	NA	NA
Mouse anti-human major basic protein for intracellular marking of eosinophils	1µg in 100µl	4180-2008; AbD Serotec, UK	Bodipy ® FL dye	Invitrogen
Mouse anti-human CLCA1 monoclonal	1µg in 100µl	H00001179-M03; Abnova, clone 2C10	Goat anti-mouse with FITC conjugate Goat anti-mouse Alexa Fluor ® 488 Bodipy ® FL dye	Beckham Coulter Invitrogen Invitrogen
Mouse anti-human CLCA2 monoclonal	1µg in 100µl	H00009635-M01; Abnova, clone 1B9 raised against a partial recombinant	Goat anti-mouse with FITC conjugate Bodipy ® FL dye	Beckham Coulter Invitrogen
Mouse anti-human Best1 monoclonal	1µg in 100µl	Novus Biologicals (E6-6) and AbCam (ab2182 clone E6-6)	Goat anti-mouse with FITC conjugate	Beckham Coulter

Rabbit anti-human Best1 polyclonal		Fabgennix (Bst-121AP)	Goat anti-mouse Alexa Fluor ® 488 Bodipy ® FL dye Mouse anti-rabbit with FITC conjugate	Invitrogen Invitrogen Invitrogen
Rabbit anti-human ANO1 monocolonal	1µg in 100µl	Abnova (clone SP31)	Donkey anti-rabbit Alexa Fluor ® 488	Invitrogen

Table 2.8: Antibodies used for immunolabelling in flow cytometry: Primary antibodies were all alloquoted to avoid freeze-thaw cycles and stored at -20 ^{o}C on receipt from the supplier. Secondary antibodies and IgG1 stored at 4 ^{o}C, protected from light. Primary antibodies were used to label the protein of interest either on the cell surface or intracellularly. Secondary antibodies used as specified above for intracellular and surface staining and were anti-primary antibody host. Alexafluor 488 used if cells were to by cytospun due to the increased photo stability in comparison to FITC. Bodipy was used for intracellular staining as it is non-polar and therefore will not non-specifically bind to intracellular granules.

Secondary antibodies were prepared by diluting to 1:200 with the appropriate staining buffer and re-suspending the cell pellet in 100µl of secondary antibody solution. Samples were incubated at 4 ^{o}C for 30 minutes, protected from light. As outlined above, the cell pellet was then washed three times in the appropriate wash buffer and finally re-suspended in 200µl of PBS for flow cytometry.

Secondary antibodies were Fab_2 fragments targeted against the host species of the primary antibodies used. Secondary antibodies were conjugated to FITC [Ex 488nm; Em 533/30nm], PE [Ex 488nm; Em 585/42nm], Bodipy® FL dye (green) [Ex 488nm; Em 533/30nm] or Alexa Fluor 488 [Ex 488nm; Em 533/30nm]. Relative expression data from flow cytometry analysis was limited to fluorophore-specific comparisons. For intracellular staining the non-polar Bodipy ® FL dye (green) was used to limit non-specific staining of the cytoplasm. For fluorescence microscopy Alexa Fluor 488 was used due to its increased resistence to photobleaching relative to FITC. Specific use of fluorosphores use is detailed appropriately in all sections of this thesis. Alexa Fluor 488 was not used for flow cytometry and therefore there was no pooling of data between the two secondary antibodies.

Each cell type for flow cytometric phenotyping included a tube with:

1. nil control: no antibodies added as an assessment of autofluorescent background,
2. negative isotype control: to check whether there was non-specific or Fc recptor-mediated binding to the host species by primary antibodies,
3. secondary control: only the secondary antibody was added to determine non-specific binding by secondary to target cells

4. positive control: to ascertain the effectiveness of cell labelling and flow cytometric analysis. CD44 was used as a positive control for surface labelling of all cells. Siglec-8 and major basic protein (MBP) were used, respectively, as positive surface and intracellular markers, for eosinophils.
5. Annexin V and propidium iodide (PI) used as indicators of apoptosis and necrosis (Section 2.3.1.2).

2.3.1.2 Apoptosis assay

To examine possible apoptosis and cellular necrosis, cells were prepared without fixation and re-suspended to 1 x 10^5 cells/ml. Cell suspensions were centrifuged at 200 RCF for 5 minutes and the supernatant removed and discarded. The cell pellet was then re-suspended in calcium buffered PBS (5mM CaCl). Calcium was required to enable annexin V to bind. 2µl of human recombinant annexin V conjugated with FITC (supplied by Invitrogen, UK) was added and incubated for 15 minutes, protected from light, at room temperature. Cells were centrifuged and washed as above with 5mM CaCl and re-suspended in 5mM CaCl. 5µl propridium iodide (PI) (Invitrogen, UK) was added and the cells immediately analysed using flow cytometry. A time course for annexin V and PI was performed by incubating cells and analysing with flow cytometry at time=5 minutes, 15 minutes and 30 minutes. Annexin V and PI were used according to manufacturers recommendations. A brief time course was performed, however, to establish whether the process of staining with Annexin V or PI caused apoptosis or necrosis in itself and to validate methodology. Optimal time for annexin V was 15 minute incubation, and PI staining required immediate analysis as it appeared to stimulate cellular necrosis. The assay was also performed before and after PFA fixing, which showed no difference

in fluorescence. Experimental conditions included group 1, annexin V only, group 2, PI only for specified time points, and group 3, annexin V incubated for time points and PI added immediately prior to analysis.

2.3.1.3 Analysis using flow cytometry

2.3.1.3.1 Beckman Coulter Epics flow cytometer

Samples were collected and prepared as in section 2.3.1.1. Analysis early in the project time course was performed using a Beckman Coulter Epics (XL IXL-MCL) flow cytometer following manufacturer recommendations for quality control measures and operation of equipment. All scatter plots were standardized to a continuous voltage and gain. Fluorescence was examined using a logarithmic scale and histogram comparisons by overlaying each experimental results, and exporting the produced image into Microsoft Paint application. In order to minimize non-specific fluorescence or multi-cellular interactions, the scatter plots were gated according to expected forward scatter for overall cellular size, and side scatter for an indication of granularity. Events recorded in the lowest range for both were excluded as considered to be cellular debris. X-mean (median of the fluorescence intensity) for each population was compared however statistical testing not completed at this stage. Laser light used was at 488nm in all machines as this was the wavelength that was able to excite all fluorpohres used. The emission for each was measured on a standardised axis; FL1 for blue/green emission and FL3 for red emissions. FITC is excited at a wavelength of 495nm whereas Alexa Fluor ® 488 is excited at 500nm. The results are comparable as both emit fluorescence at 520nm which was measured on the FL1 detector, set for blue/green emission measurement. Phycoerythrin (PE) is excited at 565nm,

however laser light can be set to 488nm. The emission wavelength is in the yellow/orange spectrum at 575nm and was measured on FL3 detectors across all machines. Results were examined using fold difference in median fluorescence intensity, from the isotype control, for each protein of interest.

2.3.1.3.2 Accuri, C6 flow cytometer

Over the course of the project, the original flow cytometer was replaced with an Accuri, C6 flow cytometer in September 2009. Initial data collected using the Beckman Coulter Epics flow cytometer was used as an indicator for further experimentation only. From this point, all flow cytometric acquisition and analysis was performed using the alternative equipment. Results were not pooled for any statistical analysis.

Preparation of samples was as outlined in 2.3.1.1 and equipment used as per manufacturers recommendations. Event collection was set to a minimum of 10000 events however this began after the gating for cellular specificity had been set to minimize contamination of results. Apoptosis using annexin V was analysed by plotting FL1 (green) on the x-axis and necrosis with PI measured by FL3 (red) on the y-axis onto a singular scatter plot and establishing cell percentages in all 4 quadrants. Cells in the upper 2 quadrants were fluorescing red and considered necrosing. Cells in the right 2 quadrants were fluorescing green and may possibly have been apoptotic.

Scales for mean fluorescence were standardized to allow comparison of pairwise means between samples and different populations. Mean fluorescence intensity was measured to 2 decimal

places (2dp) ± standard deviation (SD) to 2dp. These were compared using a two-tailed students t-test. Statistical significance was established at $p<0.05$.

2.3.2 Western blot analysis

2.3.2.1 Samples and sample preparation

2.3.2.1.1 Preparation of protein lysates

All samples were cultured as described in section 2.1. Preparation of protein initially used a process of sonication whereby cells were centrifuged at 200 RCF for 5 minutes at room temperature to pellet and washed with sterile PBS. The supernatant was removed and the cell pellet lysed with 50-100µl hot sodium dodecyl sulphate (SDS) lysis buffer. This was from a 10ml stock made up of 8.8ml dH_2O, 200µl of 0.5M Tris (pH 6.8) and 1ml of 10%SDS. The final concentration was 1% SDS and 10mM Tris. The cell lysate was sonicated and re-centrifuged for 5 minutes at 13000 RCF to pellet cell debris. Supernatant removed and kept as protein lysate. The alternative protocol was using RIPA buffer. RIPA buffer was prepared using the following Millipore (UK) protocol:

1. 790mg Tris base was made to 75 ml dH_2O and 900mg NaCl added
2. pH adjusted to 7.4 using HCl
3. 10ml Triton x100 and 2.5ml 10% sodium deoxycholate added
4. 1ml of 100mM EDTA added and volume adjusted to 100ml
5. 1 tablet of PhosSTOP (Roche, UK) in 10ml of solution was added for phosphatase inhibition
6. 1 tablet of Complete, EDTA-free cocktail (Roche, UK) was added for protease inhibition

Protein lysate was then prepared by applying 200µl RIPA buffer to the cell pellet on ice. Eppendorfs were inverted for gentle mixing and then centrifuged at 13000 RCF, at 4 ^{0}C for 15 minutes to pellet

the cellular debris. The protein of interest was removed as supernatant and stored at -20 ^{0}C until required.

2.3.2.1.2 Analysis of protein concentration

All protein samples were analysed for protein concentration to allow appropriate loading for western blot analysis. This was performed using a BCA assay kit supplied by Qiagen (UK). Stock solutions of proteins were made according to Table 2.9, using bovine serum albumin (BSA) (2.0mg/ml) diluted into dH_2O.

VIAL	DILUTENT (µl) dH_2O	VOLUME OF BSA (µl)	FINAL CONC BSA (µg/ml)
A	0	300 of stock	2000
B	125	375 of stock	1500
C	325	325 of stock	1000
D	175	175 of vial B	750
E	325	325 of vial C	500
F	325	325 of vial E	250
G	325	325 of vial F	125
H	400	100 of vial G	25
I	400	0	0

Table 2.9: Stock solutions of bovine serum albumin (BSA) for protein concentration assay: Table with protein standards prepared with BSA and dH_2O. Absorbance of protein standards were measured using spectrometry and a linear graph plotted. Samples also measured and plotted against the line of best fit with an equation generated for the linear line. This was used to calculate the concentration of samples.

BCA working reagent A was mixed with working reagent B to a ratio of 50:1. 25µl of stock solutions and samples were added to individual wells of a 96 well plate. 200µl of mixed working reagent was added to each well and the plate was shaken to mix. Samples were incubated for 30 minutes at 37^0C and then cooled to room temperature. Samples were analysed using spectrometry at 550nm to measure absorbance and a standard curve plotted to calculate concentration of the unknown samples.

Figure 2.4 shows an example of a linear graph plotted for a set of protein standards. In the same experiment, samples were loaded into the same plate to measure light absorbance using spectrometry. The measurement of absorbance was substituted for 'y' and concentration calculated as 'x'. In the above example, the equation is y=0.0006x + 0.0417. This was rearranged for each of the following samples (Table 2.10). The measured absorbance for samples was adjusted for the nil control (Sample I) by

Ab.1-(Sample I Ab.1)=Ab.2

Sample absorbance (Ab.2) then substituted into 'y' for example, for the CFPAC cells (Table 2.10) the calculation for concentration (x) was;

Absorbancy (Ab.2=y)	$\rightarrow$ 2.921 – 0.076 = 2.845
Equation	$\rightarrow$ y= 0.0006x + 0.0417
	$\rightarrow$ y-0.0417 = 0.0006x
	$\rightarrow$ (y-0.0417)/0.0006 = x
Where y =2.845	$\rightarrow$(2.845 – 0.0417)/0.0006=4672.2 µg/ml

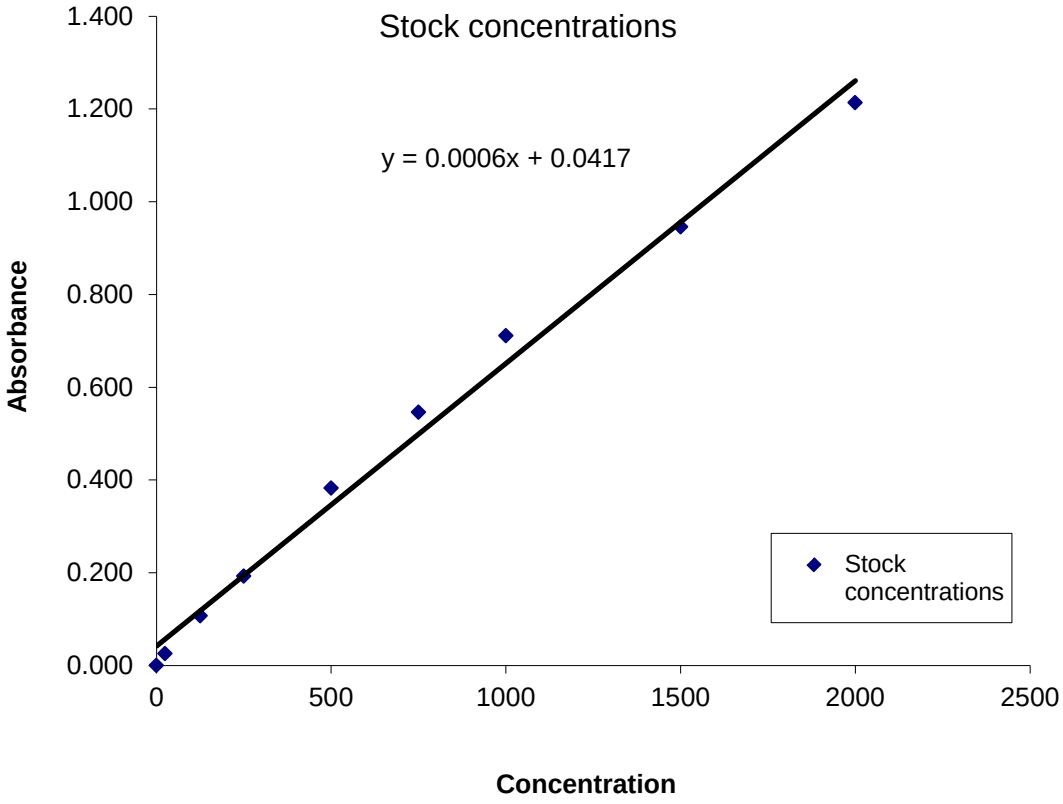

Figure 2.4: Protein standards used to measure absorbance for calculation of unknown concentration of protein samples: Protein samples were used to plot a linear graph and generate an equation for the line of best fit. This was used to calculate the concentration of protein samples of unknown concentration

	Sample	Ab.1	Conc.(ug/ml)	Ab.2
	A	1.290	2000	1.214
	B	1.022	1500	0.946
	C	0.787	1000	0.711
	D	0.622	750	0.546
	E	0.459	500	0.383
	F	0.269	250	0.193
	G	0.183	125	0.107
	H	0.102	25	0.026
	I	0.076	0	0.000
Samples	CFPAC	2.921	4672.2	2.845
	A549	0.537	698.8	0.461
	A549 (CLCA1 KD)	0.448	550.5	0.372
	PMNs	0.212	157.2	0.136
	NAEC	0.616	830.5	0.540

Table 2.10: Measures of absorbance using spectrometry for protein standards and samples: The measures of absorbance at 550nm for protein standards (samples A-I) were used to calculate a linear equation (Figure 2.4). The absorbance measured for each sample was substituted as 'y' in the equation to calculate the unknown protein concentration (x) in µg/ml. Ab.1=Measured absorbance which is adjusted for the nil (Ab.1-Sample I Ab.1)=Ab.2. Conc. = Of protein samples this is known and in the sample group, calculated from the equation.

2.3.2.1.3 Sample preparation for loading onto Western gel

Lysates of protein were prepared on ice. 20µg of sample was diluted with nuclease free water to a volume of 17µl. In the instance where samples were too dilute to allow volumes of less than 17µl they were applied to Amicon® Ultra-0.5 centrifugal filter devices in accordance with manufacturer protocols (Millipore, UK) to concentrate. Lysates were then added to sample preparation buffer

(10ml 1.5M Tris at pH 6.8, 6ml 20% SDS, 30ml glycerol, 15ml β-mercaptoethanol and 1.8mg bromphenol blue adjusted to 100ml with dH_2O). The final ratio of buffer to sample was 1:5 respectively with a final volume of 20µl. Prepared samples were heated to 95^0C for 3 minutes to denature proteins and pulse centrifuged at high speed.

2.3.2.1.4 Loading of samples and electrophoresis

12% acrylamide gels were prepared as in Figure 2.5. Gels were poured into Bio-Rad glass plates and levelled using isopropanol.

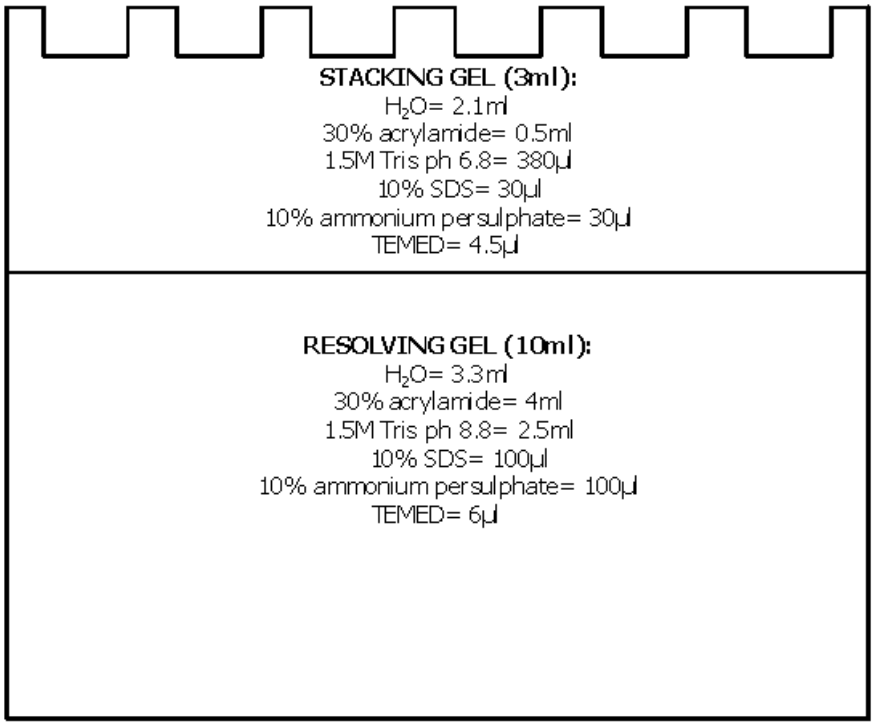

Figure 2.5: Acrylamide gel for western blot analysis: Ingredients and volumes of solutions for preparation of 12% acrylamide gel for western blot analysis. Resolving gel is set into glass plates and left to set. Stacking gel is layered onto the resolving gel and a comb inserted for well formation.

Ladder (4µl) was added to the first and last well in each gel and samples loaded in remaining wells. The gels were placed into an electrophoresis tank containing running buffer pH 8.3 (1L dH2O, 30.3g Tris base, 144.0g glycine and 10g SDS final solution diluted to 1:10) at 100V for 1.5 hours. Time course for electrophoresis was performed, at 1 hour, samples were clustered which made analysis problematic. At 2 hours, the samples had run to the bottom of the gel, and in some cases, out of the bottom of the gel.

2.3.2.2 Process of western blotting

2.3.2.2.1 Transfer of proteins onto membrane and antibody labelling

Following electrophoresis, the gel was removed from the tank and proteins transferred from the acrylamide gel onto a membrane. This was labelled with antibodies specific for the protein of interest. Figure 2.6 presents a summary of the process.

Proteins were transferred from the gel onto Immobilon-FL membrane (Millipore, UK) using a semi-dry transfer method. To permeabilise membrane, it was first soaked in ethanol for 15 minutes. This involved layering blotting paper, membrane, gel and blotting paper. Blotting paper and membrane were soaked in transfer buffer (10 times concentration of stock at pH9.2 of 390mM glycine, 480mM Tris and 0.3% SDS diluted to single strength concentration with 100ml transfer buffer, 200ml methanol and 700ml dH_2O). This was then electrophoresed for 30 minutes at 25V for two gels using Bio-Rad (UK) semi dry transfer unit.

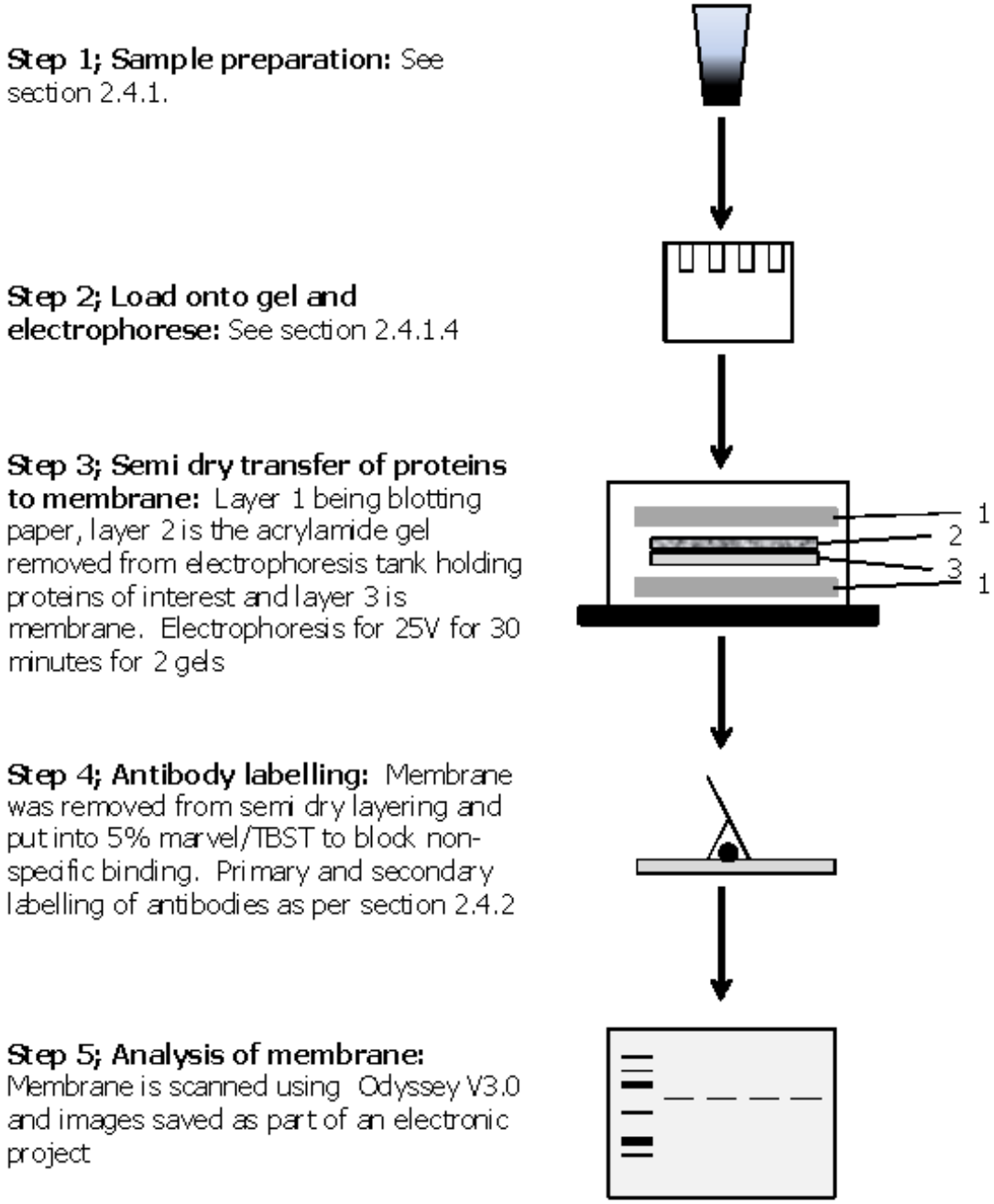

Figure 2.6: Summary of process for western blot analysis: Summary of the overall process and order of steps for western blot analysis as in section 2.3.2

When electrophoresis was complete, membranes were removed and placed into 5% marvel (milk) made with Tris buffered saline 0.5% tween (TBST) to block non-specific binding. This was put onto a fast rocker (100rpm) for 1 hour. Primary antibodies were mixed following an initial concentration assay using primary antibodies at 1:250, 1:500, 1:750, 1:1000 and 1:1500. Primary antibodies were finally made at a concentration of 1:500 with anti-actin at 1:1000 in 5% marvel/TBST which prevented excess background on analysis but allowed clear visualisation of banding. This was made to a final volume of 10ml and applied to the membrane and incubated for 12 hours at 4^0C. Secondary antibodies were also examined for optimal concentration. These were; 1:500, 1:1000, 1:2000, 1:5000 and 1:10000. Final concentration was 1:2000 as an optimal concentration for clear visualisation of bands. All primary antibodies used for western blot analysis are presented in Table 2.11. All secondary antibodies were IgG conjugated with IRDye® recommended for use with Odyssey, supplied by LI-COR Biosciences. Secondary labelling of primary antibodies that were mouse anti-human used a goat anti-mouse IgG antibody. For primaries that were rabbit anti-human, goat anti-rabbit IgG were used. All secondary antibodies were available conjugated with either IRDye®800 (green banding) or IRDye®680 (red banding). Each blot was standardised so that the protein of interest (for example hBest1, hCLCA1) was labelled with IRDye®800 and the band visualised was green for each experiment. All controls (β-actin) were labelled with IRDye®680 to give a red band on analysis.

PROTEIN OF INTEREST	CONC.	ANTIBODY	DETAILS (number and supplier)	EXPECTED MOLECULAR WEIGHT (kDa)
Rabbit anti-actin	1:1000	Rabbit anti-actin	Invitrogen, UK	42-48
Mouse anti-actin	1:1000	Mouse anti-actin monoclonal	Millipore clone C4	43
CLCA1	1:500	Mouse anti human CLCA1 monoclonal	H00001179-M03; Abnova, clone 2C10	37.11
CLCA2	1:500	Mouse anti human CLCA2 monoclonal	H00009635-M01; Abnova, clone 1B9 raised against a partial recombinant	79.9
Bestrophin 1	1:500	*Mouse anti human Best1 monoclonal*	*Novus Biologicals (E6-6) and alternative from AbCam (ab2182 clone E6-6)*	68
		Rabbit anti-human Best1 polyclonal	Fabgennix (Bst-121AP)	
Bestrophin 2	1:500	Rabbit anti human Best2 polyclonal	AbCam (ab32830)	65
Bestrophin 3	1:500	Rabbit anti-human Bestrophin 3 polyclonal	AbCam (ab94904)	51 (alternative bands at 74 and 120)
Bestrophin 4	1:500	Rabbit anti-human Bestrophin 4 polyclonal	AbCam (ab66632)	60
ANO1	1:500	*Rabbit anti human ANO1 monocolonal*	*Abnova (clone SP31). Not used previously for Western blot analysis and not successful for this*	74
		Rabbit anti human ANO1 polyclonal	AbCam (ab53212)	

Table 2.11: Antibodies used for western blot analysis: All antibodies used for western blot analysis however those highlighted in grey were non-specific. Antibodies for hBest2-4 were unable to detect a band. Blots were repeated at least 3 times. Due to constraints of resources, and the focus of the thesis, these were not repeated with different antibodies

Membranes were washed with TBST for 15 minutes, and repeated 4 times before the secondary antibody was applied. This was either red or green fluorescence, as stated, made to a concentration of 1:2000 in TBST. A further wash cycle of 15 minutes, repeated 4 times in TBST was completed before analysis using the Odyssey V3.0 scanner.

2.3.2.2.2 Western blot membrane re-probe

Membranes that contained proteins, and had been probed with antibodies were stripped using Re-Blot Plus Strong Solution (2504) 10x concentration (Millipore, UK). The process was intended to remove the antibodies that had bound to the proteins in order to allow re-probing with alternative antibodies for the same sample. Re-Blot solution was diluted to 1:10 with dH_2O and 10ml of solution applied to the membrane. Membranes were incubated at room temperature, agitated for 10 minutes. The Re-Blot solution was washed with TBST and membranes were either sotred at $4^{O}C$ for future use or immediately re-probed with antibodies using the same process as outlined previously. On examination, the process of stripping the membrane of antibodies appeared to also strip the protein of interest. The process was repeated and increasing concentrations of antibodies used however bands were either poorly visible or not present. On using new samples and completing full western blotting, bands had been visualised. The samples had been taken from the same stock. This indicated that it was the membrane stripping process that had affected results.

2.3.2.3 Analysis of results

Antibody stained membranes were placed onto a scanner plate and analysed using the Odyssey V3.0 software. As standard, the membrane was scanned at an intensity of 5 for each wavelength however this was adjusted to visualise bands as required. β-actin protein was labelled with red antibodies, as a housekeeping process, and visualised at wavelengths between 680 and 700 nanometers. All proteins of interest were labelled with green antibodies and measured at a wavelength of 800 nanometers.

2.4 Transmigration assay

Transmigration of the HL60 cell line was established. Cells were cultured as per section 2.1 and divided into 3 experimental groups; HL60 (nil) as a control, HL60 treated with transfection reagent only (no DNA added) as a control, and HL60 transfected with hBest1 (section 2.5.4) (n=3 for each experimental group) Cells were counted using trypan staining and haemocytometer technique. A total of 135 000 cells for each group were re-suspended as 250µl of sample in culture media (as per Section 2.1).

400µl of growth media (RPMI-1640 with FCS and penicillin/streptomycin additions) was added to each well of a 24 well plate. 3 experimental conditions were prepared by adding IL-13, or formyl-methionyl-leucyl-phenylalanine (fMLP) and nil to the plates. IL-13 was added to a final concentration of 10µg/ml and fMLP added to 1µM. MilliCell culture plate inserts (Millipore, UK) with a 3µm pore size were put into each well and each sample applied to the plate insert (Figure 2.7).

With a known number of cells added to the insert, cells were incubated at $37^{O}C$, 5% CO_2 for 1 hour to allow migration across the membrane. A sample of cells was taken from each well and cell counted using trypan staining and haemocytometer technique, and the total number of cells in 400µl calculated. This was converted to a percentage of the total cells added to the membrane as a percentage of cell migration across 3 experimental conditions, for three groups (n=3).

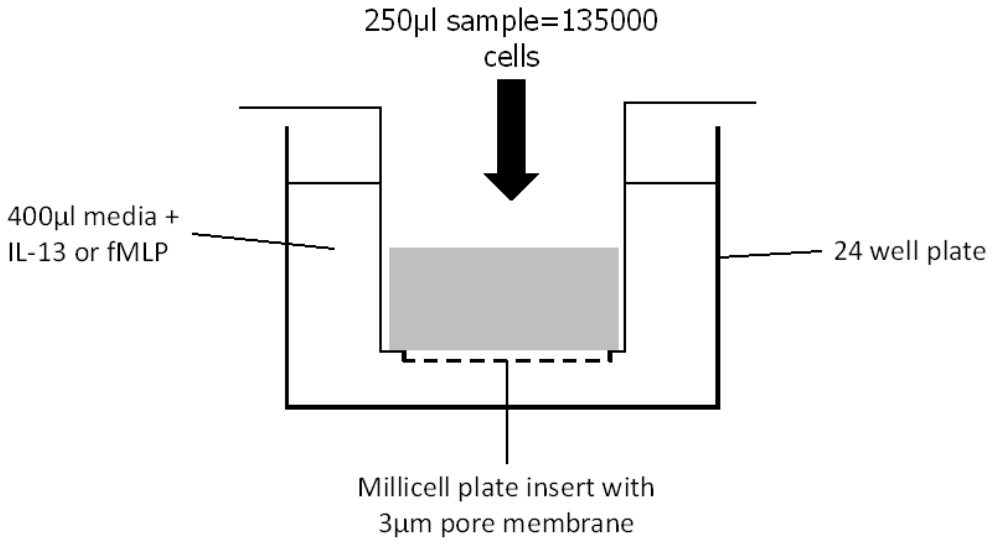

Figure 2.7: Transmigration assay equipment set up: Millicell plate insert with 3µm pore inserted into each well of a 24 well plate. Wells contained media and additives. Sample was added to the Millicell plate insert.

2.5 Chloride and calcium flux assay

HL60 cells were transfected with hBest1 as per section 2.2.2. As with the transmigration assay, there were 3 experimental groups; HL60 nil, HL60 that were treated with transfection reagents only (no DNA) and HL60 transfected with hBest1. There were three samples for each group (n=3). Chloride and calcium flux was measured in response to inhibitory or stimulatory cytokines. In order to assess intracellular chloride movement, cells were re-suspended to $1x10^6$ cells/ml and washed 3 times with Krebs ringer buffer (KRB) to mimic physiological conditions. Cells were treated with 5mM *N*-[ethoxycarbonylmethyl]-6-methoxy-quinolinium bromide (MQAE) and incubated at 37^OC by placing in a water bath, protected from light. Samples were washed five times with KRB. For calcium flux, cells were re-suspended to $4x10^6$ per ml and washed in KRB. 1µl of calcium sensor dye was added to 1ml cells (5µM) and incubated for 30 min at 37^OC in a water bath, protected from light. Cells were washed 5 times with KRB.

Each sample underwent 4 experimental treatments; nil (no additions), addition of ionomycin at 10µM, uridine 5'-triphosphate (UTP) at 100µM, and niflumic acid (100µM) followed by UTP. Samples were analysed using flow cytomtery. The chloride flux assay was performed using the BD FACS Aria II flow cytometer, whereas the calcium flux was performed on the BD Accuri C6 cytometer. All samples were run for baseline and the appropriate concentration of ionomycin, UTP or niflumic acid added accordingly. The sample run was then continued to establish the response to the inhibitors/stimulants. The final experimental group was run following the addition of niflumic acid and then stopped to add UTP and run further and changes in fluorescence measured.

2.6 Statistical analysis

Experimental replicates are represented as 'n' and all values and error bars are expressed as means ± standard error of the mean. Expressional data using RT-PCR (including cytokine stimulation assays), flow cytometry and transmigration assay were analysed using two-factor ANOVA (with replication) within Excel (as part of Microsoft Office Professional Plus 2010). Add-in "Analysis ToolPak" for Excel was downloaded and used for all statistical analysis. Two-factor ANOVA was used as data was classified along two dimensions. The null hypothesis (H_0) was that the gene or translated protein expression across cell samples, and for hCLCA1, hBest1 and hANO1 was taken from the same population, in that there was no difference across cells, or for each gene or protein. Using ANOVA, *f* values were calculated to establish whether populations were taken from different distributions. When the critical F value was shown to be less than the *f* value, the null hypothesis was rejected. $P<0.05$ was considered statistically significant, and $P<0.01$ and $P<0.001$ as highly significant, and therefore the alternate hypothesis was assumed.

Correlation coefficients were calculated for EoL-1 cells stained with hCLCA1 and propidium iodide/annexin V. A students paired t-test was used to establish any significant difference in flow cytometry between annexin V/PI staining before and after fixing EoL-1 cells, and with and without IL-5 stimulation. Levels of significance were established as $P<0.05$, $P<0.01$ and $P<0.001$.

To establish whether there was a correlation between genes expressed, scatter plots of hBest1 and hCLCA1 expression were used for linear regression and correlation coefficients were calculated. The statistical significance of any correlation was evaluated using a paired t-test and $P<0.05$ was considered statistically significant.

To compare HL60s with PMNs and eosinophils for hBest1 protein and gene expression, an unpaired 2 tailed students t-test was used to establish whether population means were statistically significant. Statistical significance was established as $P<0.05$.

2.7 Systematic review

A systematic review was performed in order to establish the expression of chloride ion channels in chronic inflammatory lung diseases. Methodology can be found in Chapter 6, Section 6.3.

2.8 Experimental summary

Throughout the project, there were numerous experiments to test methodological processes. This included western analysis following transfection to test specificity of antibodies, cell lines as models of primary cells, and preparation of RNA and proteins for analysis. Following this, experiments were focussed within 3 domains. Firstly examining the expression of molecular candidates for chloride ion channels. This was established by RT-PCR for mRNA encoding the candidates and translation into protein expression. Functional analysis explored the responses of cells transfected with hBest1 to cytokines and stimulation or inhibition of chloride and calcium flux. Finally, the project contextualised the expressional and functional experiments in chronic inflammatory lung disease through the completion of a systematic review (Chapter 6).

CHAPTER 3: CHARACTERISATION OF ANTIBODIES, SPECIFICITY OF RT-PCR PRIMERS AND METHODOLOGY OPTIMIZATION

3.1 Flow cytometry equipment

Flow cytometry was performed using two different machines, as resources became available, however, results between the two were comparable. Figure 3.1 presents the forward and side scatter plots between the two machines for EoL1 cells. Gate A in the EPICS XL (Beckman Coulter) used October 2008 corresponds to gate P5 in the Accuri C6. This was gated as these were considered the viable cells, as demonstrated in apoptosis assay (Section 3.1.2). The orientation for the data collected for forward scatter and side scatter using the Accuri C6 is on the opposite axis. Whilst this can be reversed on the Accuri C6, default settings were maintained as much as allowable to decrease the risk of computational error. In addition the settings for EPICS XL data collection allowed detectors to be set to automatically gate out smaller particles, which were considered to be cell debris. The Accuri C6 data allows this to be done during analysis. All data, and statistical analysis, was collected and performed using the Accuri C6. Data collected using the Beckman Coulter Epics flow cytometer was used as an indicator for further experimentation only and results were not pooled with the Accuri C6 data.

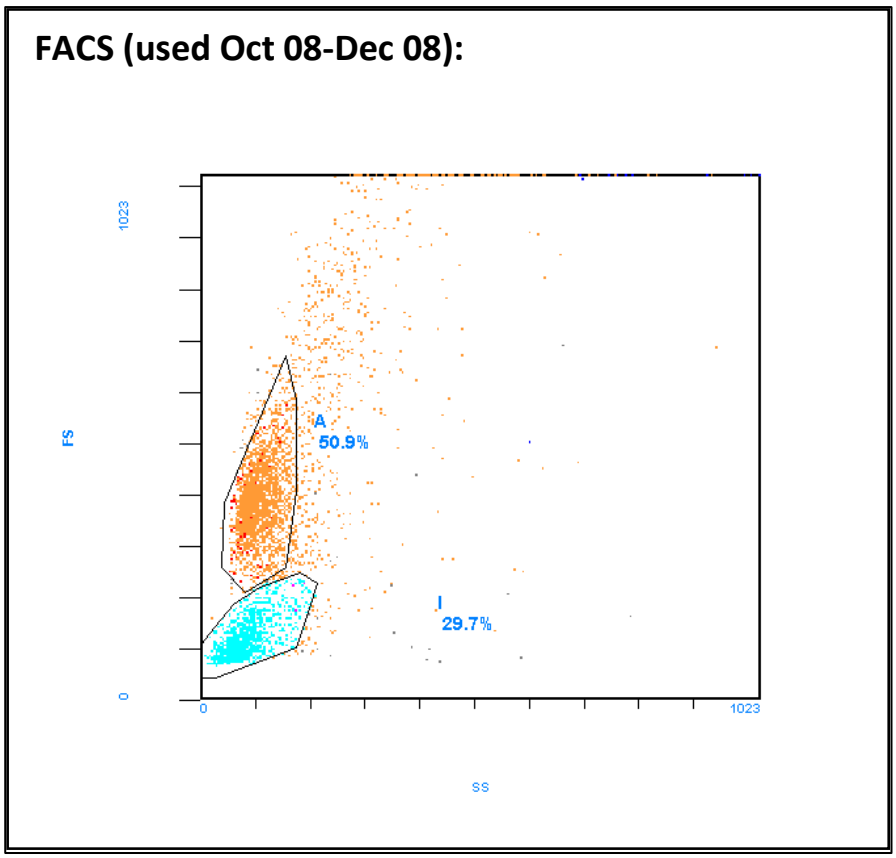

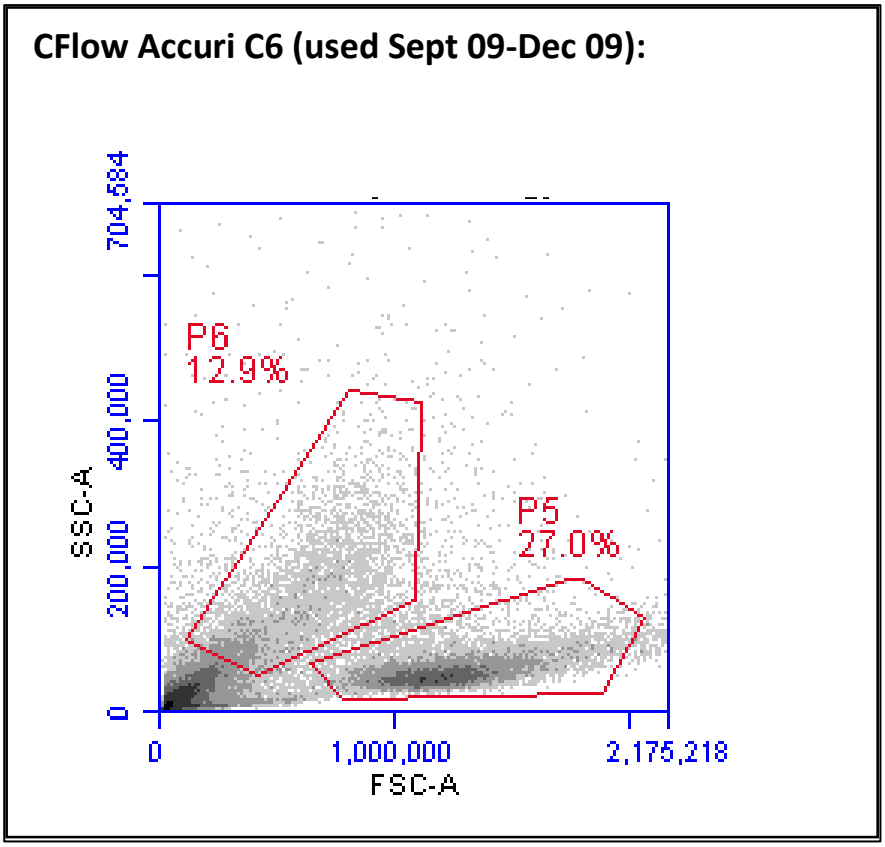

Figure 3.1: Forward scatter and side scatter for flow cytometers: Please see following page

Figure 3.1: Forward scatter and side scatter for flow cytometers: Early experiments were on the EPICS XL, Beckman Coulter, later experiments used the Accuri C6. Representative forward scatter and side scatter plots for EoL-1 cells, on both flow cytometry machines showing the comparable information between the two resources taking into consideration the opposite orientations.

3.2 Cell lines selected as an effective model of human cells

EoL1 and dEoL1 cells were initially examined to establish whether they could be used as a model for primary human cells. EoL-1 cells are considered eosinophilic however when stimulated with dbcAMP they are driven towards terminal differentiation and become more eosinophilic. Both EoL-1 and dEoL-1 cells were stained with both Annexin V and propidium iodide (PI) (see Section 2.3.1.2) as an indicator of cellular apoptosis and necrosis respectively. When PI (FL3; 670LP; Ex 488nm) was plotted against annexin V (FL1; 533/30nm; Ex 488nm) a scatter plot was produced and divided into quadrants (see Figure 3.2 for an example). Cells in the lower left quadrant (LL) were negative for both annexin V and PI and, therefore, not considered either necrotic or apoptotic. Cells in the upper right (UR) were positive for both PI and annexin V. Those in the upper left (UL were positive for PI only and the lower right (LR) were positive for annexin V only. Annexin V is a protein, which binds to phosphatidylserine as it moves to the outer leaflet of the plasma membrane as an early indicator of apoptosis. PI stains both DNA and RNA and when applied to whole cells is an indicator of cellular viability, and therefore necrosis.

When the cell population was sorted however, and annexin V/PI stained, the cells that were positive for hCLCA1 were also positive for apoptosis (n=6, see Figure 3.3). On analysis, there was a positive correlation between annexin and hCLCA1, and also between PI fluorescence and hCLCA1 (correlation coefficient 0.76 and 0.89, respectively). This was a significant relationship ($P<0.05$) (Table 3.1, Figure 3.3).

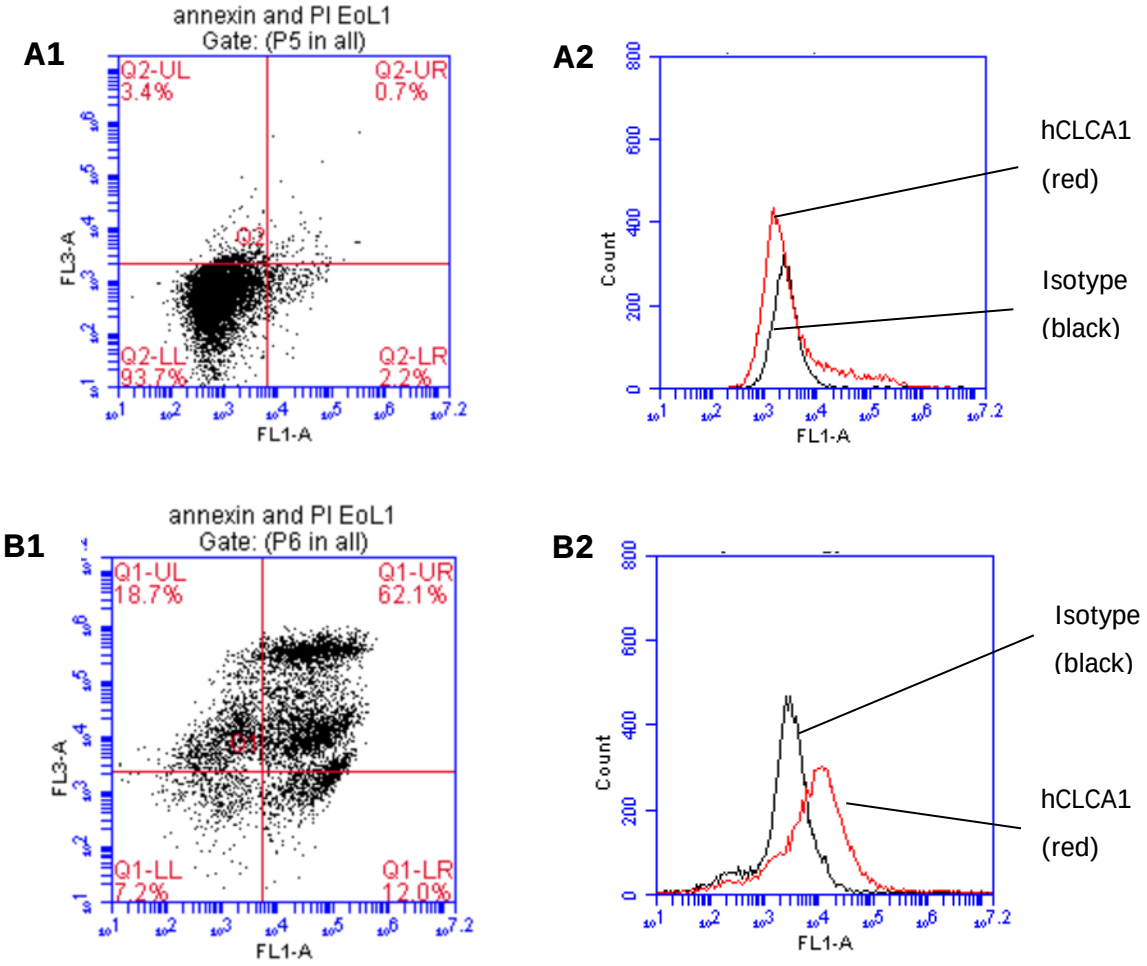

Figure 3.2: Apoptosis assay for EoL-1 and dEoL-1:
Apoptosis assay of EoL1 cells demonstrating positive annexin and propidium iodide. Results were similar for differentiated cells (dEoL-1). Apotosis assay as detailed in section 2.3.1.2. PI (FL3; 670LP; Ex 488nm) was plotted against annexin V (FL1; 533/30nm; Ex 488nm). A: EoL1 in gate P5 (Figure 3.1) were negative for PI and annexin V (A1) but also negative for hCLCA1 (A2). B: EoL1 in gate P6 (Figure 3.1) were positive for hCLCA1 (B2), however, they were also positive for PI and annexin V (B1) indicating necrosis and apoptosis (n=6).

	Median fluorescence					
Sample	Isotype control	hCLCA1	PI fresh cells	Annexin V fresh cells	PI fixed cells	Annexin V fixed cells
EoL1	535	217	729	169	740	426
EoL1	823	18839	26067	16101	24197	13546
EoL1	993	365	663	1040	532	732
EoL1	887	553	459	220		
EoL1	1056	57512	36948	15355		
EoL1	1138	14785	24208	13117		
Mean	905	15379	14846	7667	8490	4901
SD	195	20259	14773	7251	11107	6114

Table 3.1: Median fluorescence of propidium iodide (PI) and annexin V in relation to hCLCA1 in EoL-1 cells: Median fluorescence of isotype control, hCLCA1, PI and annexin V in EoL-1 (n=6 for fresh EoL-1 cells, n=3 for fixed EoL-1 cells). There is a positive correlation between hCLCA1 and PI (coefficient 0.89) and hCLCA1 and annexin V (coefficient 0.76) which was significant ($P<0.05$) (Figure 3.4). There was no statistically significant difference between fixed or fresh EoL-1 cells. PI positive cells were in either upper left or right quadrant (UL and UR), annexin V positive cells were in either the lower or upper right quadrants (LR or UR).

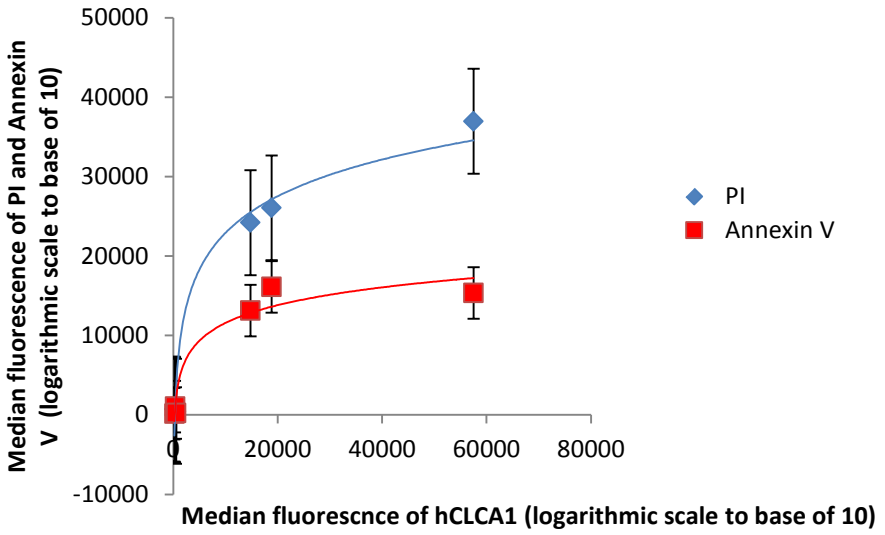

Figure 3.3: Correlation between hCLCA1 and PI / annexin V in EoL-1 cells: Median fluorescence of hCLCA1, PI and annexin V in EoL-1 cells (n=6). Error bars are standard error. There is a positive correlation between hCLCA1 and PI (coefficient 0.89) and hCLCA1 and annexin V (coefficient 0.76) which was significant ($P<0.05$)

In order to ascertain whether the process of annexin V or PI staining would induce apoptosis or necrosis, or whether it was an internal response of EoL-1 cells, a time course was performed (n=2) (Table 3.2, Figure 3.4). Whilst n=2 and, therefore, statistical analysis was not performed, this indicated that the process of annexin V surface staining was unlikely to cause spontaneous apoptosis. PI staining compared to nil controls, did increase fluorescence over time however is it known that propidium iodide is cytotoxic and therefore should only be applied immediately prior to analysis (manufacturers recommendations).

Time	Nil	Annexin V	PI (no annexin)	PI (plus annexin V)
0 mins				
1	2451	2798	19365	23751
2		4837	4360	5755
5 mins				
1	2506	2822	31949	33590
2		4920	5424	7259
10 mins				
1	2423	2845	57458	43091
2		4562	6039	9844
15 mins				
1	2404	2766	-	-
2		4269	-	-
30 mins				
1	2407	2764	-	-
2		4578	-	-
60 mins				
1	2321	2744	-	-
2		4661	-	-

Table 3.2: Time course of fluorescence for annexin V and PI staining of EoL-1 cells: EoL-1 cells (n=2) were stained with annexin V for time 0, 5, 10, 15,30 and 60 minutes and median fluorescence (logarithmic scale to base 10) measured on FL1 (FL1; 533/30nm; Ex 488nm). PI was measured on FL3 (FL3; 670LP; Ex 488nm) after 0, 5 and minutes of staining. N=2 therefore no statistical analysis could be performed however results indicate that there may be no effect of annexin V staining over time on intensity of fluorescence. PI (a known cytotoxin) caused increase fluorescence the longer it was applied to the sample (Figure 3.4). As a known cytotoxin, the time course was not continued for PI staining after 10 minutes as it is known to cause necrosis after prolonged application to cells.

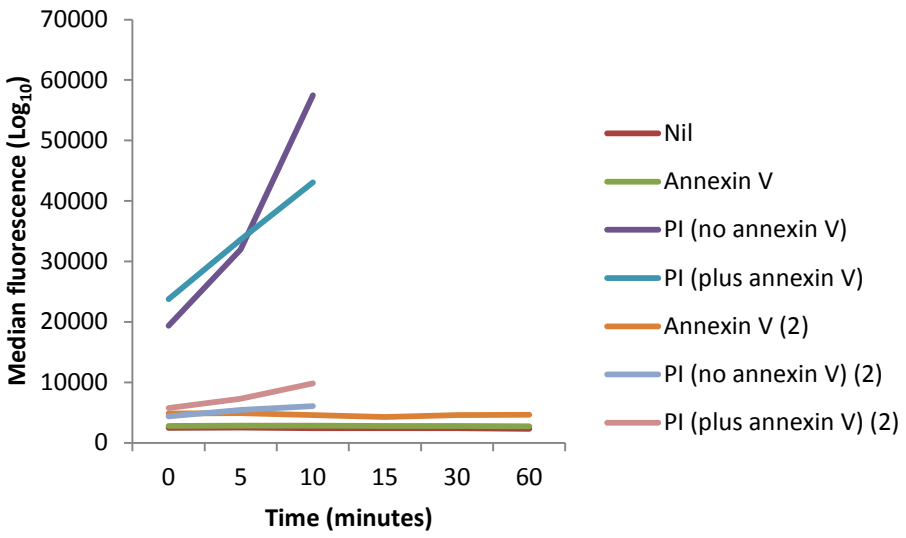

Figure 3.4: The effect of PI ± annexin V exposure, over time, on EoL-1 cell viability: Graph depicting median fluorescence following annexin V and PI staining over a time course (Table 3.2). EoL-1 cells (n=2) were stained with annexin V for time 0, 5, 10, 15, 30 and 60 minutes. PI was stained for 0, 5 and 10 minutes after staining. N=2 therefore no statistical analysis could be performed however results suggest that there may be no effect of annexin V staining over time on the intensity of fluorescence for EoL-1 cells measured on FL1 (FL1; 533/30nm; Ex 488nm). PI (a known cytotoxin) caused increase fluorescence, as measured on FL3 (FL3; 670LP; Ex 488nm) the longer it was applied to the sample. (2) in legend above denotes second sample.

Further analysis was performed on the EoL-1 cells to establish whether the process of permeabilising cells for intracellular staining caused interference in the staining technique and its specificity. This was examined to establish whether samples could be fixed and maintain annexin V staining. EoL-1 cells (n=3) were stained with annexin V and PI with and without Triton treatment (Table 3.3). Two way ANOVA was performed and there was no statistically

significant difference between nil controls (no annexin V/PI staining) and surface or intracellular staining. There was also no statistically significant difference between surface and intracellular staining for annexin V and PI ($P>0.7$).

Sample	Nil surface	Annexin V surface	Fold change Annexin V surf (2dp)	PI surface	Fold change PI surf (2dp)	Nil intracellular	Annexin V intracellular	Fold change Annexin V int (2dp)	PI intracellular	Fold change PI int.(2dp)
1	314	1150	3.66	880	2.80	174	259	1.49	923	5.30
2	219	554	2.53	194	0.89	157	1269	8.08	1147	7.31
3	3482	6265	1.80	3976	1.14	1915	5821	3.04	11407	5.96
Mean	1338	2656	2.66	1683	1.61	749	2450	4.20	4492	6.19
Standard deviation	2829	2563	0.77	1645	0.85	825	2419	2.82	4890	0.83

Table 3.3: The effect of Triton treatment on cellular viability of EoL-1 cells: EoL-1 cells (n=3) were treated with Triton (intracellular) and stained with annexin V and PI to establish whether permeabilisation causes apoptosis or necrosis in samples. This was measured as fluorescence intensity. PI was measured on FL3 (670LP; Ex 488nm) and annexin V measured on FL1 (533/30nm; Ex 488nm). These were compared to cells that had not been treated with Triton (surface). Sample 3 skewed data causing large standard deviations of fluorescence. Therefore data was normalised by calculating fold change for fluorescence intensity of PI and Annexin V from nil controls for both surface and intracellular staining. Two-way ANOVA was performed and any differences noted were not statistically significant ($P>0.7$) either from the nil, or between surface or intracellular staining. The null hypothesis (that there is no difference between populations) could not be rejected.

Under light microscopy, EoL-1 and dEoL-1 cultures that were annexin V and PI positive did not appear to be contaminated with either infection or cross culture contamination. To establish whether apoptosis or necrosis could be prevented, PI and annexin V assays were performed before and after fixing EoL-1 cells with paraformaldehyde (n=3, Table 3.1) and after stimulation with IL-5 at 10ng/ml final concentration and incubated for 24 hours (n=3, Table 3.4). There was no statistically significant difference in annexin V/PI staining between fixed or fresh cells, or stimulating with IL-5 compared to non-stimulated EoL-1s (P>0.7). There was no statistically significant difference in annexin V/PI staining between cells that had been fixed, compared to those that hadn't, prior to staining (P>0.9).

	Median fluorescence			Median fluorescence	
Sample	**PI**	**Annexin V**	**Sample**	**PI**	**Annexin V**
EoL-1 (IL-5)	23023	13421	EoL-1	42350	32459
EoL-1 (IL-5)	34329	26720	EoL-1	33251	15132
EoL-1 (IL-5)	35345	25200	EoL-1	24208	13117
Mean	30899	21780	Mean	33270	20236
SD	5585	5943	SD	7406	8682

Table 3.4: The effect of IL-5 on EoL-1 cell viability using measurements of median fluorescence for PI/annexin V: EoL-1 cells were stained with PI and annexin V after 24h stimulation with IL-5, compared to nil which were not stimulated (n=3). PI measured on FL3 (670LP; Ex 488nm) and annexin V measured on FL1 (533/30nm; Ex 488nm). There was no statistically significant difference in apoptosis/necrosis assays between the two groups (P>0.7).

EoL-1 cells are an eosinophilic leaukaemic cell line which has the phenotypical features of myeloblasts. Under microscopy myeloblasts are non-granular and consist of a large nucleus. When stimulated with N6, 2'-0-dibutyryladenosine 3':5'-cyclic monophosphate sodium (dbcAMP) (Section 2.1.1.2) EoL-1 cells differentiate into eosinophils. These cells are distinctive with development of cytoplasmic granules and a bi-lobed nucleus (Figure 1.2 shows images of primary neutrophils and eosinophils captured under microscopy). Both EoL-1 and dEoL-1 cells were stained with annexin V to identify whether cells were undergoing programmed cell death which compromises the viability of cells. Prior to differentiation, EoL-1 cells were susceptible to spontaneous apoptosis, or alternatively, the process of differentiation itself may have caused degranulation, and apoptosis. Cells can trigger apoptosis either intracellularly due to stressors, infection or hypoxia, or due to extracellular triggers such as toxins. Both EoL-1, and dEoL-1 cells were vulnerable to apoptosis which would compromised the reliability of the results.

EoL-1 and dEoL-1 cells, when stained with hCLCA1, may have been fluorescing because hCLCA1 is present intracellularly and in apoptosis/necrosis the membrane is compromised allowing the antibody access to intracellular contents, and therefore intracellular hCLCA1. Conversely however, there may have been non-specific binding. This would be due to the compromised cell membrane and release of intracellular contents, which may non-specifically bind the anti-hCLCA1 antibody. Further analysis of EoL-1 and dEoL-1 cells is indicated to confirm their use as a model for human eosinophils. Mycoplasmic infections could not be discounted. Although cultures were examined under microscopy, mycoplasma is not easily detected without the use of alternative methods such as ELISA or PCR. Additionally, further examination as to any possible correlation between apoptosis and necrosis and differentiation would be

beneficial. This could be performed by using siglec 8 and major basic protein as markers of differentiation. As indicated, the sample number for annexin V and PI staining was 2 (due to contraints of resources) and therefore statistical analysis was not performed. RT-PCR analysis was performed and no bands were visualised for hCLCA1 in either dEoL-1 or EoL-1 cells (Figure 3.5). This could not, therefore, clarify the characterisation of hCLCA1 in this cell line to support the initial flow cytometry phenotyping. Whilst EoL-1 and dEoL-1 cells cannot be discounted for use as a model for eosinophils, further experimentation is required to establish the cause of positive annexin V and PI staining, and the correlation with hCLCA1 staining. Due to the contraints of resources, and that PMNs were readily available, EoL-1 and dEoL-1s were no longer used in the project. HL60s, an alternative commercial cell line, was phenotyped to establish use as a model for eosinophils, or PMNs.

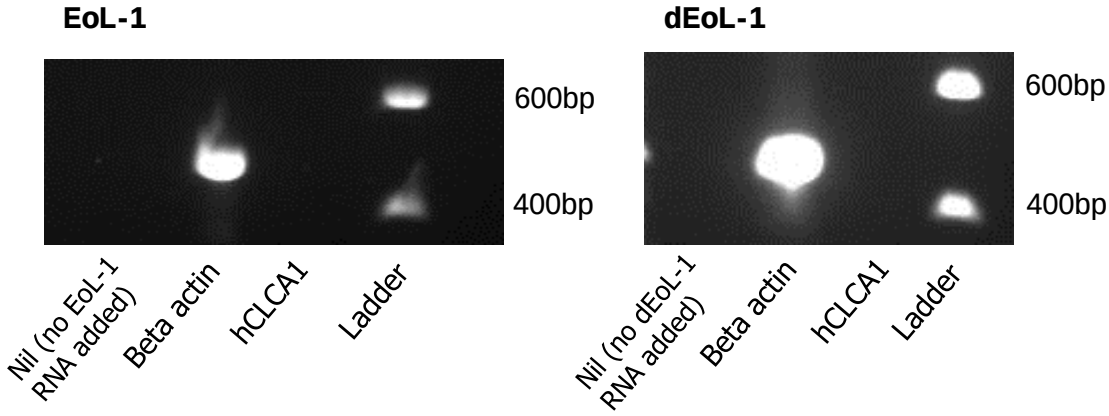

Figure 3.5: hCLCA1 expression in EoL-1 and dEoL-1 cells: EoL-1 and dEoL-1 cells analysed using RT-PCR for hCLCA1. Beta actin at the expected band size (456 bp). No band in nil control. No band visualised for hCLCA1

HL60s have been used previously as an alternative for human pro-myelocytic cells as they have a neutrophilic phenotype (Fischkoff *et al.*, 1984; Varnai *et al.*, 1993; Schrenzel *et al.*, 1995). This was confirmed by RT-PCR of HL60 cells as they demonstrated the same RNA expression pattern of bestrophin1-4, in that bands were detected for both hBest1 and hBest3, and not hBest2 or hBest4, as in PMNs and eosinophils (see Figure 3.6). Primers used were as identified in section 2.2.1.2 and gave bands at the predicted sizes (Table 2.3). HL60s were not positive for annexin or PI and so were considered an appropriate model for human PMNs in this project as the focus was hBest1. To examine functional properties of bestrophin, HL60s were cultured and used to transfect DNA and over-express protein.

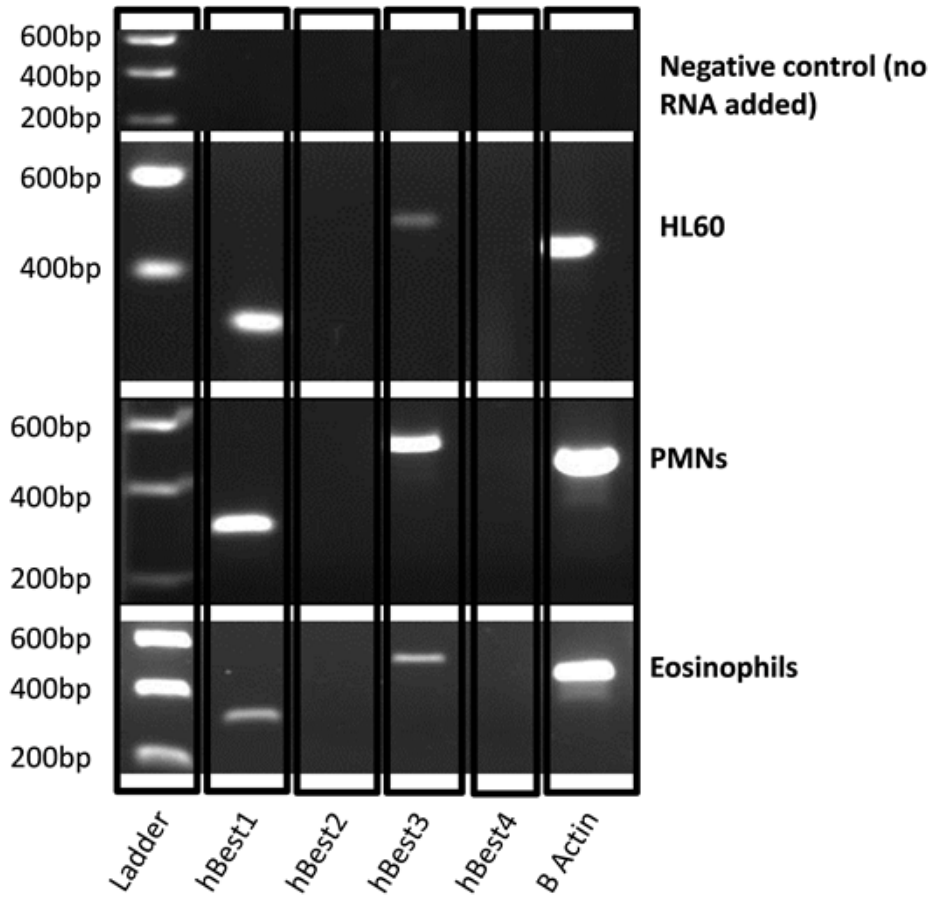

Figure 3.6: hBest1-4 expression in eosinophils, PMNs and HL60: Representative image of RT-PCR for eosinophils, PMNs (granulocytes) and HL60s for all bestrophins (n=3). Primers used as identified in section 2.2.1.2, and all bands at the predicted sizes as outlined in Table 2.3. HL60s were used as a model for PMNs in examination of hBest1-4. RT-PCR demonstrated a similar pattern of hBest1-4 in HL60s to both mixed PMNs and purified eosinophils as shown above with bands detected for hBest1 and hBest3, but not hBest2 or hBest4 in all three cell types. Nil control showed no bands when primers only (no RNA) were added RT-PCR master mix

3.3 Preparation of mRNA and proteins

Cells were prepared for RT-PCR and western blotting following a series of experiments to optimize mRNA and protein yield respectively. All prepared samples for RT-PCR were quantified using a NanoDrop spectrophotometer (Thermo Fisher Scientific) to establish concentration of mRNA yield as described in 2.3.1.3. Two preparations were compared to identify the optimum methodology for maximum yield. These are outlined in Section 2.3.1.1 and 2.3.1.2. Signosis buffer was used to prepare cell lysates and compared to the signal produced in RT-PCR using TRIzol® preparation. The amount of mRNA loaded was standardized as described in Section 2.3.1.3. Signosis buffer is recommended by the manufacturer for use when sample size is small as the resultant yield, and signal amplification, is greater. In this case, however, the preparation of mRNA was more effective using TRIzol®. There was a more distinct and brighter band for hBest1 using TRIzol® in comparison to Signosis lysate buffer. hBest3 was not detected at all using Signosis buffer. This was evident when compared to beta-actin positive control which was similar in each sample preparation (n=3) (Figure 3.7). It was concluded, therefore that in this project, TRIzol® preparation was more effective for extraction of mRNA from PMNs.

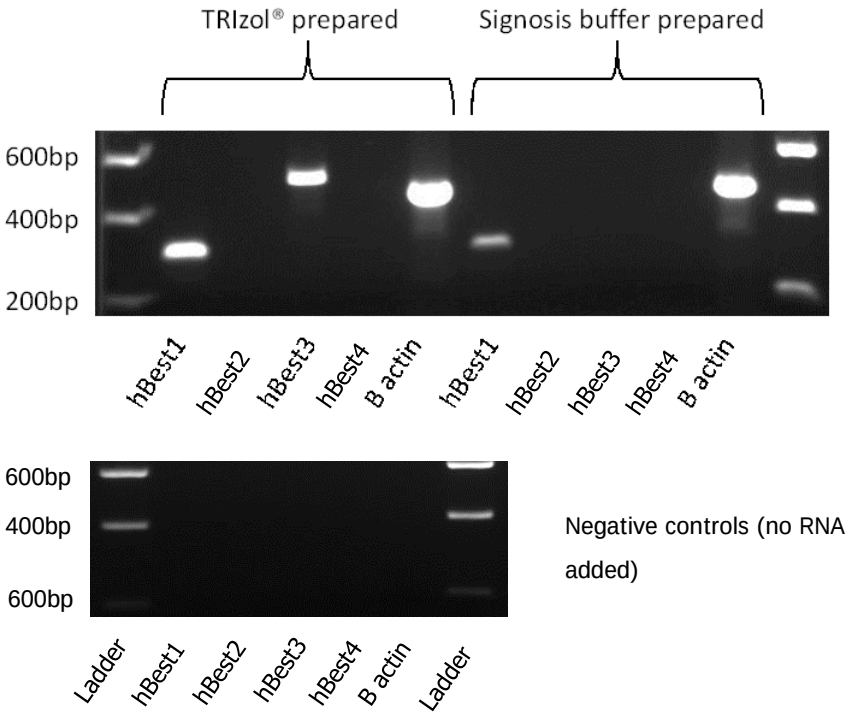

Figure 3.7: TRIzol® preparation compared to Signosis lysate buffer: Representative image of RT-PCR comparing TRIzol to Signosis buffer preparation (n=3). The two methods of mRNA preparation for RT-PCR were examined to optimize mRNA yield and signal amplification. There were clear differences between the two methods, concluding that for PMNs, the optimum preparation is using TRIzol® to examine the mRNA encoding hBest1-4. Negative control was performed at the same time as RNA added experiments

Protein samples were similarly tested for optimal preparation. Protein was extracted by either application of hot SDS and sonication method or RIPA buffer lysis (Section 2.4.1.1). On analysis of protein yield (Section 2.4.1.2) there was a greater concentration when using RIPA buffer to lyse the sample. For example, hot SDS preparation gave a granulocyte sample concentration of 127.3 µg/ml in comparison to RIPA buffer preparation from the same sample yielding a concentration of 875.9 µg/ml.

3.4 Specificity of primers for RT-PCR

A number of cell lines were screened using RT-PCR for hBest1-4, hCLCA1-4 and hANO1-10 (see Section 3.2.1 for results summary). Specific primers used are identified in Section 2.2.1.2, Table 2.3. Each positive band at the predicted size (as outlined in Table 2.3), in each cell type, was excised, purified and sent for nucleotide sequencing (Section 2.3.3.2). Using BioEdit software, the returned nucleotide sequencing was aligned with the appropriate nucleotide sequence held in the NCBI BLAST database (Figure 3.7 shows an example sequence alignment). All samples were sent for sequencing at least 3 times for confirmation. Table 3.5 summarizes the sequencing and which bands were confirmed, non-specific or indicative of a splice variant.

hBest3 has been found to have a transcript variant known as Best3 delta 2,3,6 (hBest3Δ2,3,6). This splice variant lacks exons 2, 3 and 6 which has functional implications for the protein as a Ca^{2+} activated Cl^- channel (Srivastava *et al.*, 2008) (see section 4.1.3.2 for discussion). The primer pair used for hBest3 did not span exons 2, 3 or 6 therefore were not specific enough to determine which transcript variant was being expressed.

All primers produced bands on RT-PCR, and the bands were considered to be the expected amplified product with the exception of hANO9 and hCLCA4.

Family	Summary of sequence analysis
hBest1-4 (figure 3.7 for an example of sequence alignment)	Bands were confirmed as 100% matching of sequence to hBest1and hBest3 respectively in all samples sent. hBest3 has 2 transcript variants however primers were not specific to either variant as hBest3Δ2,3,6 misses exons not spanned by primer pair. hBest2 produced a strong upper band at 1kilobase and a weaker band at 400bp. The upper band matched approximately 30% of the hBest2 sequence. hBest4 was confirmed as 100% matching the BLAST sequence in CFPAC cells however in another sample, there was a higher band visualized at approximately 900bp which was non-specific to any part of the hBest4 sequence.
hCLCA1-4	All bands for hCLCA1-3 were confirmed as 100% matching the nucleotide sequence on NCBI BLAST database. hCLCA4 was not confirmed. One sequence returned with no clear peaks so was considered to have been contaminated. All other bands sequenced were not specific despite different primer sequences. Due to the focus of the project, no further sequencing was performed due to constraints of resourcing.
hANO1-10	hANO1-8 and hANO10 were 100% confirmed for sequence alignment, however, all bands returned for hANO9 were non-specific

Table 3.5: Summary of sequence alignments for RT-PCR: All bands visualized were sent for sequencing and aligned to NCBI BLAST database using BioEdit software. Table gives a summary of all sequence alignments for RT-PCR. All samples were sent at least 3 times (n=3).

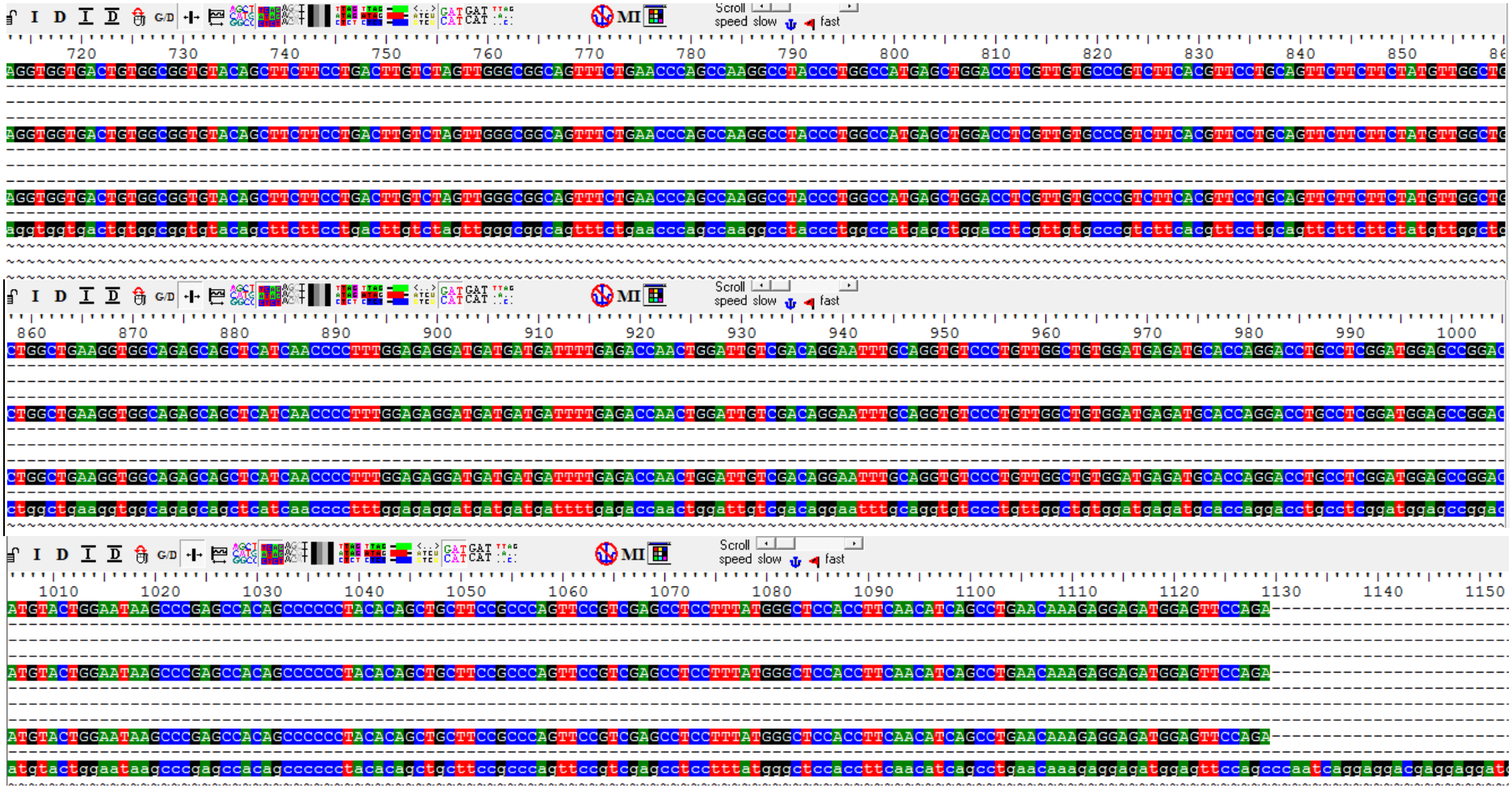

Figure 3.8: Nucleotide sequence alignment for hBest1: Alignment of nucleotide sequences demonstrating 100% alignment. A-C are samples prepared from RT-PCR bands and sent. D is cDNA sequence retrieved from NCBI.

3.5 Characterization and specificity of antibodies

The focus of this project was primarily human bestrophin 1 to human bestrophin 4. In order to demonstrate specificity of antibodies a number of cells were phenotyped to exclude any cells that had endogenous bestrophin 1-4. A number of cell lines were screened using RT-PCR which included Vero-SG, CHO and HEK293. CHO cells were the only samples that did not have endogenous hBest1-4 (n=3, see Figure 3.9).

CHO cells were cultured as per Section 2.1.1.4. Four flasks were cultured to a confluence of approximately 80%. DNA for hBest1-4 was transfected into separate samples using lentiviral transfection and bacterial delivery via *E.Coli* (Section 2.5) to over-express proteins which were then examined using RT-PCR and western blot. Each sample was successfully transfected as demonstrated in Figure 3.10 (n=3). Each transfected sample only expressed the transfected bestrophin with no other bands seen. CHO transfected with hBest4 was however very faint. CHO nil expressed only β actin as a negative control and HEK293 expressed hBest1, hBest3 and β actin as a positive control, as per previous RT-PCR. All bands were sent for sequencing with 100% alignment to NCBI BLAST database using BioEdit alignment software (method as outlines in Section 2.3.3.2).

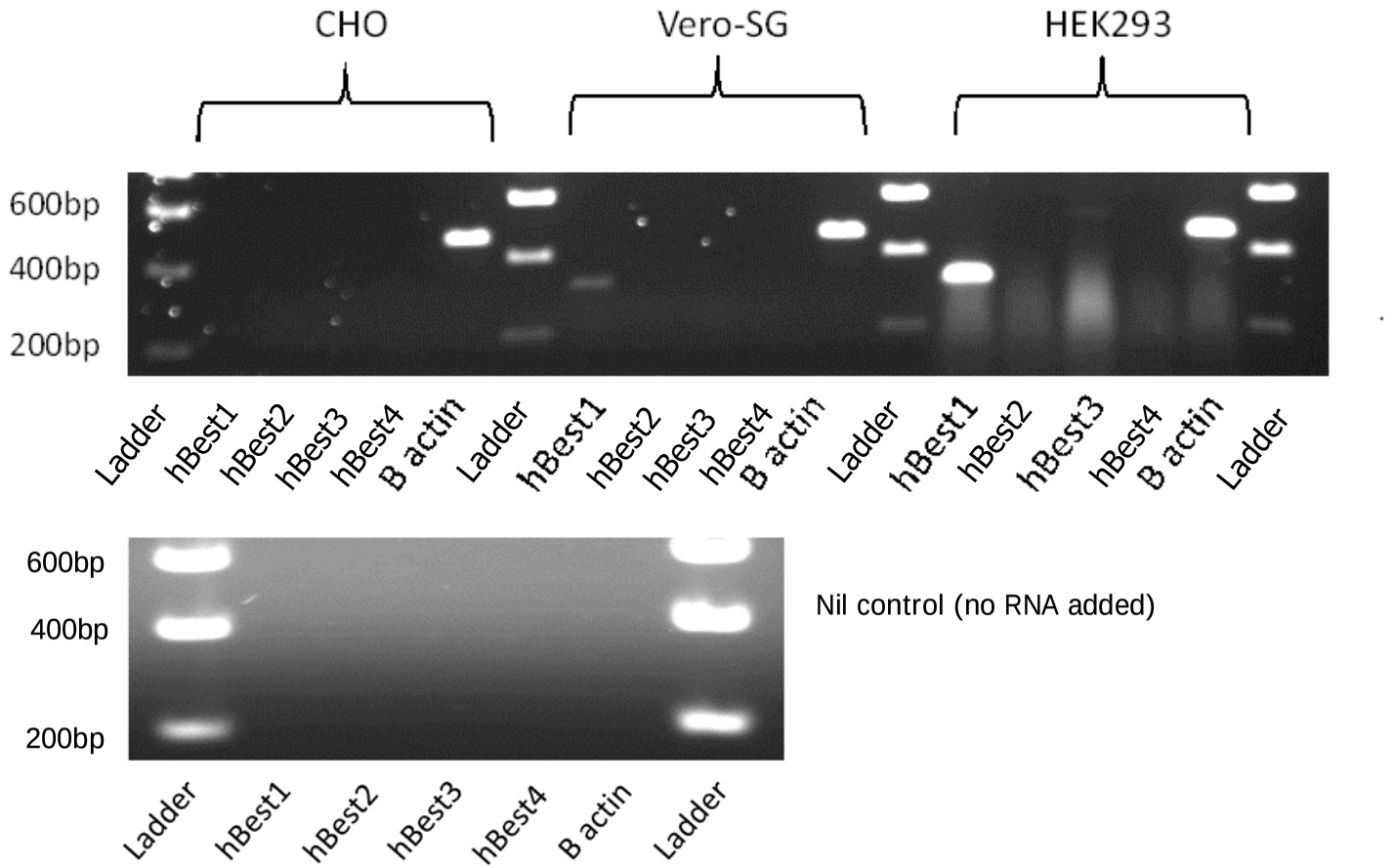

Figure 3.9: hBest1-4 expression in CHO, Vero-SG and HEK293 cells: Representative RT-PCR image for hBest1-4 screening (n=3). All samples were screened using RT-PCR to identifiy any endogenous hBest1-4. Vero-SG had a weak band for hBest1 whereas HEK293 had a strong band for hBest1 and a weaker band visualized for hBest3. HEK293 and Vero-SG therefore were not appropriate for use in transfection assays as endogenous hBest1 and hBest3 may impact on findings. Results therefore could not be clearly attributed to individual proteins. Nil controls performed at the same time as RNA added

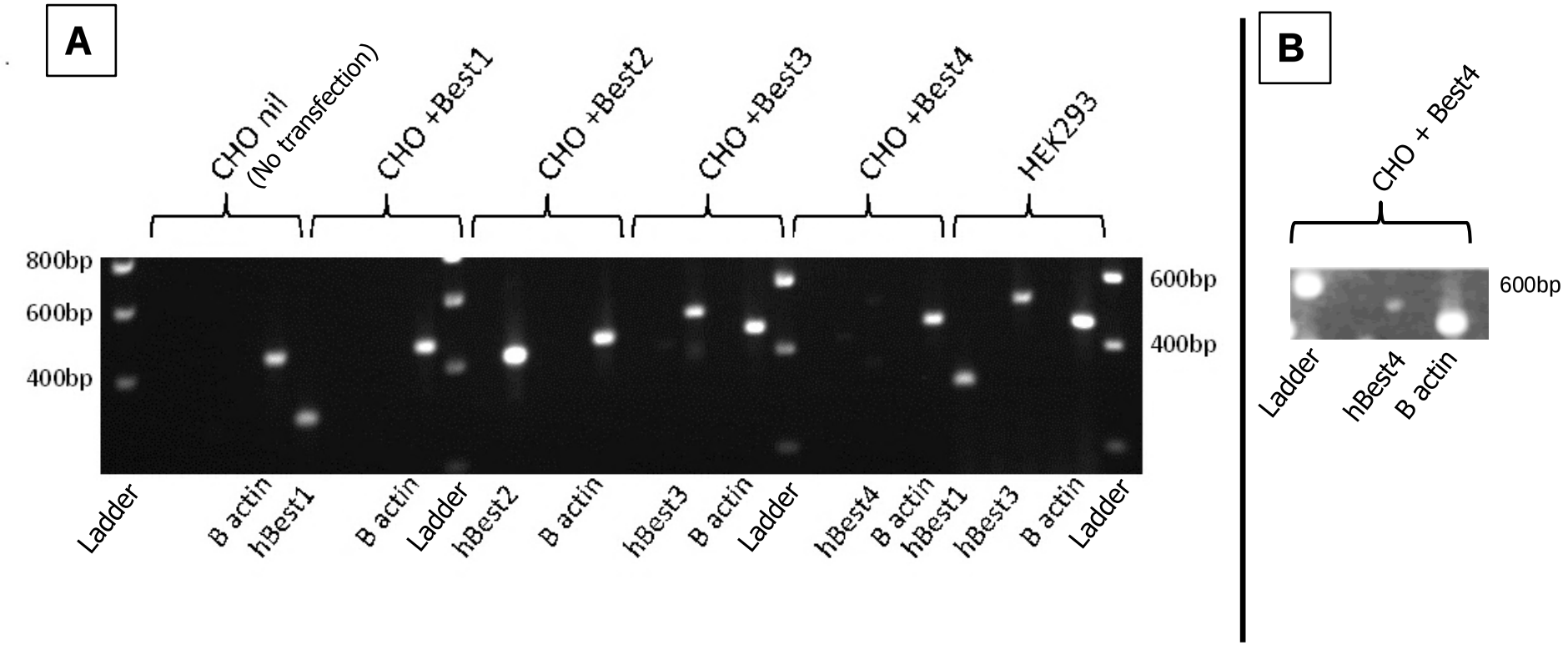

Figure 3.10: RT-PCR demonstrating successful transfection of CHO with hBest1-4: A: Representative RT-PCR image (n=3). All samples were successfully transfected with no extraneous bands visualized. For each sample, hBest1-4 was screened as in Figure 3.9. Sample run in each lane however not labelled to ensure clarity of respresentation. hBest4 band visualised in CHO transfected with Best4 however very weak. B: shows RT-PCR image for this band only with altered contrast for visualisation. All bands were at the expected weight and confirmed on sequence analysis

Antibodies for hBest1-4, used for flow cytometry and western blotting, were characterized to ensure specificity. Each transfected sample was lysed with RIPA buffer to prepare for Western Blot analysis. Each was loaded onto a single gel (using methodology as outlined in Section 2.4). Four gels were prepared and loaded with the same sample distribution across wells; CHO (nil transfected), CHO transfected hBest1, CHO transfected hBest2, CHO transfected hBest3, CHO transfected hBest4 and HEK293 as a positive control. Each membrane was labelled with either hBest1, hBest2, hBest3 and hBest4 respectively (Table 2.9 for antibodies used in western blotting with expected molecular weights). The antibodies used for hBest2, hBest3 and hBest4 were not specific and did not label CHO transfected with appropriate bestrophin (n=3). One antibody used for hBest1 was a mouse monoclonal anti-bestrophin (E6-6) (Novus Biologicals). On western blotting there was a 68kDa band visualized as expected for hBest1, however, there were bands for all samples including the nil which on RT-PCR did not express any bestrophins (Figure 3.11). This was considered non-specific, however, transfection was confirmed for hBest1 using the GFP tag on the plasmid. A similar result was found using a similar clone (AbCam ab2182, clone E6-6).

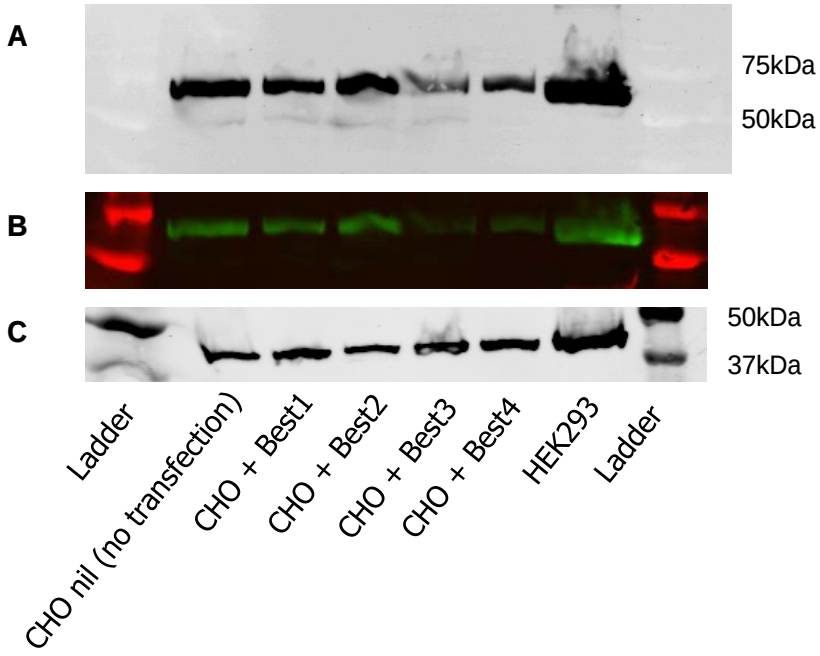

Figure 3.11: Antibody characterization using anti-bestrophin mouse monoclonal antibody: Image representing hBest1 labelling (expected molecular weight of 68kDa) for antibody characterisation. Repeated n=3 also using an alternative antibody with a similar clone. Bands visualized in all samples demonstrating non-specific binding. A is a greyscale image of anti-bestrophin label and B is colourized. Bestrophin visualized as a green band. C is greyscale of β actin as a positive house-keeping control

hBest1 transfected into CHO included a green fluorescent protein (GFP) at the C-terminus. To ensure accurate transfection three samples were loaded onto a gel for Western blot; CHO (nil with no transfection), CHO transfected with pRK5-hBest1-IRES-eGFP and a positive GFP control using MEF feeder cells with a GFP tag. This shows that the hBest1 with GFP tag was successfully transfected by using an antibody to label the GFP (Figure 3.12)

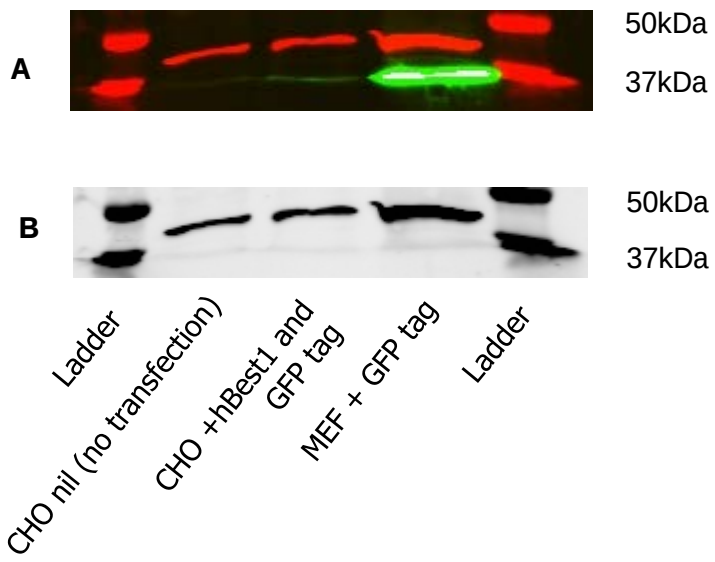

Figure 3.12: Western blot of anti-GFP labelling to demonstrate successful transfection: A is a colourised image with green labeling for green fluorescent protein and red for anti actin. Bands evident in positive control and CHO transfected with pRK5-hBest1-IRES-eGFP (well 2) and positive GFP control (well 3). GFP band at the expected molecular weight of 37kDa. B is a grey scale image of anti-actin labelling as a control for sample loading (band as expected for β actin at 43kDa). N=3

Further CHO samples were transfected and alternative antibodies used for hBest1 as the focus of the project. An antibody specific to hBest1 was identified as Bst-121AP, a rabbit polyclonal supplied by FabGennix Inc (Texas) (Figure 3.13). As identified by the manufacturer, this was appropriate for western Blot and immunohistocytochemistry analysis.

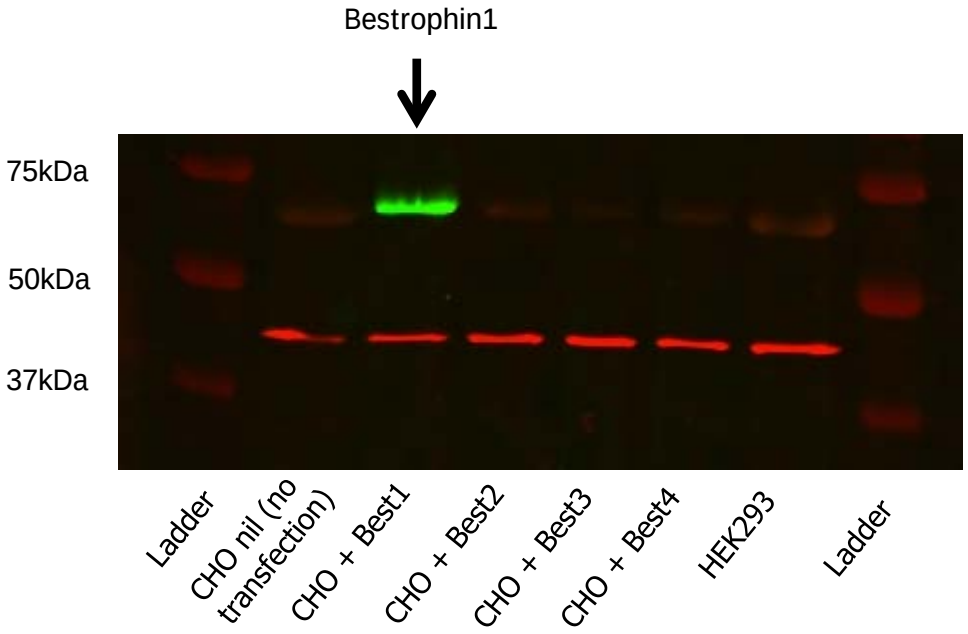

Figure 3.13: Antibody characterization for Bst-121AP (FabGennix): Clear green band visualized at the expected molecular weight of 68kDa, in CHO cells transfected with bestrophin1 and none in other transfected samples demonstrating specificity. HEK293 used as a positive control with a feint green band. Red bands depict β actin as a positive loading control. N=3

CHAPTER 4: EXPRESSION OF POTENTIAL CHLORIDE ION CHANNELS

4.1 Gene expression determination by RT-PCR

RT-PCR was performed on multiple cell types to amplify mRNA signals encoding hCLCA1-4, hBestrophin1-4 (hBest1-4) and the anoctamin (hANO1-10) family. The evidence presented in chapter 1 identifies that chloride ion channels may be implicated in granulocyte function and to date, the molecular candidates have yet to be identified. It has been shown that there is an increase in cytosolic calcium prior to recruitment and activation of pro-inflammatory processes in neutrophils. This suggests that chloride ion channels may be calcium activated. hBest1 was the focus for RT-PCR as a prime candidate. hANO1 is also examined as another potential calcium activated chloride ion channel. Chapter 1 also identified that there may be a complex relationship between hANO1, hBest1 and hCLCA1. Therefore, the RNA expression for all 3 potential candidates was examined by RT-PCR, and potential relationships identified.

4.1.1 Results

Primers used as in section 2.2.1.2 and Table 2.3. Each reaction had a corresponding nil control where no RNA was added. All bands have been confirmed by gel extraction and sequence analysis (JIC, Norwich). Primers for hCLCA4 are yet to provide a clear band for any cell line. hANO9 primers have provided bands, however, on sequence verification analysis these are non-specific. Epithelial cell lines were used as controls for RT-PCR technique and primers.

4.1.1.1 hCLCA expression

Eosinophils and PMNs express the same pattern of mRNA encoding hCLCA1-4 (Figure 4.1 of expression pattern for PMNs). hCLCA1 was detected in both PMNs (n=5) and eosinophils (n=6), however a weaker signal in PMNs was observed. HL60s however do not express hCLCA1 (n=4).

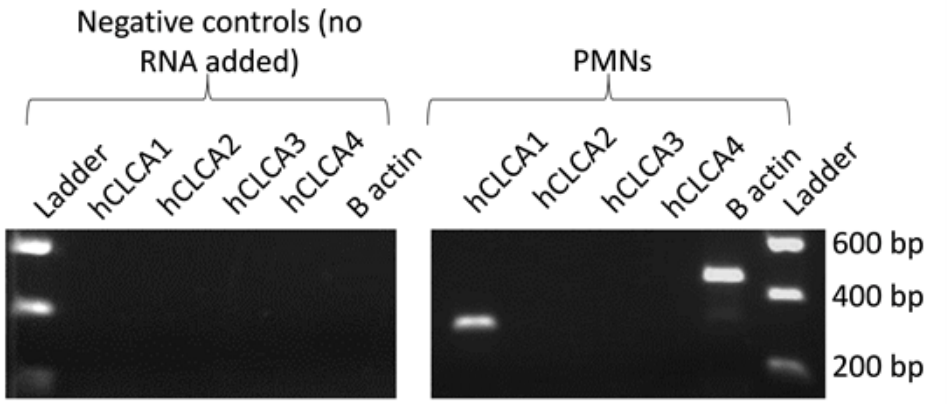

Figure 4.1: RT-PCR of PMNs for hCLCA 1-4 mRNA signal: Representative RT-PCR image of bands visualised for PMNs using primers for hCLCA 1-4. hCLCA1 at 322bp has been confirmed by sequence analysis. No bands visualised for hCLCA2-4. Beta actin was used as a control for RT-PCR enzymes and sample loading (n=5). Negative controls were master mix with primers only added and no RNA.

A549 and NAEC express hCLCA1 and 3 (Figure 4.2 & 4.3). The SAEC cells were positive for hCLCA1-3 (Figure 4.4) whereas CFPAC only clearly expressed hCLCA1, Calu-3 and HEK293 only expressed hCLCA2 (Figure 4.5). The focus of the current project was

bestrophin and therefore the implication of this spread was not considered. RT-PCR was performed however to identify positive controls and relationships to bestrophin 1.

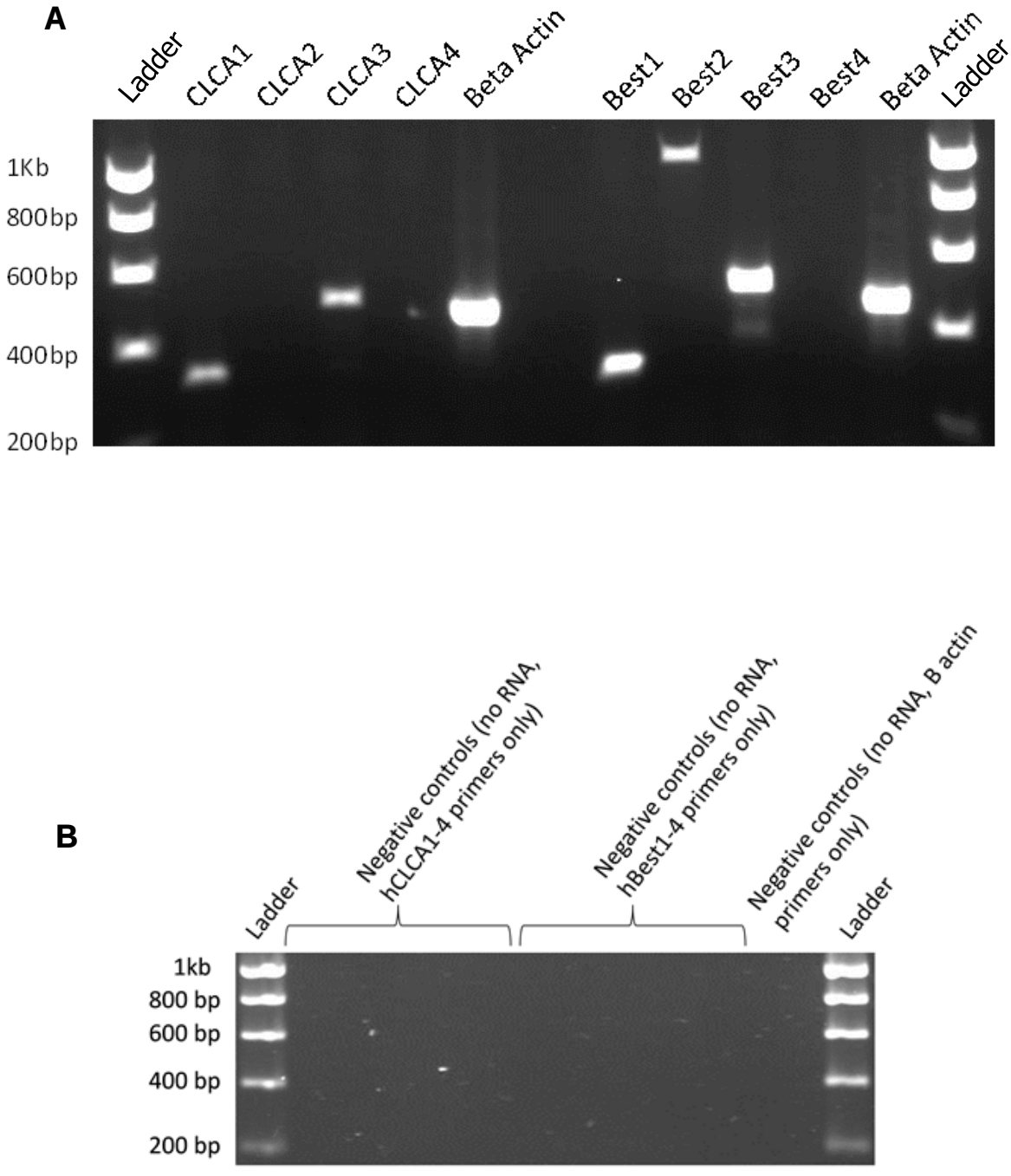

Figure 4.2: RT-PCR of A549 for hBest1-4 and hCLCA 1-4: A. Representative image of RT-PCR bands visualised for A549 cell line using primers for human hBest1-4 and hCLCA1-4. All bands confirmed by gel extraction and sequence analysis. N=3 for all RT-PCR reactions. B. Negative controls for all hCLCA1-4, hBest1-4 and beta actin primers where no RNA is added.

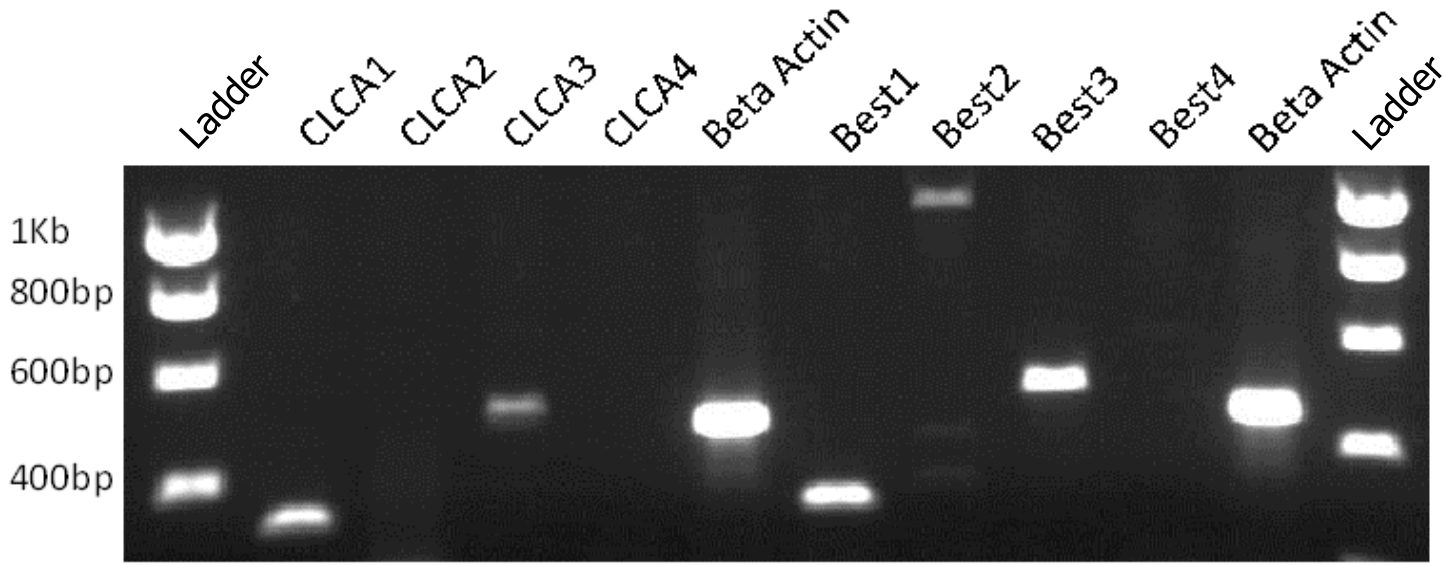

Figure 4.3: RT-PCR of NAEC for hBest1-4 and hCLCA 1-4: Representatvie image of RT-PCR bands visualised for NAEC cell line using primers for hBest1-4 and hCLCA1-4 (n=3). hBest2 as in Figure 4.7. Nil controls as in Figure 4.2 as all performed at the same time

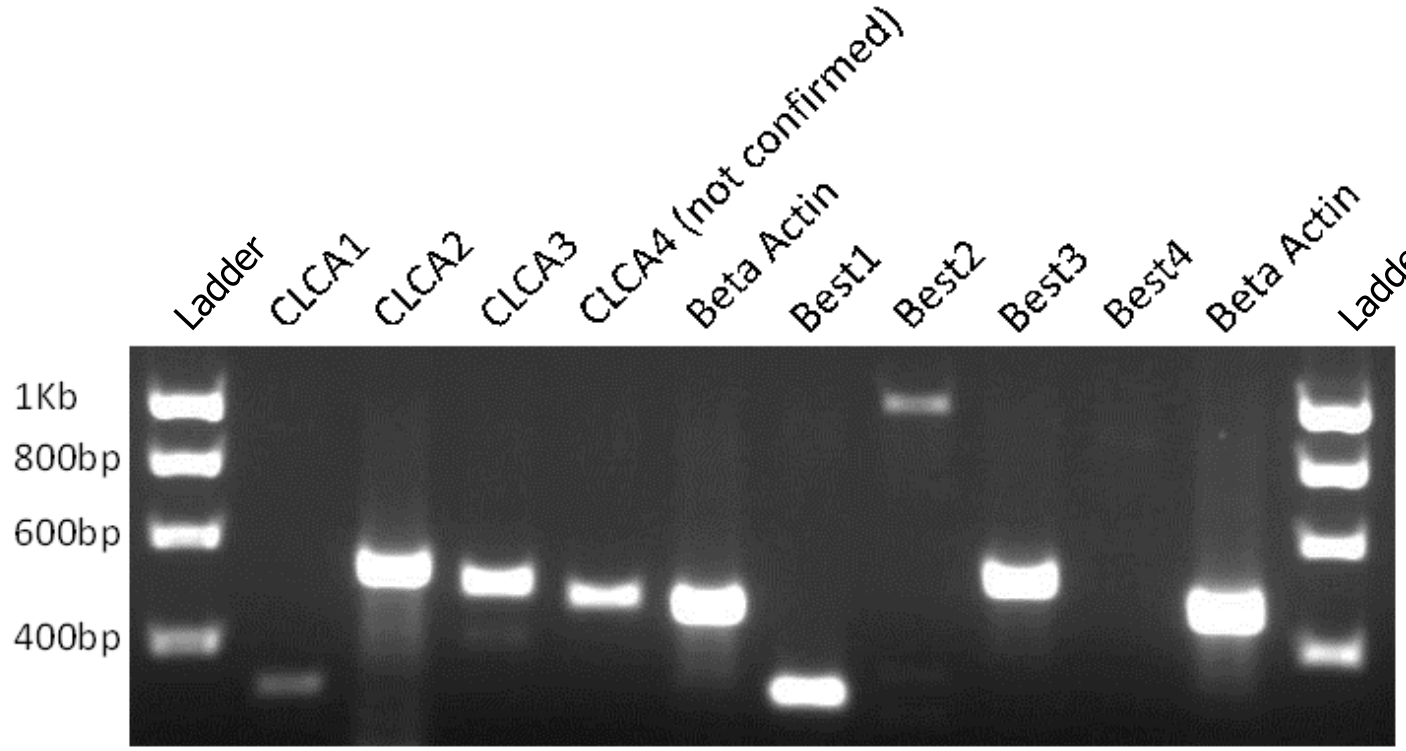

Figure 4.4: RT-PCR of SAEC for hBest1-4 and hCLCA 1-4: Representative image of RT-PCR bands visualised for SAEC cell line using primers for hBest 1-4 and hCLCA1-4. Band visualised for hCLCA4 has been extracted and purified however as yet unconfirmed on sequence analysis. hBest2 on sequence analysis appears to be a splice variant (n=3). Nil controls as in Figure 4.2 as all performed at the same time

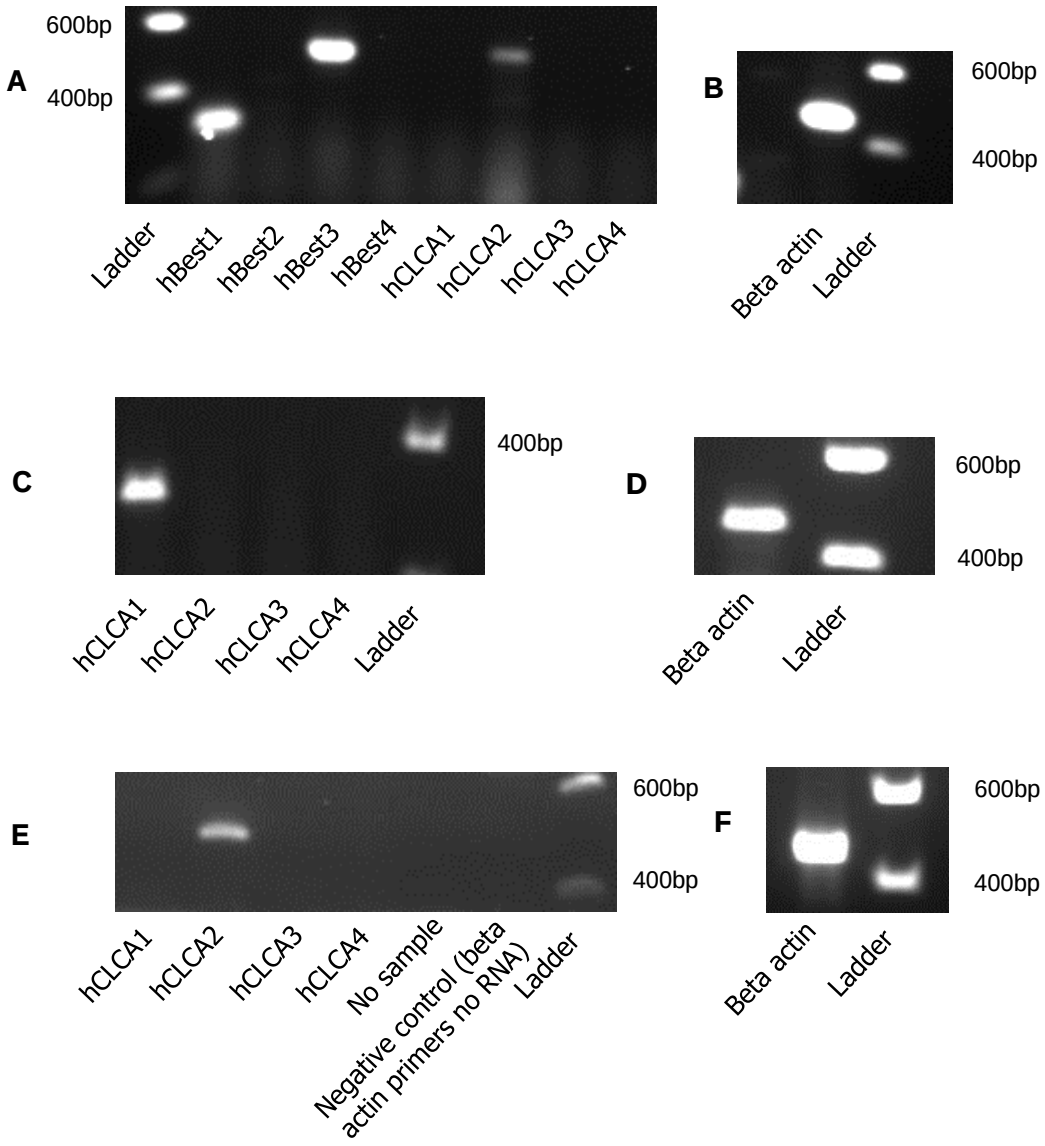

Figure 4.5: RT-PCR for HEK293, CFPAC and Calu-3 showing hCLCA1-4 expression: A. HEK293 cells screened for hBest1-4 and hCLCA1-4. Bands at expected sizes as outlined in section 2.3.2. hBest1, hBest3 and hCLCA2 expressed (n=3). Only positive bands labelled for clarity of figure B. Beta actin as positive control for HEK293. C. CFPAC screened for hCLCA1-4. Positive band at expected size for hCLCA1. D. Beta actin for CFPAC at expected size. E. Calu-3 demonstrating a band visualised for hCLCA2 at the expected size and F. Beta actin for Calu-3. All Calu-3, HEK293 and CFPAC n=3. Nil controls (no RNA) as in Figure 4.2.

4.1.1.2 Bestrophin expression

Mixed PMNs, purified eosinophil population and HL60s have clear expression of mRNA encoding hBest1 and 3 (Section 3.2, Figure 3.3). In addition, hBest1 and hBest3 are present in all cells examined, regardless of potential biological location.

Results were less comparable for the epithelial cell lines. As with the PMNs, expression of hBest1 mRNA was demonstrated on all epithelial cell lines (Figures 4.2 – 4.4) and for all except Calu-3, hBest2 was also confirmed. hBest3 was confirmed on all cell lines. Calu-3 had an mRNA signal for hBest4 however this was not at the expected size and on sequence analysis may potentially be a splice variant. CFPAC and SAEC both expressed hBest4. Figures 4.2, 4.3, and 4.4 present images of the agarose gels for A549, SAEC and NAEC for hBest1-4 and hCLCA 1-4. Figure 4.6 presents an image of SAEC and CFPAC for hBest1-4 with positive controls. Sequence analysis for hBest2 confirmed that the band at 1Kb matched to the last 3rd of the hBest2 sequence therefore this may represent a splice variant.

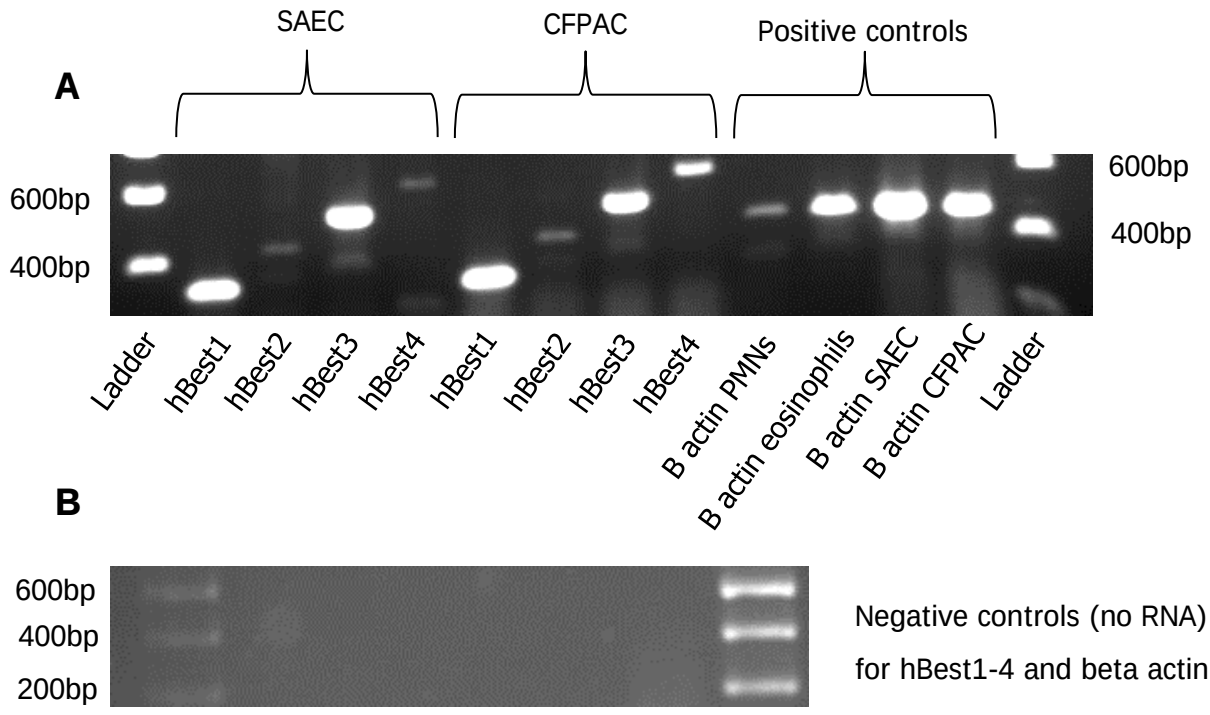

Figure 4.6: RT-PCR of SAEC and CFPAC for hBest1-4: A. Representative image of RT-PCR bands visualised for SAEC and CFPAC cell lines using primers for hBest 1-4. hBest2 on sequence analysis appears to be a splice variant (n=3). B. Negative controls were no RNA added to the master mix and primers.

4.1.1.3 hANO expression

For the anoctamin family, there was 100% sequence alignment confirmed for all with the exception of hANO9 which when analysed was non-specific. hANO6, hANO8 and hANO10 were expressed in all cell lines both commercial and primary. Of note however, hANO7 was only visualized in PMNs and eosinophils and none of the other samples examined. This may indicate a unique role of hANO7 in the function of PMNs. That it was not visualized in HL60s may also indicate a link between cellular differentiation. hANO1 was expressed in PMNs, eosinophils and SAECs however not in HL60s. It was visualized and confirmed in all other cell lines (Figure 4.7 and 4.8 shows example RT-PCR gels).

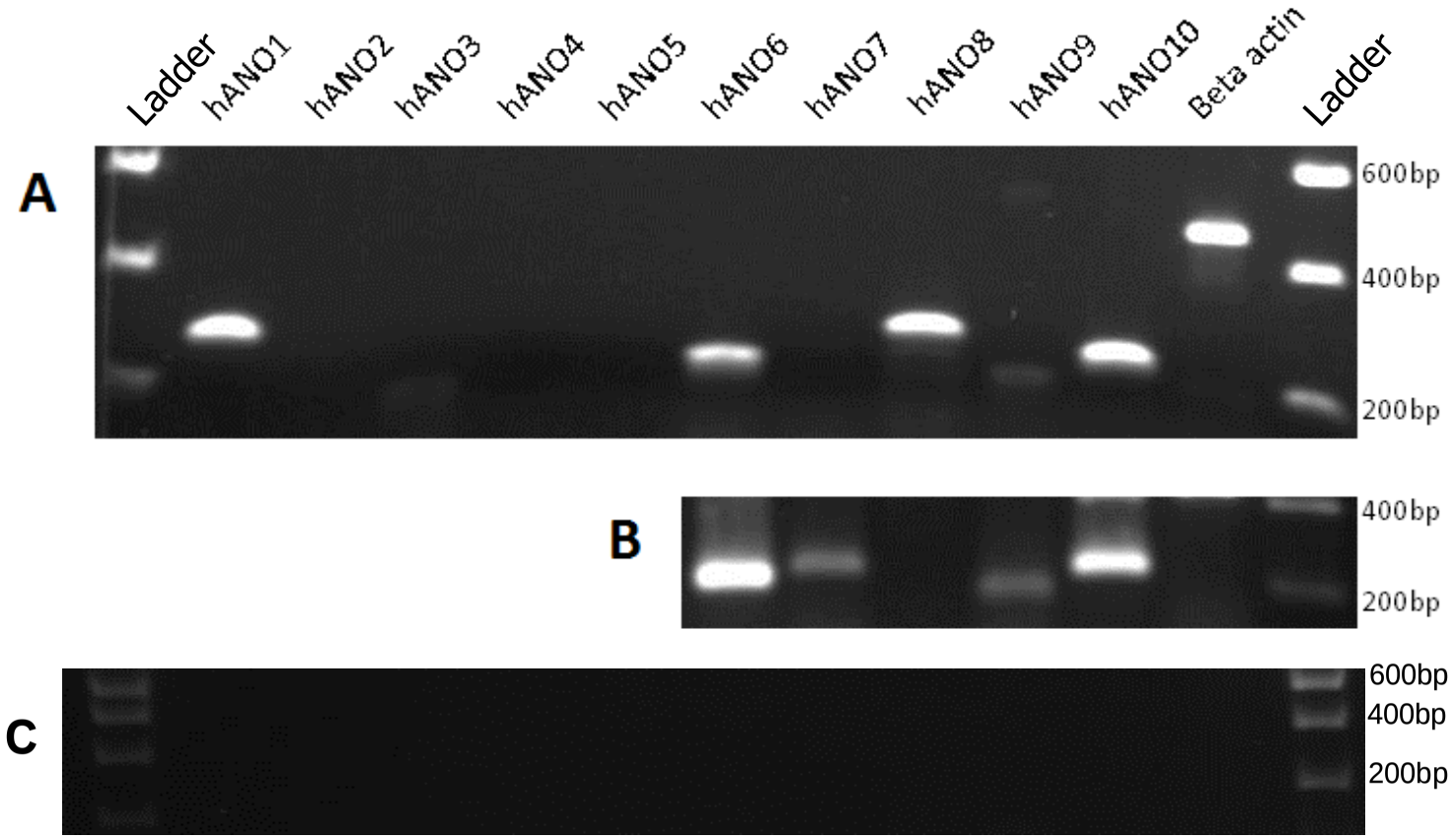

Figure 4.7: RT-PCR of PMNs for hANO1-10: Representative image of RT-PCR mRNA bands visualised for hANO1-10 on a mixed PMN population. A. A full agarose gel with hANO1, 6, 8 and 10 visualised. hANO9 a feint band which on sequence analysis is non-specific. B. A later RT-PCR with a band visualised for hANO7. C are negative controls for all ANO primers and beta actin (no RNA added) All other bands confirmed by gel extraction and sequence analysis. hANO5 was identified in a later RT-PCR

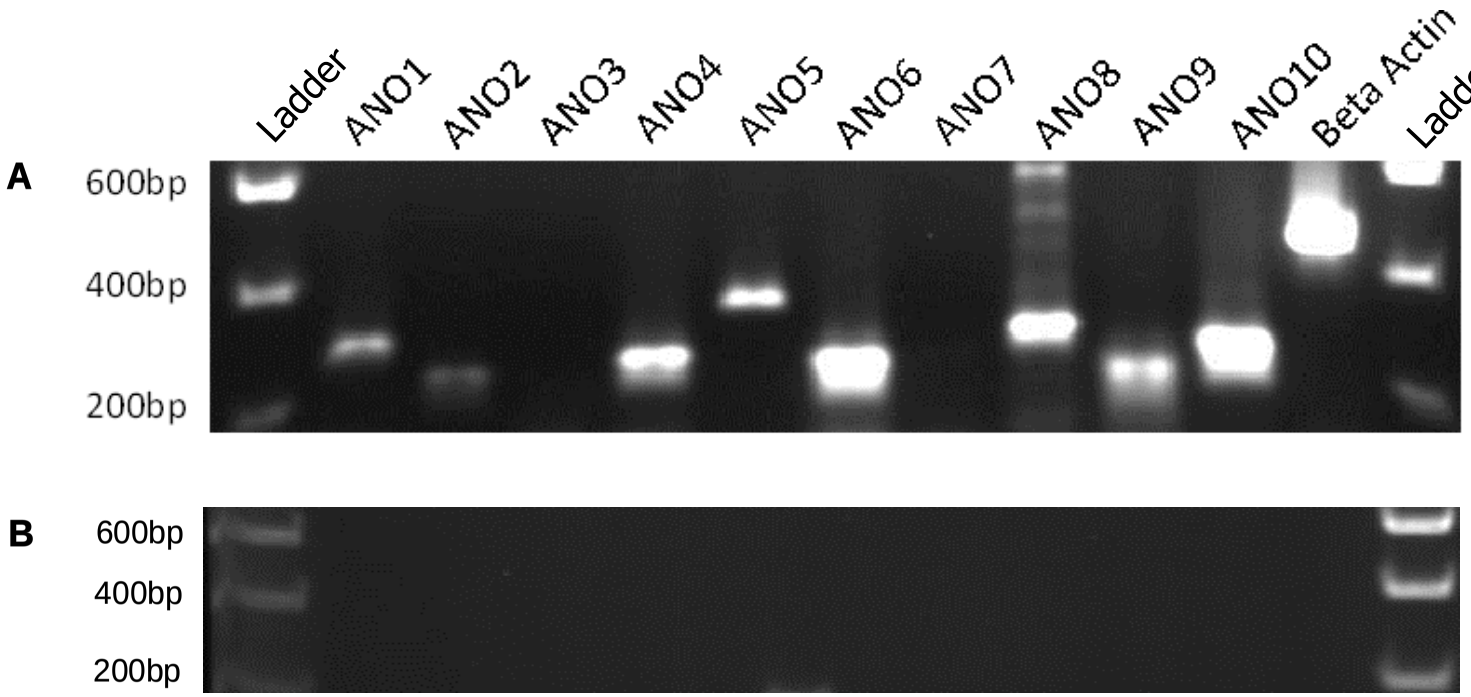

Figure 4.8: RT-PCR of SAEC for hANO1-10: A. Representative image of RT-PCR bands visualised for SAEC cell line using primers for hANO1-10. All bands extracted and purified and confirmed using sequence analysis. hANO9 on sequencing is non-specific. B negative controls for all hANO primers and beta actin (no RNA added)

4.1.1.4 RT-PCR summary and densitometry

RT-PCR was performed on multiple cell types to amplify mRNA signals encoding hCLCA1-4, hBestrophin1-4 (hBest1-4) and the anoctamin (hANO1-10) family. Primers used as in section 2.2.1.2 and Table 2.3. Table 4.1 summarises all expressional screening using RT-PCR where each reaction was repeated a minimum of 3 times (n=3). Each reaction had a corresponding nil control where no RNA was added. All bands have been confirmed by gel extraction and sequence analysis (JIC, Norwich). Primers for hCLCA4 are yet to provide a clear band for any cell line. hANO9 primers have provided bands, however, on sequence verification analysis these are non-specific. Epithelial cell lines were used as controls for RT-PCR technique and primers.

Densitometry was performed on bands for hCLCA1, hBest1 and hANO1 for eosinophils (n=6), granulocytes (n=5), HL60s (n=4) and SAEC (n=3) (Table 4.2 for optical density of bands normalised to β actin). Optical density (normailsed to β actin) was plotted as a bar chart, with error bars (Figure 4.9), and scatter plots are presented to establish any correlation between expression of genes (Figure 4.10 and 4.11).

hCLCA1 was detected in both PMNs (n=5) and eosinophils (n=6), however a weaker signal in PMNs was observed. HL60s however do not express hCLCA1 (n=4). On analysis of variance (ANOVA), this difference between cells was statistically significant ($P<0.05$) (Table 4.2, * in Figure 4.9).

It appears that hCLCA1 is up-regulated in the epithelial respiratory tissues (A549, NAEC and SAEC) (Figure 4.2, 4.3, and 4.4) relative to PMNs, however not eosinophils. Mean optical density (normalised to

β actin) for SAEC was 0.278, greater than PMNs (0.223) however less than eosinophils (0.299). This observed difference was statistically significant ($P<0.05$). The expression pattern, of hCLCA1, hBest1 and hANO1 was significantly different within each sample ($P<0.0001$). hCLCA1 was plotted against both hBest1, and hANO1 and correlation coefficients calculated (Figure 4.10 and Figure 4.11). There was a negative correlation (coefficient -0.62) between hCLCA1 and hBest1, in that as the expression of hCLCA1 increases, hBest1 decreases ($P<0.0005$). Whilst a positive correlation (0.84) was observed between hCLCA1 and hANO1, this was not statistically significant ($P>0.1$).

Semi-quantification using densitometry has shown that the expression of hBest1 is significantly greater than either hANO1 or hCLCA1 in PMNs, eosinophils, HL60s and SAECs ($P<0.0001$) (Figure 4.9). There is a negative correlation between hCLCA1 expression and hBest1 (coefficient -0.62, $P<0.0005$) (Figure 4.10). Therefore as hCLCA1 expression increases, hBest1 decreases. It has also been shown that there is a weak negative correlation between hBest1 which is statistically significant (coefficient -0.36, $P<0.0001$) (Figure 4.11). The expression of hBest1, as with hCLCA1 is greatest in eosinophils and least in PMNs (Figure 4.9). This difference across cell samples is statistically significant ($P<0.05$, $*^2$ in Figure 4.9).

HL60s were compared to both eosinophils and PMNs to establish whether they were an appropriate model for functional analysis of granulocytes. Using an unpaired 2 tailed students t-test, there was no statistically significant difference between gene expression of hBest1 in PMNs ($n=5$) and HL60s ($n=4$) ($P>0.6$). Conversely, the difference in gene expression of hBest1 in HL60s and eosinophils ($n=6$) was statistically significant ($P<0.05$).

	PMNs	Eosinophils	HL60	A549	NAEC	SAEC	CFPAC	Calu-3	HEK293
CLCA1	√	√ weak	x	√	√	√	√	x	x
CLCA2	x	x	x	x	x	√	x	√	√
CLCA3	x	x	x	√	√	√	x	x	x
CLCA4	x	x	x	x	x	x	x	x	x
Bestrophin 1	√	√	√	√	√	√	√	√	√
Bestrophin 2	x	x	x	√	√	√	√	x	x
Bestrophin 3	√	√	√	√	√	√	√	√	√
Bestrophin 4	x	x	x	x	X	√	√	x	x
ANO1	√	x	x	√	√	√	√	√	√
ANO2	x	x	x	√	√	√	√	x	√

ANO3	x	x	x	x	x	x	√	x	√
ANO4	x	x	x	√	√	√	x	√	√
ANO5	√	x	√	√	√	√	√	√	√
ANO6	√	√	√	√	√	√	√	√	√
ANO7	√	√	x	x	x	x	x	x	x
ANO8	√	√	√	√	√	√	√	√	√
ANO9	x	x	x	√	√	√	x	√	√
ANO10	√	√	√	√	√	√	√	√	√

Table 4.1: Summary of all results for RT-PCR screening: Table to summarize all RT-PCR screening (human cells). CLCA4 and ANO9 are not confirmed on sequencing and alignment. Those ticked are visualized bands which have been confirmed. PMN, eosinophils and HL60s were screened to establish whether HL60s could be used as a reliable model for human PMNs. Other cell lines were screened to establish any patterns in expression of RNA and to identify possible cell lines that could be employed as positive controls. All RT-PCR was repeated 3 times (n=3)

	hCLCA1		hBest1		hANO1		β actin
Cells/Sample	Optical density of band	Normalised to β actin (3dp)	Optical density of band	Normalised to β actin (3dp)	Optical density of band	Normalised to β actin (3dp)	Optical density of band
PMNs (n=5)							
1	12325	0.051	16943	0.070	10897	0.045	243712
2	0	0	81889	0.850	6942	0.072	96390
3	26027	0.190	52513	0.383	12530	0.091	137173
4	22967	0.461	38811	0.780	-	-	49776
5	26911	0.191	93381	0.664	-	-	140675
Mean	22058	0.223	56707	0.549	10123	0.069	133545
Standard deviation	6705	0.172	31218	0.322	2873	0.023	71761
Eosinophils (n=6)							
1	17867	0.230	0	0	16031	0.206	77775
2	49827	0.215	156366	0.674	15637	0.067	232169
3	21726	0.232	29359	0.314	8786	0.094	93619
4	6239	0.521	27982	2.336	-	-	11979
5	0	0	45577	0.388	-	-	117572
6	-	-	34357	0.332	-	-	103428
Mean	23915	0.299	58728	0.809	13485	0.122	106090
Standard deviation	18486	0.148	55018	0.866	4074	0.074	71901

HL60 (n=4)							
1	0	0	77588	0.580	0	0	133705
2	0	0	12206	0.279	0	0	43775
3	0	0	63988	0.895	0	0	71502
4	0	0	54519	0.833	0	0	65450
Mean	0	0	52075	0.647	0	0	78608
Standard deviation	0	0	28216	0.281	0	0	38612
SAEC (n=3)							
1	52581	0.376	70635	0.505	55233	0.395	139825
2	40732	0.310	69904	0.532	44234	0.337	131325
3	27302	0.147	131257	0.708	43537	0.235	185487
Mean	40205	0.278	90599	0.582	47668	0.322	152212
Standard deviation	12648	0.118	35213	0.110	6561	0.081	29128

Table 4.2: Densitometry performed on bands visualised in PMNs, eosinophils, HL60s and SAEC for hCLCA1, hBest1 and hANO1: Bands were visualised and optical density was calculated as a product of mean grey area and band area in pixels. Optical densities for each were normalised to β actin. '0' indicates samples where no band was visualised. These were excluded from the calculation of mean values. ANOVA was performed to establish whether there was a difference in the sample means, and that they are considered to be taken from different populations. Where the critical F value was less than the *f* value the null hypothesis was rejected. Statistical significance was accepted at $P<0.05$. The expression of hCLCA1, hBest1 and hANO1 was significantly different within each sample ($P<0.0001$). The expression of each hCLCA1, hBest1 and hANO1 was statistically different across each sample ($P<0.05$).

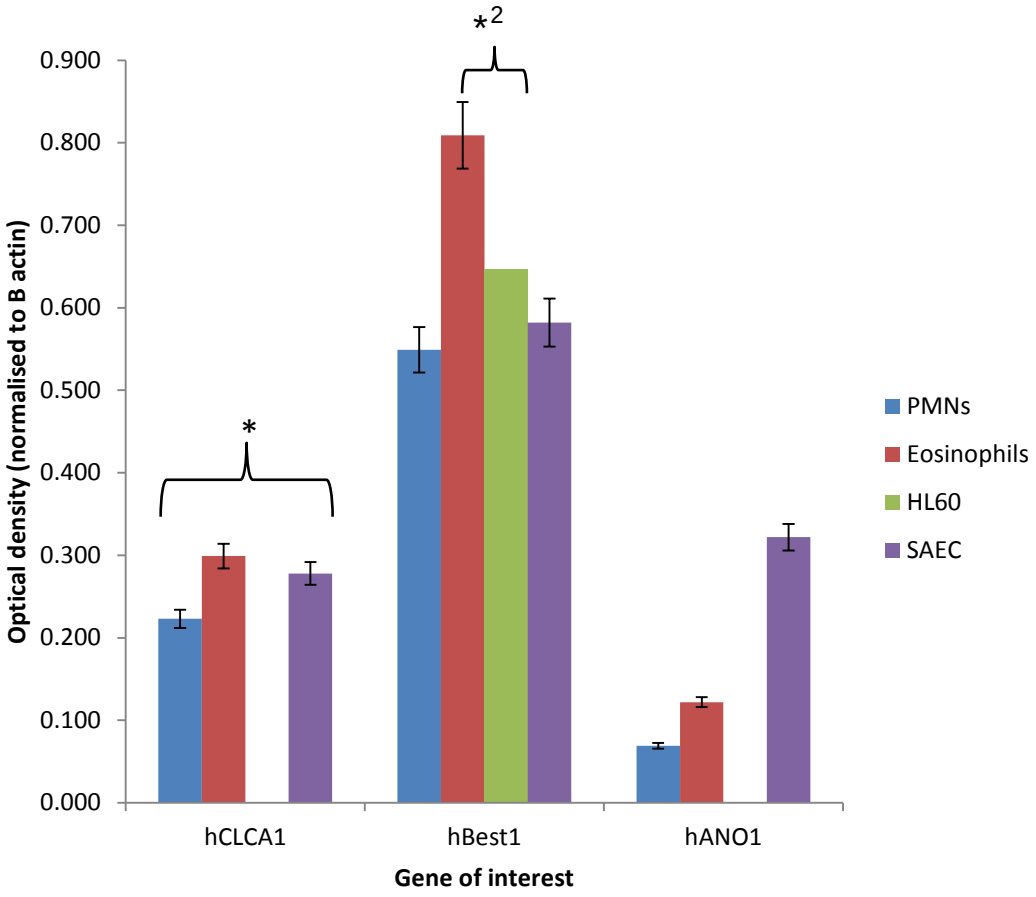

Figure 4.9: Expression of hCLCA1, hBest1 and hANO1 as optical density of bands visualised in PMNs, eosinophils, HL60s and SAEC (outlined in table 4.1): Optical density for hBest1, hCLCA1 and hANO1 in PMNs (n=5), eosinophils (n=6), HL60s (n=4) and SAECs (n=3). Error bars relate to standard error mean. Differences observed between samples, and within samples for expression of hCLCA1 and hANO1 were considered statistically significant as determined using 2-way ANOVA ($P<0.05$, * above, and $P<0.0001$ respectively). hBest1 gene expression was not significantly different between PMNs and HL60s ($P>0.6$). However, the diference between hBest1 expression in eosinophils and HL60s was significant ($P<0.05$, $*^2$ above)

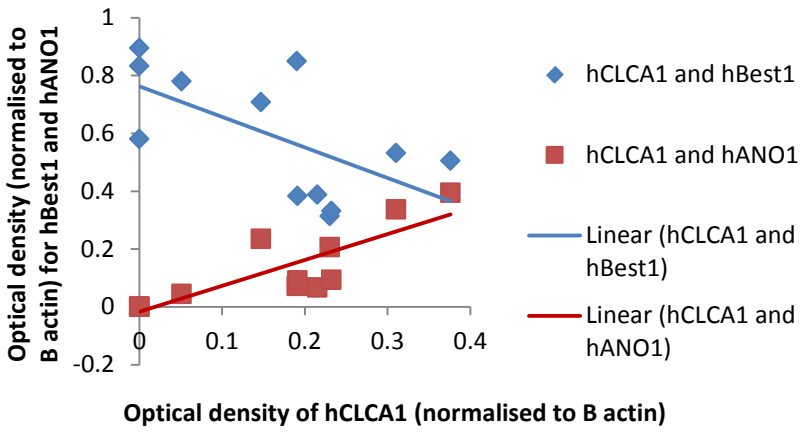

Figure 4.10: Correlations between gene expression of hCLCA1 and hANO1 and hBest1: Correlation coefficient calculated for hCLCA1 expression against hBest1 and hANO1across all samples. Negative correlation (correlation coefficient -0.62) observed between hCLCA1 and hBest1 expression which was statistically significant (P<0.0005). Whilst a positive correltation (coefficient 0.84) was observed between hCLCA1 and hANO1 this was not statistically significant (P>0.1).

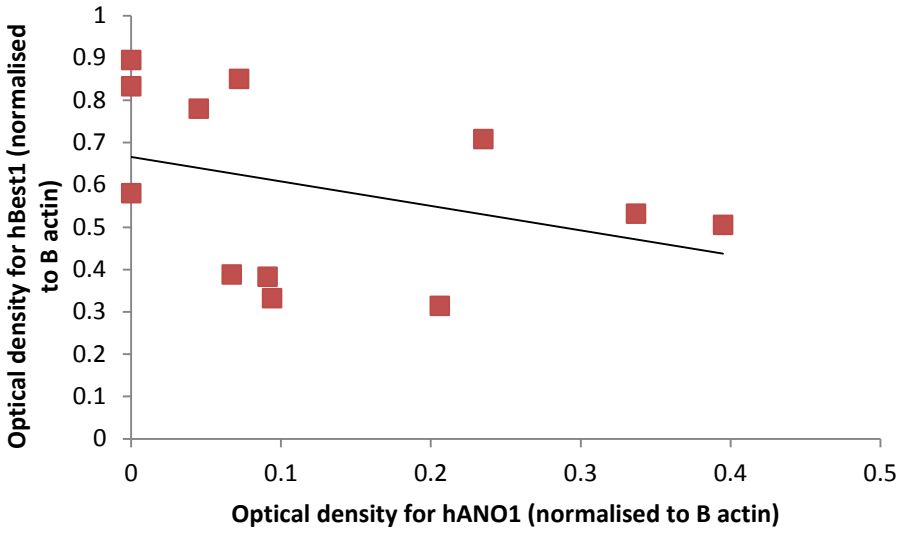

Figure 4.11: Correlation between gene expression of hANO1 and hBest1: Correlation coeeficient calculated for hANO1 expression against hBest1 expression which shows a weak negative correlation (coefficient -0.36) which is statistically significant (P<0.0001).

4.1.2 Discussion

4.1.2.1 hCLCA expression

As outlined in section 1.1.3.3, hCLCA1 is no longer considered to be a chloride ion channel itself but may have a regulatory role in the cell to modulate the activity of other chloride ion channels (Greenwood & Leblanc, 2007; Hamann *et al.*, 2009). The data presented in this project, on the lack of expression of hCLCA1 in HL60s may support this.

It has been proposed that hCLCA1 modulates the activity of other chloride ion channels. Coupled with other published evidence (as discussed in Chapter 1) and the significant differences between hCLCA1, hBest1 and hANO1 expression, and the correlation between hBest1 and hCLCA1 presented here, supports this. These observations may occur as the gene signal stops when optimal activity and modulation of an alternative channel is achieved. Conversely, it may be that the signal of hCLCA1 ceases not as a result of optimum modulation of another channel, but that hCLCA1 is implicated in the activation of cells which may be supported by the observations of differing expression across PMNs and eosinophils. In this instance, the hCLCA1 signal would be optimal as the cell is reaching maturity until electrical neutrality is restored (Loewen & Forsyth, 2005). The mature, or differentiated cell, may then have a different expression pattern of ion channel families which would be reflected in mRNA. A positive correlation between hCLCA1 and other channels (such as hANO1) may mean that an increased expression of hCLCA1 would result in modulation of alternative ion channel activity, and resultant chloride flux. This relationship within the current project was not statistically significant however but indicates the need for further examination. The relationship between hCLCA1 and

hBest1 however was negative in that as hCLCA1 increases, hBest1 decreases indicating that the modulation of this channel is inhibitory. This supports the work of others (Britton *et al.*, 2002; Loewen & Forsyth, 2005) and is further supported by the spread of hCLCA1 in the commercial cell lines examined here.

Expression of hCLCA1 in respiratory epithelia was also found by Rogers (2003) and Tyner et al (2006). The locality of mRNA encoding hCLCA1 in respiratory epithelia suggests a role in airway processes such as chloride flux and associated mucus production.

The relationship between hCLCA1, cell differentiation and other chloride ion channels may therefore be a complex relationship of several factors. Further research is required to identify whether the decrease in hCLCA1 is as a result of terminal differentiation as it is required for maturation, or because it is required for optimal activity of another chloride ion channel (such as hBest1 and hANO1). The expression of hCLCA1 would therefore be different depending on the function of hCLCA1.

4.1.2.2 Bestrophin expression

As discussed in 1.1.3.4, bestrophins are considered to be calcium activated chloride channels and it has been shown that they are sensitive to DIDs, a specific Cl^- channel blocker (Greenwood & Leblanc, 2007; Kunzelmann *et al.*, 2007; Barro-Soria *et al.*, 2010). It has been suggested that hCLCA1 may modulate the activity of hBest1 through a selective filter on the second TMD of hBest1 (Loewen & Forsyth, 2005). This is supported by the current data in that the negative correlation between hCLCA1 and hBest1 expression was significant. However, it appears that as hCLCA1 expression increases, hBest1 decreases which suggests that the role of hCLCA1

is inhibitory. Alternatively, hBest1 and hBest3 are expressed in all cells screened and may be self-regulating. Barro-Soria (2010) however, demonstrated that bestrophin1 was localized to the endoplasmic reticulum and suggested that activation of hANO1 was reliant upon intracellular calcium signalling modulated by hBest1. This relationship does not seem supported by the spread of expression. As stated, the observed relationship between hBest1 and hANO1 is negative in that as hBest1 increases, hANO1 decreases. This is not however statistically significant and therefore requires further examination. A complex interaction between hBest1, hANO1 and hCLCA1 may be evident.

hBest3 has two transcript variants, one of which does not have exons 2, 3 and 6 (hBest3Δ2,3,6), whilst the other is full length. The differences between the two may have functional implcations for bestropin 3 as a Ca^{2+} activated Cl^- channel. It has been shown in mouse studies that Best3Δ2,3,6 proteins lack two TMDs and the N-terminus which may impact upon the ability of this variant to act as a chloride channel (Srivastava *et al.*, 2008). Within these experiments, it has also been shown that there are differences in expression of the two variants. Mouse heart expresses full length Best3 whereas the variant Best3Δ2,3,6 has been found in exocrine glands, lung, testis and kidney (Srivastava *et al.*, 2008). To further examine hBest3 in human granulocytes or lung, firstly expression of variants should be established. Functional implications could be established by utilising patch clamp techniques to determine chloride flux and application of DIDs to cells transfected with full length hBest3 and hBest3Δ2,3,6. This would further clarify the expressional pattern of the Best3 variants and elucidcate functional implications.

4.1.2.3 hANO1 expression

hANO1 was expressed in PMNs, eosinophils and SAECs however not in HL60s. It was visualized and confirmed in all other cell lines. This mRNA expression pattern is similar to that of hCLCA1 and therefore may support the hypothesis that hCLCA1 is the complementary partner of an alternative chloride channel (Britton *et al.*, 2002; Loewen & Forsyth, 2005). It has been shown that there is a positive correlation between hANO1 and hCLCA1 however this is not statistically significant (coefficient 0.84, $P>0.1$) (Figure 4.10 and Figure 4.11). There is greater expression in SAECs than either PMNs or eosinophils however eosinophils have a greater expression than PMNs ($P<0.05$) (Figure 4.9). This may also suggest a relationship to the differentiation and maturation of cells.

At the point of this project, the evidence for hANO1 remained sparse and further experimentation is indicated to establish the role of hANO1 and it's relationship to other chloride ion channels.

4.2 Protein expression determination by flow cytometry

Flow cytometry phenotyped both surface, and intracellular, protein expression for PMNs, eosinophils and HL60. Flow cytometry was used to examine whether mRNA encoding for hCLCA1, hBest1 and hANO1 translated into protein expression in PMNs. Fresh PMNs purified by percoll density gradient centrifugation (see Section 2.1.2.1) were used for both intracellular and surface staining for hCLCA1, hBest1 and hANO1 (Methodology found in Section 2.2). Figure 4.12 and 4.13 present example histograms from both intracellular and surface staining respectively for both hCLCA1 and hBest1. Figure 4.14 and 4.15 present hANO1 data. Mean fluorescence was measured for PMNs (n=3), eosinophils (n=3) and HL60s (n=3) (Table 4.3 for results)

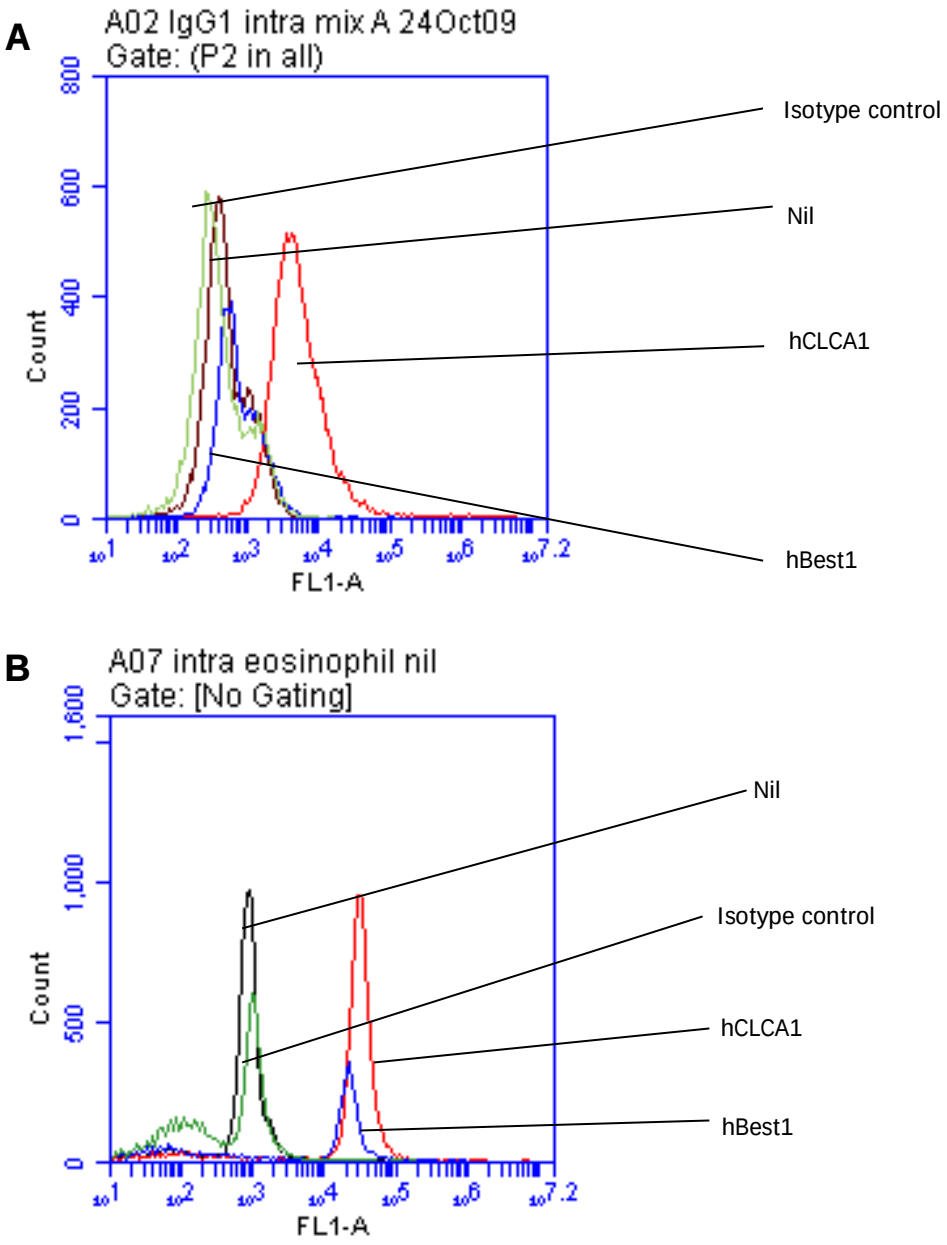

Figure 4.12: Intracellular staining of mixed PMNs and eosinophils: Representative histogram overlays demonstrating a rightward shift in fluorescence for hCLCA1 and hBest1 intracellular staining (FL1-A [533/30nm] Ex 488nm). A=PMNs and B=eosinophils. Primary labelled with hCLCA1 (red curve) and hBest1 (blue curve) and secondary labelled with bodipy as in section 3.4. Compared against the nil (black curve), and isotype control (green curve) as described in section 3.4. A rightward shift is indicative of increased fluorescence, and therefore increased protein labelled with specific antibodies. All experiments repeated 3 times (n=3)

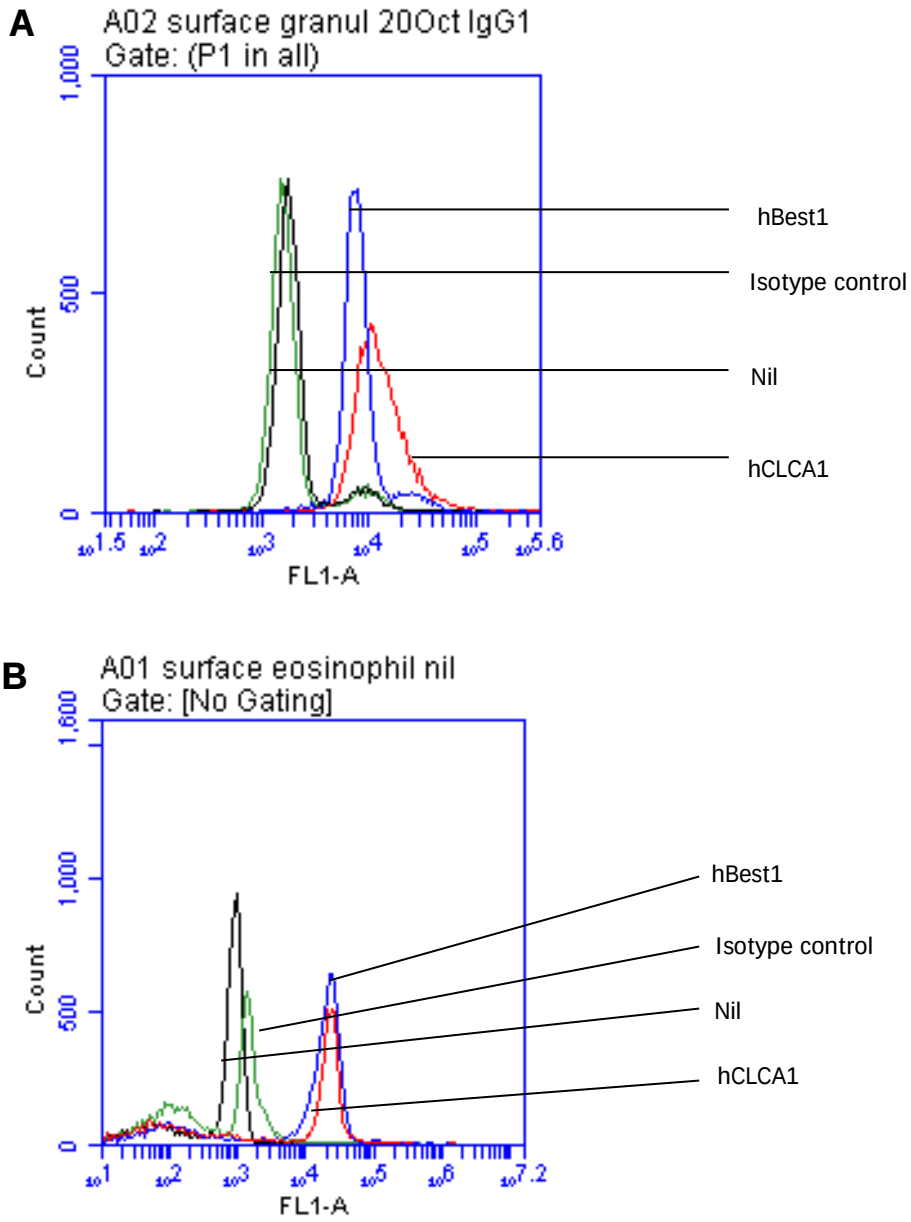

Figure 4.13: Surface staining of mixed PMNs and eosinophils: Histogram demonstrating a rightward shift of hCLCA1 and hBest1 staining on the cell surface (FL1; 533/30nm; Ex 488nm) (n=3). A=PMNs and B=eosinophils. Primary labelling for hCLCA1 (red curve) and hBest1 (blue curve) proteins and secondary labelled with goat anti-mouse FITC or alexafluor 488. Compared against nil (black curve) and isotype control (green curve). AlexaFluor 488 has a longer half-life and so is used when samples are cytospun and under microscopy for morphological assessment

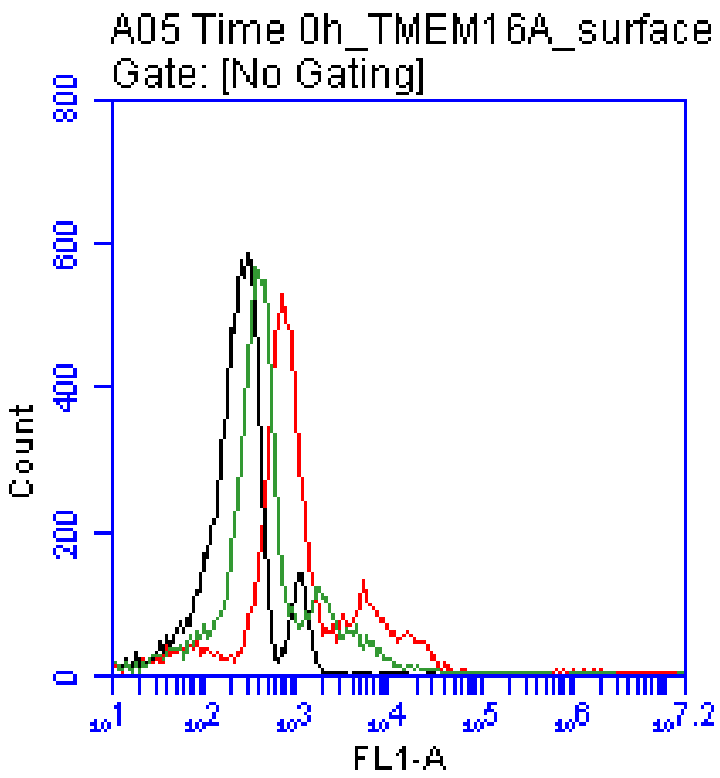

Figure 4.14: Surface hANO1 protein on mixed PMNs:
Histogram of hANO1 antibody labelling (red curve) compared to nil (black curve) and isotype control (green curve) (FL1; 533/30nm; Ex 488nm). Secondary antibody was an anti-rabbit-FITC (n=3)

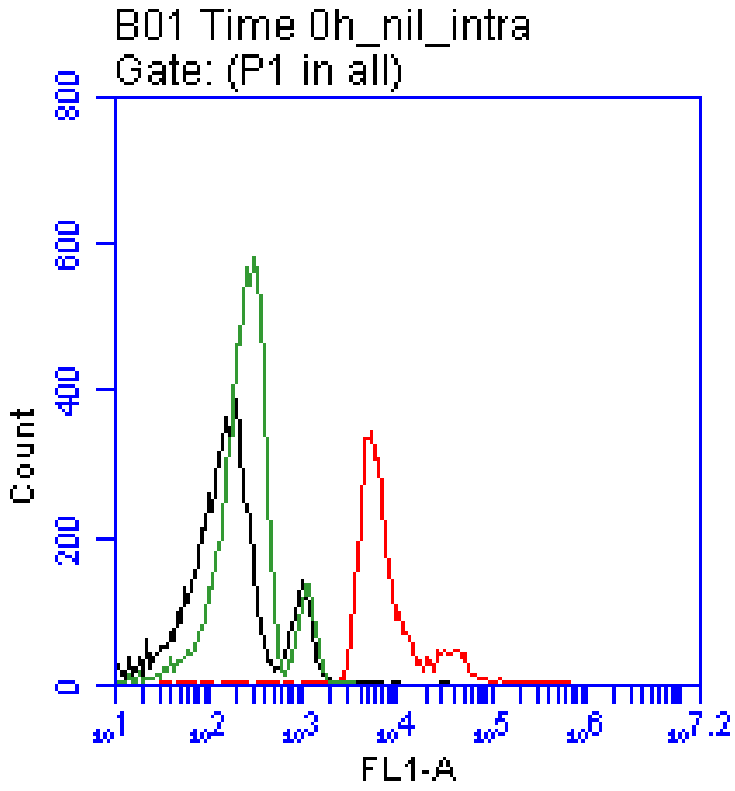

Figure 4.15: Intracellular hANO1 on mixed PMNs: Histogram of hANO1 antibody labelling (red curve) compared to nil (black curve) and isotype control (green curve) (n=3) (FL1; 533/30nm; Ex 488nm). Greater rightward shift indicates a greater expression of hANO1 protein intracellularly

A

Sample	Nil Int	Nil surface	Isotype Int	Isotype surface	CLCA1 Int	CLCA1 surface	Best1 int	Best1 surface	CD44 int	CD44 surface
PMNs (1)	352.45	244.8	303.34	405.05	33150.97	1383.79	19040.3	6161.86	31203.53	37643.76
PMNs (2)	404.51	264.83	468.9	285	27812.95	1278.82	13206.52	4523.78	26390.4	33249.02
PMNs (3)	398.87	272.17	313.45	508.14	25808.95	1974.63	18484.66	5511.75	27181.38	42427.78
Mean	385.28	260.60	361.90	399.40	28924.29	1545.75	16910.49	5399.13	28258.44	37773.52
SD	23.33	11.57	75.78	91.18	3098.67	306.28	2628.91	673.47	2107.38	3748.34

B

Sample	Nil Int	Nil surface	Isotyp. Int	Isotype surface	CLCA1 Int	CLCA1 surface	Best1 int	Best1 surface	CD44 int	CD44 surface
Eos 1	664.35	353.04	1122.03	464.98	15579.15	5678.25	3557.28	635.82	63144.44	80417.81
Eos 2	788.87	509.33	793.31	544.74	17295.57	4276.32	2571.42	824.54	51701.09	77833.66
Eos3	654.36	701.62	1079.76	891.18	20472.47	4646.65	2304.49	1025.74	47950.43	61781.45
Mean	702.53	521.33	998.37	633.63	17782.40	4867.07	2811.06	828.70	54265.32	73344.31
SD	61.19	174.60	178.84	226.58	2482.72	726.49	659.88	194.99	7914.92	10096.74

C

Sample	Nil Int	Nil surface	Isotype Int	Isotype surface	Best1 int	Best1 surface
HL601	865.37	1079.39	769.79	1076.18	1609.17	1353.73
HL602	683.43	918.23	508.64	874.08	1454.18	1373.39
HL603	725.3	782.02	682.54	812.49	1629.04	1265.36
Mean	758.03	926.55	653.66	920.92	1564.13	1330.83
SD	77.80	121.54	108.55	112.63	78.17	46.98

Table 4.3: Surface and intracellular protein expression of Best1 and CLCA1 in PMNs, eosinophils and HL60s: Samples were prepared as per previous section. Samples were labelled for protein on the cell surface and intracellularly ("int" in above) for hCLCA1 and hBest1. hBest1 is the project focus and the antibody (Bst-121AP) used was characterized for specificity (section 3.5). Median fluorescence was measured (FL1; 533/30nm; Ex 488nm) and means calculated with standard deviation (SD) all to 2dp. A=PMNs (n=3), B=eosinophils (n=3) and C= HL60 (n=3) for bestrophin only. Using 2 way ANOVA, there was no statistically significant difference between nil and isotype controls indicating that there was not any non-specific binding ($P>0.1$). Isotype controls were used to establish change in hBest1 and hCLCA1 expression. Differences in protein expression observed were between Isotype controls both intracellular and surface staining and intracellular and surface staining for hBest1 and hCLCA1 ($P<0.0001$). The differences between intracellular and surface staining for each hBest1 and hCLCA1 was also significantly different ($P<0.0001$). Figure 4.16 for bar chart of results, section 4.2.1 for summary of

4.2.1 Summary of flow cytometry experimental results

Polymorphonuclear cells and eosinophils were phenotyped for hCLCA1 and hBest1 protein expression using both surface and intracellular staining. This was to identify any relationship between these proteins (Figure 4.16, Table 4.3) and to gene expression. The bar charts presented (Figure 4.16 and 4.17) have mean fluorescence on the vertical axis measured on a logarithmic scale to base 10 (Log_{10}). Individual experiments are measured as median fluorescence of each histogram. Collective representation (n=3) is calculated as a mean of these. This was to allow visualization of values for nil, isotype and positive controls. Isotype was used as a control to measure the effect of any non-specific binding to the host species of antibody used. There was no statistically significant difference between nil and isotype controls for all cell types, and both intracellular and surface staining ($P>0.1$). Isotype controls were therefore used to compare the mean of fluorescence.

Intracellular isotype mean for PMNs was increased from 362 ± SD 76 at least 46 fold for intracellular hBest1 (* in figure 4.16) to 16910 ± SD 2629. There was, however, a much larger increase in mean fluorescence for intracellular hCLCA1 at 80 fold (hCLCA1 = 28924± SD 3099) ($*^2$ in Figure 4.16). These changes in protein expression from the isotype mean were statistically significant ($P<0.005$). The difference between fluorescence of intracellular hCLCA1 and hBest1 was also statistically significant ($P<0.0001$, indicated by $*^3$ in figure 4.16). As antibodies used were from the same animal (with the same isotype), and the same secondary antibody was used, it can be suggested that intracellularly, hCLCA1 protein expression is greater than hBest1.

The comparison between nil and isotype controls was not statistically significant (P>0.05) and, therefore, there was not considered to be any non-specific binding and isotype was used as a control.

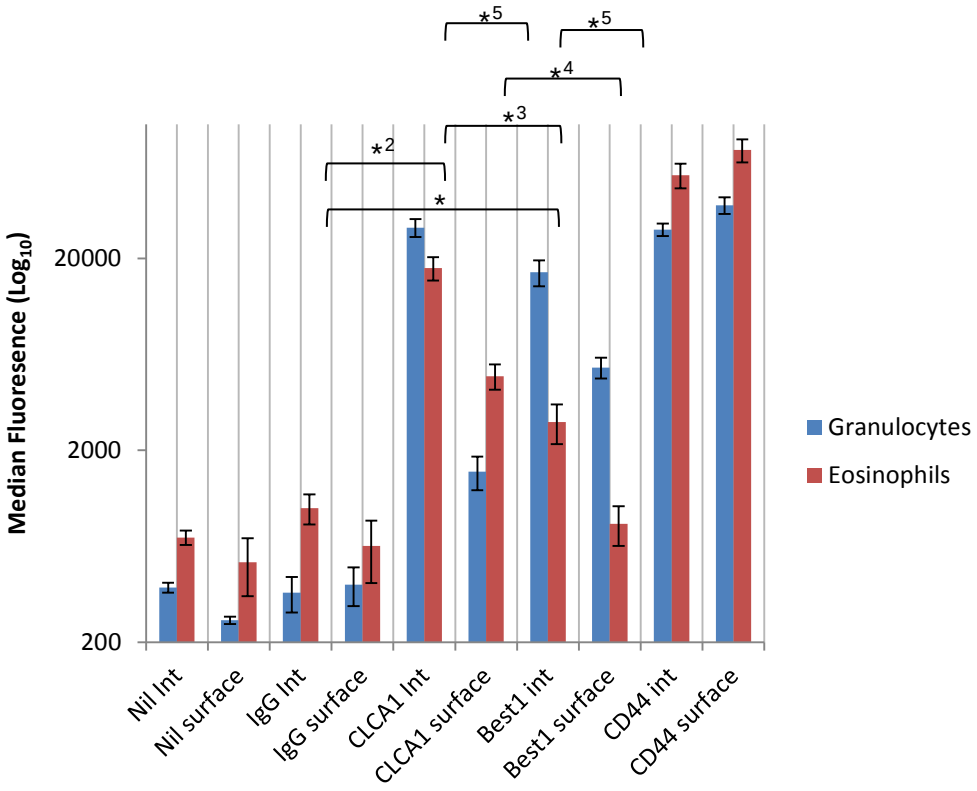

Figure 4.16: Intracellular and surface protein expression of CLCA1 and Best1 in PMNs and eosinophils: Bar chart showing the mean of median fluorescence of PMNs (labelled in graph as granulocytes, blue bar) and eosinophils (n=3) (red bar), in logarithmic scale to base 10, for hCLCA1 and hBest1 proteins both intracellularly and surface compared to negative and positive controls. Error bars are ± standard deviation (SD) to 2dp. Differences between isotype (IgG) controls (both intracellular and surface) and hCLCA1 and hBest1 are statistically significant (P<0.005). Differences between hCLCA1 and hBest1 protein expression for both intracellular and surface staining are significant. Intracellular staining shows greater hCLCA1 than hBest1 (P<0.0001, $*^3$ above). Surface staining has a greater protein expression of hBest1 compared to hCLCA1 (P<0.0001, $*^4$ above). There is a significant difference between surface staining and intracellular staining for each hCLCA1 and hBest1 ($*^5$ above)

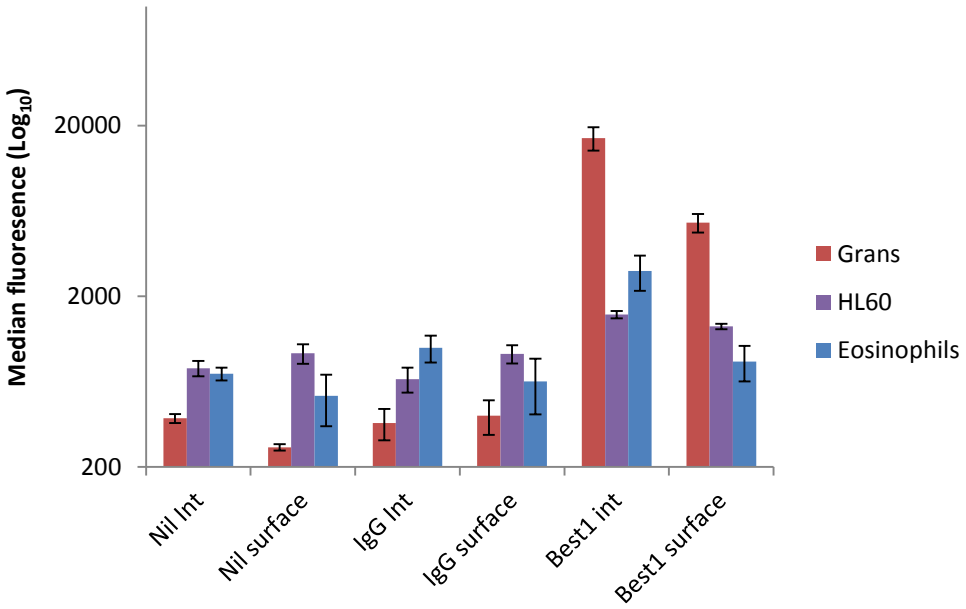

Figure 4.17: Surface and intracellular protein expression of Best1 in HL60s, PMNs and eosinophils: Graph showing the median fluorescence of PMNs (labelled as grans, red bar), in logarithmic scale to base 10, for hBest1 both intracellularly and surface stained compared to negative controls (IgG=isotype). Error bars are ± standard deviation (SD). A statistically significant ($P<0.05$) increase in fluorescence intensity for hBest1 both surface and intracellularly stained however the difference between the two was not significant ($P>0.05$). There was a significant difference between HL60s (purple) and PMNs ($P<0.01$) however the difference between HL60 and eosinophils (blue) was not significant ($P>0.07$).

When PMN cells (n=3) were surface stained, the relative fluorescence increase from isotype control for hCLCA1 was 3 fold; in contrast the hBest1 increase from isotype control was 13 fold. This increase in fluorescence from isotype for both intracellular and surface staining for hCLCA1 and hBest1 was statistically significant ($P<0.05$). The difference noted between hCLCA1 and hBest1, in that there was a greater increase in surface staining of hBest1, compared to hCLCA1 was statistically significant ($P<0.0001$, $*^4$ in Figure 4.16). Whilst both hCLCA1 and hBest1 have greater amounts of protein intracellularly than the surface stain ($P<0.005$, $*^5$ in Figure 4.16), the relationship between the two is inverse. Intracellularly there is a greater amount of hCLCA1 compared to hBest1 ($*^3$ in Figure 4.16) and on the surface a greater amount of hBest1 compared to hCLCA1 ($*^4$ in Figure 4.16).

In eosinophils (n=3), there is a similar intracellular pattern in that there is a much greater expression of hCLCA1 intracellularly (17 fold increase from isotype control, $P<0.005$), than either on the surface ($*^5$ in Figure 4.16), or compared to intracellular hBest1 (which increased by 3 fold from isotype control, $P<0.005$, $*^3$ in Figure 4.16). In comparison to PMNs, however, whilst the expression of surface hCLCA1 in eosinophils is less than intracellular (7 fold increase in surface staining from control, compared to 17 fold increase in intracellular staining), it is greater than that observed for hBest1 (1.5 fold increase). The greater expression of hCLCA1 surface staining eosinophils, compared to surface hBest1 is statistically significant ($P<0.0001$, $*^4$ in Figure 4.16). The changes in protein expression for hCLCA1 and hBest1 both from the isotype control ($P<0.005$), and surface compared to intracellular were statistically significant ($P<0.005$, $*^5$ in Figure 4.16).

CD44 has been used as a positive control for flow cytometry (Figure 4.16). CD44 is a glycoprotein used for cellular migration, and cell-cell interations. As such, it is predominantly found on the cell surface. There was, however, no significant difference found between surface and intracellular staining in either granulocytes or eosinophils (Figure 4.16). CD44 interacts with lymphocyte-specific protein tyrosine kinase (Lck) which is a protein, found intracellularly in predominantly lymphocytes. It has been found, however, that Lck is also present in granulocytes (Pulford *et al.*, 1999). In this instance, CD44 may be interacting with Lck when the cell is permeabilised and allowing entry of CD44 into the cell. Alternatively, is has been shown that a proportion of CD44 molecules cleave the C-terminal tail as an intracellular cytoplasmic domain (Mellor *et al.*, 2013). There are also non-degraded CD44 molecules that remain membrane bound. In this instance, the permeabilisation of cells would allow the antibody to enter the cell and bind to the cytoplasmic domain of CD44, or to bind to those that remain non-degraded as transmembrane proteins.

When cells are not permeabilised, antibodies have access only to surface bound proteins. Through permeabilisation, there is access to both surface and intracellular proteins. That there is little difference between surface and intracellular staining of CD44 is likely due to surface bound protein still being stained and fluorescing regardless of whether the cell is permeabilised. The antibody would still be exposed to surface proteins in addition to any that are intracellular.

The hBest1 antibody used was Bst 121-AP (Fabgennix Inc, Texas). This antibody recognises an amino acid sequence that is located at the C-terminus of bestrophin, which is an extracellular portion of the protein (Marmorstein *et al.*, 2000; Marmorstein *et al.*, 2002). hCLCA1 was labelled with monoclonal antibody (M03), clone 2C10

(Abnova). The immunogen sequence provided by the manufacturer was analysed using protein BLAST (NCBI) and mapped against the full amino acid sequence for hCLCA1. This antibody labels the amino acid sequence from 677 to 776 of the 914 amino acid sequence for hCLCA1. This is extracellular and found after any potential transmembrane domains (Gruber *et al.*, 1998). Both hBest1 and hCLCA1 had greater fluorescence when permeabilised for intracellular staining. When surface stained, antibodies would be binding only to the extracellular amino acid sequence for hCLCA and hBest1. When permeabilised, the antibody would bind to both the surface, extracellular amino acid sequence, and to any protein found intracellularly. This would result in an overall greater fluorescence than surface staining alone. That the fluorescence is greater for intracellular staining indicates that there is hCLCA1 and hBest1 intracellularly. If both proteins were bound to the cell surface only, there would be no difference in the relative fluorescence between the intracellular and surface staining.

In summary, in both PMNs and eosinophils, there is a statistically significant increase in both hBest1 and hCLCA1 both intracellularly and on surface staining compared to isotype controls. There is a greater amount of fluorescence intracellularly for both hBest1 and hCLCA1 compared to surface in both PMNs and eosinophils. In PMNs, there is a greater amount of hBest1 compared to hCLCA1 on surface staining. In eosinophils, there is a greater amount of hCLCA1 compared to hBest1 on surface staining, indicating that on the surface there is a negative correlation between hCLCA1 and hBest1. The relationship between intracellular and surface staining for PMNs and eosinophils is of interest. To date, this has not been examined elsewhere and should be further researched. The overall expression of hCLCA1 and hBest1 protein correlates to the findings of gene expression and semi-quantification using densitometry. As

discussed in section 4.1.2 and 4.1.3 there is a statistically significant negative correlation between gene expression of hCLCA1 and hBest1.

To confirm the use of HL60s as an appropriate model for human cells, samples (n=3) were phenotyped for intracellular and surface expression of hBest1 protein only. hCLCA1 or hANO1 were not screened as the functional assays were refined to hBest1 only. As identified in section 4.1.3, the gene expression of hCLCA1 and hANO1 differs between PMNs and eosinophils compared to HL60s. This is an area which requires further research. Figure 4.17 is a bar chart showing the results of HL60 screening compared to both eosinophils and mixed PMNs.

HL60 cells did not have a statistically significant difference between the nil and isotype controls. There was a statistically significant increase in both intracellular and surface expression of hBest1 protein from isotype control ($P<0.005$). The difference between surface and intracellular expression was not statistically significant. On comparison of HL60s to PMNs with a student's t-test, the difference was significant ($P=0.01$, n=3). On comparison however to eosinophils, the difference was not significant ($P>0.07$). As discussed in section 4.1.3, there was no statistically significant difference between gene expression of hBest1 in PMNs (n=5) and HL60s (n=4) ($P>0.6$). Conversely, the difference in gene expression of hBest1 in HL60s and eosinophils (n=6) was statistically significant ($P<0.05$). From the results presented, it was concluded therefore that HL60s are an appropriate model for human eosinophils or granulocytes in this instance although this may be reliant upon the stage of differentiation and cell cycle.

4.2.2 Results in context

As demonstrated in RT-PCR, and densitometry (section 4.1) there is a negative correlation between hCLCA1 gene expression and hBest1 gene expression in that as one increases, the other decreases. This is supported by and comparable with the findings of flow cytometry whereby on surface staining, there is a decreased expression of hBest1 when hCLCA1 is greater, and vice versa. This is demonstrated in the protein expression pattern of hBest1 and hCLCA1 on surface staining of eosinophils and PMNs.

In the present study, the results seem to suggest a relationship between hCLCA1 and hBest1. This is supported by the work of Loewen and Forsyth (2005). There is clear evidence using flow cytometry that there is expression of hBest1 protein intracellularly, indicated by a greater fluorescence when samples were permeabilised compared to surface staining alone. This also supports previous studies. In these, hBest1 was found to localize to the endoplasmic reticulum and was thought to activate hANO1 through calcium signalling (Kunzelmann *et al.*, 2009; Barro-Soria *et al.*, 2010). The results from both gene and protein expression analysis using RT-PCR and flow cytometry support the suggestion that there is a complex relationship between hCLCA1, hBest1 and hANO1. This, however, requires further research to gain statistical power by increasing replicates, but also to establish where the proteins are localised within the cells, and what pathways may be activated for functionality.

4.3 Western blot analysis

Western blot analysis is required to further confirm whether the genes of interest translate into proteins, whether intracellularly or membrane bound. Results were used to support the findings, and discussion, of flow cytometry. Whilst RT-PCR had shown hBest1 and hBest3 in PMNs, eosinophils and HL60s, the antibody for hBest1 (n=3) only had been characterized (Section 3.5). To date, all antibodies used for hBest3 were unsuccessful either as no band detected on Western Blotting, or that non-specific bands were visualized.

hCLCA1 has been confirmed on CFPAC, A549, NAEC, SAEC and Calu-3 on three experiments at expected weights. In granulocytes, hCLCA1 however was visible as a band at approximately 60kDa which was an unexpected weight (n=3). Whilst it could be suggested that this band may be a form of hCLCA1 following cleavage of the N-terminus, the band for β actin was faint. β actin is a cytoskeletal protein with an expected band weight of 48kDa and was used as a positive control for sample loading. A faint band may indicate inadequate sample loading however the band for hCLCA1 may be a different form of hCLCA1. There is evidence to suggest that hCLCA1 undergoes modification after translation which is different depending on the tissue expression demonstrating two subgroups of CLCA proteins (Bothe *et al.*, 2012). The pattern of protein expression shown (Figure 4.18) was seen in all three experiments, however, conclusions from this cannot be drawn with any confidence as the band was not at the expected weight and differed from other positive controls. In addition the antibody had not been characterized for specificity (Figure 4.18).

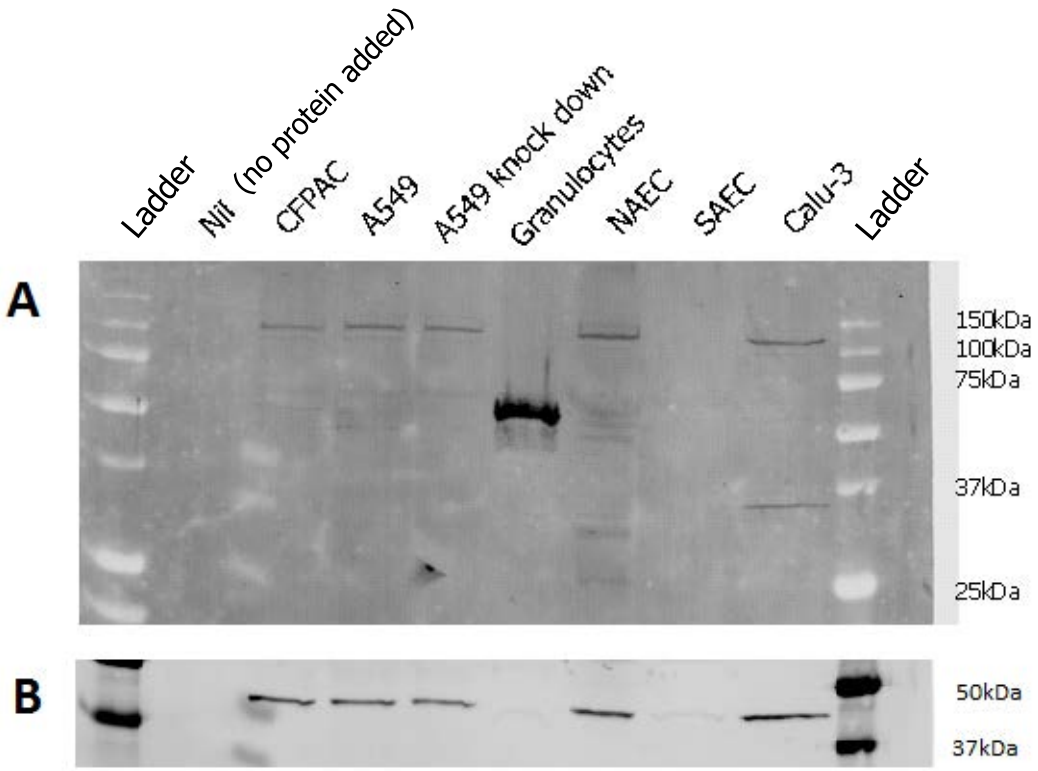

Figure 4.18: hCLCA1 protein expression in epithelial cell lines and PMNs: Representative greyscale image of a western blot labelled for hCLCA1 for epithelial samples and PMNs (granulocytes). A. Samples as listed with pre-cursor for hCLCA1 at 125kDa as expected. Protein band expected molecular weight of 37kDa. Faint band on SAEC sample however this was visualised on another earlier experiment. B. Beta actin blot demonstrating loading control of sample and bands as expected at molecular weight of 48kDa. The nil control is a sample with no protein added.

hBest1 Western blot supports the findings of RT-PCR and suggests that the mRNA encoding hBest1 translates into protein with bands seen in CFPAC, A549, NAEC and SAEC. As with hCLCA1 blot, no band was seen for PMNs however there was also a weak β actin visualised (Figure 4.19). This was repeated following optimization of process and bands were visualized at molecular weight of 68kDa, as

expected, for PMNs, NAEC, SAEC, A549 and CFPAC (Figure 4.20). Western blots were undertaken on both HL60 cells and eosinophils however no band could be detected for hBest1 in any of these samples (Figure 4.21). In addition, the beta actin for these was also weak. This may be due to the nature of the cells or the amount of bestrophin 1 at a lower concentration making detection problematic.

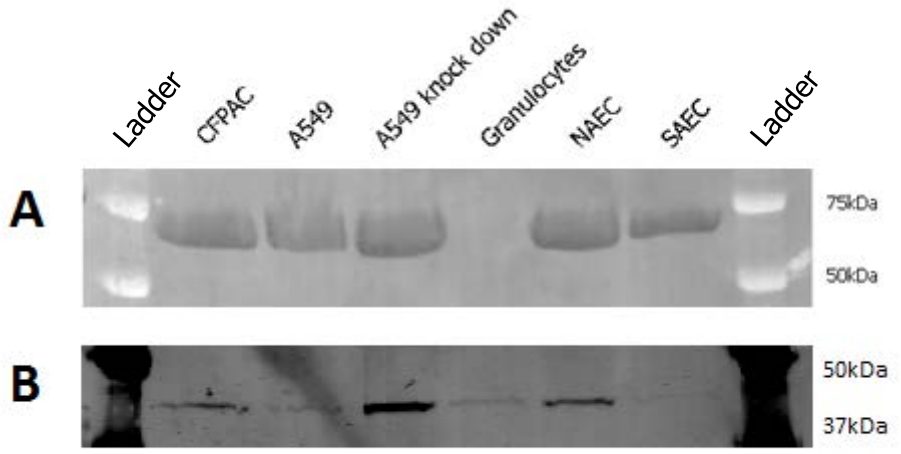

Figure 4.19: hBest1 protein expression in epithelial cell lines and PMNs: Representative greyscale image of western blot for hBest1. A. Samples as listed with bands at a molecular weight of 68kDa as expected. No band visualised for PMNs (granulocytes). B. β actin blot with bands as expected at 48kDa. Very weak band visualised for PMNs

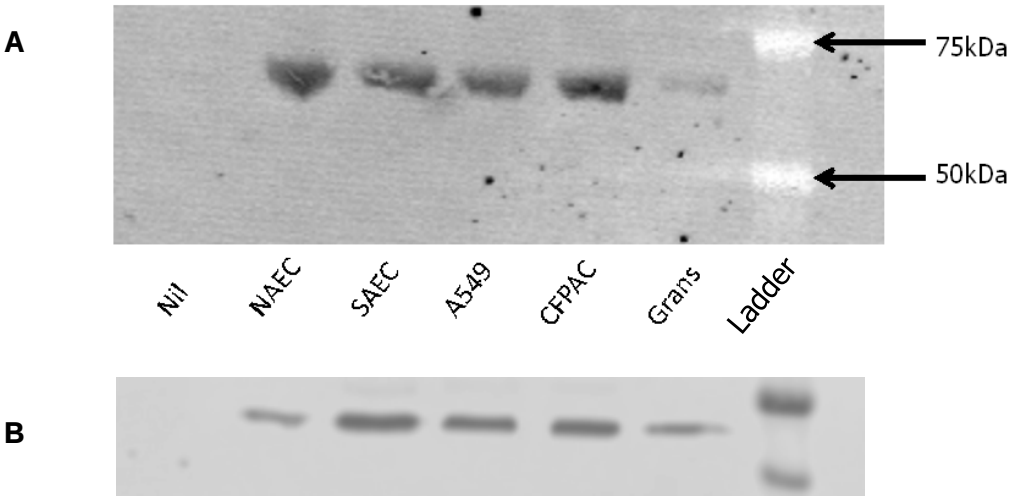

Figure 4.20: hBest1 protein expression showing a band for PMNs: A; hBest1 bands at expected molecular weight of 68kDa. Weak band for PMNs (granulocytes) however beta-actin was also weak. Nil was negative control with no protein added to the well. B; Beta actin control at the expected weight

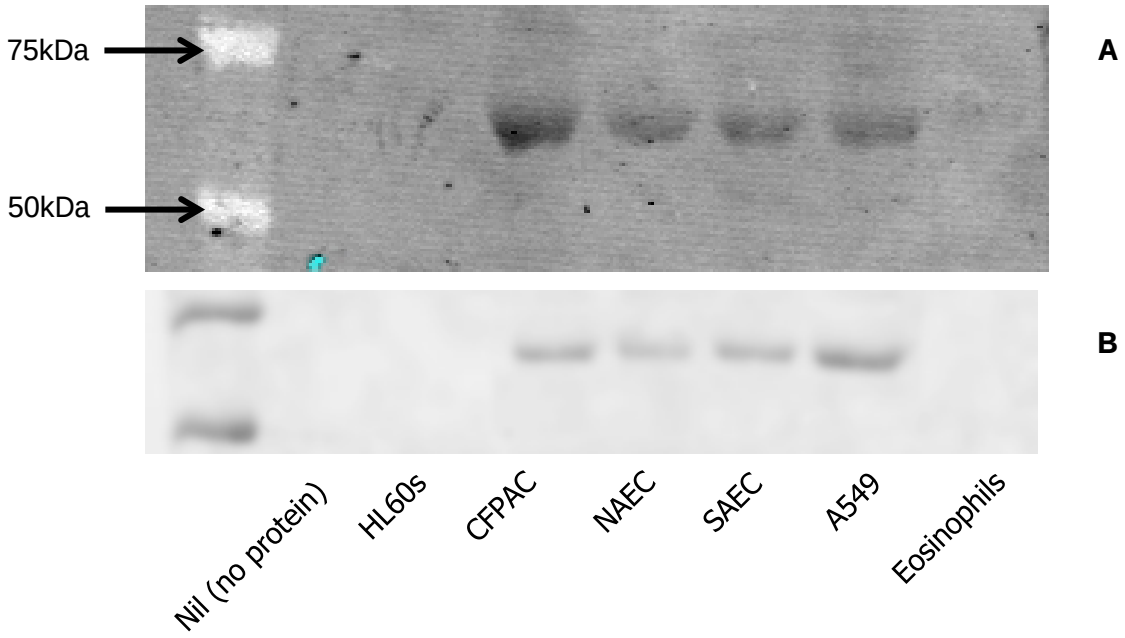

Figure 4.21: Greyscale western blot of hBest1 for positive controls, HL60s and eosinophils: A: hBest1 bands at expected molecular weight of 68kDa. No band visualised for either HL60s or eosinophils. Nil was negative control with no protein added. B: Beta actin at expected weight

The western blots do, therefore, support the findings of flow cytometry. That bands for hBest1 could not be visualized for eosinophils and HL60s correlates with the reduced expression of hBest1 in these cells as demonstrated in flow cytometry (Figure 4.17). Further experimentation is required to establish whether visualised bands of hCLCA1 are cleaved products of hCLCA1. All blots for hANO1 have been unsuccessful (n=5, Figure 4.22) although the antibody used is not recognised by the manufacturer for western blot analysis and other antibodies that were commercially available (AbCam rabbit anti-human polyclonal anti-bodies: AbCam ab53212 and AbCam ab72984) also did not produce a band on western blot.

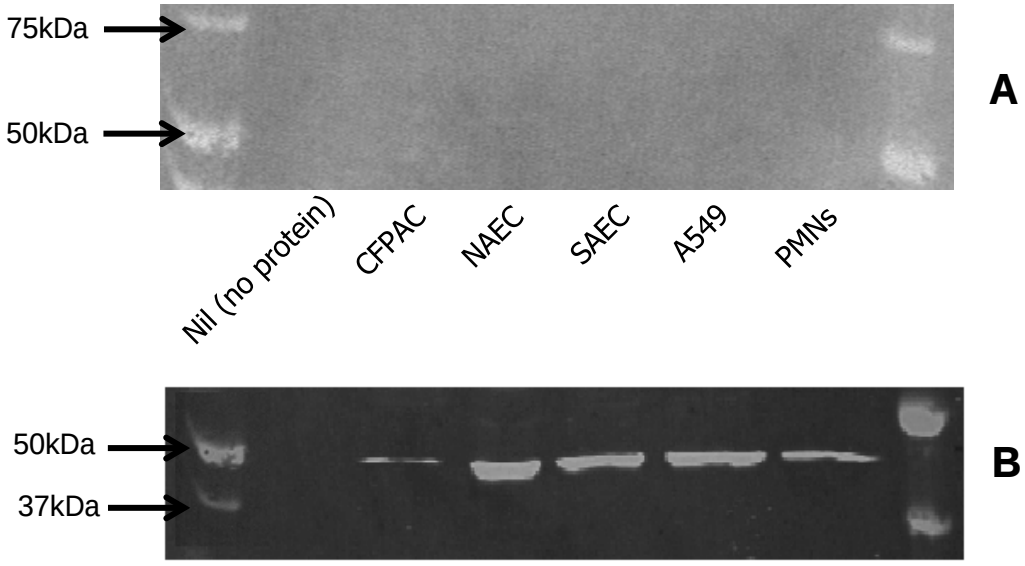

Figure 4.22: Greyscale western blot of hANO1 for positive controls and PMNs: A. hANO1 band expected at 74kDa. No band visualised in any sample. Western blot repeated n=5. B. Beta actin demonstrating samples loaded with band as expected at 48kDa. Nil was negative control with no protein added to the well

CHAPTER 5: FUNCTIONAL ANALYSIS OF hBEST1

5.1 Cytokine stimulation

Chloride ion channels may be implicated in the function of granulocytes as mediators of clinical symptoms in chronic inflammatory lung disease (Chapter 1). The current project focusses upon hBest1 as one of the candidates for chloride ion channels in granulocytes. hBest1 may have a role in granulocyte volume regulation through fluid shifts. It is hypothesised that changes in cell volume and shape will directly impact upon cellular migration and activation. hBest1 up-regulation may have therapeutic inflammatory effects such as allowing phagocytosis through cell shape modulation. In order to examine a potential role of hBest1 in granulocyte response in inflammation, functional experiments were performed. These included RT-PCR and flow cytometry following cytokine stimulation, transmigration assays and Cl^- and Ca^{2+} assays. Cytokine stimulation of PMNs, and HL60s was performed to establish whether there is upregulation in response to pro-inflammatory mediators. Transmigration assays were performed following upregulation of hBest (through transfection) to assess whether greater expression of hBest1 would impact upon the migration HL60s in response to inflammatory cytokines.

5.1.1 Results

Polymorphonuclear cells were purified from peripheral blood (see Chapter 2) and treated with cytokines over 24 and 48 hours. Samples were then antibody labelled for hBest1 protein expression on flow cytometry and prepared for RT-PCR to establish any changes in mRNA.

The gel images collected from RT-PCR demonstrated that at the gene expression level, there appeared a slight change in signal for

hBest1 in a mixed PMN population (Figure 5.1). Over time, it appeared that mRNA peaked in response to IL-13 at 24 hours and then decreased below that at time=0h (Figure 5.2, Table 5.1). Using semi-quantifiable densitometry, bands for hBest1 in PMNs that were stimulated with IL-13 over 48 hours, compared to PMNs, which were not stimulated, were measured. On ANOVA, the critical F value was much greater than the *f* value therefore the null hypothesis was accepted. Any observed differences were not statistically significant ($P>0.2$). It was not possible, therefore, to be confident that any change in band size was due to IL-13 stimulation, or as a result of natural variation. It was also not possible to be confident that any observations were not due to time as there was no significant difference either over time, or between the nil and IL-13 stimulated group. Therefore, any observations are not confirmed and further experimental analysis would be required.

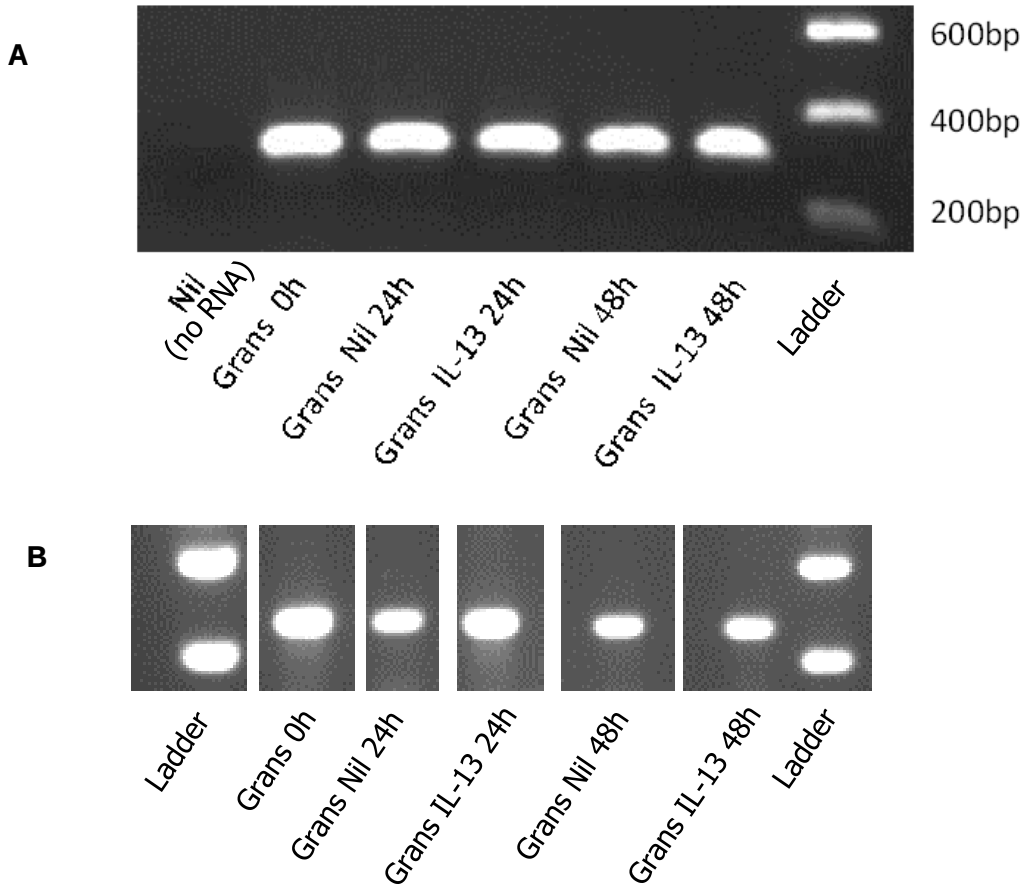

Figure 5.1: hBest1 gene expression in PMNs in response to IL-13 stimulation at 0h, 24h and 48h: A: Sample of PMNs (grans) with and without IL-13 stimulation (n=3). Intensity of the band visualized appears brighter at time=24h. There appears a weaker signal at time=48h however on densitometry and resultant ANOVA, there is no significant difference with over time, or between the nil group and the IL-13 stimulated group (P>0.2) (Table 5.1, Figure 5.2). Nil is a negative control with no RNA added to the master mix plus primers for hBest1. B: Beta actin controls for each experimental group

	hBest1 (Time=0h)		β actin	hBest1 (Time=24h)		β actin	hBest1 (Time=48h)		β actin
Cells/Sample	Optical density	Normalised to β actin	Optical density	Optical density	Normalised to β actin	Optical density	Optical density	Normalised to β actin	Optical density
PMNs (nil)									
1	76653	0.79	96991	82093	0.846	97001	64294	0.66	97478
2	18020	0.535	33677	12223	0.372	32844	26010	0.652	39899
3	67909	0.835	81325	72665	0.848	85674	59677	0.705	84680
Mean	54194	0.72	70664	55660	0.689	71840	49994	0.672	74019
SD	25827	0.132	26925	30955	0.224	27959	17063	0.023	24686
PMNs (IL-13 stimulated)									
1	75442	0.838	89992	76908	0.843	91257	54247	0.589	92165
2	20383	0.501	40681	53686	1.516	35406	24599	0.771	31909
3	68522	0.854	80257	81762	0.932	87771	49870	0.605	82448
Mean	54782	0.731	70310	70785	1.097	71478	42905	0.655	68841
SD	24488	0.163	21324	12252	0.298	25546	13067	0.082	26414

Table 5.1: Optical density (normalised to β actin) of hBest1 gene expression in PMNs in response to IL-13 stimulation over 48hrs: PMNs were stimulated with IL-13 over 48 hours and compared to a nil control (no IL-13) (n=3). Samples were analysed at time=0, 24 and 48 hours. Optical density of RT-PCR bands for hBest1 were normalised to β actin to semi-quantify results. ANOVA was used to establish significance of results. There was no statistically significant difference between the IL-13 stimulated samples and the nil samples ($P>0.2$). There was also no statistically significant difference over time ($P>0.2$).

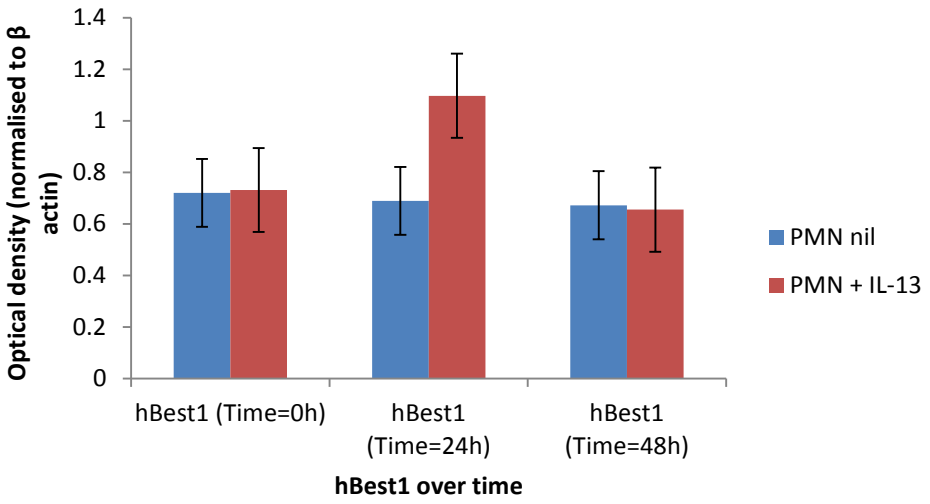

Figure 5.2: Changes in hBest1 gene expression in PMNs stimulated with IL-13 over 48 hours: Bar graph of results presented in Table 5.1. PMNs were stimulated with IL-13 over 48 hours and compared to a nil control (no IL-13) (n=3). Samples were analysed at time=0, 24 and 48 hours. Optical density of RT-PCR bands for hBest1 were normalised to β actin to semi-quantify results. ANOVA was used to establish significance of results. There was no statistically significant difference between the IL-13 stimulated samples and the nil samples (P>0.2). There was also no statistically significant difference over time (P>0.2).

To further analyse the effect of IL-13 on hBest1 protein expression, flow cytometry was performed. In PMNs (nil) (n=3), the median fluorescence on flow cytometry for hBest1 did not alter for either intracellular or surface staining over the incubation periods 24 and 48 hours. Any change noted was not statistically significant. In response to IL-13 stimulation (n=3) (section 2.1.4 for methodology)

however, the median fluorescence for hBest1 increased two-fold intracellularly and 1.5 fold for surface expression by 24 hours. As cells were incubated for a further 24 hours to reach total 48 hour incubation period, median fluorescence decreased both intracellularly and surface bound. The resultant fluorescence remained greater than control (Figure 5.3). This differences in hBest1 expression over time was statistically significant ($P<0.05$) as was the difference between both intracellular and surface staining, and the increased fluorescence from nil controls (no IL-13) ($P<0.05$). Whilst RT-PCR results were not statistically significant (Table 5.1, Figure 5.2, and Figure 5.4), this suggests responses to IL-13 may be at message level and translates into protein expression. It is acknowledged that the outlying result in RT-PCR skews data, and the number of replicates weakens the statistical power. Further replicates are required to elucidate the response to IL-13 however the flow cytometry data demonstrates that greater protein is produced, which could be indicative of either increased mRNA expression, or stabilization of synthesized mRNA. The greatest increase in hBest1 expression was intracellular and further supports the hypothesis that hBest1 may be localized to the endoplasmic reticulum, as discussed previously (Kunzelmann *et al.*, 2009; Barro-Soria *et al.*, 2010). This also supports the expressional data (Chapter 4) for both gene and protein expression of hBest1 in PMNs.

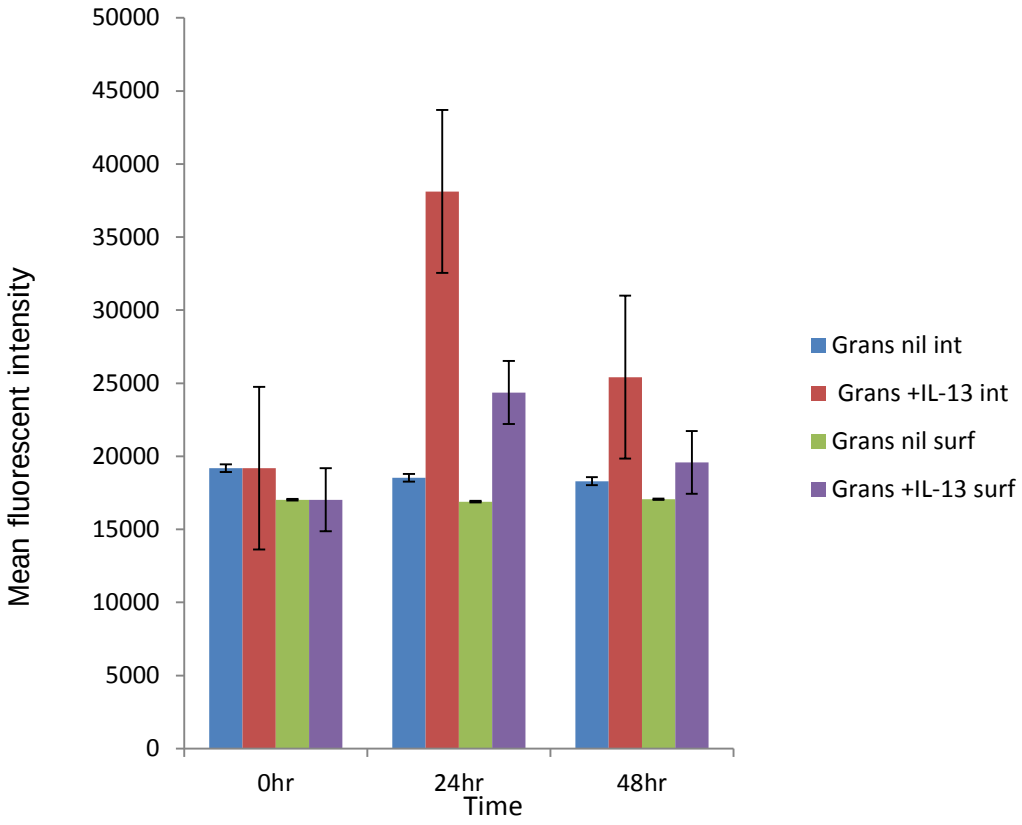

Figure 5.3: Changes in hBest1 protein expression in response to IL-13 stimulation of PMNs over 24 and 48 hours: PMNs (grans) were stimulated with IL-13 and incubated for 48 hours. Samples were taken at 0, 24 and 48 hours and analyzed using flow cytometry to label hBest1 protein intracellularly and surface bound. (n=3). Using ANOVA, the differences in hBest1 expression observed over time in response to IL-13 were statistically significant ($P<0.05$). The differences between intracellular and surface staining were statistically significant ($P<0.05$). The increased expression in response to IL-13 was statistically significantly different from nil controls (PMNs with no IL-13 stimulation)

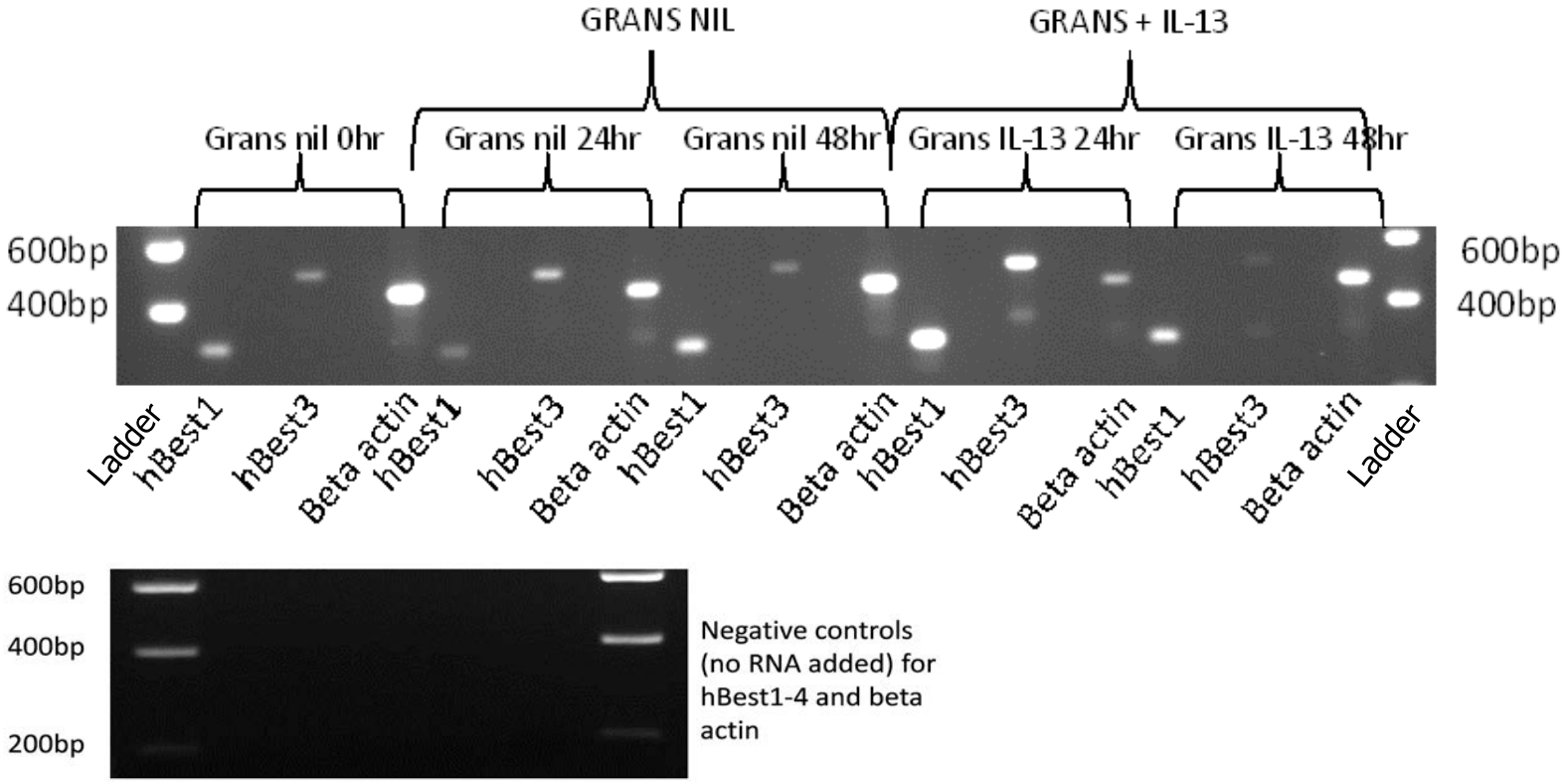

Figure 5.4: RT-PCR of hBest1-4 in PMNs stimulated with IL-13 over 48h: Representative image of RT-PCR for PMNs (grans) that were stimulated with IL-13 over 48 hours with samples taken and analysed at 0, 24 and 48 hours (n=3). Samples run in each well for each sample for hBest1-4 consecutively. Only beta actin, hBest1 and hBest 3 labelled for clarity of Figure. All bands analysed using densitometry and normalised to beta actin. Any differences in hBest1 band intensity were not statistically significant (P>0.2) (Table 5.1, Figure 5.2). Grans nil are not treated with IL-13 and samples collected at 0 hour, 24 and 48 hours.

RT-PCR and flow cytometric analysis suggests that changes in mRNA encoding hBest1 is translated into protein expression (Figure 5.4). Polymorphonuclear cells that were stimulated with IL-13 appeared to have greater expression of hBest1 mRNA which was most evident at 24 hours of incubation. It should be noted that this is observational only and any changes are not statistically significant. Further replication is indicated. The band becomes weaker for hBest1 after 48 hours however is greater than that seen in PMNs with no stimulation as a control.

The data presented suggests that IL-13 up-regulates both the hBest1 gene expression and translation into protein. There appears to be greater expression of hBest1 protein intracellularly which peaks at 24 hours when exposed to the pro-inflammatory cytokine IL-13. This is a statistically significant up-regulation of protein ($P<0.05$)

Figure 5.5 (Table 5.2, eosinophil data) shows that intracellular protein expression of hCLCA increases from isotype control marginally however, in response to all cytokines, there is a decrease in hCLCA1 expression from the nil control in eosinophils. This is also observed on surface staining however the difference in expression is less. Conversely, there is a marked increase in hBest1 expression intracellularly in response to cytokine stimulation with a marginal increase in surface expression. After 24 hours, the greatest response was observed in intracellular hBest1 expression following stimulation with IL-5 and IL-13. Intracellular hBest1 also had an observed increase in response to IL-13 alone. The peak in hBest1 at 24 hours after cytokine stimulation may correlate with the manifestations of inflammatory responses, however, further research is required to examine the relationship between cytokines and chloride ion channel expression.

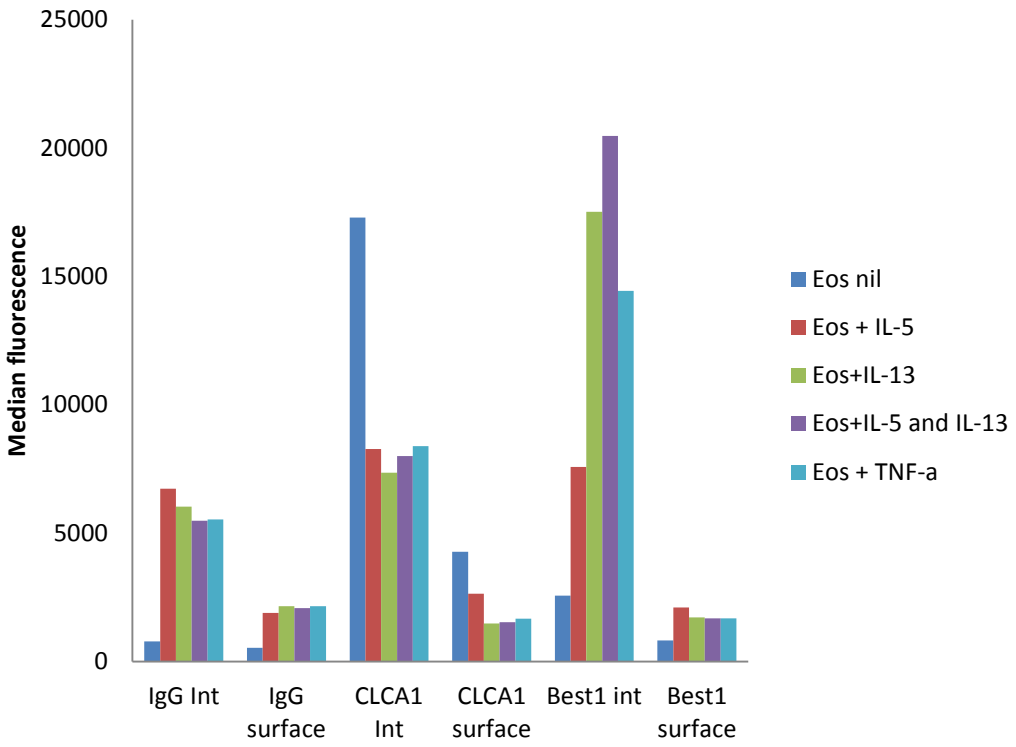

Figure 5.5: Changes in protein expression of intracellular and surface CLCA1 and Best1 in response to cytokine stimulation: Graph showing mean fluorescence of eosinophils following stimulation with cytokines for 24 hours. Experiment performed once (n=1) due to the constraints of resources however further repetition would benefit to allow statistical analysis

Sample	Isotype Int	Isotype surface	CLCA1 Int	CLCA1 surface	Best1 int	Best1 surface
Eos nil	793.31	544.74	17295.57	4276.32	2571.42	824.54
Eos +IL-5	6738.52	1898.03	8274.37	2640.68	7578.83	2107.77
Eos +IL-13	6031.5	2164.87	7356.97	1490.86	17510.61	1719.65
Eos + IL-5 and IL-13	5493.26	2087.66	8001.59	1536.89	20465.77	1692.04
Eos and TNF-a	5543.37	2157.78	8394.59	1674.05	14439.62	1683.94

Table 5.2: Changes in intracellular and surface protein expression of CLCA1 and Best1 in response to cytokine stimulation: Table showing mean fluorescence of eosinophils for hCLCA1 and hBest1 intracellularly and surface expression. Eosinophil samples were in five experimental groups using cytokines to stimulate cells and measured after 24 hours incubation. Experiment performed once (n=1) due to the constraints of resources however further repetition would benefit to allow statistical analysis

5.1.2 Discussion

It has been shown that the symptoms of inflammatory lung diseases are linked to migration and activation of granulocytes. Particularly, asthma is considered to be primarily an eosinophilic disease with symptoms positively correlated to eosinophil migration to the site of inflammation (Kyoh *et al.*, 2008; KanKaanranta *et al.*, 2010). It has been previously shown that peak in eosinophil accumulation occurs 24 hours after exposure to an allergen (O'Byrne *et al.*, 2004; Holgate & Polosa, 2008). The activation of eosinophils has been linked to IL-13 as this cytokine is pre-formed and stored in granules and released in response to stimuli (Spencer & Weller, 2010; Walsh & August, 2010). The positive correlation between IL-13, eosinophils and exacerbation of chronic inflammatory lung disease symptoms is therefore clear and well documented in murine models. The role of chloride ion channels in this, particularly hBest1 has not been clearly established.

The data presented has implied that gene expression may increase at 24 hours following stimulation with IL-13. In the current project, this has not been shown to be statistically significant. At protein level, there is a statistically significant increase in hBest1 (Figure 5.3) in PMNs stimulated with IL-13, both from time 0h and compared to nil controls. There may also be a similar response in eosinophils as implied by initial cytokine stimulation and flow cytometry (Figure 5.5, Table 5.2) however further repetition is required. This may be mediated by hCLCA1 as Nakano et al (2006) have demonstrated that in response to IL-13, there is increased expression of mCLCA3 (human isoform hCLCA1). This was not the case in the current project which found that in response to IL-13, there was a decrease in hCLCA1 in eosinophils. This is observational only however and further replication is required to eludicate the expression of hCLCA1

in response to IL-13. In RT-PCR gene expression screening (Chapter 4) however, it has been shown that the relationship between hCLCA1 and hBest1 is negative. In this instance, if there were an increase in hCLCA1, it would be expected that there would be a decrease in hBest1, and vice versa. This appears to support the observations in Figure 5.5. It may be suggested therefore, that hCLCA1 and hBest1 may work in a complementary way and that either one may be up-regulated in response to IL-13. This is supported by the findings of Nakano *et al* (2006) and the expressional screening presented in Chapter 4 and 5.

The relationship between granulocytes, chronic inflammatory lung disease and symptoms seems supported as the data shows a response to IL-13 stimulation with a peak in hBest1 intracellularly at 24 hours, which decreases after 48 hours. This also supports the findings of others who suggest that hBest1 is located primarily intracellularly and may be linked to activation of hANO1 (Kunzelmann *et al.*, 2009; Barro-Soria *et al.*, 2010). In this process, inflammation may stimulate IL-13 release and therefore an increase in hCLCA1 (Nakano *et al.*, 2006). This may be responsible for maturation and differentiation of granulocytes, which peaks at 24 hours after stimulation (Holgate & Polosa, 2008). Alternatively, there may be an increase in hBest1 expression primarily intracellularly (Kunzelmann *et al.*, 2009; Barro-Soria *et al.*, 2010), with exacerbation of symptoms. As a result, activation of hANO1 may occur. As activated granulocytes begin apoptosis at 24 hours (KanKaanranta *et al.*, 2010), this supports the findings and possible process as the expression of hBest1 begins to decrease after this point. Conversely, the expression of eosinophils in this study do not fully support this hypothesis (Figure 5.5 and Table 5.2). This was performed once (n=1) due to the constraints of resources and therefore conclusions cannot be statistically supported.

The peak hBest1 in eosinophils in response to IL-13 and IL-5 together (Figure 5.5) supports Willis-Karp (2004) who state that in the presence of IL-5, eosinophils are further activated to increase IL-13 release. This combined action and process would increase the expression of hBest1 protein as demonstrated in figure 5.5. This is indicative of the *in vivo* responses to inflammation as IL-5 and IL-13 are considered to act in partnership (Kim *et al.*, 2010; Spencer & Weller, 2010). IL-5 alone demonstrates an increase in hBest1 protein however this is not as great as any of the other experimental groups. This may not be a true reflection of *in vivo* responses. IL-5 response in inflammation has been shown to terminally differentiate eosinophils, increase recruitment and attraction of eosinophils to the site of inflammation and to delay apoptosis (Kariyawasam & Robinson, 2007; Simon & Simon, 2007; Matsumoto *et al.*, 2008). In this study, the true biological response would have been prohibited as the number of eosinophils was defined and the action of recruiting further eosinophils was not possible. It would be beneficial to examine this in more depth, possibly in combination with transmigration techniques so that eosinophil recruitment could be established.

TNF-a also caused a significant increase in hBest1 protein intracellularly however this needs replication (n=1). The role of TNF-a is considered to be a neutrophilic chemo-attractant. As discussed previously, this process would be inhibited by the *in vitro* limitations.

5.2 Transmigration assay

5.2.1 Transmigration results

In order to establish a potential function for hBest1 in PMNs the transmigration of HL60s with over-expressed (transfected) hBest1 protein was measured as a response to N-formyl-methionyl-leucyl-phenylalanine (fMLP) and IL-13 (see section 2.6 for concentration and methodology). The number of cells were counted in one large square ($1mm^2$ = 100nl) using a haemocytometer (A in Table 5.3). This was converted to cells/ml and then total number of cells in 400µl by;

Cell count in $1mm^2$ x 10^4 x 2 (dilution factor) = cells/ml

Cell/ml x 0.4 = Total cells in 400µl (B in Table 5.3)

The total number of cells in 400µl was used to calculate a percentage of total cells migrated across the membrane. The known number of cells added into the well were 13.5 x 10^4 therefore the final percentage (C in Table 5.3) was calculated as;

(Cells in 400µl / (13.5 x 10^4)) x 100 = Percentage migration

	Well additive = nil			Well additive = fMLP			Well additive = IL-13		
	A	**B**	**C**	**A**	**B**	**C**	**A**	**B**	**C**
Sample									
1. HL60 (nil)	2	16000	12	2	16000	12	10	80000	59
2. HL60 (nil)	4	32000	24	4	32000	24	8	64000	47
3. HL60 (nil)	3	24000	18	2	16000	12	4	32000	24
Mean HL60 (nil) (n=3)	**3**	**24000**	**18**	**3**	**21333**	**16**	**7**	**58667**	**43**
Standard Deviation	**NA**	**8000**	**NA**	**NA**	**9238**	**NA**	**NA**	**24440**	**NA**
1. HL60 +hBest1	3	24000	18	10	80000	59	13	104000	77
2. HL60 +hBest1	2	16000	12	9	72000	53	14	112000	83
3. HL60 + hBest1	2	16000	12	7	56000	41	11	88000	65
Mean HL60 +hBest1 (n=3)	**2.33**	**18667**	**14**	**9**	**69333**	**51**	**13**	**101333**	**75**
Standard Deviation	**NA**	**4619**	**NA**	**NA**	**12220**	**NA**	**NA**	**12220**	**NA**
1. HL60 + JetPrime	2	16000	12	3	24000	18	11	88000	65
2. HL60 + JetPrime	3	24000	18	1	8000	6	9	72000	53
3. HL60 + JetPrime	3	24000	18	0	0	0	8	64000	47
Mean HL60 + JetPrime (n=3)	**2.67**	**21333**	**16**	**1**	**10667**	**8**	**9**	**74667**	**55**
Standard Deviation	**NA**	**4619**	**NA**	**NA**	**12220**	**NA**	**NA**	**12220**	**NA**

Table 5.3: Effects of transfecting hBest1 into HL60s on transmigration in response to fMLP and IL-13: HL60 cells were transfected with hBest1. Three experimental groups (nil, hBest1 transfected and JetPrime only treated) were applied to a 3µm pore membrane and the number of cells migrated across in response to fMLP and IL-13 measured (section 2.6 for concentration). A= Cell count using haemocytometer, B= Conversion to number of cells in 400µl of cell media, C= Percentage of cells migrated. N=3 and mean of cell count with ± standard deviation (SD).

The transmigration of nil HL60s, compared to HL60s treated with transfection reagent, JetPrime only (n=3), were not statistically significant (P>0.05) (see section 2.8 for statistical analysis method). Therefore, it was considered that the process of transfection itself, did not affect the transmigration of cells either due to cell shape or alterations in function. This was also the case for each experimental group (nil, fMLP and IL-13 addition, section 2.6 for concentrations) in that the HL60 nil group were not statistically different from the HL60s treated with JetPrime only. Therefore, the HL60 group with no treatment were used as a control group. In the control group, the number of cells migrating through the membrane in response to IL-13 was double that in the nil, and the fMLP group, with 43% of cells migrated. Using ANOVA, this was a statistically significant migration in response to IL-13 for HL60s (nil) (P<0.05, n=3, * in figure 5.6).

However, when HL60s were transfected with hBest1 (n=3), the response to fMLP and IL-13 addition in the well was statistically significant (P<0.05) ($*^2$ in Figure 5.6). When examining hBest1 transfected cells, there was no difference between nil HL60s and those transfected with hBest1 when there was no addition to the well. In response to fMLP, there was a statistically significant 4 fold increase in the number of cells migrating across the membrane, into the well containing fMLP (P<0.01, $*^2$ in Figure 5.6). Whilst there was migration in the HL60 nil group in response to IL-13 (* in Figure 5.6), there was a greater migration of HL60s transfected with hBest1 when IL-13 was added to the well. The migration was over 5 times greater than nil which was statistically significant (P<0.01). This was also nearly twice the migration observed in HL60s (nil) in response to IL-13. This was statistically significant and therefore responses in migration when IL-13 is added to the well were thought to be hBest1 specific (P<0.05, $*^3$ in Figure 5.6). Moreover, the different migration

responses to fMLP and IL-13 were also statistically significant ($P<0.05$). From this assay, it is reasonable to conclude that hBest1 has a role in cellular migration. The role of hBest1 intracellularly requires further experimentation however it may be implicated in cell signalling, and maturation of cells. It has also been suggested that there is an interaction between hBest1 and hCLCA1 or hANO1. In this instance, there may be a secondary impact upon cell volume through activation of alternative chloride ion channels. This relationship requires further clarity.

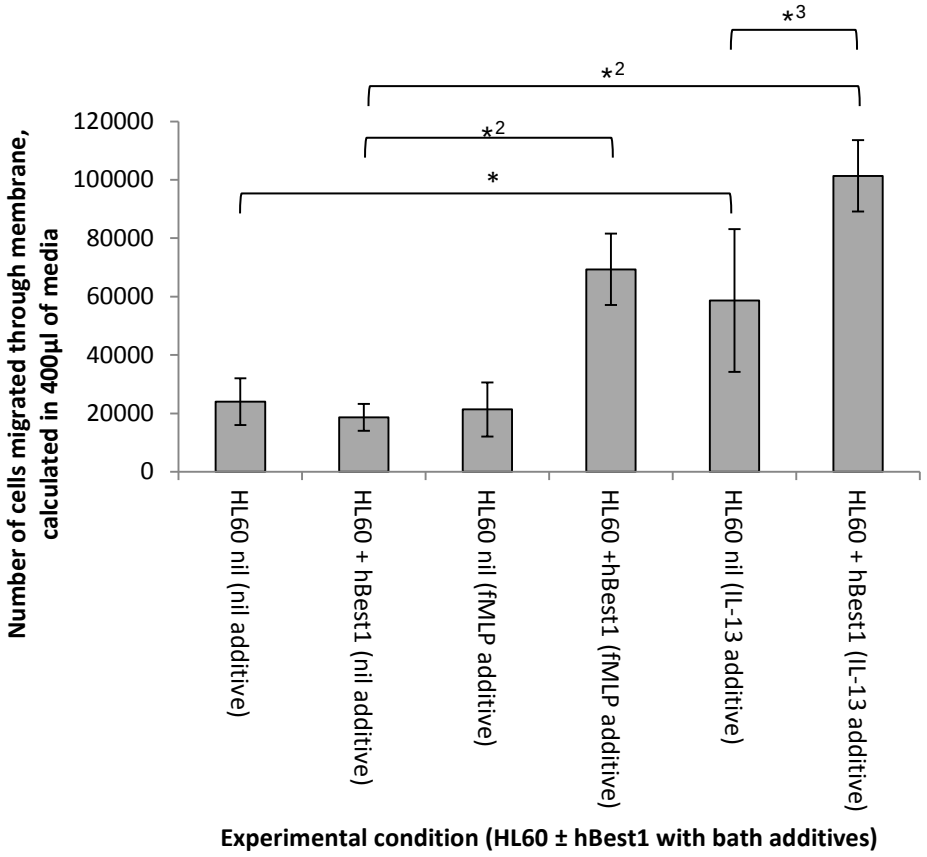

Figure 5.6: The effect of transfection with hBest1 on the transmigration of HL60s in response to fMLP and IL-13: Transmigration of HL60 cells transfected with hBest1, compared to nil, and transfection reagent treated only. This was in response to fMLP and IL-13 additive to the well (n=3 for each experimental group). Error bars for standard deviation. There was no statistically significant difference between HL60 (nil) and those treated with transfection reagent only. The migration when transfected with hBest1 in response to both fMLP and IL-13 was statistically significant ($P<0.05$, $*^2$ above) with a greater migration in response to IL-13 (* and $*^3$ above) . This appears to suggest a role for hBest1 in cellular migration

5.2.2 Implications and discussion

hBest1 has previously been linked to Best's disease, in which fluid shifts occur as a result of dysfunction of the hBest1 chloride channel (Qu *et al.*, 2004; Chien *et al.*, 2006). Additionally there is evidence suggesting that hBest1 is involved in the conductance of airway epithelial cells (Duta *et al.*, 2004).

fMLP is found *in vivo* following bacterial protein breakdown. It is also present in the inflammatory process as a bi-product of mitochondrial protein degradation, which would also be present in epithelial tissues of the lungs in chronic inflammatory lung diseases. The transmigration assay, therefore, was performed to establish any link between inflammation and the potential function of hBest1 in granulocytes.

fMLP is a powerful chemo attractant which has been shown to attract neutrophils, specifically during inflammation (Virchow *et al.*, 1998; Zhu *et al.*, 2005). It would seem reasonable to expect migration of HL60s, as a model of PMNs, in the presence of fMLP therefore, regardless of whether hBest1 was transfected. This was not a statistically significant observation in the current assay. However, it has been shown that fMLP stimulated neutrophils have a role to play in the inflammatory process. Zhu et al (2005) have shown that neutrophils stimulated with fMLP have a role in inflammation and cellular permeability. That neutrophils are essential in this response is demonstrated when fMLP was applied directly to tissues with no response in permeability. fMLP has been implicated in inflammation as it initially attracts neutrophils to the site of inflammation, and increases granulocyte respiratory burst, with an increase in oxygen free radical species (Virchow *et al.*, 1998;

Zhu *et al.*, 2005). It is the oxygen free radicals that are responsible for the observed cellular permeability in inflammation and infection. In addition, fMLP stimulates an increase in intracellular Ca^{2+}(Zhu *et al.*, 2005) in neutrophils. This is specifically relevant to the current transmigration assay. As discussed previously, hBest1 is a Ca^{2+} activated chloride channel (Suzuki *et al.*, 2006; Greenwood & Leblanc, 2007). Therefore, if intracellular Ca^{2+} rises in response to fMLP, it may result in increased activity of hBest1 as a chloride ion channel, if the transfected HL60s have an over-expression of hBest1. Whether this is by direct Cl^- movement, or by stimulating another channel such as ANO1 (Kunzelmann *et al.*, 2009) is not clear in the current study.

It has been suggested that hBest1 acts to volume regulate the cell however this has been established in the retina in Bests disease (Duta *et al.*, 2004; Qu *et al.*, 2004; Chien *et al.*, 2006). The increased transmigration of HL60s when transfected with hBest1, may be due to increasing Ca^{2+} stimulating the over-expressed hBest1 and therefore an increased conductance of Cl^- and resultant fluid movement. This is through the interaction between intracellular and membrane bound chloride ion channels

It has been suggested that there is a complex interaction between hBest1, hCLCA1 and hANO1 expressed intracellularly, and cell membrane bound. The functions of intracellular and surface chloride channels may complement each other in the control of cell volume in granulocytes. Intracellular chloride channels are considered to have several roles. Among these is regulation of intracellular pH through electrogenic transport of cations, such as vacuolar proton ATPase. In this instance, using energy released from ATP hydrolysis, hydrogen ions are pumped across the membranes of intracellular organelles (Edwards & Kahl, 2010). However, it has been

hypothesised that another role intracellular chloride channels, such as hBest1, is to increase intracellular calcium. There is a release of calcium ions from the endoplasmic reticulum through counterion movement (Pollock *et al.*, 1998; Barro-Soria *et al.*, 2010; Edwards & Kahl, 2010). This control of calcium intracellularly, through hBest1, may therefore modulate the activity of membrane bound calcium activated chloride channels such as hBest1 or hANO1 (Edwards & Kahl, 2010). In granulocytes, the activation of membrane bound chloride channels would impact upon overall cell volume. Increasing chloride conductance across the membrane would increase movement of sodium, coupled as salt (NaCl). By osmosis, there would be a greater movement of water across the cell membrane (Figure 5.6). This would decrease cell volume and allow a greater migration of HL60s through the defined 3µm pore membrane. This process would be similar in physiological inflammation however there would be further exacerbation of epithelial symptoms as granulocytes go through respiratory burst, degranulate and release oxygen free radicals in response to fMLP (Virchow *et al.*, 1998; Zhu *et al.*, 2005). This in turn would increase permeability of airway epithelia, exacerbation of sputum clearance, and airway hyper-responsiveness.

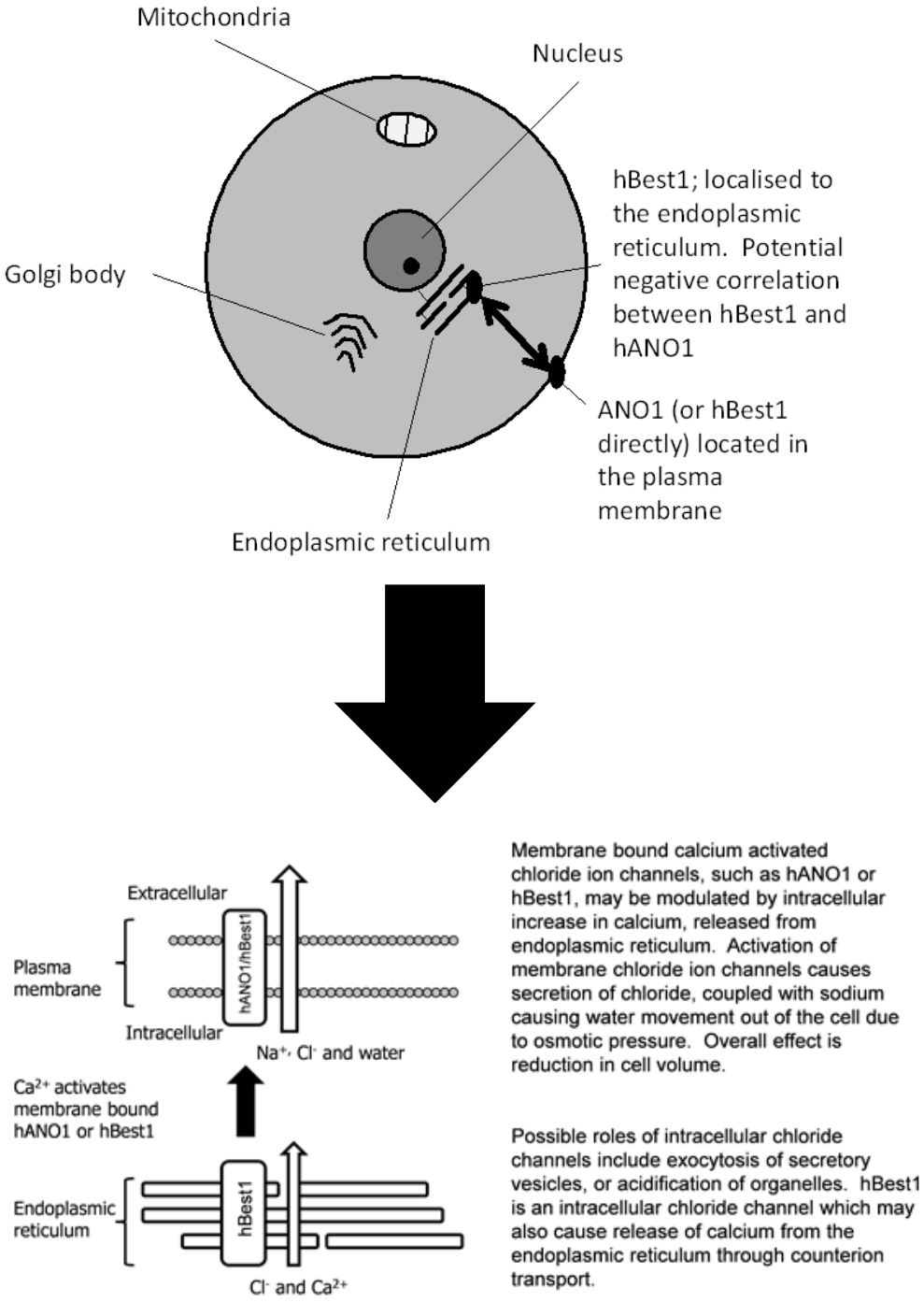

Figure 5.7: Diagrammatic representation of the hypothesis of cell volume control through interactions between intracellular and surface bound chloride ion channels: Intracellular hBest1 may modulate the activity of surface bound chloride ion channels by increasing release of calcium from endoplasmic reticulum. This increase in intracellular calcium may activate surface bound calcium activated chloride ion channels causing an increase in secretion of chloride, coupled with sodium, across the cell membrane. A resultant movement of fluid, due to osmosis, would regulate overall cell volume.

In the current transmigration assay, there was a larger migration of HL60s in response to IL-13 additive to the well. This difference in migration in response to IL-13 and fMPL was statistically significant. The larger migration supports a possible role of hBest1 with hCLCA1 and hANO1. IL-13 addition may cause a positive feedback system as during inflammation, IL-13 causes PMNs, particularly eosinophils, to migrate to the site of inflammation. This causes an increase in IL-13 release from eosinophils which further increases migration. This may account for the differences observed in Figure 5.4 however may suggest a further relationship between alternative chloride channels. As identified, IL-13 up-regulates mCLCA3 (human ortholog hCLCA1) (Nakano *et al.*, 2006). In the human model, this may increase the expression of hCLCA1 in HL60s. There has also been suggestion of a correlation between hCLCA1 expression and up-regulation of hBest1 ((Kunzelmann *et al.*, 2007; Hamann *et al.*, 2009). In cells transfected with hBest1, there is already over-expression and the result may be an increase in hBest1 greater than that observed in the fMLP experimental condition. As stated, hBest1 may be localized to the endoplasmic reticulum and responsible for mediation and activation of hANO1 (Kunzelmann *et al.*, 2009; Barro-Soria *et al.*, 2010). This would result in an overall increase in net efflux of Cl^-, and therefore fluid, decreasing cell volume with greater migration, as observed.

The transmigration assay supports the hypothesis that hBest1 may be involved in cellular migration during periods of inflammation, and increase in epithelial responses. Polymorphonuclear cells, particularly HL60s in this assay, are responsive to fMLP and IL-13 release during inflammatory responses. This may be due to an overall net increase in Cl^- flux changing cell volume, or an increased expression of Ca^{2+} activated Cl^- ion channel mediators. It would

indicate further analysis as to the relationship between hCLCA1, hBest1 and hANO1.

5.3 Cl^- and Ca^{2+} flux assays

The flux of Cl^- would further add evidence to the growing discussions regarding hBest1 and the role in either granulocyte migration or activation, and the links to exacerbation of clinical symptoms in chronic inflammatory lung diseases.

N-(ethoxycarbonylmethyl-6-methoxyquinolinium bromide (MQAE) was used in accordance with manufacturers recommendations (Invitrogen) and previous laboratories (Koncz & Daugirdas, 1994). The MQAE fluorescent probe has been used in a number of cell types (Koncz & Daugirdas, 1994; Marandi *et al.*, 2002) however the level at which MQAE is either self-quenching, or quenched by non-chloride anions, specifically in HL60s is unclear at this point, therefore analysis using this technique is problematic. Marandi et al (2002) highlight the limitations of MQAE and state that quantification of Cl^- flux is difficult and a limitation of these studies as the dye is non-ratiometric. In addition, the leakage of MQAE from different cell types is varied, and dependent upon the preparation of samples. One extraneous variable is temperature. This indicates the need for extensive methodology modification however, it should be justified given that results are difficult to quantify.

The calcium flux assay used a calcium sensor dye eFluor®514 (eBioscience). On initial flow cytometry there appeared to be clear changes in fluorescence however when the cells were stained with propridium iodide (PI) (Figure 5.8), there appeared to be evidence of cellular necrosis. The increase in calcium flux was correlated with PI positive staining (PI binding to DNA material). As the calcium dye is a membrane permeable dye, it may be that this stimulates cellular apoptosis, and further necrosis. This may also be due to preparation of the dye as it is constituted in DMSO, as per manufaturers

instruction, at the recommended concentration. This in itself is a nucleophilic acid which may cause cellular necrosis. It seems, therefore, that results are inconclusive possibly due to issues in methodology which would require extensive optimization. The change in fluorescence cannot be specifically attributed to any experimental condition as the dye may be non-specifically binding as the cell becomes necrotic.

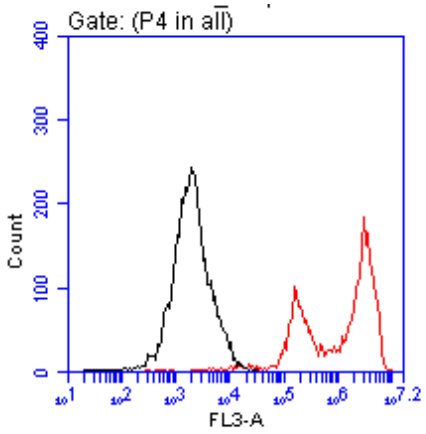

Figure 5.8: Effect of calcium sensor dye staining on HL60 cell viability

HL60 cells (n=3) were treated with calcium sensor dye [2nM final conc.] for 30min at 37°C/5% CO_2/humidified air. The cells were then assessed for viability by propidium iodide (PI) exclusion immediately before analysis on a BD Accuri C6 flow cytometer (Ex 488nm; Em 533/30nm (Calcium sensor dye; FL-1A), 670LP (PI; FL-3A). This representative histogram overlay reveals that dye labelled cells exhibited dual peaks in the PI channel (red line) while undyed cells exhibited a single PI negative peak (black line).

CHAPTER 6: SYSTEMATIC REVIEW:

IS THE GENE AND PROTEIN EXPRESSION OF CHLORIDE ION CHANNELS UPREGULATED IN THE RESPIRATORY EPITHELIA, OR GRANULOCYTES, OF SUBJECTS WITH CHRONIC INFLAMMATORY LUNG DISEASE

6.1 Rationale for systematic review

Systematic reviewing is a rigorous research method designed to collate all of the evidence on a specific question. The Cochrane Handbook defines a systematic review as;

"A systematic review attempts to collate all empirical evidence that fits pre-specified eligibility criteria in order to answer a specific research question. It uses explicit, systematic methods that are selected with a view to minimizing bias, thus providing more reliable findings from which conclusions can be drawn and decisions made" (Higgins & Green, 2008, pg6).

It is acknowledged, however, that systematic reviewing is designed predominantly for collating a large number of randomized control trials in order to apply findings to healthcare. In this project, the principles of systematic reviewing are applied to laboratory based studies.

It has been established in the literature review (Chapter 1, Introduction) that granulocytes are implicated in the process, and symptoms, of chronic inflammatory lung disease. There has also been considerable discussion as to the role of chloride ion channels in these cells. Through laboratory experiments, the expression of a number of putative chloride ion channels, and some of the functional properties of bestrophin 1 in humans (hBest1) has been established in granulocytes, and HL60s. The relationship between chloride ion channels and chronic inflammatory lung disease needs to be assessed to address the project question. It may be possible to

identify whether chloride ion channels are up-regulated, or implicated in lung disease. Provisionally experimental plans were formulated to address this question and to further explore functional properties of hBest1, such as using patch clamping techniques to establish calcium and chloride flux. However, due to changes in funding, and therefore available resources, further experimental work was prohibited. In discussion with, and under the guidance of an expert in systematic reviewing alternative methods for addressing the hypothesis were explored. It was considered that, whilst the preferred research method would be primary laboratory work, systematic reviewing of evidence could be utilised. However, this systematic review may be subject to publication bias and must be acknowledged. The studies identified may not be representative of all experiments conducted due to the risks of publishing only "positive" results. Limitations of the systematic review will however be explored in section 6.5.1.

A systematic review was undertaken to examine evidence on the expression of chloride ion channels in subjects with chronic inflammatory lung diseases.

6.2 Objectives of systematic review

The systematic review aims to study whether the gene and protein expression of chloride ion channels is different in chronic inflammatory lung disease compared to health. The term "granulocytes" will be used in this section as this was the prevalent term in the literature found. With a focus on chronic inflammatory lung disease, and a control of those without disease, specific objectives are;

- To examine both granulocytes and airway epithelial cells, in order to establish whether there is a different expression pattern in health and disease. This relates specifically to the different family groups (bestrophins, CLCAs, anoctamins, ClCs, CFTR and Tweety)

- To consider both protein and gene expression to establish whether there is up-regulation, and increased protein expression in the presence of disease

This will complement the experimental data on expressional screening and functional analysis in granulocytes.

6.3 Methodology

6.3.1 Formulation of systematic review question

A protocol was formulated and has been used to develop the methodology reported. The question to be answered through systematic review was formulated using a framework of case, control and mechanism/factor (Table 6.1).

Cases	Controls	Mechanism/factor
Subjects with chronic inflammatory lung disease Granulocytes (eosinophils, neutrophils and basophils) Epithelia (tracheal, bronchial and small airways) Chronic inflammatory lung disease (COPD and asthma)	**Subjects without chronic inflammatory lung disease**	**Chloride ion channel expression** Bestrophins (1-4), CLCAs, ANOs, ClCs, Tweety Protein and gene expression

Table 6.1: Table using case/control/mechanism to formulate systematic review question: Bold font signifies the population within the case, control and factor groups. Detail of inclusions within this population are listed beneath. From this the systematic review question was formulated

From this, the systematic review question was formulated; Is the gene and protein expression of chloride ion channels upregulated in the respiratory epithelia, or granulocytes, of subjects with chronic inflammatory lung disease, as assessed by Bestrophins (1-4), CLCAs, ANOs, ClCs, Tweety protein and gene expression, using all available cohort, case control and laboratory studies?

6.3.2 Inclusion/exclusion criteria

The systematic review was performed using guidelines adapted from the Cochrane Handbook (Higgins & Green, 2008). The inclusion and exclusion criteria were defined (Table 6.2) and all primary research papers identified were considered for inclusion, which included both cohort studies and laboratory based experimental studies.

Criteria no.	Inclusion/Exclusion criteria
1	Is the study laboratory based/cohort study? (Include all primary laboratory research. Exclude all opinion papers, reviews, meta-analyses, editorials, letters and studies published only in abstract form)
2	Are the samples/subjects mammalian? (Include all studies using either human subjects, mammals or mammalian commercial cell lines. Exclude all samples taken from non-mammals such as amphibians, reptiles and fish)
3	Is the focus upon blood cells or airway tissue? (Include all blood cell types such as granulocytes and agranulocytes, and all airway cells such as tracheal, bronchial etc. Exclude cells/samples from other organs such as pancreas. Exclude nasal)
4	Focussed upon chronic inflammatory lung diseases? (Include all inflammatory lung diseases. Exclude non-inflammatory disease of the lungs such as cancers, inflammatory disease or symptoms not of the airways such as bowel, exclude cystic fibrosis)
5	Chloride ion channels? (To include all types such as voltage gated, volume regulated, calcium activated and ligand gated. Include those assumed to be either regulators of chloride flux or a channel; CLCA, bestrophins, ClC, tweety etc. Exclude all other ion channels such as potassium and sodium)

Table 6.2: Table of inclusion and exclusion criteria for selection of evidence for systematic review: All inclusion and exclusion criteria identified by which studies were selected, or rejected for use in the systematic review

Comparison groups were control (considered “healthy” tissue) and tissues involved in chronic inflammatory lung disease. Those disease processes for inclusion were primarily COPD and asthma. Cystic fibrosis was excluded due to multiple pathological processes. Other diseases excluded were; rhinitis, asbestosis and cancer. These diseases were considered to have physiological processes that would not be generalizable to COPD or asthma.

Outcome measures and factors for inclusion were chloride channels and channel families. This included; CLCA, bestrophins, anoctamins, ClCs, CFTR and Tweety. Other channels, such as potassium or sodium, were excluded from the systematic review. Studies were included if they considered protein or gene expression of these channels using methodologies such as RT-PCR, Western and Northern blot analysis, immunohistocytochemistry and flow cytometry.

6.3.3 Identification of studies and search protocol

To identify appropriate studies Medline and EMBASE databases were searched using the OVID platform on 19th May 2012. Search terms for these databases are outlined in Table 6.3. In addition, the Cochrane library was searched to ensure that the review question had not already been addressed in another systematic review. A personal collection of studies was hand-searched to identify potential papers for inclusion. Reference lists of all papers were scanned for potentially included studies. Full text of those identified was accessed as appropriate. To ensure that all potential studies were considered, letters were written to key laboratories in Europe to ask if any unpublished data could be shared for the purpose of the systematic review (Appendix 2 presents a copy of the letter).

Search terms with Boolean operators and truncation
1. gene expression regulation/ or gene expression/ 2. (western blot adj5 analys*).ti,ab. 3. RT-PCR.ti,ab. 4. (reverse adj3 transcript*).ti,ab. 5. (gene* adj3 upreg*).ti,ab. 6. (protein adj3 express*).ti,ab. 7. 1 or 2 or 3 or 4 or 5 or 6 8. exp lung disease/ or exp respiratory tract disease/ or exp bronchiolitis/ or exp chronic lung disease/ or exp chronic obstructive lung disease/ or exp lung alveolitis/ or exp lung emphysema/ 9. (chronic adj5 lung adj5 disease).ti,ab. 10. (resp* adj5 lung adj5 disease*).ti,ab. 11. COPD.ti,ab. 12. (chronic adj5 obstructive adj5 pulmonary adj5 disease*).ti,ab. 13. (chronic adj5 obstructive adj5 airway* adj5 disease*).ti,ab. 14. COAD.ti,ab. 15. asthma*.ti,ab. 16. (inflammato* adj5 lung adj5 disease*).ti,ab. 17. 8 or 9 or 10 or 11 or 12 or 13 or 14 or 15 or 16 18. exp chloride channel/ or exp chloride channelopathy/ 19. (chloride adj5 ion adj5 chan*).ti,ab. 20. bestrophin.ti,ab. 21. CLCA.ti,ab. 22. anoctamin.ti,ab. 23. anoc*.ti,ab. 24. ClC.ti,ab. 25. tweety.ti,ab. 26. (volume adj5 regulated).ti,ab. 27. (ligand adj5 gate*).ti,ab. 28. (voltage adj5 act*).ti,ab. 29. calcium act*.ti,ab. 30. 18 or 19 or 20 or 21 or 22 or 23 or 24 or 25 or 26 or 27 or 28 or 29 31. 7 and 17 and 30

Table 6.3: Search terms with Boolean operators and truncation: All terms used to search Medline and Embase using OVID as a platform

The initial list of identified studies was examined and any duplicates across databases identified. Any duplicates were removed prior to assessing inclusion and exclusion criteria. A standardized "inclusion/exclusion" form was used to assess whether studies met the inclusion criteria (Appendix 3). This was performed at two points in the literature search process. The first exclusion point (Point A in Figure 6.1, in Section 6.4) used title and abstract to assess eligibility for inclusion. The second point (Point B in Figure 6.1, in section 6.4) used the full text articles for each identified study. At exclusion point C, the focus was narrowed to expression of genes or protein in order to accurately assess the systematic review question.

6.3.4 Assessing the risk of bias

To complete the selection process, papers were assessed for the risk of bias. A tool (Appendix 4) was developed from adapting the Cochrane Handbook risk of bias tool for randomized controlled trials (Higgins & Green, 2008). This was combined with an adapted tool from the National Institute for Clinical Excellence (NICE, 2007). Final selected papers were independently assessed by two reviewers to reduce the risk of bias in the systematic review process. To judge the studies for eligibility to be included, the risk of bias was assessed in three domains; internal validity, overall assessment and study description. Each domain was rated as low, medium or high risk of bias by totaling the number of areas that were either not addressed or not reported. Studies that scored 15% or less were considered to have a low risk of bias and the conclusions were very unlikely to alter. Any study that was assessed with medium or high risk of bias in any of the three domains was excluded from the systematic review.

Publication bias has been considered however thorough assessment is problematic. Systematic reviewing, as stated, is intended for randomised controlled trials which maybe subject to registration at the beginning of the study (Song *et al.*, 2010). This would allow identification of all prospective data sets, regardless of whether they are null or not. Laboratory experiments are not subject to registration and therefore identification of all prospective studies is unlikely. Publication bias was addressed during the systematic review by writing to key European laboratories requesting all data collected relevant to the research question, regardless of whether results were considered "positive" or null. However, non-response may be due to results not being processed if considered null. A funnel plot was considered however not performed following final

selection of studies due to the differences in populations examined, and the limited number of studies identified. It has been assumed, therefore, that the review presented has a high risk of publication bias and therefore application of findings is unlikely.

6.3.5 Data extraction and synthesis of results

Data from identified studies, meeting inclusion criteria, was intended to be pooled using outcomes measures of protein, and gene expression. Variables to be considered were; with or without chronic inflammatory lung disease (as the independent variable), and protein and gene expression of each potential chloride ion channel (as the dependent variable). Pooled results were to be tabulated with the mean, and standard deviation, calculated for protein and gene expression, for each identified chloride ion channel. The mean gene and protein expression in samples with chronic inflammatory lung disease was to be compared to samples without disease. Statistical significance would have been identified using ANOVA to assess whether there was upregulation of chloride ion channels in chronic inflammatory lung diseases, compared to those without.

Whilst this was the intended method of data extraction and synthesis, the limited number of studies identified used differing outcome measures and therefore pooling data was not possible.

To ensure transparency and full reporting of the systematic review, a PRISMA checklist was completed (Appendix 5).

6.4 Results

6.4.1 Literature search results

Database searches, and hand-searching, yielded 560 potential papers for inclusion. There were however 36 duplicates therefore 524 studies were considered for inclusion by scanning the title and abstract. From the initial search, 438 studies were excluded as they did not meet inclusion criteria (Figure 6.1, exclusion point A). This was assessed by accessing the title and abstract only. Of these 187 were excluded as they didn't focus upon inflammatory lung disease. These studies primarily considered either cystic fibrosis or cancer. A large number of the 438 excluded were due to the tissue type used. 117 used tissues other than lung or blood cells, such as intestinal, pancreatic, brain. Other reasons for excluding studies were that they were not primary research, or that the focus was on other ion channels such as sodium or potassium. Of the 86 papers initially identified, a further 46 were excluded after accessing the full text (Figure 6.1, exclusion point B). At exclusion point C, a further 25 studies were excluded as the focus was not upon expression of genes or proteins. There were 15 studies selected for possible inclusion in the systematic review following assessment of the risk of bias. Figure 6.1 summarizes the results of the literature searching process.

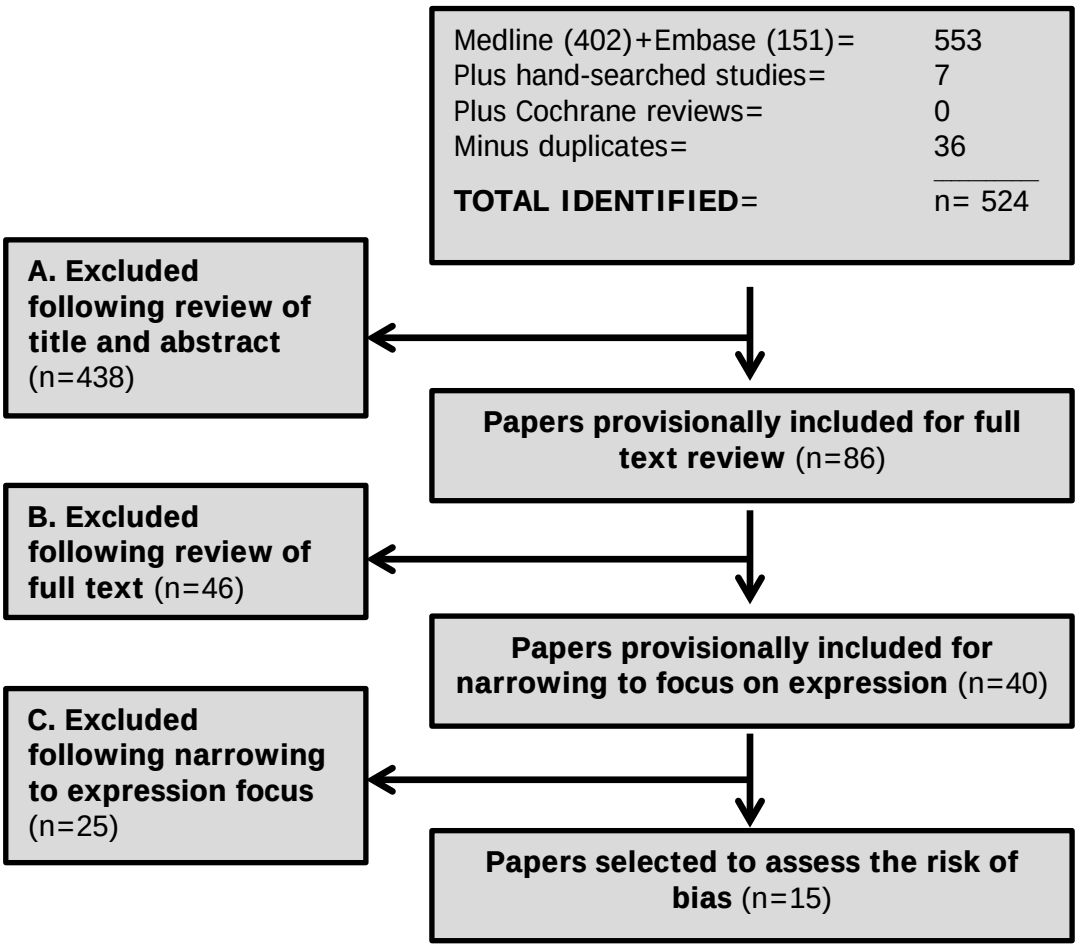

Figure 6.1: Flow chart of process for literature searching: 524 papers were initially identified for assessment against the inclusion/exclusion criteria. A standardized form (appendix 2) was used at exclusion point A and B. Final papers were selected at point C by narrowing the focus to expressional data only. 15 papers were identified for possible inclusion

6.4.2 Assessing the risk of bias

Five of the papers selected scored as a high or medium risk of bias in at least one domain. These were excluded from the systematic review. 10 of the studies were finally included. Table 6.4 summarizes the 15 papers and the risk of bias scoring for each domain. Two of the papers which scored a high or medium risk of bias were due to the limits of only accessing abstract. One study was a conference presentation and published in abstract only and the other was published in Chinese and abstract only available in English. Whilst this paper may have offered a valuable contribution to the review, there were limitations to accessing translation. The other three studies excluded due to a high or medium risk of bias did not present all required information, such as not defining the sample size or control group.

Study	Risk of bias		
	Risk of bias within internal validity domain	**Risk of bias in overall assessment**	**Risk of bias in study description**
(Anton *et al.*, 2005)	Low	Low	Low
(Gerber *et al.*, 2009)	Low	Low	Low
(Hoshino *et al.*, 2002)	Low	Low	Low
(Kuperman *et al.*, 2005)	Low	Low	Low
(Liu *et al.*, 2004)	High	High	Low
(Moore *et al.*, 2008)	Low	High	Medium
(Nakano *et al.*, 2006)	Medium	Low	Medium
(Range *et al.*, 2007)	Low	Low	Low
(Ryhner *et al.*, 2008)	Low	Low	Low
(Toda *et al.*, 2002)	Low	Low	Low
(Wang *et al.*, 2007a)	Low	Low	Low
(Wang *et al.*, 2007b)	Low	Low	Low
(Woodruff *et al.*, 2007)	Low	Low	Low
(Yim *et al.*, 2011)	Low	Medium	Low
(Zhou *et al.*, 2001)	Low	Medium	Medium

Table 6.4: Summary of identified papers and resultant risk of bias assessment: Table outlines the risk of bias assessment in all three domains for each paper identified. Those highlighted in grey were excluded from the final systematic review as they attracted a medium or high risk of bias in at least one of the three domains assessed.

6.4.3 Characteristics of included studies

The key characteristics of the final selected studies are presented in Table 6.5. Seven of the 10 selected studies were published within the last five years and all were within 10 years. 60% had a sample of humans whereas the remaining 40% were equine. All tissues were extracted from the bronchus of each species. Of the studies, the majority focused upon asthma (90%) with three of these also considering COPD. Only one study focused upon COPD alone however it was noted that the first author of this was also first author on a similar paper that considered asthma. The title, methodologies and conclusions for these two papers were similar, and the title only differed by interchanging “COPD” and “asthma”. These were considered two papers arising from the same study as discussed in later text. All studies used the expression of RNA as an outcome measure through experimental techniques such as quantitative RT-PCR or immunohistochemistry.

Study	Sample size		Sample species	Tissue type	Disease focus	Chloride ion channel focus	Experimental techniques	Outcome measures
	Experimental	Control						
(Anton *et al.*, 2005)	3	3	Equine	Lung	Asthma	eCLCA1	Northern blot, immunoblotting, electrophysiology and quantitative RT-PCR	RNA and protein
(Gerber *et al.*, 2009)	5	5	Equine	Small cartilaginous conducting airway	Asthma and COPD	eCLCA1	Quantitative RT-PCR	RNA and neutrophil count
(Hoshino *et al.*, 2002)	21	13	Human	Bronchial	Asthma	Calcium-activated chloride channel 1	Quantitative RT-PCR, histochemical analysis	RNA
(Kuperman *et al.*, 2005)	30	28	Human and murine	Bronchial	Asthma	hCLCA1 and mCLCA3	Microarray analysis and quantitative RT-PCR	Gene expression by fold change
(Range *et al.*, 2007)	9	9	Equine	Trachea and bronchus	Asthma and COPD	eCLCA1	Immunohistochemistry and quantitative RT-PCR	RNA and protein

(Ryhner *et al.*, 2008)	19	11	Equine	Bronchial	Asthma and COPD	eCLCA1	Cytology and quantitative RT-PCR	RNA
(Toda *et al.*, 2002)	9	10	Human	Bronchial	Asthma	hCLCA1	Hybridization, histochemistry and immunocytochemistry	RNA
(Wang *et al.*, 2007a)	25	20	Human	Bronchial	COPD	Calcium-activated chloride channel 1	RT-PCR, immunohistochemistry	RNA and protein
(Wang *et al.*, 2007b)	6	10	Human	Bronchial	Asthma	Calcium-activated chloride channel 1	RT-PCR, immunohistochemistry	RNA and protein
(Woodruff *et al.*, 2007)	42	28	Human	Bronchial	Asthma	hCLCA1	Quantitative RT-PCR, immunohistochemistry	RNA and protein

Table 6.5: Table summarizing the key characteristics of the selected studies: The studies were assessed for the risk of bias and key characteristics identified to allow comparability within discussion. The final ten selected papers are presented in this table

6.4.4 Data extraction

Data from the ten selected studies could not be pooled for meta-analysis due to the variety of outcome measures that were used. Some studies used fold difference gene expression whereas others used copy number per nanogram of total RNA. Data extraction therefore is from individual papers and the outcome measures discussed in principle.

6.4.5 Summary of results

Of the ten finally selected studies, nine focused upon asthma, five of which used human bronchial epithelial tissue to explore the expression of particular chloride ion channels (Hoshino *et al.*, 2002; Toda *et al.*, 2002; Kuperman *et al.*, 2005; Wang *et al.*, 2007b; Woodruff *et al.*, 2007). The remaining four used equine bronchial tissues as a model of asthma in humans (Anton *et al.*, 2005; Range *et al.*, 2007; Ryhner *et al.*, 2008; Gerber *et al.*, 2009). Equine studies have been included for systematic review as it has been suggested that horses with recurrent airway obstruction (RAO) are a model for human asthma due to similar clinical features (Anton *et al.*, 2005; Gerber *et al.*, 2009). It must be reiterated however that equine models are weak due to the potential environmental effects of stabling (Range *et al.*, 2007). There have been previous studies that use murine models for chloride ion channels and it has been shown that that mCLCA3 is homologous with hCLCA1 (Section 1.1.3.3). It has been previously suggested that mCLCA3 and hCLCA1 have a similar isoform to eCLCA1 however there are slight structural differences. To what extent this may impact upon function is not clearly addressed in the selected studies. The findings of the systematic review however must be considered with the limitations. That there were only 10 papers finally selected, and that there was a mix of human, murine and equine studies, suggests that findings cannot be used to support or reject the hypothesis.

Of the nine studies, CLCA was the only chloride channel that was examined. However, as discussed in section 1.1.3.3, CLCA is not considered a chloride ion channel in itself (Greenwood & Leblanc, 2007). Hamann (2009) has suggested that CLCA modulates the function of other Ca^{2+} activated Cl^- channels. CLCAs are therefore implicated in the conductance of chloride and have been included in

the systematic review. Two of the selected studies measured expression of Ca^{2+}-activated Cl^- channel 1 (CaCC1) (Hoshino *et al.*, 2002; Wang *et al.*, 2007b) which is considered an alternative name for hCLCA1 (homologous to mCLCA3 and eCLCA1) (Wang *et al.*, 2007b). Hoshino et al (2002) suggest that it is similar in distribution and structure to murine gob-5 which is considered as an alias for mCLCA3 (Anton *et al.*, 2005). Both Wang et al (2007b) and Hoshino et al (2002) state that CaCC1 has similar homology to gob-5. All studies reported an increase in the expression of CLCA in response to inflammation. That only CLCA has been identified, and is not considered a chloride ion channel in itself is another limitation of the current systematic review.

6.5 Discussion

The symptoms of chronic inflammatory lung disease include mucus over-production, airway inflammation and hyper-reactivity (Toda *et al.*, 2002; Kuperman *et al.*, 2005; Wang *et al.*, 2007b). It has been suggested that chloride ion channels are responsible for these symptoms as discussed in Chapter 1 (Anton *et al.*, 2005; Wang *et al.*, 2007b). The expression of the bestrophin family has been screened in numerous cell types, and preliminary functional properties explored (Chapter 4 and Chapter 5). To establish whether chloride ion channels are implicated in chronic inflammatory lung disease, a systematic review question was formulated; Is the gene and protein expression of chloride ion channels upregulated in the respiratory epithelia, or granulocytes, of subjects with chronic inflammatory lung disease, as assessed by Bestrophins (1-4), CLCAs, ANOs, ClCs, Tweety protein and gene expression, using all available cohort, case control and laboratory studies?

This question remains unanswered through this systematic review. It appears there is an increase in hCLCA1 expression in those with chronic inflammatory lung disease however this cannot be necessarily applied to chloride ion channels until the relationship between hCLCA1 and other potential molecular candidates is clarified. In addition, there is a high risk of bias due to the limited number of studies that could be compared as four used an equine population. The consistency between studies was also problematic due to variables in controls, sample size and sample preparation. Outcomes (gene and protein expression) were also not comparable due to different measures used across the studies. It is also important to acknowledge that there is a high risk of publication bias, as discussed, which further limits the ability to draw conclusions from the systematic review.

6.5.1 Limitations of the systematic review

Whilst the methodology has followed the principles of systematic reviewing it must be acknowledged that the results are extremely limited. Primarily, a weakness of the systematic review is that methods have been adapted from processes designed to collate RCT evidence and answer questions related directly to healthcare (as discussed in Section 6.1). The intention was to identify whether chloride ion channels are upregulated in chronic inflammatory lung diseases. Whilst the the validity of each paper was reliably assessed, due to the limits of adapting a process designed for alternative evidence, any discussion must be considered cautiously.

A limitation of the current systematic review may also be the search terms used. To ensure that every available paper was accessed, the search terms were broad and a systematic process to exclude evidence was used. This resulted in a large number of papers being identified (524 as in Figure 6.1) which were initially screened for abstract and title leaving 86 which were examined in further depth for possible inclusion. Alternative search terms were initially identified however there were no papers identified using the databases described. By broadening search terms, papers that met criteria were included (Section 6.4.1 for further discussion regarding inclusion and exclusion of papers). It could be argued however that by broadening the search terms it encouraged a thorough and systematic search for all potential studies. The final number of papers selected was very limited as only 10 met criteria, and whilst they were considered to have a low risk of bias, the population of each differed, making comparability difficult. This must also be considered when assessing the validity and reliability of the systematic review.

A further limitation is that of the 10 studies that were finally included, 40% used equine samples. Anton *et al* (2005) suggest that human COPD and human asthma can be modelled effectively using RAO affected horses. They state that there are similarities between RAO and human COPD/asthma pathologies, clinical symptoms and allergic responses. Whilst this is supported by Gerber *et al* (2009) who acknowledge the similarities in clinical features, they also acknowledge that stabling horses in itself can cause many of the allergic symptoms that are considered similar to COPD and asthma in humans. This includes the effect of both allergic and non-allergic irritants such as dust or mould spore irritation. RAO in horses is therefore considered a relatively weak model for human asthma and COPD (Range *et al.*, 2007). As a result, the findings of equine studies can only be considered in the current systematic review with caution. Further research to examine the similarities between human and equine studies is required in order to draw conclusions with any confidence.

A substantial limitation of the systematic review is that there is a high risk of publication bias. Whilst key laboratories were written to requesting potential data, both positive and null, there were no responses. This may indicate that there were no prospective studies that should be included, regardless of whether they have been published or not. However, if a researcher perceives results to be null, it is unlikely that data would be in an appropriate format and available for dissemination. Therefore, that none of the laboratories responded is not a reliable measure of reduced publication bias. Furthermore, that the populations were not comparable, and sample sizes were small, prohibited use of a funnel plot to assess bias. As a result, it is likely that findings from the current systematic review over-estimate any potential correlation between chloride ion

channels and chronic inflammatory lung disease due to publication bias (Song *et al.*, 2010).

6.5.2 Expression of chloride ion channels in asthma

6.5.2.1 Equine studies

Equine studies are considered to be an appropriate animal model for asthma in humans due to the similarities in clinical symptoms and pathophysiology between RAO and asthma (Anton *et al.*, 2005; Ryhner *et al.*, 2008). It has been argued however that due to the environmental effects of stabling, and non-allergic irritants, equine models for asthma and COPD are weak. However, Anton et al (2005) suggested from their data that eCLCA1 is the equine orthologue of hCLCA1, mCLCA3 and pCLCA1. The distribution of eCLCA1 and mCLCA3 is similar in each species with some differences noted in sweat glands of both animals (Leverkoehne & Gruber, 2002; Anton *et al.*, 2005). It has been established, however, that there is similar expression of mCLCA3 and eCLCA1 in the mucin producing cells of animal airways (Anton *et al.*, 2005; Range *et al.*, 2007). Anton et al (2005) has shown in their study of horses that eCLCA1 mRNA is strongly up-regulated in the RAO lung compared to healthy horses. They used Northern blot hybridization on horses (n=3) spontaneously affected with RAO compared to healthy controls (n=3). They also demonstrated that eCLCA1 protein was up-regulated in RAO horse lung, compared to a weak signal in healthy lung on Western blotting. They suggested therefore that this would be indicative of an increase in the human asthmatic lung. As stated however, this is not conclusive due to the variables that would impact upon the expression of symptoms in RAO that are associated with asthma or COPD and that equine models are not considered a strong animal model for humans. In addition, Anton et al (2005) did not quantify the number of goblet cells in the RAO affected horses, compared to controls. It has been shown in a later study on horses with RAO, that the observed increased expression of eCLCA1 is not

at transcription (Range *et al.*, 2007). In this study, there was a larger sample of 9 horses in the RAO group, and 9 healthy controls. Range et al (2007) quantified goblet cells by using the housekeeping gene EF-la as a marker of goblet cells. They found that there was a direct correlation between eCLCA1 mRNA and protein expression with goblet cell metaplasia and hyperplasia. This is an essential component in understanding the role that eCLCA1 may have in RAO affected horses.

Range et al (2007) demonstrated that by using whole lungs from RAO affected horses could lead to misinterpretation and that in their study, the up-regulation of eCLCA1 was due to increased numbers of mucin-producing goblet cells. If there was transcriptional up-regulation of hCLCA1, and increase in protein, it would seem reasonable to assume that this has a role to play in the symptoms of the disease. However, if there is observed up-regulation of goblet cells, and as a result, a correlated increase in expression of eCLCA1 then it may be that it is the goblet cells that have a pivotal role. In the study by Range *et al* (2007) they also demonstrated that the eCLCA1 protein was completed secreted, with no association with the plasma membrane of a cell. This was established using Western blot techniques to establish glycosylation patterns in both cell lysate and supernatant of HEK293 transfected cells. As discussed, this further suggests that horses are not an appropriate model for human disease. In human studies, there is some evidence to suggest that hCLCA1 retains a membrane bound portion, however in the Range *et al* (2007) study, the protein was completed secreted. This difference in CLCA structure between species further limits findings of equine studies when applying to human asthma and COPD. In opposition to the study by Anton *et al* (2005) it was suggested by Range *et al* (2007) that there is no clear role for eCLCA1 in the symptoms and pathophysiology of RAO in horses. It was suggested, however, that

the symptoms observed in RAO were as a direct result of increased goblet cell hyperplasia and metaplasia which may be regulated by eCLCA1 in horses.

The relationship between mucous production in RAO is examined in another equine study by Gerber *et al* (2009). In this study RAO affected horses (n=5) and control horses (n=5) were euthanized by barbiturate overdose following five days of stabling. Each subject was dissected and airway samples collected from a number of sites. Additionally, neutrophil count was established by cytology brushing of intraluminal secretions. It was concluded that in RAO affected horses, neutrophil count in airways was significantly increased, compared to control horses, and correlated with intensity of symptoms. Conversely, there was not a significant change in eosinophil count. However, in the study by Gerber *et al* (2009) there was no significant difference between control groups or the RAO affected horses in intraepithelial mucous production, or up-regulation of eqMUC5AC. They found similar values in both groups of horses however have acknowledged that by stabling the horses prior to euthanasia, they may experience dust irritation. This would result in similar irritation to airways in both RAO horses and control horses. Dust irritation may account for any of the observed symptoms. Gerber *et al* (2009) in contrast to Range *et al* (2007) found no significant difference between experimental groups in goblet cell metaplasia or hyperplasia however did suggest that there was an increase in both groups due to stabling, compared to healthy horses that had been kept in pasture.

Despite the similarities in control and RAO affected horses, Gerber *et al* (2009) has shown that there is a positive correlation between eqMUC5AC and eCLCA1 expression. In each group, the relationship differed however. In the experimental group, there was a

comparatively larger expression of eCLCA1 in relation to MUC5AC. Conversely, there was a greater expression of MUC5AC in relation to eCLCA1 in the control group of horses. It was suggested that eCLCA1 acts as a regulator of MUC5AC in response to IL-13 (Gerber *et al.*, 2009). This was also supported by an earlier study on mice which showed a larger increase in mCLCA3 in mice compared to MUC5AC when IL-13 was administered intra-tracheally (Thai *et al.*, 2005). In the human asthmatic airway, symptoms are often exacerbated by allergen or dust exposure, which would increase IL-13 and therefore may have similar responses as the RAO horses in this study. However, as highlighted, equine studies may not prove to be a useful model, particularly due to differences in the structure of CLCAs between species. Gerber *et al* (2009) suggest that the relationship between IL-13, eqMUC5AC and eCLCA1 that is observed is likely to be as a consequence of neutrophilic inflammation and that eCLCA1 is an important molecule in the regulation of mucous production in RAO affected horses.

In contrast to the three previous equine studies, Ryhner *et al* (2008) has shown that despite an increase in mucous production in the RAO affected horses (n=12) compared to healthy controls (n=11), there is no significant difference in MUC5AC or eCLCA1 genes. They also found that IL-13 was down-regulated in RAO horses. This contradicts the hypothesis that in RAO IL-13 is increased in response to, and causing a response in, eosinophil accumulation (Lee *et al.*, 2001; Nakano *et al.*, 2006). It has also previously been found that increased IL-13 will up-regulate CLCA1, and goblet cell metaplasia (Nakanishi *et al.*, 2001). The findings of the study by Ryhner *et al* (2008) demonstrated that increased mucous secretion is not correlated to IL-13 or eCLCA1 and suggested this to be as a result of neutrophilic airway inflammation. The horses used in this study, however, were chronically affected with RAO and

as acknowledged, IL-13 and increases in MUC5AC and eCLCA1 may only occur in the acute phase of disease.

Equine studies which consider the expression of chloride channels in RAO are contradictory to date. There are 3 studies which demonstrate an up-regulation of eCLCA1 in horses with RAO, as an animal model for asthma. One of which presents this as a transcriptional up-regulation (Anton *et al.*, 2005). As second study states that whilst the is an overall increase in eCLCA1, this is because eCLCA1 is expressed in goblet cells and during RAO, there is an increase in goblet cell metaplasia and hyperplasia (Range *et al.*, 2007). A third study found no difference between RAO and control horses in the expression of MUC5AC or eCLCA1 but did find an increase in mucous production and eCLCA1 in both groups. This was attributed to both groups being stabled for five days prior to euthanasia and both being exposed to allergen and dust irritants. They also presented a positive correlation between MUC5AC and eCLCA1 which was postulated to be IL-13 driven (Gerber *et al.*, 2009). Controversially, the final equine study found no significant difference in gene expression between RAO horses and control horses and that IL-13 was controversially decreased in RAO horses compared to the control group (Ryhner *et al.*, 2008). In this instance, the horses were chronically affected with RAO and it was considered that the differences in study results may be because eCLCA1 and MUC5AC may only be up-regulated in the acute phase of disease.

In summary, it appears that equine studies may not be directly applicable to human asthmatic responses and results should only be considered with caution. First and foremost, RAO shares similar symptoms to asthma however it cannot be used as a model for asthma due to differing pathologies, and variables such as dust

irritation in equine studies. It has also become evident that there may be structural differences in CLCA between humans and horses. As previously discussed (Chapter 1) CLCA1 is not considered a channel in itself however there is a correlation between CLCA1 and chloride flux. This may be attributable to the postulated regulatory role of CLCA1 on other Ca^{2+} activated Cl^- ion channels. However, that it is not a channel in itself is another limitation. Using the equine studies, the hypothesis cannot be supported in light of the acknowledged limitations.

6.5.2.2 Human studies

Human studies seem to support the hypothesis that hCLCA1 expression is greater in the airway epithelial tissues of people with asthma. Woodruff et al (2007) found that asthmatic subjects had a 6.2 fold greater expression of hCLCA1 compared to healthy control subjects. This was compared against smokers as a disease control group which found that the expression of hCLCA1 was not increased in this group. The likely mechanism by which hCLCA1 is up-regulated is a response to inflammation. Within this study, primary airway cells were grown as a monolayer and stimulated with IL-13. The result was a marked increase in hCLCA1 expression (Woodruff *et al.*, 2007). IL-13 is released during inflammation, such as that in asthma, which may correlate the observed response *in vitro* with primary airway cells, to that found *in vivo* from the bronchial brushings of asthmatic subjects. In addition, the expression of hCLCA1 was decreased in response to inhaled cortico-steroids. However, the study by Woodruff *et al* (2007) did not quantify goblet cell hyperplasia or metaplasia. Given the suggestion from the equine studies that CLCA1 is up-regulated due to its distribution in goblet cells, this may have been useful to establish in the Woodruff *et al*

(2007) study. This would indicate whether, in humans, hCLCA1 is up-regulated in relation to goblet cell numbers.

Toda et al (2002) have supported this in humans by examining the expression of hCLCA1, IL-9 and the quantity of mucous producing cells. They found that in asthmatic subjects, there is greater expression of hCLCA1 but equally, the number of mucous producing cells is increased in asthmatic subjects, compared to healthy controls. Toda et al (2002) have considered hCLCA1 as a chloride ion channel however, as previously discussed, since the publication of this study it has been found that CLCA1 is not in itself a channel but may, however, regulate other channels. The correlation between mucous producing epithelial cells and hCLCA1 is further supported however, as the increased expression of hCLCA1 is correlated with increased IL-9 which is thought to stimulate goblet cells (Toda *et al.*, 2002). If hCLCA1 is found to interact with other chloride ion channels, it seems reasonable to suggest that chloride ion channels are implicated in the disease process and symptoms of asthma.

The increased expression of CLCA1 has been confirmed in a study that used both human samples, and mouse models of asthma (Kuperman *et al.*, 2005). In the murine model, there were three experimental groups; control mice that were allergen challenged, IL-13-over-expressing transgenic mice with signal transducer and activator of transcription factor 6 (STAT6) limited to airway epithelial cells, and IL-13 over-expressing mice with normal STAT6. Those with normal STAT6 produce symptoms of asthma however those with STAT6 limited to airway epithelial cells produced symptoms of asthma but without inflammation, fibrosis or emphysema. By using the three murine models of asthma, Kuperman *et al* (2005) were able to establish which genes were over-expressed as a result of allergen stimulation only, and which were attributable to certain

symptoms of asthma, such as mucous hyper-secretion and inflammation. By using the two models +/- STAT6 the effects of IL-13 as a single mediator were established. Kuperman *et al* (2005) found that in all three murine asthmatic models, there was increased expression of mCLCA3 (human orthologue hCLCA1). This suggests that in allergen stimulated asthma, there is increased expression of mCLCA3. This pattern was similar in human subjects with asthma, compared to controls however the over-expression of hCLCA1 in airway epithelial cells was greater in humans, than observed in murine models as measured by fold change.

The two other studies which used human subjects used the term CaCC1 (calcium activated chloride channel 1) (Hoshino *et al.*, 2002; Wang *et al.*, 2007b). This is an alternative term for hCLCA1 as identified by Wang et al (2007b).

Hoshino et al (2002) found that there was a marked increase in hCaCC1 in asthmatic subjects compared to control subjects. They found that the distribution of this chloride channel was similar to that of eCLCA1 (Range *et al.*, 2007) and hCLCA1 (Woodruff *et al.*, 2007). Also, similarly, Hoshino *et al* (2002) demonstrated that hCaCC1 was expressed in the epithelium of the bronchus, and particularly in the goblet cells. However, as with the Woodruff *et al* (2007) study, there was no quantification of goblet cells and so the up-regulation was not clearly transcriptional, or whether it was due to metaplasia of goblet cells. The images provided within the study by Hoshino *et al* (2002) do clearly demonstrate a correlation between location of hCaCC1 and goblet cells by immunohistochemical staining.

The observations from Hoshino *et al* (2002) were supported by Wang *et al* (2007b) in their study however they also examined the correlation with goblet cells. hCaCC1 had a greater expression in the

asthmatic subjects, throughout the bronchial tissues, compared to controls. This was statistically significant and was positively correlated with the expression of MUC5AC protein and quantities of goblet cells.

The studies of hCLCA1 support that there is significant up-regulation of this gene in asthmatic subjects. It is not clear whether this is because there is more expression within goblet cells, and these are up-regulated, or whether it is transcriptional up-regulation is not clear. However, there appears more evidence to suggest that the increased expression of hCLCA1 is due to hyperplasia and metaplasia of goblet cells. That the relationship between hCLCA1 and goblet cells is unclear, and that was a limited number of studies identified, further limits application of findings to the current project. As with equine studies, only hCLCA1 has been identified and therefore not a chloride ion channel in itself. In light of these limitations, the findings of the human studies do not support the hypothesis and further evidence is required.

6.5.3 Expression of chloride ion channels in chronic obstructive pulmonary disease (COPD)

Four of the included studies discussed chloride ion channels in COPD. Of these, only one considered COPD alone and the remaining three were both asthma and COPD. It should be noted, however, that the study by Wang *et al* (2007b) was published by the same laboratory group that published a similar paper which focused upon asthma only with the same chloride ion channels examined (Wang *et al.*, 2007a). The abstracts and methodology for each of the papers by the Wang laboratory are similar with "asthma" substituted with "COPD". It seems reasonable, therefore, to assume that these differing papers are a result of a single study (Wang *et al.*, 2007a; Wang *et al.*, 2007b). The discussion therefore for COPD can be directly extracted from section 6.5.2.2 for equine studies (Range *et al.*, 2007; Ryhner *et al.*, 2008; Gerber *et al.*, 2009) and 6.5.2.3 for human studies (Wang *et al.*, 2007a; Wang *et al.*, 2007b).

6.5.4 Systematic review concluding remarks

The studies examining chloride ion channels all focus upon hCLCA1 or the animal homologue, eCLCA1. As discussed in section 1.1.3.3, hCLCA1 is no longer considered a chloride ion channel in itself but may modulate other Ca^{2+} activated Cl^- channels. Therefore, the increased expression of hCLCA1 can be correlated with an increased flux of chloride. The exact relationship between hCLCA1 and alternative channels, such as hBest1 or hANO1, is not yet clear. In light of this, the findings cannot be applied with confidence to the current project and do not support the hypothesis that chloride ion channels are upregulated in chronic inflammatory lung diseases.

The papers used in the systematic review have suggested a positive correlation between increased hCLCA1 expression and goblet cell hyperplasia and metaplasia. There is also a relationship between increased hCLCA1 and increased IL-13 and IL-9. From these results it appears that hCLCA1 expression is increased in inflammatory aiways as a result of cytokine release and goblet cell metaplasia and hyperplasia. The interaction between hCLCA1 and other chloride ion channels requires further experimentation to be established. The relationship between goblet cell metaplasia and hyperplasia also requires further clarity before the findings of the current systematic review can be applied with confidence to the hypothesis.

There are several limitations to the systematic review highlighted (Section 6.5.1). These include; adaptation of systematic reviewing methods intended for RCTs in healthcare, mixed species evidence, a small number of papers finally selected, that CLCA1 is not considered a chloride ion channel in itself, structural differences in CLCA1 across species and that findings across papers are contradictory. In light of these limitations, the systematic review has not answered the

question posed, nor proved supportive of the current project and the hypothesis is not supported.

CHAPTER 7: CONCLUSIONS

7.1 Limitations

There are limitations to the current project which need defining in order to assess any risk of bias or application of results.

Initial experimental data was using commercial cell lines and primary cells from “healthy” donors. It could be argued that in order to further elucidate potential candidates for chloride ion channels then there should be a comparison to granulocytes in either donors with allergic responses, or chronic inflammatory lung diseases. This may further be examined by using alternative experimental groups and defining specific lung diseases within each. For example, healthy donors as control, COPD and asthma as experimental groups. This would clarify any changes or up-regulation during the disease process. It may also be useful to expand the tissue types to include nasal or bronchial brushings, again from three experimental groups. Ethics approval, scope of the project timeline and financial constraints prohibited this in the current project.

Some methodological concerns regarding calcium and chloride flux assays which would need extensive optimization in order to achieve significant results. This could also be used on primary cells with different experimental groups. HL60s however could be used to establish method as the financial commitment is less, and the cells are more readily available than primary cells.

Systematic reviewing is an established technique in research which is considered rigorous in the hierarchy of evidence. There are, however, limitations for this project. There are many systematic reviews that have been published however they are more commonly employed when examining randomized controlled trials. Therefore,

much of the guidance, and tools available are structured towards this particular field of research. The tool used for assessing the risk of bias was designed using several different tools and applying them to primary, laboratory experiments. In addition, there were many limitations (Section 6.5.1) which suggest that the systematic review was not productive in the current project. Any discussion cannot support the hypothesis. Further research should be directed towards laboratory experimentation, using human subjects, to identify which chloride ion channels may be upregulated in chronic inflammatory lung diseases.

7.2 Addressing the hypothesis

The aim of this project (section 1.2) was initially to elucidate the potential candidates for chloride ion channels in granulocytes, and the commercial cell line, HL60s. There has also been considerable screening of epithelial cells used as controls. It was shown that HL60s are an appropriate model for human granulocytes as they have a similar phenotype for the bestrophin family of chloride ion channels (section 3.2).

RT-PCR has been employed to screen a number of positive controls, and airway epithelial tissues to examine the potential candidates. Many of the airway cells were used as positive controls and all bands for hCLCA1-4, hBest1-4 and hANO1-10 were confirmed by sequence analysis with the exception of hCLCA4 and hANO9. These were non-specific (Table 3.5). As a result, phenotyping for all cells was considered to be an accurate reflection of the physiological expression of mRNA. For the purpose of this project, the putative channels were narrowed to focus upon hCLCA1, hBest1 and hANO1 for further analysis using flow cytometry and western blotting for protein expression. The aim was to clarify whether these were surface or membrane bound proteins. Secondly, there has been some suggestion that hCLCA1 may interact with hBest1 to modulate activity (Greenwood & Leblanc, 2007; Hamann *et al.*, 2009). Previous studies have demonstrated that hBest1 is localized to the endoplasmic reticulum and have suggested that in turn, hANO1 is activated (Loewen & Forsyth, 2005; Barro-Soria *et al.*, 2010). This was not supported with the RT-PCR data however, this may be due to cessation of mRNA signal when optimal activity is reached. Flow cytometry does however, support this hypothesis. Section 4.2 shows that there is a statistically significant difference in hCLCA1 and hBest1 expression. There is a negative correlation between the two

proteins in that as hCLCA1 decreases, hBest1 increases and vice versa. The overall expression of hBest1 is less than hCLCA1 as supported by the work of Loewen and Forsyth (2005). In addition, as highlighted in section 4.2, there is a greater fluorescence when hBest1 is labelled intracellulary which supports other studies stating that hBest1 is predominantly localised to the endoplasmic reticulum (Barro-Soria *et al.*, 2010). There was also an increased expression of hANO1 which also correlated with decreased expression of hBest1 (figure 4.2 and 4.3). This was statistically significant. Also of note, and potentially important in discussion of the hypothesis is that there is a statistically significant greater expression of both hCLCA1 and hBest1 in granulocytes, compared to eosinophils. It has been postulated that hCLCA1 may have a role in maturation and differentiation of granulocytes (Loewen & Forsyth, 2005) which may be supported by the difference between granulocytes and eosinophils. It is hypothesised that hCLCA1 is involved in the terminal differentiation of eosinophils, secondary to an increase in hBest1 expression. This, in turn, increases the recruitment and activation of granulocytes at the site of inflammation (Matsumoto *et al.*, 2008; Spencer & Weller, 2010).

That granulocytes are implicated in COPD and asthma is clear (Barnes, 2008) however the role of hBest1 in granulocyte function in these disease processes needs clarity. This may be of importance when considering the differing granulocyte sub groups associated with pathology of differing inflammatory lung diseases (Part 1.1). In this instance, it may be that eosinophils have a different expression of chloride ion channels than neutrophils which may be attributable to the differing clinical manifestations of the diseases. This may support a role for chloride ion channels in chronic inflammatory lung diseases.

To address the secondary aim exploring potential role of hBest1 in granulocyte during inflammation, cells were stimulated with cytokines and examined with RT-PCR and flow cytometry. Results indicate that hBest1 peaks after 24 hours stimulation with pro-inflammatory cytokine, IL-13. This was demonstrated using flow cytometry with changes measured in median fluorescence and RT-PCR (Section 5.1). This supports a potential role for hBest1 in inflammation, and possibly inflammatory lung disease. In particular asthma which is known to have a peak in eosinophil accumulation, and symptoms, at 24 hours after exposure to allergens (O'Byrne *et al.*, 2004; Holgate & Polosa, 2008). The role of hBest1 is not clear at this point, whether involved in maturation of granulocytes and differentiation, or whether up-regulation may be linked to accumulation of granulocytes to sites of inflammation. The evidence presented in this project and current literature indicates hBest1 has a role in the migration and attraction of granulocytes in inflammatory responses (Raap & Wardlaw, 2008; Walsh & August, 2010). Flow cytometry has demonstrated that hBest1 is up-regulated in response to IL-4, IL-5 and IL-13 which is likely to occur *in vivo*. The mechanism by which hBest1 may be responsible in migration of granulocytes may be through Cl^- flux and resultant changes in cell volume and shape.

Migration of granulocytes in COPD and asthma, secondary to up-regulation of hBest1 as observed in the project, may have a direct impact upon severity of symptoms. It has been suggested that granulocyte accumulation results in up-regulation of MUC5A, therefore hyper secretion and hyperplasia of goblet cells (Rogers, 2003; Caramori *et al.*, 2004; Barnes, 2008). This would result in mucous hyper secretion. Martinez-Anton et al (2006) however relate granulocyte accumulation to mucous secretion through MUC4 and MUC8.

The accumulation of granulocytes in inflammatory lung disease has been implicated in symptoms such as airway hyper-responsiveness and fibrosis (Kariyawasam & Robinson, 2007; Cheng *et al.*, 2008; Venge, 2010). Whilst these processes are linked to detrimental responses leading to tissue damage, hBest1 may also be implicated in therapeutic inflammatory responses. Up-regulation of hBest1 would increase flux of Cl^-, and in turn fluid shift. This has an important role in cell volume and shape regulation in granulocytes. This is implicated in the process of phagocytosis, an important process in defence mechanisms.

Transmigration assay was performed and it was found that when HL60s were transfected with hBest1, there was a statistically significant greater migration of cells, compared to controls towards both fMLP and IL-13. This supports then hypothesis that hBest1 in granulocytes may be involved in migration, and therefore cellular accumulation. There may also be a role in increasing cellular permeability at the site of inflammation. It has been demonstrated that fMLP stimulated neutrophils are attracted to the site of inflammation, and stimulates an increase in intracellular Ca^{2+} (Zhu *et al.*, 2005). This may cause a greater stimulation of hBest1 as a calcium activated chloride channel. It has also been postulated that hBest1 may be responsible for respiratory burst and release of oxygen free radical species (Tintinger *et al.*, 2005). This is supported by (Menegazzi *et al.*, 1999) who state that granulocytes must migrate to the area of inflammation, and be immobilised by fibronectin. Further stimulation by TNF alpha results in respiratory burst which is associated with symptom exacerbation and tissue damage in COPD and asthma. This further suggests a role for hBest1 as it has been shown that airway epithelium directly stimulated with fMLP do not respond. However, when neutrophils

are stimulated with fMLP there is accumulation at the site of inflammation, and a greater respiratory burst with release of oxygen free radicals causing cellular permeability (Virchow *et al.*, 1998; Zhu *et al.*, 2005).

To establish a link between chloride ion channels and inflammatory lung disease, a systematic review was performed to identify whether the expression of chloride ion channels is different in the cells of people with inflammatory lung diseases. The papers identified for inclusion into the systematic review focussed upon predominantly hCLCA1 (or animal orthologues) in either asthma or COPD (Chapter 6). As identified in previous studies, hCLCA1 is no longer considered an ion channel in itself but may modulate the activity of hBest1. There were only 10 papers identified for inclusion of which 40% were equine studies. The limitations were acknowledged within Chapter 6 and as a result, the systematic review did not support the hypothesis.

7.3 Concluding remarks and recommendations

This project has demonstrated that there is expression of a number of chloride ion channels in granulocytes in both health and disease. The focus was on hBest1 primarily which has been up-regulated in response to pro-inflammatory cytokine stimulation with IL-13 and fMLP stimulation. hBest1 may have a complex relationship with both hCLCA1 and hANO1 which requires further clarity. There may be a direct role for these chloride ion channels in symptoms when localised to respiratory epithelium however the role within granulocytes in subjects with inflammatory lung diseases may be multi-facetted. Firstly, the relationship between hCLCA1, hBest1 and hANO1 may cause a flux of chloride that is directly responsible for cell volume, particularly for those channels that are volume regulated. In this instance, cells may migrate with ease through permeable membranes, such as those in inflammatory responses. Secondly, the up-regulation of hCLCA1, and hBest1 may be responsible for granulocyte differentiation, maturation and eventual apoptosis and necrosis. This is stimulated by pro-inflammatory cytokines further increasing accumulation at the site of inflammation, and release of cytokines from granulocytes themselves. Another positive feedback relationship is evident and may be self-terminating as cells become terminally differentiated, and apoptotic. This may relate to the termination of clinical manifestations and symptoms. hBest1 may also have a role in respiratory burst and superoxide release which will directly increase inflammation and cell permeability of respiratory epithelia when there is accumulation of granulocytes.

There is a complex picture emerging which indicates several areas for further research. Primarily, the relationship between hCLCA1, hBest1 and hANO1 requires clarity. This may also be examined over several time courses and in relation to cellular development, maturity

and differentiation. Further examination of function of hBest1 relating to chloride or calcium flux, particularly in granulocytes as a currently under-researched area. Other research would be indicated looking at primary granulocytes from both allergic, and control subjects. Also, differentiation between diseases such as asthma and COPD may further enlighten expression and function of alternative chloride ion channels. These areas would further illuminate the complex physiological processes in chronic inflammatory lung diseases and particular focus should be on the potential relationship between the key candidates for chloride ion channels.

Evidence from the literature, and the presented experimental data, shows that hBest1 is up-regulated in granulocytes in response to inflammatory mediators. It has been postulated from this project that hBest1 is implicated in the attraction of granulocytes to the site of inflammation and the maturation and activation of such. This may occur predominantly through cell volume regulation, possibly in a complex relationship between hCLCA1, hBest1 and hANO1. hBest1 may also have a role in symptom exacerbation in COPD and asthma through stimulation of goblet cell hyperplasia and metaplasia with resultant mucous hyper-secretion. There is also suggestion that through stimulation of respiratory burst in granulocytes, hBest1 is implicated in fibrosis and airway hyper-responsiveness. It has been acknowledged, however, that through modulation of cell shape, hBest1 has a role in phagocytosis, a therapeutic inflammatory response.

In early responses to inflammation, therefore, hBest1 may have a therapeutic effect. Prolonged inflammation, however can cause tissue damage through processes such as fibrosis and airway hyper-responsiveness. hBest1, and potentially hCLCA1 and hANO1, may be involved in these processes.

REFERENCES

Abdel-Ghany M, Cheng HC, Elble RC & Pauli BU. (2001). The breast cancer beta 4 integrin and endothelial human CLCA2 mediate lung metastasis. *Journal of Biological Chemistry* **276,** 25438-25446.

Ackerman SJ, Liu L, Kwatia MA, Savage MP, Leonidas DD, Swaminathan GJ & Acharya KR. (2002). Charcot-Leyden crystal protein (Galectin-10) is not a dual function galectin with lysophospholipase activity but binds a lysophospholipase inhibitor in a novel structural fashion. *The Journal of Biological Chemistry* **277,** 14859-14868.

Agnel M, Vermat T & Culouscou J. (1999). Identification of three novel members of the calcium-dependent chloride channel (CaCC) family predominantly expressed in the digestive tract and trachea. *FEBS lett* **455,** 295.

Agrawal DK, Cheng G, Kim M-J & Kiniwa M. (2008). Interaction of suplatast tosilate (IPD) with chloride channels in human blood eosinophils: a potential mechanism underlying its anti-allergic and anti-asthmatic effects. *Clinical and Experimental Allergy* **38,** 305-312.

Ahluwalia J. (2008). Tamoxifen does not inhibit the swell activated chloride channel in human neutrophils during the respiratory burst. *Biochemical and Biophysical Research Communications* **375,** 596-601.

Ahmen N, Ramjeesingh M, Wong S, Varga A, Garami E & Bear CE. (2000). Chloride channel activity of ClC-2 is modified by the actin cytoskeleton. *Biochemical Journal* **352,** 789-794.

Al-Jumaily M, Kozlenkov A, Mechaly I, Fichard A, Matha V, Scamps F, Valmier J & Carroll P. (2007). Expression of three distinct families of calcium-activated chloride channel genes in the mouse dorsal root ganglion. *Neuroscience Bulletin* **23,** 293-299.

Aldehni F, Spitzner M, Martins JR, Barro-Soria R, Schreiber R & Kunzelmann K. (2009). Bestrophin 1 promotes epithelial-to-mesenchymal transition of renal collecting duct cells. *Journal of the American Society of Nephrology* **20,** 1556-1564.

Allakhverdi Z, Comeau MR, Smith DE, Toy D, Endam L, Desrosiers M, Liu Y-J, Howie KJ, Denburg JA, Gauvreau GM & Delespesse G. (2009). CD34+ hemopoietic progenitor cells are potent effectors of alergic inflammation. *Journal of Allergy and Clinical Immunology* **123,** 472-478.

Almaça J, Tian Y, Aldehni F, Ousingsawat J, Kongsuphol P, Rock JR, Harfe BD, Schreiber R & Kunzelmann K. (2009). TMEM16 proteins produce volume-regulated chloride currents that are reduced in mice lacking TMEM16A. *The Journal of Biological Chemistry* **284,** 28571-28578.

Altenberg GA. (2005). Guest Editorial: The multidrug resistance protein P-glycoprotein and the regulation of chloride channels. *Leukemia Research* **29,** 983-984.

Anton F, Leverkoehne I, Mundhenk L, Thoreson WB & Gruber AD. (2005). Overexpression of eCLCA1 in Small Airways of Horses with Recurrent Airway Obstruction. *Journal of Histochemistry and Cytochemistry* **53,** 1011-1021.

Bakall B, Marmorstein LY, Hoppe G, Peachey NS, Wadelius C & Marmorstein AD. (2003). Expression and localization of bestrophin during normal mouse development. *Investigative Opthalmology and Visual Science* **44,** 3622-3628.

Bakall B, McLaughlin PJ, Stanton JB, Zhang Y, Hartzell C, Marmorstein LY & Marmorstein AD. (2008). Bestrophin-2 is involved in the generation of intraocular pressure. *Investigative Opthalmology and Visual Science* **49,** 1563-1570.

Bangel N, Dahlhoff C, Sobczak K, Weber W-M & Kusche-Vihrog K. (2008). Upregulated expression of ENaC in human CF nasal epithelium. *Journal of Cystic Fibrosis* **7,** 197-205.

Barnes PJ. (2008). Immunology of asthma and chronic obstructive pulmonary disease. *Nature Review* **8,** 183-191.

Barro-Soria R, Aldehni F, Almaça J, Witzgall R, Schreiber R & Kunzelmann K. (2010). ER-Localized Bestrophin 1 Activates Ca²+- Dependent Ion Channels TMEM16A and SK4 Possibly by Acting as a Counterion Channel. *Pflugers Archiv-European Journal of Physiology* **459,** 485-497.

Barro-Soria R, Schreiber R & Kunzelmann K. (2008). Bestrophin 1 and 2 are components of the Ca^{2+} activated Cl^- conductance in mouse airways. *Biochemica et Biophysica Acta* **1783,** 1993-2000.

Barro-Soria R, Spitzner M, Schreiber R & Kunzelmann K. (2009). Bestrophin-1 enables Ca^{2+}-activated Cl^- conductance in epithelia. *The Journal of Biological Chemistry* **284,** 29405-29412.

Bauman RW. (2006). *Microbiology*. Pearson Benjamin Cummings.

Berlin AA, Lincoln P, Tomkinson A & Lukacs NW. (2004). Inhibition of stem cell factor reduces pulmonary cytokine levels during allergic airway responses. *Clinical and Experimental Immunology* **136,** 15-20.

Berryman M & Bretscher A. (2000). Identification of a novel member of the chloride intracellular channel gene family (CLIC5) that associates with the actin cytoskeleton of placental microvilli. *Molecular Biology of the Cell* **11,** 1509-1521.

Board PG, Coggan M, Watson S, Gage PW & Dulhunty AF. (2004). CLIC-2 modulates cardiac ryanodine receptor Ca2+ release channels. *International Journal of Biochemistry and Cell Biology* **36,** 1599-1612.

Bonfield TL, Konstan MW & Berger M. (1999). Altered respiratory epithelial cell cytokine production in cystic fibrosis. *Journal of Allergy and Clinical Immunology* **104,** 72-78.

Boon CJF, Klevering BJ, Leroy BP, Hoyng CB, Keunen JEE & Hollander AI. (2009). The spectrum of ocular phenotypes caused by mutations in the BEST1 gene. *Progress in Retinal and Eye Research* **28,** 187-205.

Bothe MK, Braun J, Mundhenk L & Gruber AD. (2008). Murine mCLCA6 is an integral apical membrane protein of non-goblet cell enterocytes and co-localizes with the cystic fibrosis transmembrane conductance regulator. *Journal of Histochemistry and Cytochemistry* **56,** 495-509.

Bothe MK, Mundhenk L, Beck CL, Kaup M & Gruber AD. (2012). Impaired autoproteolytic cleavage of mCLCA6, a murine integral membrane protein expressed in enterocytes, leads to cleavage at the plasma membrane instead of the endoplasmic reticulum. *Molecules & Cells* **33,** 251-257.

Boucher RC. (2007). Evidence for airway surface dehydration as the initiating event in CF airway disease. *Journal of Internal Medicine* **261,** 5-16.

Boudes M, Sar C, Menigoz A, Hilaire C, Péquignot MO, Kozlenkov A, Marmorstein AD, Carroll P, Valmier J & Scamps F. (2009). Best1 is a gene regulated by nerve injury and required for Ca^{2+}-activated Cl^- current expression in axotomized sensory neurons. *The Journal of Neuroscience* **29,** 10063-10071.

Braun J, Bothe MK, Mundhenk L, Beck CL & Gruber AD. (2010). Murine mCLCA5 is expressed in granular layer keratinocytes of stratified epithelia. *Histochemistry and Cell Biology* **133,** 285-299.

Britton FC, Ohya S, Horowitz B & Greenwood IA. (2002). Comparison of the properties of *CLCA1* generated currents and $I_{Cl(Ca)}$ in murine portal vein smooth muscle cells. *The journal of Physiology* **539,** 107-117.

Brouillard F, Bensalem N, Hinzpeter A, Tondelier D, Trudel S, Gruber AD, Ollero M & Edelman A. (2005). Blue native/SDS-PAGE analysis reveals reduced expression of the mCLCA3 protein in cystic fibrosis knock-out mice. *Molecular and Cellular Proteomics* **4,** 1762-1775.

Bubien JK. (2001). CFTR may play a role in regulated secretion by lymphocytes: a new hypothesis for the pathophsiology of cystic fibrosis. *Pflugers Archiv-European Journal of Physiology* **443,** S36-S39.

Bubien JK, Kirk KL, Rado TA & Frizzell RA. (1990). Cell cycle dependence of chloride permeability in normal and cystic fibrosis lymphocytes. *Science* **248,** 1416-1419.

Burgess R, Millar ID, Leroy BP, Urquhart JE, Fearon IM, Baere E, Brown PD, Robson AG, Wright GA, Kestelyn P, Holder GE, Webster AR, Manson FDC & Black GCM. (2008). Biallelic mutation of BEST1 causes a distinct retinopathy in humans. *The American Journal of Human Genetics* **82,** 19-31.

Bykova EA, Zhang XD, Chen TY & Zheng J. (2006). Large movement of C terminus of ClC-0 chloride channel during slow gating. *Nature Structural and Molecular Biology* **13,** 1115-1119.

Caputo A, Caci E, Ferrera L, Pedemonte N, Barsanti C, Sondo E, Pfeffer U, Ravazzolo R, Zegarra-Moran O & Galietta LJ. (2008). TMEM16A, a membrane protein associated with calcium-dependent chloride channel activity. *Science* **322,** 590-594.

Caramori G, Gregorio C, Carlstedt I, Casolari P, Guzzinati I, Adcock IM, Barnes PJ, Ciaccia A, Cavallesco G, Chung KF & Papi A. (2004). Mucin expression in peripheral airways of patients with chronic obstructive pulmonary disease. *Histopathology* **45,** 477-484.

Chen JH, Schulman H & Gardner P. (1989). A cAMP-regulated chloride channel in lymphocytes that is affected in cystic fibrosis. *Science* **243,** 657-660.

Chen TY. (2005). Structure and function of CLC channels. *Annual Review of Physiology* **67,** 809-839.

Cheng G, Ramanathan A, Shao Z & Agrawal DK. (2008). Chloride channel expression and functional diversity in the immune cells of allergic diseases. *Current Molecular Medicine* **8,** 401-407.

Chien L-T & Hartzell HC. (2007). Drosophila bestrophin-1 chloride current is dually regulated by calcium and cell volume. *The Journal of General Physiology* **130,** 513-524.

Chien L-T, Zhang Z-R & Hartzell C. (2006). Single Cl^- channels activated by Ca^{2+} in Drosophila S2 cells are mediated by bestrophins. *The Journal of General Physiology* **128,** 247-259.

Chmiel JF, Berger M & Konstan MW. (2002). The role of inflammation in the pathophysiology of CF lung disease. *Clinical Reviews in Allergy and Immunology* **23,** 5-27.

Choi JS, Jang AS, Park JS, Park SW, Paik SH, Uh ST & Kim YH. (2012). Role of neutrophils in persistent airway obstruction due to refractory asthma. *Respirology* **17,** 322-329.

Chuang J-Z, Milner TA, Zhu M & Sung C-H. (1999). A 29kDa intracellular chloride channel p64H1 is associated with large dense-core vesicles in rat hippocampal neurons. *The Journal of Neuroscience* **19,** 2919-2928.

Coelho RR, Souza EP, Soares PMG, Meireles AVP, Santos GCM, Scarparo HC, Assreuy AMS & Criddle DN. (2004). Effects of chloride channel blockers on hypotonicity-induced contractions of the rat trachea. *British Journal of Pharmacology* **141,** 367-373.

Connon CJ, Kawasaki S, Yamasaki K, Quantock AJ & Kinoshita S. (2005). The quantification of hCLCA2 and colocalisation with integrin beta4 in stratified human epithelia. *Acta Histochemistry* **106,** 421-425.

Connon CJ, Yamasaki K, Kawasaki S, Quantock AJ, Koizumi N & Kinoshita S. (2004). Calcium-activated chloride channel-2 in human epithelia. *Journal of Histochemistry and Cytochemistry* **52,** 415-418.

Cromer BA, Gorman MA, Hansen G, Adams JJ, Coggan M, Littler DR, Brown LJ, Mazzanti M, Breit SN, Curmi PMG, Dulhunty AF, Board PG & Parker MW. (2007). Structure of the Janus protein human CLIC2. *Journal of Molecular Biology* **374,** 719-731.

Cunningham SA, Awayda MS, Bubien JK, Ismailov II, Arrate MP, Berdiev BK, Benos DJ & Fuller CM. (1995). Cloning of an epithelial chloride channel from bovine trachea. *Journal of Biological Chemistry* **270,** 31016-31026.

Davidson AE, Millar ID, Urquhart JE, Burgess-Mullan R, Shweikh Y, Parry N, O'Sullivan AJ, Maher GJ, McKibbin M, Downes SM, Lotery AJ, Jacobson SG, Brown PD, Black GCM & Manson FDC. (2009). Missense mutations in a retinal pigment epithelium protein, Bestrophin-1, causes retinitis pigmentosa. *The American Journal of Human Genetics* **85,** 581-592.

Davis-Volk AP, Heise CK, Hougen JL, Artman CM, Volk KA, Wessels D, Soll DR, Nauseef WM, Lamb FS & Moreland JG. (2008). ClC-3 and ICl_{swell} are required for normal neutrophil chemotaxis and shape change. *Journal of Biological Chemistry* **283,** 34315-34326.

Döring G & Gulbins E. (2009). Cystic fibrosis and innate immunity: how chloride channel mutations provoke lung disease. *Cellular Microbiology* **11,** 208-216.

Duan D, Winter C, Cowley S, Hume JR & Horowitz B. (1997). Molecular identification of a volume-regulated chloride channel. *Nature* **390,** 417-421.

Ducharme G, Newell EW, Pinto C & Schlichter LC. (2007). Small conductance Cl^- channels contribute to volume regulation and phagocytosis in microglia. *European Journal of Neuroscience* **26,** 2119-2130.

Duta V, Duta F, Puttagunta L, Befus2 D & Duszyk M. (2006). Regulation of Basolateral Cl^- Channels in Airway Epithelial Cells: The Role of Nitric Oxide. *The Journal of Membrane Biology* **213,** 165-174.

Duta V, Szkotak AJ, Nahirney D & Duszyk M. (2004). The role of bestrophin in airway epithelial ion transport. *Federation of European Biochemical Societies* **577,** 551-554.

Dutzler R. (2006). The ClC family of chloride channels and transporters. *Current Opinion in Structural Biology* **16,** 439-446.

Dutzler R, Campbell EB, Cadene M, Chait BT & MacKinnon R. (2002). X-ray structure of a ClC chloride channel at 3.0A reveals the molecular basis of anion selectivity. *Nature* **415,** 287-294.

Dyer KD & Rosenberg HF. (1996). Eosinophil Charcot-Leyden Crystal protein binds to beta-galactoside sugars. *Life Sciences* **58,** 2073-2082.

Edwards JC. (1999). A novel p64-related Cl^- channel: subcellular distribution and nephron segment-specific expression. *American Journal of Physiology Renal Physiology* **276,** F398-F408.

Edwards JC & Kahl CR. (2010). Chloride channels of intracellular membranes. *FEBS Journal* **584,** 2102-2111.

Eggermont J. (2004). Calcium-activated chloride channels: (Un)known, (un)loved? *Proceedings of the American Thoracic Society* **1,** 22-27.

Eggermont J, Buyse G, Voets T, Tytgat J, De Smedt H, Droogmans G & Nilius B. (1997). Alternative splicing of ClC-6 (a member of the ClC chloride-channel family) transcrips generates three truncated isoforms one of which, ClC-6c, is kidney-specific. *Biochemical Journal* **325,** 269-276.

Eksandh L, Adamus G, Mosgrove L & Andréasson S. (2008). Autoantibodies against bestrophin in a patient with vitelliform paraneoplastic retinopathy and a metastatic choroidal malignant melanoma. *Archives of Opthalmology* **126,** 432-435.

Elble RC, Ji G, Nehrke K, DeBiasio J, Kingsley PD, Kotlikoff MI & Pauli BU. (2002). Molecular and functional characterization of a murine calcium-activated chloride channel expressed in smooth muscle. *The Journal of Biological Chemistry* **277,** 18586-18591.

Elble RC, Walia V, Chen H-c, Connon CJ, Mundhenk L, Gruber AD & Pauli BU. (2006). The putative chloride channel hCLCA2 has a single transmembrane segment. *The Journal of Biological Chemistry* **281,** 29448-29454.

Elble RC, Widom J, Gruber AD, Abdel-Ghany M, Levine R, Goodwin A, Cheng HC & Pauli BU. (1997). Cloning and characterization of lung-endothelial cell adhesion molecule 1 suggest it is an endothelial chloride channel. *Journal of Biological Chemistry* **272,** 27853-27861.

Engh AM, Faraldo-Gomez JD & Maduke M. (2007). The mechanism of fast-gate opening in ClC-0. *Journal of General Physiology* **130,** 335-349.

Evans SR, Thoreson WB & Beck CL. (2004). Molecular and functional analyses of two new calcium-activated chloride channel family members from mouse eye and intestine. *The Journal of Biological Chemistry* **279,** 41792-41800.

Fahlke C, Beck CL & George ALJ. (1997a). A mutation in autosomal dominant myotonia congenita affects pore properties of the muscle chloride channel. *Proceedings of the National Academy of Sciences USA* **94,** 2729-2734.

Fahlke C, Dürr C & George ALJ. (1997b). Mechanism of ion permeation in skeletal muscle chloride channels. *Journal of General Physiology* **110,** 551-564.

Fahlke C, Rhodes TH, Desai RR & George ALJ. (1998). Pore stoichiometry of a voltage-gated chloride channel. *Nature* **394,** 687-690.

Fahlke C, Rosenbohn A, Mitrovic N, George AL & RÜdel R. (1996). Mechanism of voltage-dependent gating in skeletal muscle chloride channels. *Biophysical Journal* **71,** 695-706.

Femling JK, Cherny VV, Morgan D, Rada B, Davis AP, Czirják G, Enyedi P, England SK, Moreland JG, Ligeti E, Nauseef WM & DeCoursey TE. (2006). The antibacterial activity of human neutrophils and eosinophils requires proton channels but not BK channels. *Journal of General Physiology* **127,** 659-672.

Fischkoff SA, Pollak A, Gleich GJ, Testa JR, Misawa S & Reber TJ. (1984). Eosinophilic differentiation of the human promyelocytic leukemia cell line, HL60. *Journal of Experimental Medicine* **160,** 179-196.

Fischmeister R & Hartzell C. (2005). Volume sensitivity of the bestrophin family of chloride channels. *Journal of Physiology* **562,** 477-491.

Freedman SD, Weinstein D, Blanco PG, Martinez-Clark P, Urman S, Zaman M, Morrow JD & Alvarez JG. (2002). Characterization of LPS-induced lung inflammation in *cftr* -/- mice and the effect of docosahexaenoic acid. *Journal of Applied Physiology* **92,** 2169-2176.

Friedli M, Guipponi M, Bertrand S, Bertrand D, Neerman-Arbez M, Scott HS, Antonarakis SE & Reymond A. (2003). Identification of a novel member of the CLIC family, CLIC6, mapping to 21q22.12. *Gene* **320,** 31-40.

Galli SJ, Kalesnikoff J, Grimbaldeston MA, Piliponsky AM, Williams CMM & Tsai M. (2005). Mast cells as "tunable" effector and immunoregulatory cells: Recent advances. *Annual Review of Immunology* **23,** 749-786.

Gaspar KJ, Racette KJ, Gordon JR, Loewen ME & Forsyth GW. (2000). Cloning a chloride conductance mediator from the apical membrane of porcine ileal enterocytes. *Physiological Genomics* **3,** 101-111.

Gauvreau GM, Plitt JR, Baatjes A & MacGlashan DW. (2005). Expression of functional cysteinyl leukotriene receptors by human basophils. *The Journal of Allergy and Clinical Immunology* **116,** 80-87.

Gerber V, De Feijter-Rupp H, Wagner J, Harkema JR & Robinson NE. (2009). Differential association of MUC5AC and CLCA1 expression in small cartilaginous airways of RAO-affected and control horses. *Equine Veterinary Journal* **41,** 817-823.

Gibbs BF. (2005). Human basophils as effectors and immunomodulators of allergic inflammation and innate immunity. *Clinical and Experimental Medicine* **5,** 43-49.

Gibson A, Lewis AP, Affleck K, Aitken AJ, Meldrum E & Thompson N. (2005). hCLCA1 and mCLCA3 Are Secreted Non-integral Membrane Proteins and Therefore Are Not Ion Channels. *The Journal of Biological Chemistry* **280,** 27205-27212.

Gleich GJ, Loegering DA, Mann KG & Maldonado JE. (1976). Comparative properties of the Charcot-Leyden Crystal protein and the major basic protein from human eosinophis. *The Journal of Clinical Investigation* **57,** 633-640.

Gonem S, Raj V, Wardlaw AJ, Pavord ID, Green R & Siddiqui S. (2012). Phenotyping airways disease: an A to E approach. *Clinical & Experimental Allergy* **42,** 1664-1683.

Graeber SY, Zhou-Suckow Z, Schatterny J, Hirtz S, Boucher RC & Mall MA. (2013). Hypertonic saline is effective in the prevention and treatment of mucus obstruction but not airway inflammation in mice with chronic obstructive lung disease. *American Journal of Respiratory Cell & Molecular Biology*.

Greenwood IA & Leblanc N. (2007). Overlapping pharmacology of Ca^{2+}-activated Cl^- and K^+ channels. *TRENDS in Pharmacological Sciences* **28,** 1-5.

Griffon N, Jeanneteau F, Prieur F, Diaz J & Sokoloff P. (2003). CLIC6, a member of the intracellular chloride channel family, interacts with dopamine D2-like receptors. *Molecular Brain Research* **117,** 47-57.

Gritli-Linde A, Sani FV, Rock JR, Hallberg K, Iribarne D, Harfe BD & Linde A. (2009). Expression patterns of the Tmem16 gene family during cephalic development in the mouse. *Gene Expression Patterns* **9,** 178-191.

Gruber AD, Elble RC, Ji HL, Schreur KD, Fuller CM & Pauli BU. (1998). Genomic cloning, molecular characterization, and functional analysis of human CLCA1, the first human member of the family of Ca2+-activated Cl- channel proteins. *Genomics* **54,** 200-214.

Gruber AD & Pauli BU. (1999a). Clustering of the human CLCA gene family on the short arm of chromosome 1 (1p22-31). *Genome* **42,** 1030-1032.

Gruber AD & Pauli BU. (1999b). Molecular cloning and biochemical characterization of a truncated, secreted member of the human family of Ca^{2+}-activated Cl^- channels. *Biochimica et Biophysica Acta* **1444,** 418-423.

Gruber AD & Pauli BU. (1999c). Tumorigenicity of human breast cancer is associated with loss of Ca^{2+}-activated Cl^- channel CLCA2. *Cancer Research* **59,** 5488-5491.

Gruber AD, Schreur KD, Ji HL, Fuller CM & Pauli BU. (1999). Molecular cloning and transmembrane structure of hCLCA2 from human lung, trachea, and mammary gland. *American Journal of Physiology and Cellular Physiology* **276,** 1261-1270.

Guziewicz KE, Zangert B, Lindauer SJ, Mullins RF, Sandmeyer LS, Grahn BH, Stone EM, Acland GM & Aguirre GD. (2007). Bestrophin gene mutations cause canine multifocal retinopathy: A novel animal model for best disease. *Investigative Opthalmology and Visual Science* **48,** 1959-1967.

Hagen AR, Barabote RD & Saier MH. (2005). The bestrophin family of anion channels: identification of prokaryotic homologues. *Molecular Membrane Biology* **22,** 291-302.

Hagiwara G, Krouse M, Müller U & Wine J. (1989). Is regulation of a chloride channel in lymphocytes affected in cystic fibrosis? *Science* **246,** 1049-1050.

Hamann M, Gibson A, Davies N, Jowett A, Walhin JP, Partington L, Affleck K, Trezise D & Main M. (2009). Human ClCa1 Modulates Anionic Conduction of Calcium-Dependent Chloride Currents. *The Journal of Physiology* **587,** 2255-2274.

Harada Y, Tanaka K, Yamashita K, Ishibashi M, Miyazaki H & Katori M. (1983). The anti-inflammatory mechanism of MK-447 in rat carrageenin-induced pleurisy. *Prostaglandins* **26,** 79-90.

Hauber H-P, Goldmann T, Vollmer E, Wollenberg B, Hung H-L, Levitt RC & Zabel P. (2007). LPS-induced mucin expression in human sinus mucosa can be attenuated by hCLCA1 inhibitors. *Journal of Endotoxin Research* **13,** 109-116.

Hauber H-P, Steffen A, Goldmann T, Vollmer E, Hung H-L, Wollenberg B & Zabel P. (2008). Effect of steroids, acetyl-cysteine and calcium-activated chloride channel inhibitors on allergic mucin expression in sinus mucosa. *Laryngoscope* **118,** 1528-1533.

Hegab AE, Sakamoto T, Nomura A, Ishii Y, Morishima Y, Iizuka T, Kiwamoto T, Matsuno Y, Homma S & Sekizawa K. (2007). Niflumic acid and AG-1478 reduce cigarette smoke-induced mucin synthesis: the role of hCLCA1. *Chest* **131,** 1149-1156.

Hegab AE, Sakamoto T, Saitoh W, Massoud HH, Massoud HM, Hassanein KM & Sekizawa K. (2004). Polymorphisms of *IL4*, *IL13*, and *ADRB2*
Genes in COPD*. *Chest* **126,** 1832-1839.

Heinemann A, Sturm GJ, Ofner M, Sturm EM, Weller C, Peskar BA & Hartnell A. (2005). Stem cell factor stimulates the chemotaxis, integrin upregulation, and survival of human basophils. *The Journal of Allergy and Clinical Immunology* **116,** 820-826.

Heiss NS & Poustka A. (1997). Short Communication: Genomic structure of a novel chloride channel gene, CLIC2, in Xq28. *Genomics* **45,** 224-228.

Higgins JPT & Green S, ed. (2008). *Cochrane Handbook for Systematic Reviews of Interventions*. John Wiley and Sons Ltd, Chichester.

Holgate ST & Polosa R. (2008). Treatment strategies for allergy and asthma. *Nature Reviews* **8,** 218-230.

Horowitz B, Tsung SS, Hart P, Levesque PC & Hume JR. (1993). Alternative splicing of CFTR Cl- channels in heart. *American Journal of Physiology* **264,** H2214-H2220.

Hoshino M, Morita S, Iwashita H, Sagiya Y, Nagi T, Nakanishi A, Ashida Y, Nishimura O, Fujisawa Y & Fujino M. (2002). Increased expression of the human Ca^{2+}-activated Cl^- channel 1 (CaCC1) gene in the asthmatic airway. *American Journal of Respiratory and Critical Care Medicine* **165,** 1132-1136.

Huan C, Greene KS, Shui B, Spizz G, Sun H, Doran RM, Fisher PJ, Roberson MS, Elble RC & Kotlikoff MI. (2008). mCLCA4 ER processing and secretion requires luminal sorting motifs. *American Journal of Cell Physiology* **295,** C279-C287.

Huang F, Rock JR, Harfe BD, Cheng T, Huang X, Jan YN & Jan LY. (2009). Studies on expression and function of the TMEM16A calcium-activated chloride channel. *Proceedings of the National Academy of Sciences* **106,** 21413-21418.

Illek B, Fu Z, Schwarzer C, Banzon T, Jalickee S, Miller SS & Machen TE. (2008). Flagellin-stimulated Cl- secretion and innate immune responses in airway epithelia: role for p38. *American Journal of Physiology- Lung Cell and Molecular Physiology* **295,** L531-L542.

Ishibashi K, Yamasaki J, Okamura K, Teng Y, Kitamura K & Abe K. (2006). Roles of CLCA and CFTR in electrolyte re-absorption from rat saliva. *Journal of Dental Research* **85,** 1101-1105.

Ito Y, Satoh T, Takayama K, Miyagishi C, Walls AF & Yokozeki H. (2011). Basophil recruitment and activation in inflammatory skin diseases. *Allergy* **66,** 1107-1113.

Itoh R, Kawamoto S, Miyamoto Y, Kinoshita S & Okubo K. (2000). Isolation and characterization of a Ca^{2+}-activated chloride channel from human corneal epithelium. *Current Eye Research* **21,** 918-925.

Iyer R, Iverson TM, Accardi A & Miller C. (2002). A biological role for prokaryotic ClC chloride channels. *Nature* **419,** 715-718.

Izuhara K, Ohta S, Shiraishi H, Suzuki S, Taniguchi K, Toda S, Tanabe T, Yasuo M, Kubo K, Hoshino T & Aizawa H. (2009). The mechanism of mucus production in bronchial asthma. *Current Medicinal Chemistry* **16,** 2867-2875.

Jacobsen EA, Taranova AG, Lee NA & Lee JJ. (2007). Eosinophils: Singularly destructive effector cells or purveyors of immunoregulation? *The Journal of Allergy and Clinical Immunology* **119,** 1313-1320.

Jacquot J, Tabary O, Le Rouzic P & Clement A. (2008). Airway epithelial cell inflammatory signalling in cystic fibrosis. *The International Journal of Biochemistry and Cell Biology* **40,** 1703-1715.

Jame AJ, Lackie PM, Cazaly AM, Sayers I, Penrose JF, Holgate ST & Sampson AP. (2007). Human bronchial epithelial cells express an active and inducible biosynthetic pathway for leukotrienes B4 and C4. *Clinical and Experimental Allergy* **37,** 880-892.

Jeck N, Konrad M, Peters M, Weber S, Bonzel KE & Seyberth HW. (2000). Mutations in the chloride channel gene, CLCNKB, leading to a mixed Bartter-Gitelman phenotype. *Pediatric Research* **48,** 754-758.

Jentsch TJ. (2008). CLC chloride channels and transporters: from genes to protein structure, pathology and physiology. *Critical Reviews in Biochemistry and Molecular Biology* **43,** 3-36.

Jentsch TJ, GÜnther W, Pusch M & Schwappach B. (1995). Properties of voltage-gated chloride channels of the ClC gene family. *Journal of Physiology* **482,** 19S-25S.

Jentsch TJ, Maritzen T & Zdebik AA. (2005). Chloride channel diseases resulting from impared transepithelial transport or vesicular function. *The Journal of Clinical Investigation* **115,** 2039-2046.

Jentsch TJ, Stein V, Weinreich F & Zdebik AA. (2002). Molecular Structure and Physiological Function
of Chloride Channels. *Physiological Reviews* **82,** 503-568.

Jiang B, Hattori N, Liu B, Kitagawa K & Inagaki C. (2002). Expression of swelling- and/or pH-regulated chloride channels (ClC-2, 3, 4 and 5) in human leukemic and normal immune cells. *Life Sciences* **70,** 1383-1394.

Jiang B, Hattori N, Liu B, Nakayama Y, Kitagawa K, Sumita K & Inagaki C. (2004). Expression and roles of Cl^- channel ClC-5 in cell cycles of myeloid cells. *Biochemical and Biophysical Research Communications* **317,** 192-197.

KanehisaLaboratories. (2009). http://www.genome.jp/dbget-bin/show_pathway?ecb04740+100052615.

KanKaanranta H, Janka-Junttila M, Ilmarinen-Salo P, Ito K, Jalonen U, Ito M, Adcock IM, Moilanen E & Zhang X. (2010). Histone deacetylase inhibitors induce apoptosis in human eosinophils and neutrophils. *Journal of Inflammation* **7,** 9-24.

Kariyawasam HH & Robinson DS. (2007). The role of eosinophils in airway tissue remodelling in asthma. *Current Opinion in Immunology* **19,** 681-686.

Khan TZ, Wagener JS, Bost T, Martinez J, Accurso FJ & Riches DW. (1995). Early pulmonary inflammation in infants with cystic fibrosis. *American Journal of Respiratory and Critical Care Medicine* **151,** 1075-1082.

Khodoun MV, Orekhova T, Potter C, Morris S & Finkelman FD. (2004). Basophils initiate IL-4 production during memory T-dependent response. *The Journal of Experimental Medicine* **200,** 857-870.

Kim K, Suzuki N, Ohneda K, Minegishi N & Yamamoto M. (2010). Fractionation of mature eosinophils in GATA-reporter transgenic mice. *Tohoku Journal of Experimental Medicine* **220,** 127-138.

Klimmeck D, Daiber PC, Bruhl A, Baumann A, Frings S & Möhrlen F. (2009). Bestrophin 2: An anion channel associated with neurogenesis in chemosensory systems. *The Journal of Comparative Neurology* **515,** 585-599.

Knight DA, Yang IA, Ko FWS & Lim TK. (2012). Year in review 2011: Asthma, chronic obstructive pulmonary disease and airway biology. *Respirology* **17,** 563-572.

Komiya T, Tanigawa Y & Hirohashi S. (1999). Cloning and identification of the gene gob-5, which is expressed in intestinal goblet cells in mice. *Biochemical and Biophysical Research Communications* **255,** 347-351.

Koncz C & Daugirdas J. (1994). Use of MQAE for measurement of intracellular [Cl^-] in cultured aortic smooth muscle cells. *American Journal of Physiology (Heart and Circulatory Physiology 36)***,** H2114-H2123.

Korchak HM, Eisenstat BA, Hoffstein ST, Dunham PB & Weissmann G. (1980). Anion channel blockers inhibit lysosomal enzyme secretion from human neutrophils without affecting generation of superoxide anion. *Proceedings of the National Academy of Sciences* **77,** 2721-2725.

Kornak U, Kasper D, Bosl MR, Kaiser E, Schweizer M, Schulz A, Friedrich W, Delling G & Jentsch TJ. (2001). Loss of the ClC-7 chloride channel leads to osteopetrosis in mice and man. *Cell* **104,** 205-215.

Krause K-H & Welsh MJ. (1990). Voltage-dependent and Ca^{2+}-activated ion channels in human neutrophils. *The Journal of Clinical Investigation* **85,** 491-498.

Krauss RD, Bubien JK, Drumm ML, Zheng T, Peiper SC, Collins FS, Kirk KL, Frizzell RA & Rado TA. (1992). Transfection of wild-type CFTR into cystic fibrosis lymphocytes restores chloride conductance at G1 of the cell cycle. *The EMBO Journal* **11,** 875-883.

Kunzelmann K, Kongsuphol P, Aldehni F, Tian Y, Ousingsawat J, Warth R & Schreiber R. (2009). Bestrophin and TMEM16-Ca^{2+} activated Cl^- channels with different functions. *Cell Calcium* **46,** 233-241.

Kunzelmann K, Milenkovic VM, Spitzner M, Soria RB & Schreiber R. (2007). Calcium-dependent chloride conductance in epithelia: is there a contribution by bestrophin? *Pflugers Archiv-European Journal of Physiology* **454,** 879-889.

Kuperman DA, Lewis CC, Woodruff PG, Rodriguez MW, Yee HY, Dolganov GM, Fahy JV & Erle DJ. (2005). Dissecting asthma using focused transgenic modeling and functional genomics. *Journal of Allergy and Clinical Immunology* **116,** 305-311.

Kyoh S, Kanazawa H, Tochino Y, Kodama T, Asai K & Hirata K. (2008). Comparison of N-(carboxymethyl) lysine levels and percentage of eosinophils in induced sputum for

assessment of small airway involvements in asthma. *Medical Science Monitor* **14,** CR375-380.

Laan M, Lotvall J, Chung KF & Linden A. (2001). IL-17 induced cytokine release in human bronchial epithelial cells *in vitro*: role of mitogen-activated protein (MAP) kinases. *British Journal of Pharmacology* **133,** 200-206.

Landry DW, Sullivan S, Nicolaides M, Redhead CR, Edelman AE, Field M, Al-Awqati Q & Edwards J. (1993). Molecular cloning and characterization of p64, a chloride channel protein from kidney microsomes. *The Journal of Biological Chemistry* **268,** 14948-14955.

Leblanc N, Ledoux J, Saleh S, Sanguinetti A, Angermann J, O'Driscoll K, Britton F, Perrino BA & Greenwood IA. (2005). Regulation of calcium-activated chloride channels in smooth muscle cells: a complex picture is emerging. *Canadian Journal of Physiology and Pharmacology* **83,** 541-556.

Leckie MJ, ten Brinke A, Khan J, Diamant Z, O'Connor BJ, Walls CM, Mathur AK, Cowley HC, Chung KF, Djukanovic R, Hansel TT, Holgate ST, Sterk PJ & Barnes PJ. (2000). Effects of an interleukin-5 blocking monoclonal antibody on eosinophils, airway hyper-responsiveness and the late asthmatic response. *Lancet* **356,** 2144-2148.

Lee JH, Kaminski N, Dolganov G, Grunig G, Koth L, Solomon C, Erle DJ & Sheppard DN. (2001). Interleukin-13 induces dramatically different transcriptional programs in three human airway cell types. *American Journal of Respiratory Cell and Molecular Biology* **25,** 474-485.

Lee SH, Goswami S, Grudo A, Song LZ, Bandi V, Goodnight-White S, Green L, Hacken-Bitar J, Huh J, Bakaeen F, Coxson HO, Cogswell S, Storness-Bliss C, Corry DB & Kheradmand F. (2007). Antielastin autoimmunity in tobacco smoking-induced emphysema. *Nature Medicine* **13,** 567-569.

Leonidas DD, Elbert BL, Zhou Z, Leffler H, Ackerman SJ & Acharya KR. (1995). Crystal structure of human Charcot-Leyden crystal protein, an eosinophil lysophospholipase, identifies it as a new member of the cardohydrate-binding family of galectins. *Structure* **3,** 1379-1393.

Lepple-Wienhues A, SzabÒ I, Laun T, Kaba NK, Gulbins E & Lang F. (1998). The tyrosine kinase $p56^{lck}$ mediates activation of swelling-induced chloride channels in lymphocytes. *The Journal of Cell Biology* **141,** 281-286.

Lepple-Wienhues A, Wieland U, Laun T, Heil L, Stern M & Lang F. (2001). A src-like kinase activates outwardly rectifying chloride channels in CFTR-defective lymphocytes. *The FASEB Journal* **15,** 927-931.

Leverkoehne I & Gruber AD. (2002). The murine mCLCA3 (Alias gob-5) protein is located in the mucin granule membranes of intestinal, respiratory, and uterine goblet cells. *The journal of Histochemistry and Cytochemistry* **50,** 829-838.

Leverkoehne I, Holle H, Anton F & Gruber AD. (2006). Differential expression of calcium-activated chloride channels (CLCA) gene family members in the small intestine of cystic fibrosis mouse models. *Histochemistry and Cell Biology* **126,** 239-250.

Leverkoehne I, Horstmeier BA, Samson-Himmelstjerna G, Scholte BJ & Gruber AD. (2002). Real-time RT-PCR quantitation of mCLCA1 and mCLCA2 reveals differntially regulated expression in pre- and postnatal murine tissues. *Histochemistry and Cell Biology* **118,** 11-17.

Linley JE, Boese SH, Simmons NL & Gray MA. (2009). A voltage-dependent Ca2+ influx pathway regulates the Ca2+-dependent Cl- conductance of renal IMCD-3 cells. *Journal of Membrane Biology* **230,** 57-68.

Littler DR, Harrop SJ, Goodchild SC, Phang JM, Mynott AV, Jiang L, Valenzuela SM, Mazzanti M, Brown LJ, Breit SN & Curmi PMG. (2010). The enigma of the CLIC proteins: Ion channels, redox proteins, enzymes, scaffolding proteins? *FEBS Letters* **584,** 2093-2101.

Liu JB, Zhang ZX, Xu YJ, Xing LH & Zhang HL. (2004). Effects of interleukin-13 on the gob-5 and MUC5AC expression in lungs of a murine asthmatic model. *Zhonghua jie he he hu xi za zhi = Zhonghua jiehe he huxi zazhi = Chinese journal of tuberculosis and respiratory diseases* **27,** 837-340.

Liu YJ. (2006). Thymic stromal lymphoprotein: master switch for allergic inflammation. *Journal of Experimental Medicine* **203,** 269-273.

Lloyd CM & Saglani S. (2010). Between Bedside and Bench: The Emerging Epithelium. *Nature Medicine* **16,** 273-274.

Loewen ME, Bekar LK, Gabriel SE, Walz W & Forsyth GW. (2002a). pCLCA1 becomes a cAMP-dependent chloride conductance mediator in Caco-2 cells. *Biochemical and Biophysical Research Communications* **298,** 531-536.

Loewen ME, Bekar LK, Walz W, Forsyth GW & Gabriel SE. (2004). pCLCA1 lacks inherent chloride channel activity in an epithelial colon carcinoma cell line. *American Journal of Physiology- Gastrointestinal and Liver Physiology* **287,** G33-G41.

Loewen ME & Forsyth GW. (2005). Structure and function of CLCA proteins. *Physiological Reviews* **85,** 1061-1092.

Loewen ME, Gabriel SE & Forsyth GW. (2002b). The calcium-dependent chloride conductance mediator pCLCA1. *American Journal of Cell Physiology* **283,** C412-C421.

Loewen ME, Smith NK, Hamilton DL, Grahn BH & Forsyth GW. (2003). CLCA protein nd chloride transport in canine retinal pigment epithelium. *American Journal of Cell Physiology* **285,** C1314-C1321.

Lollike K, Lindau M, Calafat J & Borregaard N. (2002). Compound exocytosis of granules in human neutrophils. *Journal of Leukocyte Biology* **71,** 973-980.

Ludewig U, Jentsch TJ & Pusch M. (1997). Analysis of a protein region involved in permeation and gating of the voltage-gated *Torpedo* chloride channel ClC-0. *Journal of Physiology* **498,** 691-702.

Mall M, Gonska T, Thomas J, Schreiber R, Seydewitz HH, Kuehr J, Brandis M & Kunzelmann K. (2003). Modulation of Ca2+-activated Cl- secretion by basolateral K+ channels in human normal and cystic fibrosis airway epithelia. *Pediatric Research* **53,** 608-618.

Marandi N, Konnerth A & Garaschuk O. (2002). Two-photon chloride imgaing in neurons of brain slices. *Pflugers Archiv- European Journal of Physiology***,** 357-365.

Markovic S & Dutzler R. (2007). The structure of the cytoplasmic domain of the chloride channel ClC-Ka reveals a conserved interaction interface. *Structure* **15,** 715-725.

Marmorstein AD, Marmorstein LY, Rayborn M, Wang X, Hollyfield JG & Petrukhin K. (2000). Bestrophin, the product of the Best vitelliform macular dystrophy gene (VMD2), localizes to the basolateral plasma membrane of the retinal pigment epithelium. *Proceedings of the National Academy of Sciences* **97,** 12758-12763.

Marmorstein LY, McLaughlin PJ, Stanton JB, Yan L, Crabb JW & Marmorstein AD. (2002). Bestrophin interacts physically and functionally with protein phosphatase 2A. *The Journal of Biological Chemistry* **277,** 30591-30597.

Marmorstein LY, Wu J, McLaughlin PJ, Yocom J, Karl MO, Neussert R, Wimmers S, Stanton JB, Gregg RG, Strauss O, Peachey NS & Marmorstein AD. (2006). The light peak of the electroretinogram is dependent on voltage-gated clacium channels and antagonized by bestrophin (best-1). *Journal of General Physiology* **127,** 577-589.

Marone G, Triggiani M & de Paulis A. (2005). Mast cells and basophils: friends as well as foes in bronchial asthma. *TRENDS in Immunology* **26,** 25-31.

Marsey LL & Winpenny JP. (2009). Bestrophin expression and function in the human pancreatic duct cell line, CFPAC-1. *The journal of Physiology* **587,** 2211-2224.

Martínez-Antón A, de Bolós C, Garrido M, Roca-Ferrer J, Barranco C, Alobid I, Xaubet A, Picado C & Mullol J. (2006). Mucin genes have different expression patterns in healthy and diseased upper airway mucosa. *Clinical and Experimental Allergy* **36,** 448-457.

Matchkov VV, Larsen P, Bouzinova EV, Rojek A, Boedtkjer DM, Golubinskaya V, Pedersen FS, Aalkjaer C & Nilsson H. (2008). Bestrophin-3 (vitelliform macular dystrophy 2-like 3 protein) is essential for the cGMP-dependent calcium-activated chloride conductance in vascular smooth muscle cells. *Circulation Research* **103,** 864-872.

Matsumoto K, Tamari M & Saito H. (2008). Involvement of eosinophils in the onset of asthma. *The Journal of Allergy and Clinical Immunology* **121,** 26-27.

Matulef K & Maduke M. (2007). The ClC 'chloride channel' family: revelations from prokaryotes. *Molecular Membrane Biology* **24,** 342-350.

McCann FV, McCarthy DC & Noelle RJ. (1990). Patch-clamp profile of ion channels in resting murine B lymphocytes. *Journal of Membrane Biology* **114,** 175-188.

Mellor L, Knudson CB, Hida D, Askew EB & Knudson W. (2013). Intracellular Domain Fragment of CD44 Alters CD44 Function in Chondrocytes. *Journal of Biological Chemistry* **288,** 25838-25850.

Menegazzi R, Busetto S, Decleva E, Cramer R, Dri P & Patriarca P. (1999). Triggering of chloride ion efflux from human neutrophils as a novel function of leukocyte β_2 integrins: relationship with spreading and activation of the respiratory burst. *The Journal of Immunology* **162,** 423-434.

Middleton RE, Pheasant DJ & Miller C. (1996). Homodimeric architecture of a ClC-type chloride channel. *Nature* **383,** 337-340.

Milenkovic VM, Barro-Soria R, Aldehni F, Schreiber R & Kunzelmann K. (2009). Functional assembly and purinergic activation of bestrophins. *Pflugers Archiv-European Journal of Physiology* **458,** 431-441.

Milenkovic VM, Langmann T, Schreiber R, Kunzelmann K & Weber BHF. (2008). Molecular evolution and functional divergence of the bestrophin protein family. *BMC Evolutionary Biology* **8,** 72-82.

Milenkovic VM, Rivera A, Horling F & Weber BHF. (2007). Insertion and topology of normal and mutant bestrophin-1 in the endoplasmic reticulum membrane. *The Journal of Biological Chemistry* **282,** 1313-1321.

Moore B, Cheng G, Shao Z, Bewtra AK & Agrawal DK. (2008). Abstract 175: ClC-3 channels and migration of eosinophils in asthma: Effect of TGF-B1. *Journal of Allergy & Clinical Immunology* **121,** S45.

Moran O & Zegarra-Moran O. (2008). On the measurement of the functional properties of the CFTR. *Journal of Cystic Fibrosis***,** 1-12.

Moreland JG, Davis AP, Bailey G, Nauseef WM & Lamb FS. (2006). Anion channels, including ClC-3, are required for normal neutrophil oxidative function, phagocytosis and transendothelial migration. *Journal of Biological Chemistry* **281,** 12277-12288.

Moreland JG, Davis AP, Matsuda JJ, Hook JS, Bailey G, Nauseef WM & Lamb FS. (2007). Endotoxin priming of neutrophils requires NADPH oxidase-generated oxidants and is regulated by the anion transporter ClC-3. *Journal of Biological Chemistry* **282,** 33958-33967.

Mullins RF, Kuehn MH, Faidley EA, Syed NA & Stone EM. (2007). Differential macular and peripheral expression of bestrophin in human eyes and its implication for Best disease. *Investigative Opthalmology and Visual Science* **48,** 3372-3380.

Mummery JL, Killey J & Linsdell P. (2005). Expression of the chloride channel CLC-K in human airway epithelial cells. *Canadian Journal of Physiology and Pharmacology* **83,** 1123-1128.

Mundhenk L, Alfalah M, Elble RC, Pauli BU, Naim HY & Gruber AD. (2006). Both cleavage products of the mCLCA3 protein are secreted soluble proteins. *The Journal of Biological Chemistry* **281,** 30072-30080.

Murzin AG. (2008). Biochemistry. Metamorphic proteins. *Science* **320,** 1725-1726.

Nakanishi A, Morita S, Iwashita H, Sagiya Y, Ashida Y, Shirafuji H, Fujisawa Y, Nishimura O & Fujino M. (2001). Role of gob-5 in mucus overproduction and airway hyperresponsiveness in asthma. *Proceedings of the National Academy of Sciences of the United States of America* **98,** 5175-5180.

Nakano T, Inoue H, Fukuyama S, Matsumoto K, Matsumura M, Tsuda M, Matsumoto T, Aizawa H & Nakanishi Y. (2006). Niflumic acid suppresses interleukin-13-induced asthma phenotypes. *American Journal of Respiratory and Critical Care Medicine* **173,** 1216-1221.

Neagoe I, Stauber T, Fidzinski P, Bergsdorf EY & Jentsch TJ. (2010). The late endosomal ClC-6 mediates proton/chloride countertransport in heterologous plasma membrane expression. *Journal of Biological Chemistry* **285,** 21689-21697.

Neussert R, Müller C, Milenkovic VM & Straub O. (2010). The presence of bestrophin-1 modulates the Ca^{2+} recruitment from Ca^{2+} stores in the ER. *Pflugers Archiv-European Journal of Physiology* **460,** 163-175.

NICE. (2007). The Guidelines Manual; Appendix C Methodology Checklist: Randomised Controlled Trials. In *wwwniceorguk/niceMedia/pdf/GDM_AppendixC_0305pdf*.

Nishizawa T, Nagao T, Iwatsubo T, Forte JG & Urushidani T. (2000). Molecular Cloning and Characterization of a Novel Chloride Intracellular Channel-related Protein, Parchorin, Expressed in Water-secreting Cells. *Journal of Biological Chemistry* **275,** 11164-11173.

Nouri-Aria KT & Durham SR. (2004). Basophils in human allergen-induced late-phase responses. *Revue Francaise D'Allergologie et D'Immunologie Clinique* **44,** 138-143.

Ntimbane T, Comte B, Mailhot G, Berthiaume Y, Poitout V, Prentki M, Rabasa-Lhoret R & Levy E. (2009). Cystic fibrosis-related diabetes: from CFTR dysfunction to oxidative stress. *Clinical Biochemical Reviews* **30,** 153-177.

O'Byrne PM, Inman MD & Adelroth E. (2004). Reassessing the Th2 cytokine basis of asthma. *TRENDS in Pharmacological Sciences* **25,** 244-248.

O'Driscoll KE, Hatton WJ, Burkin HR, Leblanc N & Britton F. (2008). Expression, localization, and functional properties of bestrophin 3 channel isolated from mouse heart. *American Journal of Cell Physiology* **295,** C1610-C1624.

O'Driscoll KE, Leblanc N, Hatton WJ & Britton F. (2009). Functional properties of murine bestrophin 1 channel. *Biochemical and Biophysical Research Communications* **384,** 476-481.

Onuma Y, Haramoto Y, Nejigane S, Takahashi S & Asashima M. (2009). Bestrophin genes are expressed in Xenopus development. *Biochemical and Biophysical Research Communications* **384,** 290-295.

Page C & Pitchford S. (2013). Neutrophil and platelet complexes and their relevance to neutrophil recruitment and activation. *International Immunopharmacology*.

Painter RG, Marrero L, Lombard GA, Valentine VG, Nauseef WM & Wang G. (2010). CFTR-mediated halide transport in phagosomes of human neutrophils. *Journal of Leukocyte Biology* **87,** 933-942.

Painter RG, Valentine VG, Lanson NA, Leidal K, Zhang Q, Lombard G, Thompson C, Viswanathan A, Nauseef WM, Wang G & Wang G. (2006). CFTR expression in human neutrophils and the phagolysosomal chlorination defect in cystic fibrosis. *Biochemistry* **45,** 10260-10269.

Park H, Oh S-J, Han K-S, Woo DH, Park H, Mannaioni G, Traynelis SF & Lee CJ. (2009). Bestrophin-1 encodes for the Ca^{2+} activated anion channel in hippocampal astrocytes. *Journal of Neuroscience* **29,** 13063-13073.

Parnham MJ, Adolfs MJP & Bonta IL. (1979). Effects of 2-aminomethyl-4-t-butyl-6-iodophenol (MK-447) on granulomatous inflammation: Lack of correlation with changes in levels of prostaglandin-like material. *Inflammation Research* **9,** 275-279.

Patel AC, Brett TJ & Holtzman MJ. (2009). The role of CLCA proteins in inflammatory airway disease. *Annual Review of Physiology* **71,** 425-449.

Paul CC, Ackerman SJ, Mahrer S, Tolbert M, Dvorak AM & Baumann MA. (1994). Cytokine induction of granule protein synthesis in an eosinophil-inducible human myeloid cell line, AML14. *Journal of Leukocyte Biology* **56,** 74-79.

Pauli BU, Abdel-Ghany M, Cheng H-C, Grunig G, Archibald HA & Elble RC. (2000). Molecular characteristics and functional diversity of CLCA family members. *Clinical and Experimental Pharmacology and Physiology* **27,** 901-905.

Pawlowski K, Lepisto M, Meinander N, Sivars U, Varga M & Wieslander E. (2006). Novel conserved hydrolase domain in the CLCA family of alleged calcium-activated chloride channels. *PROTEINS: Structure, Function, and Bioinformatics* **63,** 424-439.

Phipps DJ, Branch DR & Schlichter LC. (1996). Chloride-channel block inhibits T lymphocyte activation and signalling. *Cellular Signalling* **8,** 141-149.

Picollo A, Liantonio A, Babini E, Camerino DC & Pusch M. (2007). Mechanism of interaction of niflumic acid with heterologously expressed kidney CLC-K chloride channels. *Journal of Membrane Biology* **216,** 73-82.

Picollo A & Pusch M. (2005). Chloride/proton antiporter activity of mammalian CLC proteins ClC-4 and ClC-5. *Nature* **436,** 420-423.

Pifferi S, Dibattista M & Menini A. (2009a). TMEM16B induces chloride currents activated by calcium in mammalian cells. *Pflugers Archiv* **458,** 1023-1038.

Pifferi S, Dibattista M, Sagheddu C, Boccaccio A, Qteishat AA, Ghirardi F, Tirindelli R & Menini A. (2009b). Calcium-activated chloride currents in olfactory sensory neurons from mice lacking bestrophin-2. *Journal of Physiology* **587,** 4265-4279.

Pifferi S, Pascarella G, Boccaccio A, Mazzatenta A, Gustincich S, Menini A & Zucchelli S. (2006). Bestrophin-2 is a candidate calcium-activated chloride channel involved in olfactory transduction. *Proceedings of the National Academy of Sciences* **103,** 12929-12934.

Piirsoo M, Meijer D & Timmusk T. (2009). Expression analysis of the CLCA gene family in mouse and human with emphasis on the nervous system. *BMC Developmental Biology* **9,** 10-21.

Planells-Cases R & Jentsch TJ. (2009). Chloride channelopathies. *Biochemica et Biophysica Acta* **1792,** 173-189.

Plath KES, Grabbe PJ, Strenzke N, Wolff HH & Gibbs BF. (2001). Effect of chloride channel blockers on anti-IgE-stimulated histamine and IL-4/IL-13 release from human basophils. *Inflammation Research* **50,** S51-S52.

Plog S, Grotzsch T, Klymiuk N, Kobalz U, Gruber AD & Mundhenk L. (2012). The porcine chloride channel calcium-activated family member pCLCA4a mirrors lung expression of the human hCLCA4. *Journal of Histochemistry and Cytochemistry* **60,** 45-56.

Plog S, Mundhenk L, Klymiuk N & Gruber AD. (2009). Genomic, tissue expression, and protein characterization of pCLCA1, a putative modulator of cystic fibrosis in the pig. *Journal of Histochemistry and Cytochemistry* **57,** 1169-1181.

Pollock NS, Kargacin ME & Kargacin GJ. (1998). Chloride channel blockers inhibit Ca2+ uptake by the smooth muscle sarcoplasmic reticulum. *Biophysical Journal* **75,** 1759-1766.

Polosa R & Blackburn MR. (2009). Adenosine receptors as targets for therapeutic intervention in asthma and chronic obstructive pulmonary disease. *TRENDS in Pharmacological Sciences* **30,** 528-535.

Pulford K, Jones M, Banham AH, Haralambieva E & Mason DY. (1999). Lymphocyte-specific protein 1: a specific marker of human leucocytes. *Immunology* **96,** 262-271.

Pusch M, Ludewig U, Rehfeldt A & Jentsch TJ. (1995). Gating of the voltage-dependent chloride channel ClC-0 by the permeant anion. *Nature* **373,** 527-531.

Qian Z, Okuhara D, Abe MK & Rosner MR. (1999). Molecular cloning and characterization of a mitogen-activated protein kinase-associated intracellular chloride channel. *The Journal of Biological Chemistry* **274,** 1621-1627.

Qiang Z, Yu K, Cui YY, Ying C & Hartzell C. (2007). Activation of bestrophin Cl^- channels is regulated by C-terminal domains. *Journal of Biological Chemistry* **282,** 17460-17467.

Qu Z, Cheng W, Cui Y, Cui Y & Zheng J. (2009). Human disease-causing mutations disrupt an N-C-terminal interaction and channel function of bestrophin 1. *The Journal of Biological Chemistry* **284,** 16473-16481.

Qu Z, Cui Y & Hartzell C. (2006). A short motif in the C-terminus of mouse bestrophin 4 inhibits its activation as a Cl channel. *Federation of European Biochemical Societies* **580,** 2141-2146.

Qu Z, Fischmeister R & Hartzell C. (2004). Mouse Bestrophin-2 Is a Bona fide Cl- Channel: Identification of a Residue Important in Anion Binding and Conduction. *The Journal of General Physiology* **123,** 327-340.

Qu Z, Han X, Cui Y & Li C. (2010). A PI3 kinase inhibitor found to activate bestrophin 3. *Journal of Cardiovascular Pharmacology* **55,** 110-115.

Qu Z & Hartzell C. (2008). Bestrophin Cl- channels are highly permeable to HCO_3^-. *American Journal of Cell Physiology* **294,** C1371.

Qu Z, Wei RW, Mann W & Hartzell C. (2003). Two bestrophins cloned from xenopus laevis oocytes express Ca^{2+}-activated Cl^- currents. *The Journal of Biological Chemistry* **278,** 49563-49572.

Raap U & Wardlaw AJ. (2008). A new paradigm of eosinophil granulocytes: neuroimmune interactions. *Experimental Dermatology* **17,** 731-738.

Range F, Mundhenk L & Gruber AD. (2007). A soluble secreted glycoprotein (eCLCA1) is overexpressed due to goblet cell hyperplasia and metaplasia in horses with recurrent airway obstruction. *Veterinary Pathology* **44,** 901-911.

Redhead CR, Edelman AE, Brown D, Landry DW & Al-Awqati Q. (1992). A ubiquitous 64-kDa protein is a component of a chloride channel of plasma and intracellular membranes. *Proceedings of the National Academy of Sciences USA* **89,** 3716-3720.

Robinson NC, Huang P, Kaetzel MA, Lamb FS & Nelson DJ. (2004). Identification of an N-terminal amino acid of the ClC-3 chloride channel critical in phosphorylation-dependent activation of a CaMKII-activated chloride current. *The journal of Physiology* **556,** 353-368.

Rock JR, Futtner CR & Harfe BD. (2008). The transmembrane protein TMEM16A is required for normal development of the murine trachea. *Developmental Biology* **321,** 141-149.

Rock JR, Lopez MC, Baker HV & Harfe BD. (2007). Identification of genes expressed in the mouse limb using

a novel ZPA microarray approach. *Gene Expression Patterns* **8,** 19-26.

Rogers DF. (2003). The airway goblet cell. *The International Journal of Biochemistry and Cell Biology* **35,** 1-6.

Rosenberg HF, Phipps S & Foster PS. (2007). Eosinophil trafficking in allergy and asthma. *The Journal of Allergy and Clinical Immunology* **119,** 1303-1310.

Rosenthal R, Bakall B, Kinnick T, Peachey NS, Wimmers S, Wadelius C, Marmorstein AD & Strauss O. (2005). Expression of bestrophin-1, the product of the VMD2 gene, modulates voltage-dependent Ca^{2+} channels in retinal pigment epithelial cells. *The FASEB Journal* **20,** 178-180.

Ross PE, Garber SS & Cahalan MD. (1994). Membrane chloride conductance and capacitance in jurkat T lymphocytes during osmotic swelling. *Biophysical Journal* **66,** 169-178.

Roussa E, Wittschen P, Wolff NA, Torchalski B, Gruber AD & Thévenod F. (2010). Cellular distribution and subcellular localization of mCLCA1/2 in murine gastrointestinal epithelia. *Journal of Histochemistry and Cytochemistry* **58,** 653-668.

Rychkov GY, Pusch M, Roberts ML, Jentsch TJ & Bretag AH. (1998). Permeation and block of the skeletal muscle chloride channel, ClC-1, by foreign anions. *Journal of General Physiology* **111,** 653-665.

Ryhner T, Muller N, Balmer V & Gerber V. (2008). Increased mucus accumulation in horses chronically affected with recurrent airway obstruction is not associated with up-regulation of CLCA1, EGFR, MUC5AC, Bcl-2, IL-13 and INF- expression. *Veterinary Immunology and Immunopathology* **125,** 8-17.

Salmon MD & Ahluwalia J. (2009). Swell activated chloride channel function in human neutrophils. *Biochemical and Biophysical Research Communications* **381,** 462-465.

Sanz J, von Kanel T, Schneider M, Steiner B, Schaller A & Gallati S. (2010). The *CFTR* frameshift mutation 3905insT and its effect at transcript and protein level. *European Journal of Human Genetics* **18,** 212-217.

Schreiber R, Uliyakina I, Kongsuphol P, Warth R, Mirza M, Martins JR & Kunzelmann K. (2010). Expression and Function of Epithelial Anoctamins. *The Journal of Biological Chemistry* **285,** 7838-7845.

Schrenzel J, Demaurex N, Foti M, Van Delden C, Jacquet J, Mayr G, Lew DP & Krause K-H. (1995). Highly co-operative Ca2+ elevations in response to Ins (1,4,5) P3 microperfusion through a patch-clamp pipette. *Biophysical Journal* **69,** 2378-2391.

Schroeder BC, Cheng T, Jan YN & Jan LY. (2008). Expression Cloning of TMEM16A as a Calcium-Activated Chloride Channel Subunit. *Cell* **134,** 1019-1029.

Schwiebert EM, Benos DJ, Egan ME, Stutts MJ & Guggino WB. (1999). CFTR is a conductance regulator as well as a chloride channel. *Physiological Reviews* **79,** S145-S166.

Schwingshackl A, Moqbel R & Duszyk M. (2000). Involvement of ion channels in human eosinophil respiratory burst. *The Journal of Allergy and Clinical Immunology* **106,** 272-279.

Sheppard DN & Welsh MJ. (1999). Structure and function of the CFTR chloride channel. *Physiological Reviews* **79,** S23-S45.

Siddiqui S, Cruse G, Mckenna S, Monteiro W, Mistry V, Wardlaw A & Brightling C. (2009). IL-13 expression by blood T cells and not eosinophils is increased in asthma compared to non-asthmatic eosinophilic bronchitis. *BMC Pulmonary Medicine* **9,** 34-41.

Simchowitz L, Textor JA & Cragoe EJ. (1993). Cell volume regulation in human neutrophils: 2-(aminomethyl) phenols as Cl^- channel inhibitors. *American Journal of Physiology* **265,** C143-C155.

Simon D & Simon H-U. (2007). Eosinophilic disorders. *The Journal of Allergy and Clinical Immunology* **119,** 1291-1300.

Singh H & Ashley RH. (2007). CLIC4 (p64H1) and its putative transmembrane domain form poorly selective, redox-regulated ion channels. *Molecular Membrane Biology* **24,** 41-52.

Singh H, Cousin MA & Ashley RH. (2007). Functional reconstitution of mammalian 'chloride intracellular channels' CLIC1, CLIC4 and CLIC5 reveals differential regulation by cytoskeletal actin. *FEBS Journal* **274,** 6306-6316.

Sokol CL, Chu N-Q, Yu S, Nish SA, Laufer TM & Medzhitov R. (2009). Basophils function as antigen presenting cells for an allergen-induced Th2 response. *Nat Immunol* **10,** 713-720.

Song F, Parekh S, Hooper L, Loke YK & Ryder J. (2010). Dissemination and publication of research findings : an updated review of related biases. *Health Technology Assessment* **14,** 234.

Song J, Zhang XD, Qi Z, Sun G, Chi S, Zhu Z, Ren J, Qiu Z, Liu K, Myatt L & Ma RZ. (2009). Cloning and characterization of a calcium-activated chloride channel in rat uterus. *Biology of Reproduction* **80,** 788-794.

Spencer LA & Weller PF. (2010). Eosinophils and Th2 immunity: contemporary insights. *Immunology and Cell Biology* **88,** 250-256.

Spitzner M, Martins JR, Soria RB, Ousingsawat J, Scheidt K, Schreiber R & Kunzelmann K. (2008). Eag1 and bestrophin 1 are up-regulated in fast growing colonic cancer cells. *The Journal of Biological Chemistry* **283,** 7421-7428.

Srivastava A, Romanenko VG, Gonzalez-Begne M, Catalán MA & Melvin JE. (2008). A variant of the Ca^{2+}-activated Cl channel Best3 is expressed in mouse exocrine glands. *Journal of Membrane Biology* **222,** 43-54.

Stanton JB, Goldberg AFX, Hoppe G, Marmorstein LY & Marmorstein AD. (2006). Hydrodynamic properties of porcine bestrophin-1 in Triton X-100. *Biochemica et Biophysica Acta* **1758,** 241-247.

Steinmeyer K, Lorenz C, Pusch M, Koch MC & Jentsch TJ. (1994). Multimeric structure of ClC-1 chloride channel revealed by mutations in dominant myotonia congenita (Thomsen). *EMBO Journal* **13,** 737-743.

Steinmeyer K, Ortland C & Jentsch TJ. (1991). Primary structure and functional expression of a developmentally regulated skeletal muscle chloride channel. *Nature* **354,** 301-304.

StÖhr H, Marquardt A, Nanda I, Schmid M & Weber BHF. (2002). Three novel human VMD2-like genes are members of the evolutionary highly conserved RFP-TM family. *European Journal of Human Genetics* **10,** 281-284.

Sturton G, Persson C & Barnes PJ. (2008). Small airways: An important but neglected target in the treatment of obstructive airway diseases. *TRENDS in Pharmacological Sciences* **29,** 340-345.

Sun H, Tsunenari T, Yau KW & Nathans J. (2002). The vitelliform macular dystrophy protein defines a new family of chloride channels. *Proceedings of the National Academy of Sciences USA* **99,** 4008-4013.

Suzuki M. (2006). The *Drosophila tweety* family: molecular candidates for large-conductance Ca^{2+}-activated Cl^- channels. *Experimental Physiology* **91,** 141-147.

Suzuki M, Morita T & Iwamoto T. (2006). Review: Diversity of Cl– Channels. *Cellular and Molecular Life Sciences* **63,** 12-24.

Taraseviciene-Stewart L, Douglas IS, Nana-Sinkam PS, Lee JD, Tuder RM, Nicolls MR & Voelkel NF. (2006). Is alveolar destruction and emphysema in chronic obstructive pulmonary disease an immune disease? *Proceedings of the American Thoracic Society* **3,** 687-690.

Terheggen-Lagro SW, Rijkers GT & van der Ent CK. (2005). The role of airway epithelium and blood neutrophils in the inflammatory response in cystic fibrosis. *Journal of Cystic Fibrosis* **4,** 15-23.

Thai P, Chen Y, Dolganov G, Wu R, Thai P, Chen Y, Dolganov G & Wu R. (2005). Differential regulation of MUC5AC/Muc5ac and hCLCA-1/mGob-5 expression in airway epithelium. *American Journal of Respiratory Cell & Molecular Biology* **33,** 523-530.

Tintinger G, Steel HC & Anderson R. (2005). Taming the neutrophil: calcium clearance and influx mechanisms as novel targets for pharmacological control. *Clinical and Experimental Immunology* **141,** 191-200.

Tintinger GR & Anderson R. (2004). Counteracting effects of NADPH oxidase and the Na+/Ca2+ exchanger on membrane repolarisation and store-operated uptake of Ca2+ by chemoattractant-activated neutrophils. *Biochemical Pharmacology* **67,** 2263-2271.

Toda M, Tulic MK, Levitt RC, Hamid Q, Toda M, Tulic MK, Levitt RC & Hamid Q. (2002). A calcium-activated chloride channel (HCLCA1) is strongly related to IL-9 expression and mucus production in bronchial epithelium of patients with asthma. *Journal of Allergy & Clinical Immunology* **109,** 246-250.

Tonini R, Ferroni A, Valenzuela SM, Warton K, Campbell TJ, Breit SN & Mazzanti M. (2000). Functional characterization of the NCC27 nuclear protein in stable transfected CHO-K1 cells. *FASEB Journal* **14,** 1171-1178.

Tsunenari T, Nathans J & Yau KW. (2006). Ca^{2+}-activated Cl^- current from human bestrophin-4 in excised membrane patches. *Journal of General Physiology* **127,** 749-754.

Tsunenari T, Sun H, Williams J, Cahill H, Smallwood P, Yau KW & Nathans J. (2003). Structure-function analysis of the bestrophin family of anion channels. *The Journal of Biological Chemistry* **278,** 41114-41125.

Tulk BM, Kapadia S & Edwards JC. (2002). CLIC1 inserts from the aqueous phase into phospholipid membranes where it functions as an anion channel. *American Journal of Cell Physiology* **282,** C1103-C1112.

Tyner JW, Kim EY, Ide K, Pelletier MR, Roswit WT, Morton JD, Battaile JT, Patel AC, Patterson A, Castro M, Spoor MS, You Y, Brody SL & Holtzman MJ. (2006). Blocking airway mucous cell metaplasia by inhibiting EGFR antiapoptosis and IL-3 transdifferentiation signals. *The Journal of Clinical Investigation* **116,** 309-321.

Ulrich M, Worlitzsch D, Viglio S, Siegmann N, Iadarola P, Shute JK, Geiser M, Pier GB, Friedel G, Barr ML, Schuster A, Meyer KC, Ratjen F, Bjarnsholt T, Gulbins E & Döring G. (2010). Alveolar inflammation in cystic fibrosis. *Journal of Cystic Fibrosis* **9,** 217-227.

Valenzuela SM, Martin DK, Por SB, Robbins JM, Warton K, Bootcov MR, Schofield PR, Campbell TJ & Breit SN. (1997). Molecular Cloning and Expression of a Chloride Ion Channel of Cell Nuclei. *Journal of Biological Chemistry* **272,** 12575-12582.

Varnai P, Demaurex N, Jaconi M, Schlegel W, Lew DP & Krause K-H. (1993). Highly co-operative Ca2+ activation of intermediate-conductance K+ channels in granulocytes from a human cell line. *Journal of Physiology* **472,** 373-390.

Venge P. (2010). The eosinophil and airway remodelling in asthma. *The Clinical Respiratory Journal* **4,** 15-19.

Vercelli D. (2008). Discovering susceptibility genes for asthma and allergy. *Nature Reviews* **8,** 169-182.

Virchow S, Ansorge N, RÃ¼bben H, Siffert G & Siffert W. (1998). Enhanced fMLP-stimulated chemotaxis in human neutrophils from individuals carrying the G protein Î²3 subunit 825 T-allele. *FEBS Letters* **436,** 155-158.

Walsh E, Sahu N & August A. (2007). Abstract 600: Eosinophils are Required for T Cell Infiltration of Lungs During Allergic Asthma Responses. *The Journal of Allergy and Clinical Immunology; Supplement* **119,** S153.

Walsh ER & August A. (2010). Eosinophils and allergic airway disease: there is more to the story. *TRENDS in Immunology* **31,** 39-44.

Wang G, Qian Y, Qiu Q, Lan X, He H & Guan Y. (2006). Interaction between Cl^- channels and CRAC-related Ca^{2+} signalling during T lymphocyte activation and proliferation. *Acta Pharmacologica Sinica* **27,** 437-446.

Wang K, Feng YL, Wen FQ, Chen XR, Ou XM, Xu D, Yang J, Deng ZP, Wang K, Feng Y-L, Wen F-Q, Chen X-R, Ou X-M, Xu D, Yang J & Deng Z-P. (2007a). Increased expression of human calcium-activated chloride channel 1 is correlated with mucus overproduction in the airways of Chinese patients with chronic obstructive pulmonary disease. *Chinese Medical Journal* **120,** 1051-1057.

Wang K, Wen FQ, Feng YL, Ou XM, Xu D, Yang J, Deng ZP, Wang K, Wen F-Q, Feng Y-L, Ou X-M, Xu D, Yang J & Deng Z-P. (2007b). Increased expression of human calcium-activated chloride channel 1 gene is correlated with mucus overproduction in Chinese asthmatic airway. *Cell Biology International* **31,** 1388-1395.

Wartosch L, Fuhrmann JC, Schweizer M, Stauber T & Jentsch TJ. (2009). Lysosomal degradation of endocytosed proteins depends on the chloride transport protein ClC-7. *FASEB Journal* **23,** 4056-4068.

Willis-Karp M. (2004). Interleukin-13 in asthma pathogenesis. *Immunological Reviews* **202,** 175-190.

Winpenny JP, Marsey LL & Sexton DW. (2009). The CLCA gene family: Putative therapeutic target for respiratory diseases. *Inflammation and Allergy* **8,** 146-160.

Woodruff PG, Boushey HA, Dolganov GM, Barker CS, Yee HY, Donnelly S, Ellwanger A, Sidhu SS, Dao-Pick TP, Pantoja C, Erle DJ, Yamamoto KR & Fahy JV. (2007). Genome-wide profiling identifies epithelial cell genes associated with asthma and with treatment response to corticosteroids. *Proceedings of the National Academy of Sciences of the United States of America* **104,** 15858-15863.

Xanthou G, Duchesnes CE, Williams TJ & Pease JE. (2003). CCR3 functional responses are regulated by both CXCR3 and its ligands CXCL9, CXCL10 and CXCL11. *European Journal of Immunology* **33,** 2241-2250.

Xiao Q, Prussia A, Yu K, Cui Y-Y & Hartzell C. (2008). Regulation of bestrophin Cl channels by calcium: role of the C terminus. *Journal of General Physiology* **132,** 681-692.

Xiao Q, Yu K, Cui Y-Y & Hartzell C. (2009). Dysregulation of human bestrophin-1 by ceramide-induced dephosphorylation. *Journal of Physiology* **587,** 4379-4391.

Yamazaki J, Okamura K, Ishibashi K & Kitamura K. (2005). Characterization of CLCA protein expressed in ductal cells of rat salivary glands. *Biochemica et Biophysica Acta* **1715,** 132-144.

Yang YD, Cho H, Koo JY, Tak MH, Cho Y, Shim WS, Park SP, Lee JD, Lee B, Kim BM, Raouf R, Shin YK & Oh U. (2008). TMEM16A confers receptor-activated calcium-dependent chloride conductance. *Nature* **455,** 1210-1215.

Ye J, Coulouris G, Zaretskaya I, Cutcutache I, Rozen S & Madden TL. (2012). Primer-BLAST: A tool to design target-specific primers for polymerase chain reaction. *BMC Bioinformatics* **13,** 134.

Yim PD, Gallos G, Xu D, Zhang Y, Emala CW, Yim PD, Gallos G, Xu D, Zhang Y & Emala CW. (2011). Novel expression of a functional glycine receptor chloride channel that attenuates contraction in airway smooth muscle. *FASEB Journal* **25,** 1706-1717.

Yoon I-S, Jeong SM, Lee SN, Lee J-H, Kim J-H, Pyo MK, Lee J-H, Lee B-H, Choi S-H, Rhim H, Choe H & Nah S-Y. (2006). Cloning and heterologous expresion of a Ca^{2+}-activated chloride channel isoform from rat brain. *Biological and Pharmaceutical Bulletin* **29,** 2168-2173.

Yoshimura K, Nakamura H, Trapnell BC, Chu C-S, Dalemans W, Pavirani A, Lecocq J-P & Crystal RG. (1991). Expression of the cystic fibrosis transmembrane conductance regulator gene in cells of non-epithelial origin. *Nucleic Acids Research* **19,** 5417-5423.

Yu K, Cui YY & Hartzell C. (2006). The bestrophin mutation A243V, linked to adult-onset vitelliform macular dystrophy, impairs its chloride channel function. *Investigative Opthalmology and Visual Science* **47,** 4956-4961.

Yu K, Lujan R, Marmorstein AD, Gabriel SE & Hartzell C. (2010). Bestrophin-2 mediates bicarbonate transport by goblet cells in mouse colon. *The Journal of Clinical Investigation* **120,** 1722-1735.

Yu K, Qu Z, Cui YY & Hartzell C. (2007). Chloride channel activity of bestrophin mutants associated with mild or late-onset macular degeneration. *Investigative Opthalmology and Visual Science* **48,** 4694-4705.

Yu K, Xiao Q, Cui G, Lee A & Hartzell C. (2008). The best disease-linked Cl^- channel *hBest1* regulates Ca_v1 (L type) Ca^{2+} channels via src-homology-binding domains. *The Journal of Neuroscience* **28,** 5660-5670.

Zhang SJ, Steijaert MN, Lau D, Schutz G, Delucinge-Vivier C, Descombes P & Bading H. (2007). Decoding NMDA receptor signaling: identification of genomic programs specifying neuronal survival and death. *Neuron* **53,** 549-562.

Zhang Y, Davidson BR, Stamer WD, Barton JK, Marmorstein LY & Marmorstein AD. (2009). Enhanced inflow and outflow rates despite lower IOP in bestrophin-2-deficient mice. *Investigative Opthalmology and Visual Science* **50,** 765-770.

Zhang Y, Patil RV & Marmorstein AD. (2010). Bestrophin 2 is expressed in human non-pigmented ciliary epithelium but not retinal pigment epithelium. *Molecular Vision* **16,** 200-206.

Zholos A, Beck B, Sydorenko V, Lemonnier L, Bordat P, Prevarskaya N & Skryma R. (2005). Ca^{2+} - and Volume-sensitive Chloride Currents Are Differentially Regulated by Agonists and Store-operated Ca^{2+} Entry. *The Journal of General Physiology* **125,** 197-211.

Zhou Y, Dong Q, Louahed J, Dragwa C, Savio D, Huang M, Weiss C, Tomer Y, McLane MP, Nicolaides NC & Levitt RC. (2001). Characterization of a calcium-activated chloride channel as a shared target of Th2 cytokine pathways and its potential involvement in asthma. *American Journal of Respiratory Cell and Molecular Biology* **25,** 486-491.

Zhu L, Castranova V & He P. (2005). fMLP-stimulated neutrophils increase endothelial [Ca2+]i and microvessel permeability in the absence of adhesion: role of reactive oxygen species. *American Journal of Physiology - Heart and Circulatory Physiology* **288,** H1331-H1338.

Zifarelli G, Liantonio A, Gradogna A, Picollo A, Gramegna G, De Bellis M, Murgia AR, Babini E, Camerino DC & Pusch M. (2010). Identification of sites responsible for the potentiating effect of niflumic acid on ClC-Ka kidney chloride channels. *British Journal of Pharmacology* **160,** 1652-1661.

APPENDICES

Appendix 1: Letter of ethics approval for blood harvest

Mr Darren Sexton

Biomedical Research Centre
School of Medicine, Health Policy and Practice

UEA

NR4 7TJ

Faculty of Health

Research Office

University of East Anglia
Norwich NR4 7TJ
United Kingdom

Email: Jane.Carter@uea.ac.uk
Tel: +44 (0) 1603 591023
Fax: +44 (0) 1603 591132

Web:www.uea.ac.uk

20.04.2009

Dear Darren,

Mechanisms of airway diseases - 2008042

The resubmission of your above proposal has now been considered by the Chair of the FOH Ethics Committee and we can now confirm that your proposal has now been approved.
Please could you ensure that any amendments to either the protocol or documents submitted are notified to us in advance and also that any adverse events which occur during your project are reported to the committee. Please could you also arrange to send us a report once your project is completed.
The committee would like to wish you good luck with your project.

Yours sincerely,

Dr. Jane Carter

+44 (0) 1603 591023
Jane.Carter@uea.ac.uk

Appendix 2: Letter to laboratories for systematic review

Biomedical Research Centre address

Lab address

Dear

I am currently undertaking a PhD examining the role of calcium activated chloride ion channels, in granulocytes, during chronic inflammatory lung disease. As part of my study I am undertaking a systematic review of all the studies that examine the expression of chloride ion channels in people with, and without, chronic inflammatory lung diseases. I am including granulocytes, agranulocytes and airway epithelial cells from all mammals and mammalian cell lines.

As you may be aware, in order to enable a rigorous systematic review, it is important that I can access any potential sources, including unpublished works. In order to complete this, I am writing to ask if you, your colleagues, or any member of your laboratory, have undertaken research that may be published or unpublished at this point, for consideration for inclusion in the systematic review.

Research to be included in the review will:

- Study any chloride channels
- Assess factors relating to chronic inflammatory lung disease
- Methodology could include expression and/or functional studies.

- Inclusion criteria; mammals or mammalian cell lines and all chloride ion channels
- Whether the results were positive, negative or unclear is not important to inclusion in the review

Please could you send me contact details of any researchers (including yourself) who have conducted potentially relevant research? I would like to negotiate access to the raw data from any relevant studies, in return for co-authorship on the published systematic review. It is anticipated that this would be published within 18 months. Therefore any help, or contribution, from you that you would be able to give would be invaluable. If you are able to contribute information for this systematic review, I would ask that you forward this to the above address, for the attention of my supervisor, Dr John Winpenny.

With many thanks for your time.

Yours Sincerely

Kirsty Kirk
RN (Dip) HE, BA(Hons), PGC(M)E, MSc, FHEA

Appendix 3: Inclusion/exclusion form for systematic review

In/Out form for inclusion of studies in systematic review: Is the expression of chloride ion channels different in cells from people with and without chronic inflammatory lung disease?

Study Ref: **Reviewer:**

Criteria no.	Inclusion/Exclusion criteria	Meets inclusion?
1	Is the study laboratory based/cohort study? (Include all primary laboratory research. Exclude all opinion papers, reviews, meta-analyses, editorials, letters and studies published only in abstract form)	Y N Unsure
2	Are the samples/subjects mammalian? (Include all studies using either human subjects, mammals or mammalian commercial cell lines. Exclude all samples taken from non-mammals such as amphibians, reptiles and fish)	Y N Unsure
3	Is the focus upon blood cells or airway tissue? (Include all blood cell types such as granulocytes and agranulocytes, and all airway cells such as nasal, bronchial etc. Exclude cells/samples from other organs such as pancreas)	Y N Unsure
4	Focussed upon chronic inflammatory lung diseases? (Include all inflammatory lung diseases. Exclude non-inflammatory	Y N Unsure

	disease of the lungs such as cancers, inflammatory disease or symptoms not of the airways such as bowel, exclude cystic fibrosis)	
5	Chloride ion channels? (To include all types such as voltage gated, volume regulated, calcium activated and ligand gated. Include those assumed to be either regulators of chloride flux or a channel; CLCA, bestrophins, ClC, tweety etc. Exclude all other ion channels such as potassium and sodium)	Y N Unsure

If all answers to the above are "Y" circle "include". If any answers are "N" then circle "exclude". If any are unsure then circle "pending" and detail action to resolve:

Include **Exclude** **Pending**

(Action?):

Summary: (Brief summary of reasons for exclusion if applicable)

Appendix 4: Risk of bias tool for systematic review

Risk of Bias Assessment

Tool adapted from Cochrane Risk of Bias checklist for RCT and the National Institute for Health and Clinical Excellence (www.nice.org.uk/niceMedia/pdf/GDM_AppendixC_0305.pdf) from Scottish Intercollegiate Guidelines Network

Study ID: Reference			
Completed by:		Date:	
INTERNAL VALIDITY			
1.1	The question is clear and focussed which is addressed by the study	Well covered Adequately covered Poorly addressed	Not addressed Not reported Not applicable
1.2	Methodology is appropriate to the defined question	Well covered Adequately covered Poorly addressed	Not addressed Not reported Not applicable
1.3	The treatment and control groups are similar at the start of the study	Well covered Adequately covered Poorly addressed	Not addressed Not reported Not applicable
1.4	The only difference between groups is the treatment under investigation	Well covered Adequately covered Poorly addressed	Not addressed Not reported Not applicable
1.5	All relevant outcomes are measured in a standard, valid and reliable way	Well covered Adequately covered Poorly addressed	Not addressed Not reported Not applicable

1.6	Was the attrition of the sample from the study considered/defined	Well covered Adequately covered Poorly addressed	Not addressed Not reported Not applicable
JUDGEMENT	Overall risk of bias: (50% or more "not addressed/not reported"=high risk of bias, 30% or more=medium risk of bias, 15% or less =low risk of bias)	High Medium	Low Unknown
	What is the likely effect of bias? (High=conclusions are likely to alter, medium=unlikely to alter conclusions and low = very unlikely to alter)		
OVERALL ASSESSMENT			
2.1	How well was the risk of bias identified and considered	Well covered Adequately covered Poorly addressed	Not addressed Not reported Not applicable
2.2	Evaluation of the methodology to the overall outcome of the study and the power of statistical analysis	Well covered Adequately covered Poorly addressed	Not addressed Not reported Not applicable
2.3	Is it likely that the	Well covered	Not addressed

	overall effect is due to the study intervention	Adequately covered Poorly addressed	Not reported Not applicable
2.4	Are the results likely to be generalizable due to study design?	Well covered Adequately covered Poorly addressed	Not addressed Not reported Not applicable
JUDGEMENT	Overall risk of bias:	High Medium	Low Unknown
	What is the likely effect of bias?		

STUDY DESCRIPTION			
3.1	What was the sample size? Was it appropriate/adequate?	Yes	No
3.2	Was the sample mammalian or mammalian cell line?	Yes	No
3.3	Is the sample applicable to blood cells or airway tissue?	Yes	No
3.4	Is the study generalizable to chronic inflammatory lung diseases?	Yes	No
3.5	Is the study focussed upon chloride ion channels?	Yes	No
3.6	Is there an intervention that is appropriate to systematic	Yes	No

	review?		
3.7	Is there an adequate measure of controls?	Yes	No
3.8	Are the outcome measures appropriate?	Yes	No
3.9	Was the study externally funded?	Yes	No
3.10	Is any external funding considered to reduce the risk of bias?	Yes	No
3.11	Does the study help to answer systematic review question?	Yes	No
JUDGEMENT	Overall risk of bias:	High Medium	Low Unknown
	What is the likely effect of bias?		

DESCRIPTORS (for tabulating key characteristics of the study)	
What was the sample size?	
What was the sample species?	
What was the tissue type?	
What disease was focussed on?	
What type of study was it? (experimental/cohort study etc)	
What chloride ion channels were examined?	
What were the experimental techniques used?	

What were the controls?	
What were the outcome measures?	

PRISMA 2009 Checklist APPENDIX 5: Completed PRISMA checklist for systematic review

Section/topic	#	Checklist item	Reported on page #
TITLE			
Title	1	Identify the report as a systematic review, meta-analysis, or both.	262
ABSTRACT			
Structured summary	2	Provide a structured summary including, as applicable: background; objectives; data sources; study eligibility criteria, participants, and interventions; study appraisal and synthesis methods; results; limitations; conclusions and implications of key findings; systematic review registration number.	NA
INTRODUCTION			
Rationale	3	Describe the rationale for the review in the context of what is already known.	263
Objectives	4	Provide an explicit statement of questions being addressed with reference to participants, interventions, comparisons, outcomes, and study design (PICOS).	265
METHODS			
Protocol and registration	5	Indicate if a review protocol exists, if and where it can be accessed (e.g., Web address), and, if available, provide registration information including registration number.	266
Eligibility criteria	6	Specify study characteristics (e.g., PICOS, length of follow-up) and report characteristics (e.g., years considered, language, publication status) used as criteria for eligibility, giving rationale.	268
Information sources	7	Describe all information sources (e.g., databases with dates of coverage, contact with study authors to identify additional studies) in the search and date last searched.	270
Search	8	Present full electronic search strategy for at least one database, including any limits used, such that it could be repeated.	271
Study selection	9	State the process for selecting studies (i.e., screening, eligibility, included in systematic review, and, if applicable, included in the meta-analysis).	268
Data collection process	10	Describe method of data extraction from reports (e.g., piloted forms, independently, in duplicate) and any processes for obtaining and confirming data from investigators.	275
Data items	11	List and define all variables for which data were sought (e.g., PICOS, funding sources) and any assumptions and simplifications made.	275
Risk of bias in individual studies	12	Describe methods used for assessing risk of bias of individual studies (including specification of whether this was done at the study or outcome level), and how this information is to be used in any data synthesis.	273
Summary measures	13	State the principal summary measures (e.g., risk ratio, difference in means).	275

Synthesis of results	14	Describe the methods of handling data and combining results of studies, if done, including measures of consistency (e.g., I^2) for each meta-analysis.	275
Risk of bias across studies	15	Specify any assessment of risk of bias that may affect the cumulative evidence (e.g., publication bias, selective reporting within studies).	273
Additional analyses	16	Describe methods of additional analyses (e.g., sensitivity or subgroup analyses, meta-regression), if done, indicating which were pre-specified.	NA
RESULTS			
Study selection	17	Give numbers of studies screened, assessed for eligibility, and included in the review, with reasons for exclusions at each stage, ideally with a flow diagram.	276
Study characteristics	18	For each study, present characteristics for which data were extracted (e.g., study size, PICOS, follow-up period) and provide the citations.	280
Risk of bias within studies	19	Present data on risk of bias of each study and, if available, any outcome level assessment (see item 12).	278
Results of individual studies	20	For all outcomes considered (benefits or harms), present, for each study: (a) simple summary data for each intervention group (b) effect estimates and confidence intervals, ideally with a forest plot.	284
Synthesis of results	21	Present results of each meta-analysis done, including confidence intervals and measures of consistency.	NA
Risk of bias across studies	22	Present results of any assessment of risk of bias across studies (see Item 15).	288
Additional analysis	23	Give results of additional analyses, if done (e.g., sensitivity or subgroup analyses, meta-regression [see Item 16]).	NA
DISCUSSION			
Summary of evidence	24	Summarize the main findings including the strength of evidence for each main outcome; consider their relevance to key groups (e.g., healthcare providers, users, and policy makers).	289
Limitations	25	Discuss limitations at study and outcome level (e.g., risk of bias), and at review-level (e.g., incomplete retrieval of identified research, reporting bias).	286
Conclusions	26	Provide a general interpretation of the results in the context of other evidence, and implications for future research.	299
FUNDING			
Funding	27	Describe sources of funding for the systematic review and other support (e.g., supply of data); role of funders for the systematic review.	NA

From: Moher D, Liberati A, Tetzlaff J, Altman DG, The PRISMA Group (2009). Preferred Reporting Items for Systematic Reviews and Meta-Analyses: The PRISMA Statement. PLoS Med 6(6): e1000097. doi:10.1371/journal.pmed1000097